NOAA Atlas NESDIS 13

ATLAS OF SURFACE MARINE DATA 1994 SUPPLEMENT A: ANOMALIES OF DIRECTLY OBSERVED QUANTITIES AND SURFACE MARINE FLUXES FOR 1990-1993

Washington, D.C.
March 1997

U.S. DEPARTMENT OF COMMERCE
National Oceanic and Atmospheric Administration
National Environmental Satellite, Data, and Information Service

NOAA Atlas NESDIS 13

ATLAS OF SURFACE MARINE DATA 1994 SUPPLEMENT A: ANOMALIES OF DIRECTLY OBSERVED QUANTITIES AND SURFACE MARINE FLUXES FOR 1990-1993

Christine C. Young-Molling
Department of Geosciences
University of Wisconsin-Milwaukee

Arlindo M. da Silva
Data Assimilation Office
NASA/Goddard Space Flight Center

and

Sydney Levitus
National Oceanographic Data Center
Ocean Climate Laboratory
Silver Spring, Maryland 20910

Washington, D.C.
March 1997

U.S. DEPARTMENT OF COMMERCE
William M. Daley, Secretary

National Oceanic and Atmospheric Administration
D. James Baker, Under Secretary

National Environmental Satellite, Data, and Information Service
Robert S. Winokur, Assistant Administrator

National Oceanographic Data Center
USER SERVICES

Additional copies of this publication, as well as information about NODC data holdings, products, and services, are available on request directly from the NODC. NODC information and data are also available over the Internet through the NODC World Wide Web and Gopher sites.

National Oceanographic Data Center
User Services Branch
NOAA/NESDIS E/OC1
SSMC3, 4th Floor
1315 East-West Highway
Silver Spring, MD 20910-3282

Telephone: (301) 713-3277

Fax: (301) 713-3302

E-mail: services@nodc.noaa.gov

NODC World Wide Web site: http://www.nodc.noaa.gov/

NODC Gopher site: gopher.nodc.noaa.gov

Contents

Acknowledgments

The results described in this atlas supplement would not have been possible without the continued dedication of the people in the COADS Project (Slutz *et al.* 1985; Woodruff *et al.* 1987, 1993) and the perpetual efforts of the observers on the many ships of the Voluntary Observing Fleet. We are particularly grateful to Steven Worley, who cheerfully assisted us with the new data release. Special thanks go to Steven Carson, Richard Greatbatch, and Joseph Umoh for reviewing the manuscript. The calculations reported here were conducted at the University of Wisconsin-Milwaukee (UWM) Department of Geosciences. The support of the UWM Geosciences Faculty is greatly appreciated. This research has been supported by NSF grant ATM 9310959 (Tsonis/CCYM) and by NOAA's Climate and Global Change Program (SL/CCYM). A. da Silva is supported by NASA's EOS Interdisciplinary Science Program. The data sets and products represented by this atlas are for distribution internationally, without restriction.

Atlas of Surface Marine Data 1994 Supplement A: Anomalies of Directly Observed Quantities and Surface Marine Fluxes for 1990–1993

CHRISTINE C. YOUNG-MOLLING
Department of Geosciences, University of Wisconsin–Milwaukee
ARLINDO M. DA SILVA
Data Assimilation Office, NASA/Goddard Space Flight Center
AND
SYDNEY LEVITUS
NOAA/National Oceanographic Data Center

Abstract

This atlas supplement presents objectively analyzed fields of surface marine anomalies of selected observed quantities and fluxes of heat, momentum, and fresh water. These fields are based on the 1945–1989 climatology presented in Volumes 1–5 of this atlas series. Anomaly fields are derived from individual observations in the Comprehensive Ocean-Atmosphere Data Set (COADS) Release 1a from January 1990 to December 1993 and are analyzed on a 1-degree by 1-degree global grid. Corrections have been made to reduce wind speed bias associated with an erroneous Beaufort equivalent scale, to quality control night-time fractional cloud cover observations according to the brightness of the sky, and to assign clear weather to certain Present Weather observations recorded as missing. This supplement presents seasonal plots of observation density and anomalies for the years 1990 through 1993, along with the 1945-89 climatology for each quantity.

1 Introduction

The compilation of the Comprehensive Ocean-Atmosphere Data Set (COADS) as documented by Slutz *et al.* (1985) and Woodruff *et al.* (1987, 1993) has provided climate researchers with the most complete record of surface marine climate to date. The availability of this data set has contributed significantly to advancing our understanding of the atmosphere-ocean climate system. In addition to observational studies based on COADS, atmospheric and oceanic modelers have relied on this data set for boundary conditions in long-term integrations of atmospheric and oceanic circulation models.

One of the main contributions of the COADS project was to unify several historical data sets in a single, consistent format, and to subject the reports to the same quality control procedure. This homogenized data set is available in two forms: as monthly mean summaries in 2- by 2-degree boxes over the global oceans, and as raw individual observations. Due to the massive number of individual reports, the majority of researchers have used the monthly mean summaries.

In an attempt to extend and improve the oceanic fluxes in COADS, a collaborative project between the Department of Geosciences of the University of Wisconsin-Milwaukee (UWM) and the NOAA National Oceanographic Data Center was initiated. The main goal of this project was to produce high resolution (1-degree by 1-degree), stability dependent heat and momentum fluxes, as well as evaporation, precipitation and radiational fluxes which were absent from the COADS monthly mean summaries. In addition to improved resolution and boundary layer parameterizations, a new scientific Beaufort equivalent scale was developed which reduces wind speed bias and artificial wind speed trends in the post World War II pe-

riod. These results, based on COADS Release 1 and an interim release covering 1980-89 were published in *Atlas of Surface Marine Data 1994* (da Silva *et al.* 1994). The data associated with that atlas series will be henceforth referred to as the UWM/COADS data set.

Recently, COADS Release 1a (COADS1a) became available (Woodruff *et al.* 1993). This release, covering 1980 through 1992, with an update for 1993, includes more data sources in the 1980's, more detailed metadata, and a wider choice of quality control options. An immediate concern, before a reanalysis was attempted, was to use this data to extend the UWM/COADS data set through 1993. In this light, we have used the methods of da Silva *et al.* (1994) on COADS1a to compute anomalies of selected quantities in the UWM/COADS data set only for the years 1990–1993. We wish to emphasize that the new data from the 1980's was not used to update our 1945-89 climatology nor the anomalies in the 1980's (see sections 3 and 4 for discussions of flaws in the previous analysis, specifically the 1980's). It is our intention to compute a full reanalysis in the future, including all new data available.

Our 1990-93 extension to the UWM/COADS data set (henceforth referred to as the UWM/COADS Extended data set) is available in the form of raw monthly means, standard deviations, and number of observations in 1- by 1-degree boxes over the global oceans, from 1990 to 1993. These raw data are made available along with the raw 1945-89 data for those users wishing to perform their own objective analysis. In addition, the monthly mean fields have been objectively analyzed with the same successive correction scheme used in da Silva *et al.* (1994). As with the UWM/COADS data set, it is important to note that although the analyzed fields are given with a 1-degree grid spacing, only wavelengths greater than about 770 km remain due to the smoothing effects of the analysis.

In this atlas supplement we present objectively analyzed seasonal mean anomalies along with climatology and observation density. In order to conserve space, we show seasonally averaged anomalies computed from the monthly anomalies. This volume documents the anomaly structure of the directly observed quantities and selected heat, momentum, and fresh water fluxes for the period 1990–1993. The seasonal climatology is the same 1945-89 climatology shown in da Silva *et al.* (1994). The anomalies shown are based on the analyzed difference from this 1945–89 climatology.

Readers of da Silva *et al.* (1994) will note that much of the documentation presented in this supplement is identical to that in Volume 1. We repeat this material in order to give context to the corrections and clarifications to Volume 1 and to the more complete discussions of subjects such as the calculation of constrained heat flux anomalies.

2 Overview of data products

The UWM/COADS Extended data set is a collection of global $1^\circ \times 1^\circ$ raw and analyzed gridded fields covering the period from January 1990 to December 1993. These fields have been derived primarily from individual observations in COADS Release 1a (Woodruff *et al.* 1993), with the same corrections as described in da Silva *et al.* (1994). We also implement the same quality control procedure as used in da Silva *et al.* (1994) in which a more stringent criterion is used over regions climatologically covered by sea ice.

The data are stored using Unidata's network Common Data Format (netCDF) described in Rew *et al.* (1993). NetCDF is self-describing and system-independent software for storing scientific data and is currently available for most Unix workstations, supercomputers and personal computers. A description of the UWM/COADS Extended data formats, and FORTRAN subroutines needed to read the data can be found in section 12. FORTRAN access software and examples of how to read the data are included in the data distribution.

The objectively analyzed anomaly files are listed in Table 1. The companion raw (unanalyzed) monthly mean files appear in Table 2.

3 Data source and COADS quality control

The primary data source for this study is Release 1a of COADS which covers the period 1980–1992 (Woodruff *et al.* 1993) with an update to 1993 (recently made available). Release 1a adds more observations to the interim data base (1980's) used in da Silva *et al.* (1994). In all years of the set, there exists a more complete array of information for each observation. This improved data base, which was not available in time for our first atlas, is used in the 1990-93 extension to our analyses.

As described below, our detailed calculations require the consideration of individual ship reports. One product of COADS Release 1A is the *Long Marine Reports—Fixed* format (LMRF) and contains individual reports of surface marine and atmospheric observations from merchant vessels, research vessels, buoys, platforms, rigs, etc. (Woodruff *et al.* 1987). Among the quantities available in each report in LMRF are the following:

Table 1: List of objectively analyzed quantities in the UWM/COADS Extended data set, along with netCDF file name and units. Each file contains 48 monthly mean anomaly grids from January/90 to December/93. The size of each file (with the exception of `icemask.nc`) is approximately 4 Megabytes.

Directly Observed Quantities		
File Name	Units	Description
cloud.nc2	%/100.	fractional cloudiness
q.nc2	g/kg	specific humidity
sat.nc2	C	air temperature at measurement height
slp.nc2	hPa	sea level air pressure
sst.nc2	C	sea surface temperature
u3.nc2	m/s	zonal wind speed
v3.nc2	m/s	meridional wind speed
w3.nc2	m/s	scalar wind speed
Heat and Momentum Fluxes		
ac.nc2	W/m^2	short wave cloudiness sensitivity parameter
achi.nc2	W/m^2	long wave Chi sensitivity parameter
ae.nc2	hPa	long wave vapor pressure sensitivity parameter
latent3.nc2	W/m^2	latent heat flux
longrad.nc2	W/m^2	net long wave radiation
netheat.nc2	W/m^2	constrained net heat flux
sensib3.nc2	W/m^2	sensible heat flux
shortrad.nc2	W/m^2	net short wave radiation
taux3.nc2	N/m^2	zonal wind stress
tauy3.nc2	N/m^2	meridional wind stress
Fresh Water Fluxes		
eminusp.nc2	mm/(3 hours)	constrained evap. minus precip. rate
evaprate.nc2	mm/(3 hours)	evaporation rate
precip.nc2	mm/(3 hours)	precipitation rate
Miscellaneous Derived Quantities		
airdens.nc2	kg/m^3	sea level air density
qs_qa.nc2	g/kg	sea minus air specific humidity
sst_sat.nc2	C	sea minus air temperature
vappress.nc2	hPa	vapor pressure
Other (about 1 Mb each)		
icemask.nc	(none)	ice masks (Alexander and Mobley 1976)

Table 2: List of raw (unanalyzed) quantities in the UWM/COADS Extended data set, along with netCDF file names and units. For each quantity, there are 4 files: one for each of the years from 1990 to 1993. Each file contains monthly mean data for each month. Files for the years 1945 through 1989 and a 1945–89 climatological file are also available in the same set. Each annual file contains monthly means, standard deviations and number of observations for each calendar month. In the file names below, *yy* stands for 2 digits denoting the year. For example, `sst_91.nc` is the file with sea surface temperature data for 1991. File sizes are variable.

Directly Observed Quantities		
File Name	Units	Description
cld_*yy*.nc	%/100.	fractional cloudiness
q_*yy*.nc	g/kg	specific humidity
sat_*yy*.nc	C	air temperature at measurement height
slp_*yy*.nc	hPa	sea level pressure
sst_*yy*.nc	C	sea surface temperature
u3_*yy*.nc	m/s	zonal wind speed
v3_*yy*.nc	m/s	meridional wind speed
w3_*yy*.nc	m/s	scalar wind speed
Heat and Momentum Fluxes		
achi_*yy*.nc	W/m^2	long wave Chi sensitivity coefficient
ae_*yy*.nc	W/m^2	long wave vapor pressure sensitivity coefficient
latn_*yy*.nc	W/m^2	latent heat flux
long_*yy*.nc	W/m^2	net long wave radiation
sens_*yy*.nc	W/m^2	sensible heat flux
taux_*yy*.nc	N/m^2	zonal wind stress
tauy_*yy*.nc	N/m^2	meridional wind stress
Fresh Water Fluxes		
evap_*yy*.nc	mm/(3 hours)	evaporation rate
prcp_*yy*.nc	mm/(3 hours)	precipitation rate
Miscellaneous Derived Quantities		
rho_*yy*.nc	kg/m^3	sea level air density
dq_*yy*.nc	g/kg	sea minus air specific humidity
dt_*yy*.nc	C	sst minus sat
e_*yy*.nc	hPa	vapor pressure

- wind speed and direction
- air temperature
- sea surface temperature
- sea level pressure
- dew point temperature
- cloudiness
- present weather

along with measurement method flags and quality control indicators. The interested reader should consult the original COADS documentation (Slutz *et al.* 1985) and supplemental information regarding Release 1a (Woodruff *et al.* 1993) for a detailed description of available information and the quality control procedure. Note that on ships, the wind, dew point and sea level pressure are not directly observed but rather calculated by ship personnel. When measured, the reported wind speed and direction are computed from the anemometer reading, taking into consideration the ship velocity—a procedure that often introduces errors. Dew point temperature is computed from the measured dry and wet bulb temperatures. Sea level pressure is computed from the measured pressure with a height correction to reduce it to sea level. WMO Publication No. 47 (e.g., WMO 1990), available yearly since 1955 (in digital form since 1973), lists all the Ships of the Voluntary Observing Fleet along with the ship instrumentation and routes. Kent and Taylor (1991) describes in some detail observing practice by ships of the Voluntary Observing Fleet and the instruments they used during the VSOP-NA project (May/88 to September/90).

Quality control in COADS is implemented by means of a multiple step statistical procedure to identify "outliers." The limits used to identify outliers in Release 1a are taken from the 1950–1979 limits generated for Release 1 (Slutz *et al.* 1985). These limits were calculated as follows: The first step is to generate *Decadal Summary Untrimmed Limits* for six variables: sea surface temperature, air temperature, air pressure, zonal wind, meridional wind, and humidity. Sextiles are calculated for each variable in every 2° box for each decade and month. Next, the third sextile (the median), the third minus first sextile difference, and the fifth minus third sextile difference for each box are averaged with those in boxes adjacent in latitude, longitude and decade (a 27-box "cube"). Averaging is done for three non-overlapping periods (1854–1909, 1910–1949, 1950–79) in an attempt to separate possible climatic epochs or observational discontinuities. Further smoothing is done for the resulting 216 sets of sextile triplets (6 variables $\times$ 3 periods $\times$ 12 months). The result is three sets of smoothed lower and upper limits (σ_1, σ_5) around the smoothed mean ($\overline{x}$) for each variable, month, and 2° box. These means and limits are used to create trimming bounds for the variables. A detailed description of the statistical process can be found in Slutz *et al.* (1985), section C. Trimming flags for sea surface temperature, air temperature, humidity, wind and sea level pressure are included in LMRF for each observation. Note that trimming does not take into account different methods of observation within the same period, nor were bias corrections applied when the limits were generated.

We have used the COADS1a/LMRF flags to perform quality control on the data used as input to our 1-degree statistics and analysis. Table 3 summarizes the possible values of the quality control flags in COADS1a/LMRF. Although the more relaxed 4.5σ limits are available in LMRF, we use the same methods as in da Silva *et al.* (1994) in order to produce a consistent product. In general, then, an observation is rejected if it differs from the smoothed median by more than 3.5 "standard deviations" (flag value greater than 3) or the smoothed limits are missing or not applicable (flag value equal to 11-15). However, over the regions climatologically covered by sea ice, this trimming procedure still yields very noisy fields. This is due to the irregular coverage of observations in ice-covered regions in both area and time. In an effort to generate smoother fields in regions where sea ice is common, a more stringent trimming criterion is used. If an observation occurs in a climatologically ice-covered region, the observation is trimmed if it differs from the smoothed median by more than 2.8 "standard deviations" (flag value greater than 1).

Usage of the 3.5σ trimming limits, as opposed to the more relaxed 4.5σ limits can introduce error into the analysis by eliminating extremes of climate, such as a strong ENSO. Wolter (1992) discusses the effects of the 3.5σ trimming on the 1982–83 El Niño, in which up to 35% of SSTs in the region were trimmed. On the other hand, using the 4.5σ trimming limits would allow more spurious observations to be retained. In an effort to produce an analysis consistent with da Silva *et al.* (1994), we chose to retain the 3.5σ trimming limits for the present. The user should be aware that extreme events will subsequently be eliminated or show diminished intensity in the analyses presented here and in da Silva *et al.* (1994). In the future, however, it is our intent to use the less strict 4.5σ trimming limits as data allow.

Table 3: Quality control flags in COADS1a/LMRF, where x is an individual observation of the variable under scrutiny, $\overline{x}$ is the smoothed median and σ_1 and σ_5 are the smoothed lower and upper median deviation. See text for details.

Flag Value	Trimming Limits	Trim?
1	$\overline{x} - 2.8\sigma_1 \leq x \leq \overline{x} + 2.8\sigma_5$	no
2	$\overline{x} - 3.5\sigma_1 \leq x < \overline{x} - 2.8\sigma_1$	if obs. over ice
3	$\overline{x} + 2.8\sigma_5 < x \leq \overline{x} + 3.5\sigma_5$	if obs. over ice
4	$\overline{x} - 4.5\sigma_1 \leq x < \overline{x} - 3.5\sigma_1$	yes
5	$\overline{x} + 3.5\sigma_5 < x \leq \overline{x} + 4.5\sigma_5$	yes
6	$x < \overline{x} - 4.5\sigma_1$	yes
7	$x > \overline{x} + 4.5\sigma_5$	yes
11	limits missing; MEDS data correct	yes
12	limits missing	yes
13	landlocked 2-degree box	yes
14	data outside physical limits	yes
15	data missing or not computable	yes

4 Known biases in COADS

The purpose of this section is to discuss some of the known biases and other problems in COADS surface marine reports. In subsequent sections, we describe our bias correction schemes for wind speed, cloudiness, and Present Weather.

4.1 Sea surface temperature

Biases in sea surface temperature are associated with different methods of measurements (basically *bucket* and *intake*), which also respond in different ways to atmospheric conditions. On average, measurement with an uninsulated canvas bucket introduces an error of about 0.5°C due to evaporative cooling. Folland and Hsiung (1986) [see also Folland 1991] have developed a physical model for a typical canvas bucket that predicts the amount of evaporative cooling as a function of the atmospheric conditions and exposure time of the bucket. This model has been used effectively to correct the bias in bucket observations (Farmer *et al.* 1989). However, Farmer *et al.* (1989) have used the bucket correction method only for pre-World War II observations. Observations after that time were assumed to be almost exclusively measured by intake or by insulated buckets. This is consistent with the fact that the largest discontinuity in SST due to changes in measurement procedure (approximately one-half degree rise in SST around 1940) took place prior to our analysis period (Bottomley *et al.* 1990, Kushnir 1994).

Recently, the *Voluntary Observing Ships Special Observing Program for the North Atlantic* (VSOP-NA, Kent *et al.* 1993a) has found that observations of SST from insulated buckets and hull contact sensors are reliable. A constant bias of 0.35°C was found in observations from ships' intake thermometers compared to those measured by bucket.

The unreliability of the bucket/intake indicator in COADS and the lack of reliable information about the kind of bucket used make this correction impractical from individual observations. Therefore, we do not include a sea surface temperature correction in this version of our calculations.

4.2 Air temperature

Systematic errors in air temperature are believed to be caused primarily by the heating of the ship superstructure, causing biases of 0.4°–0.8°C in some regions of the tropics (Isemer and Hasse 1987 and references within). In view of this, some authors (Folland *et al.* 1984) have preferred to discard daytime observations. Although night time observations may be adequate to study long term trends in air temperature, we feel that it significantly reduces the number of observations and tends to bias the data toward a generally lower night time temperature.

Kent *et al.* (1993b) devised a method of correction for daytime surface air temperature based on wind speed and the incoming short wave radiation. Preliminary calculations by these authors indicate correcting daytime air temperature results in increases in mean sensible and latent heat fluxes of 3.3 and 1.0 W/m^2, respectively, in the North Atlantic Ocean (Kent and Taylor 1995). We intend to include such a correction in future versions of our data set, but to be consistent with da Silva *et al.* (1994), we do not

do so at this time.

4.3 Dew point temperature

Biases in dew point temperature are generally associated with contamination of the wet bulb thermometer by salt or insufficient moistening of the wet bulb thermometer wick. These instrumentation problems lead to a systematically higher value of the specific humidity. On average, the dew point temperature is biased about 0.5°C (Isemer and Hasse 1987 and references within). Since this bias is due mainly to human errors for which no record is available, it is very difficult to devise a correction.

Kent *et al.* (1993a) have found that wet bulb temperatures measured by psychrometers were on average lower than those reported from ships using screens. By considering the many factors that might have contributed to this discrepancy, Kent *et al.* (1993a) concluded that psychrometer observations were more reliable and a simple regression equation was devised to correct screen-measured dew point temperatures. Because of inadequate metadata in COADS (there is no indicator of the method of measurement for dew point temperature) this correction could not be implemented at the present time.

Recently, the compilers of COADS have identified errors in some dew point temperature reports from January through May of 1988 and from May through November of 1992. These erroneous dew point reports are found in deck 927, which contains U. S.–recruited ship logbook data digitized by the National Climatic Data Center. The 1988 bias seems to have been caused by the substitution of wet bulb temperature for dew point, from which wet bulb temperature was recalculated. This resulted in reported dew points too large by several tenths of a degree Celsius. There also appears to be an unreasonably large number of observations with saturated conditions. The error in deck 927 for 1992 involved dew point temperatures that averaged too high by about 1 degree Celsius. Deck 927 constitutes, globally, about 20% of dew point observations during these months. The majority of deck 927 observations lie in the North Atlantic and North Pacific. The compilers of COADS have estimated the bias in dew point results in a mean global bias in relative humidity of +1%. Due to the location of the observations, the bias is most pronounced in the North Pacific, and to a lesser extent in the North Atlantic. Elsewhere, biases in humidity should be small.

The compilers of COADS have recently attempted to correct the dew point errors found in deck 927 (S. Woodruff, personal communication). These corrected data, however, were not available in time for our calculations of 1988 anomalies. The corrected 1992 data *were* used for the calculation of the Extended anomalies. Users should be aware that all humidity quantities and derived quantities using humidity (e.g. latent heat flux) presented in da Silva *et al.* (1994) are biased during the first five months of 1988. Such biases are highest in the North Pacific, smaller in the North Atlantic, and likely small elsewhere. The impact on the long-term (1945-89) climatology is expected to be small. There should be no bias in humidity-dependent quantities in 1992.

4.4 Wind speed

Because wind is a key parameter for the determination of the air-sea fluxes at the ocean surface, a great deal of effort has been devoted to sort out the problems with ship winds. Wind speeds reported by ships are either directly measured with anemometers or are estimated from the *sea state*. Instrumentation problems with anemometers are believed (or better, assumed) to be non-systematic and are expected to cancel out when spatial/temporal averages are taken. Estimated winds are somewhat subjective and depend on the skill of the observer. But even when a correct identification of the sea state is made, it still needs to be converted to wind speed through a Beaufort equivalent scale.

Since 1946, a Beaufort equivalent scale developed by Simpson (1906), combined with a well defined sea state devised by Petersen (1927), has been used by meteorological weather services (Roll 1965; Isemer and Hasse 1991). This scale is known as Code 1100 and is sometimes referred to as the *old* WMO scale. It is now widely accepted that the old WMO Beaufort equivalent scale results in systematic biases when compared to anemometer measured winds. There are a few alternative Beaufort equivalent scales (WMO 1970; Cardone 1969; Kaufeld 1981), and they all suggest that the old WMO scale underestimates the winds for Beaufort numbers less than about 6 and overestimates winds for Beaufort numbers greater than about 6. As pointed out by Isemer and Hasse (1991), this systematic error causes climatological wind speeds to be underestimated, and climatological wind speed standard deviation to be overestimated in the North Atlantic Ocean. Concerning long term variability, Cardone *et al.* (1990) have shown that a Beaufort scale correction, ship anemometer height adjustment, and stability correction strongly reduce artificial trends in wind speed, and drastically improve the agreement between measured and estimated winds.

Finally, most definitions of transfer coefficients are calibrated to work with winds from a reference level of 10 m above the ocean surface. Cardone *et al.* (1990) suggest that the average ship anemometer height is

actually 20 m. Kent *et al.* (1993a) shows that during VSOP-NA a typical anemometer height is in the range 15–20 m, but on modern container ships the anemometer heights are about 30 m. A common approximation is to take the 20 m wind in place of the required 10 m. Since virtually all ship anemometers are higher than 10 m, this approximation introduces a systematic error. Isemer and Hasse (1991) estimated that the 10 m wind speed is on average 93% of the wind speed at 20 m. Calculations by the authors show that for light winds under stable conditions, the surface layer has strong shear and the wind at 10 m can be as low as 40% of the wind speed at 20 m. This result suggests that a careful stability dependent correction is warranted.

The ship type indicator, however, is often incorrect or missing in COADS/CMR-5. This is particularly significant in the 1980's when large numbers of drifting buoys were placed in the southern oceans. We have found that nearly all buoy observations in the COADS/CMR-5 1980's interim product are not identified correctly. The result is that a wind observation measured at 5 m is treated as if it were taken at 20 m. Winds in regions sampled mainly by drifting buoys will be biased toward lower values. This problem has apparently been fixed in COADS Release 1a. Although a few errors still remain, the majority of buoys and ships are correctly identified in COADS 1a, yielding a lower bias in the Extended data set wind analysis.

4.5 Cloudiness

Cloudiness observations on board ships are estimated visually. In very low light conditions, observers often miss high level clouds. This tends to bias night time cloudiness toward a smaller fraction of cloud cover (Sverdrup 1933; Riehl 1947; Schneider *et al.* 1989). It is possible to reduce this bias by rejecting cloudiness observations taken during dark sky conditions. These conditions can be determined by the altitude of the sun and the phase and altitude of the moon.

Another bias in cloudiness results from *sky obscured* observations. A sky obscured observation means that clouds are not visible due to smoke, blowing dust, fog, snow, or some other phenomenon. This condition represents over 6% of the observations in the period 1952–81 (Hahn *et al.* 1992). Sky obscured observations are coded separately and cannot be assigned one cloudiness value, as not all sky obscuring phenomena are associated with clouds. But if none of these observations are included, heavy fog– or snow–associated cloudiness would be eliminated and the cloudiness would be biased toward a lower value. To eliminate this bias, the *present weather* code can be checked for each sky obscured observation (see section 5.2).

4.6 Present Weather

A code number signifying the present weather conditions is recorded as a standard part of a ship's observation. This code can be used as a proxy for precipitation, as precipitation is rarely measured on ships. Beginning in the early 1980's, the WMO no longer required Present Weather (PW) to be recorded for clear weather observations (S. Woodruff, personal communication). Previously, in clear weather episodes, the observer entered a code number indicating there was no weather observed. When the observations in the 1980's were entered into the COADS interim product, the missing clear weather observations were given the missing flag, just as truly missing PW observations were. Using such observations as they are recorded in COADS would eliminate most if not all clear weather (rainless and snowless) reports. If few clear weather reports are available, the result would be a wet bias in the 1980's precipitation. This effect would be particularly evident in climatologically clear areas, such as below the subtropical highs. In the course of this investigation, it was discovered that there is indeed a sharp increase in the number of missing PW observations beginning in 1982. Beginning Nov 2, 1994, the WMO reversed its requirements so that clear weather was again coded differently from missing weather observations (Baron 1994).

5 Bias corrections

This section documents our bias correction procedures for wind speed, cloudiness and Present Weather. No additional correction is applied to the other directly observed quantities.

5.1 Wind speed

Several scientific Beaufort equivalent scales have been developed to correct WMO Code 1100 (WMO 1970; Cardone 1969; Kaufeld 1981). Data used to generate these scales have mainly been limited to the North Atlantic and North Pacific oceans. In Vol. 1 of da Silva *et al.* (1994), we have examined the performance of several Beaufort equivalent scales by comparing monthly mean estimated and anemometer measured wind speeds in the Northern Hemisphere oceans. The analysis was conducted for the two decades from 1970 to 1989, a period which has a good mix of estimated and measured wind observations. Taking the wind speed measurement indicator

(flag WI in COADS/CMR-5) at face value, all available Beaufort equivalent scales showed climatological biases in at least some part of the wind speed range. This fact prompted the authors to empirically derive a Beaufort equivalent scale which attempts to reduce the climatological wind speed bias in COADS. After much experimentation we derived a wind speed correction of the form

$$W_{\text{new}} = x_1 W_{\text{old}} + x_2 \sqrt{W_{\text{old}}} \qquad (1)$$

where W_{old} is the WMO Code 1100 speed of the estimated wind and W_{new} is the corrected wind speed. We find that this functional form fits the relationship between measured and estimated winds reasonably well and can also accurately express the other alternative Beaufort equivalent scales. In particular, it is shown in Vol. 1 of da Silva *et al.* (1994) that this method also produces consistent measured/estimated wind speed standard deviations. It is important to note that the formula above is valid only for individual observations and should not be used to correct monthly mean quantities. The factors x_1 and x_2 were determined for several averaging periods (annual and monthly means), and for several regions of the world oceans by means of a least squares fit. After examining the seasonal/regional sensitivity of the correction, it was concluded that a single set of parameters x_1,x_2 based on Northern Hemisphere January data was sufficient, as the maximum error in measured/estimated regression slopes was only 5%. Errors in regression slopes were as large as 7% for the annual-based scale and 8% for the July-based scale. The chosen values are

$$x_1 = 0.7870, \qquad x_2 = 0.9547. \qquad (2)$$

This choice of parameters gives mean measured/estimated wind speeds with regression slopes within 5% of 1 and standard deviations less than 0.4 m/s (see Vol. 1 of da Silva *et al.* [1994]). The parameters also produce a good relationship between measured and estimated pseudo stress (W^2): January climatological pseudo stress has a regression slope of 0.98 and a bias of -0.08 m^2/s^2, and a regression slope of 0.99 and a bias of -0.11 m^2/s^2 for July. Table 4 lists equivalent wind speed for WMO Code 1100 and our new Beaufort equivalent scale. It is important to realize that this new Beaufort equivalent scale produces wind speeds valid at a 20 meter reference level. Whenever 10 meter wind speed is required, the proper conversion from 20 meters should be performed using stability dependent surface layer similarity theory. For additional details on this wind speed correction procedure, the reader is referred to Vol. 1 of da Silva *et al.* (1994).

Table 4: WMO Code 1100 and the revised Beaufort equivalent scale. The equivalent wind speed is given in m/s.

Beaufort Number	**Equivalent Wind Speed** Code 1100	Revised Scale
0	0	0
1	0.8	1.5
2	2.4	3.4
3	4.3	5.4
4	6.7	7.7
5	9.4	10.4
6	12.3	13.0
7	15.5	16.0
8	18.9	19.0
9	22.6	22.4
10	26.4	25.7
11	30.6	29.3
12	34.9	33.1

5.2 Cloudiness

To reduce the bias caused by the underestimation of cloudiness in low light levels, we reject all observations taken under dark skies. A cloudiness observation is considered acceptable only if one of the following *bright sky* conditions apply (Hahn *et al.* 1992):

$$a_s \geq -8^\circ \qquad (3)$$

or

$$P_m \sin a_m \geq 0.2 \qquad (4)$$

where a_s and a_m are the altitudes of the sun and moon, respectively. The phase of the moon P_m can vary between 0 (new moon) and 1 (full moon). Equations to determine the altitude of the sun and altitude and phase of the moon can be found in Volume 1 of da Silva *et al.* (1994) and in the *Astronomical Almanac* (U.S. Government Printing Office 1990).

We also use the treatment of the *sky obscured* observation after Hahn *et al.* (1992). Some of the phenomena which obscure the sky, such as fog, are associated with overcast skies. If the Present Weather code indicates that the sky is obscured due to rain, snow, fog, or any other cloud-induced phenomenon, we consider the fractional cloudiness for the *sky obscured* observation to be 1 and include it as a valid observation.

5.3 Present Weather

From 1982 through late 1994, clear weather observations were often recorded with a missing Present

Weather indicator. This practice has an adverse effect on our precipitation estimates as it introduces a *wet* bias. In order to circumvent this problem we have devised a method of correction which links PW with cloudiness. It is assumed that any observer making a cloud cover observation will also make a PW observation, and vice versa. Therefore, when encountering a missing observation from 1982 through 1993, cloudiness is checked. If cloudiness is missing, PW is assumed to be missing, and is not included in the precipitation calculation. If a cloudiness observation is present, however, it is assumed that there was a PW observation and that the weather was clear. The observation is used as a clear weather observation in the precipitation calculation. As a test, PW and cloudiness observations were checked prior to 1982. Cases in which a cloudiness observation was present but the PW observation was missing were very rare. We are confident, therefore, that our method of correcting PW is reliable.

6 Parameterizations

This section describes the parameterizations used in the production of the data sets. The thermodynamic quantities described below (e.g., specific humidity, vapor pressure, etc.) are computed as in COADS (Slutz *et al.* 1985) using the software documented in Schlatter *et al.* (1981).

Symbols

A_a	water vapor and O_3 coefficient (unitless)
c	fractional cloud cover (unitless)
c_p^{air}	specific heat of air constant (J $K^{-1}kg^{-1}$)
C_D	drag coefficient (unitless)
C_{DN}	neutral drag coefficient (unitless)
C_E	Dalton number (unitless)
C_{EN}	neutral Dalton number (unitless)
C_T	Stanton number (unitless)
C_{TN}	neutral Stanton number (unitless)
e	atmospheric vapor pressure (mb or Pa)
E	evaporation rate (m s^{-1} or mm/(3hr))
L	Monin-Obukhov length (m)
L_E	latent heat of evaporation (J kg^{-1}), $L_E(T_a) = (2494 - 2.2 * T_a) * 1000$, T_a in Celsius.
p	sea level pressure (mb or Pa)
P	precipitation rate (m s^{-1} or mm/(3hr))
q	specific humidity (g kg^{-1})
q_s	saturation specific humidity at the surface (g kg^{-1}), $q_s = 0.98 q_{satur}(T_s)$
Q_0	incident radiation at the top of the atmosphere (W m^{-2})
Q_L	latent heat flux (W m^{-2})
Q_S	sensible heat flux (W m^{-2})
R	gas constant for dry air (J $K^{-1}kg^{-1}$)
R_{clear}	incident short wave radiation under clear skies (W m^{-2})
R_{diff}	diffuse component of short wave radiation (W m^{-2})
R_{dir}	direct component of short wave radiation (W m^{-2})
R_L	long wave radiation (W m^{-2})
R_S	short wave radiation (W m^{-2})
T_a	surface air temperature (° C or K)
T_s	sea surface temperature (° C or K)
u	zonal wind speed (m s^{-1})
v	meridional wind speed (m s^{-1})
W	wind speed (m s^{-1})
z	zenith angle (degrees)
Z	height above sea surface (m)
α	ocean surface albedo (unitless)
β	solar noon altitude (degrees)
ϵ	emissivity of the ocean (0.97) (unitless)
θ	potential temperature ($\theta \approx T + \gamma Z$, $\gamma = 0.01°\text{K/m}$) (K)
θ_a	potential temperature of air (Z = measurement height) (K)
θ_s	sea surface potential temperature ($Z = 0$) (K)
ρ	air density (kg m^{-3})
ρ_0	fresh water density as a function of temperature (kg m^{-3})
σ	Stefan-Boltzmann constant (W $m^{-2}K^{-4}$)
τ	wind stress (N m^{-2})
τ_a	atmospheric transmission coefficient (unitless)
χ	cloud cover coefficient (unitless)

6.1 Wind stress

The zonal and meridional components of the wind stress are defined, respectively, by

$$\tau_x = \rho C_D W u \quad (5)$$

$$\tau_y = \rho C_D W v . \quad (6)$$

The air density, including the effect of moisture, is given by

$$\rho = \frac{p}{RT_a(1 + 0.61q)} . \quad (7)$$

The drag coefficient is parameterized as $C_D = f(Z/L)C_{DN}$, where C_{DN} is the neutral drag coefficient and $f(Z/L)$ is a stability correction depending on the Monin-Obukhov length. The neutral drag coefficient formulation is based on Large and Pond (1981) modified for low wind speeds as in Trenberth

et al. (1990):

$$C_{DN} = \begin{cases} 2.18 \times 10^{-3} \text{ for } W \leq 1\text{m/s} \\ (0.62 + 1.56/W) \times 10^{-3} \text{ for } 1 < W < 3\text{m/s} \\ 1.14 \times 10^{-3} \text{ for } 3 \leq W < 10\text{m/s} \\ (0.49 + 0.065W) \times 10^{-3} \text{ for } W \geq 10\text{m/s} \end{cases}$$

Details of the surface layer formulation are given in Volume 1 of da Silva *et al.* (1994). The stability dependent drag coefficient C_D is a function of several surface marine variables:

$$C_D = C_D(W, T_a, \Delta\theta, \Delta q) \tag{8}$$

where

$$\Delta\theta = \theta_s - \theta_a \tag{9}$$

$$\Delta q = q_s - q \tag{10}$$

where θ_s is merely the temperature of the sea surface ($Z = 0$). Analysis of the functional form of C_D indicates that for the observed range of parameters, the dependence of C_D on wind speed is the most important; the thermodynamic quantities only enter through the boundary layer stability correction.

As seen from the expressions above, the computation of wind stress requires simultaneous observations of the following quantities: u, v, p, T_a, T_s and q. In practice it is difficult to obtain complete ship reports, and cases in which one or more of the above quantities is missing are very common (Cardone *et al.* 1990). In order to circumvent the problem, wind stress is computed for all ship reports in which the wind data are available (neither missing nor trimmed by the quality control procedure). If the thermodynamic quantities are available, then they are used to compute C_D. Otherwise the missing thermodynamic quantities are *filled in* with the analyzed monthly mean for that particular month. The accuracy of using monthly means in the calculation of this stability correction is discussed by Esbensen and Reynolds (1981).

Also note that the formulation for wind stress neglects the effects of the ocean's surface current. Over much of the ocean, wind speed is one or two orders of magnitude greater than the surface current. The surface current can be neglected in such circumstances. In the tropics, however, wind speeds are low and current speeds can be high. Halpern (1988) estimated the uncertainty in zonal wind stress due to the surface current is $\pm 17\%$ in the tropics. Unfortunately, COADS does not include surface current information. However, wind stress calculated from visually estimated winds will include current effects. Wind stress calculated with measured winds will contain error, but the degree of error is mitigated by a ship's tendency to drift with the current (W. Large, personal communication). The wind stress values in this atlas series, therefore, presumably contain only a small degree of uncertainty in the tropics.

6.2 Evaporation, sensible and latent heat fluxes

The bulk formulas for evaporation and sensible and latent heat fluxes are given by

$$E = \frac{\rho}{\rho_0} C_E W \Delta q \tag{11}$$

$$Q_S = \rho c_p^{\text{air}} C_T W \Delta\theta \tag{12}$$

$$Q_L = \rho L_E C_E W \Delta q \tag{13}$$

where Δq is unitless (grams per gram).

The transfer coefficients C_T and C_E are estimated using the Large and Pond (1982) formulation (see Vol. 1 of da Silva *et al.* [1994]), which gives

$$C_T = C_T(W, T_a, \Delta\theta, \Delta q) \tag{14}$$

$$C_E = C_E(W, T_a, \Delta\theta, \Delta q)\,. \tag{15}$$

For reference, the neutral transfer coefficients are given by

$$C_{TN} = \begin{cases} 1.2 \times 10^{-3} & \text{(unstable)} \\ 0.75 \times 10^{-3} & \text{(stable)} \end{cases} \tag{16}$$

$$C_{EN} = 1.2 \times 10^{-3}\,. \tag{17}$$

Like the wind stress calculation, the heat fluxes require a complete ship report for their calculation. The wind stress procedure is modified slightly: sensible (latent) heat fluxes are computed for all those reports in which W and $\Delta\theta$ (Δq) are available. The remaining thermodynamic quantities are *filled in* with the analyzed monthly mean value for that grid point, if not available. Evaporation, however, is calculated only when all required variables are present. Evaporation is converted from units of m/s to mm/(3 hours) in order to match precipitation's units.

6.3 Precipitation

Accurate measurements of precipitation at sea are extremely difficult to take. As a result, precipitation rate is not included in ship reports. However, the type of weather the ship encounters is recorded and can be used as a precipitation proxy.

Precipitation rate is estimated using the method developed by Tucker (1961). The method uses the Present Weather (PW) information of standard ship reports and relates it to precipitation rate according to a regression formula.

The PW is reported at 3 hour intervals (usually less frequently) with the results being coded from 00 to 99. Tucker considers that weather associated with codes 50 to 99 contribute significantly to precipitation. Based on data for 12 stations around the British

Isles, Tucker derived a regression formula which relates precipitation during the 3 hour sampling interval to the amount of light, moderate, or heavy precipitation (x, y, and z respectively). Each PW code is then expressed as a linear combination of x, y, and z as shown in Table 5. Tucker's estimates for these coefficients are $x = 1.85$ mm, $y = 5.66$ mm, and $z = 8.13$ mm per 3 hour period.

Because the PW does not have an adequate range to accommodate the tropics, Dorman and Bourke (1978) derived an additional correction which takes into consideration the local air temperature:

$$P_{\text{corrected}} = P_{\text{Tucker}}(a + bT_a + cT_a^2) . \qquad (18)$$

Dorman and Bourke (1978) give correction coefficients a, b, and c for each month of the year. The coefficients are shown in Table 6. The corrected values for P are used to calculate monthly mean precipitation rate.

The precipitation fields obtained with the formula above showed an unrealistic minimum in Spring when compared to estimates from NMC and NASA/Goddard (Schubert *et al.* 1993) reanalyses, as well as Arkin and Meisner's (1987) GOES Precipitation Index. This abrupt decrease of precipitation in spring is not present in the uncorrected P_{Tucker}, but is introduced, rather, by the correction factor $(a + bT_a + cT_a^2)$. In order to remove this spurious seasonal cycle in precipitation, we have used the annual mean of Dorman and Bourke's (1978) correction factor in our precipitation calculations: the monthly mean correction was calculated from the 12 monthly climatologies of air temperature and averaged to form the annual mean correction. This modification has little effect on the annual mean precipitation and fresh water fluxes into the ocean.

6.4 Net short wave and net long wave radiation

The incoming solar radiation at the top of the atmosphere is computed from the formulas given in *Smithsonian Meteorological Tables* (List 1958), with an attenuation by clouds as in Reed (1977). The formula adopted here is the same as described in Rosati and Miyakoda (1988):

$$R_S = R_{\text{clear}}\,(1 - 0.62c + 0.0019\beta)\,(1 - \alpha) . \qquad (19)$$

The parameter R_{clear}, the incident radiation under clear skies, is composed of direct and diffuse components of short wave radiation:

$$R_{\text{clear}} = R_{\text{dir}} + R_{\text{diff}} . \qquad (20)$$

The direct component of short wave radiation is

$$R_{\text{dir}} = Q_0 \tau_a^{\sec z} \qquad (21)$$

where the atmospheric transmission coefficient $\tau_a = 0.7$, z is the zenith angle of the sun , and Q_0 is the incident radiation at the top of the atmosphere. The diffuse component of net short wave radiation is

$$R_{\text{diff}} = [(1 - A_a)Q_0 - R_{\text{dir}}]/2 \qquad (22)$$

where $A_a = 0.09$ is the absorption due to water vapor and ozone. The solar noon altitude in degrees (β), Q_0, and z are computed from present day astronomy (see Volume 1 of da Silva *et al.* [1994]).

The ocean surface albedo α is taken from Payne (1972). In order to compute monthly means of R_S, results from the formula are averaged for each day of the month, using analyzed monthly means of cloudiness for c.

The net long wave radiation is based on an empirical formula which includes the effect of air-sea temperature difference (e.g., Rosati and Miyakoda 1988)

$$\begin{aligned} R_L &= \epsilon\sigma T_s^4 \left(0.39 - 0.05\sqrt{e}\right)\left(1 - \chi c^2\right) \\ &\quad + 4\epsilon\sigma T_s^3 \left(T_s - T_a\right) . \end{aligned} \qquad (23)$$

The dimensionless cloud coefficient χ is allowed to vary with latitude in order to account for different cloud types (Budyko 1974, Oberhuber 1988). This bulk parameterization is based on a formula originally given by Brunt (1932), later modified to include the term proportional to $T_s - T_a$ which attempts to include the effects of the temperature difference between the surface layer and the lower layer of air (Budyko 1974). Although several authors have adopted the parameterization using T_s^4 and T_s^3 as above (e.g., Simpson and Paulson 1979, Rosati and Miyakoda 1988), others (Bunker 1976, Hsiung 1986, Oberhuber 1988, Isemer *et al.* 1989) have used T_a^4 and T_a^3 instead.

In COADS, on average, sea surface temperature is warmer than air temperature, when considered on an annual, global scale. The usage of T_a in the parameterization of R_L, therefore, would produce a smaller average long wave radiation than does the usage of T_s. Rough comparisons show that, on an annual mean basis, T_a^4 is within 2% of T_s^4 over most of the global ocean, but is 2–5% lower over the far northern oceans (north of about 60° N), the Gulf Stream, the Kuroshio Current, and the southern extent of the Agulhas Current. This would imply that the two different parameterizations of R_L agree to within a few percent over most of the global ocean, with the T_s version producing larger R_L on average. One argument for using the T_s parameterization is that in the case of our COADS analyses, a smaller average long wave radiation would increase the imbalance in the annual net heat flux (see Volume 1, Figure 8).

Table 5: Precipitation rate in terms of x, y, and z for Present Weather codes 50 through 99 (from Tucker 1961): $x = 1.85$ mm/(3 hours), $y = 5.66$ mm/(3 hours), and $z = 8.13$ mm/(3 hours).

PW	0	1	2	3	4	5	6	7	8	9
50	0	$x/2$	$x/2$	x	y	$2y$	$x/2$	$y/2$	$x/2$	$y/2$
60	$x/2$	x	$y/2$	y	$z/2$	z	x	$(y+z)/2$	x	$(y+z)/2$
70	$x/2$	x	$y/2$	y	$z/2$	z	0	0	0	0
80	$x/2$	$y/2$	$z/2$	$x/2$	$(y+z)/4$	$x/2$	$(y+z)/4$	$x/2$	$(y+z)/2$	$x/2$
90	$(y+z)/2$	x	$(y+z)/2$	x	$(y+z)/2$	$(x+y)/2$	$(x+y)/2$	z	0	z

6.5 Air-sea temperature and moisture difference terms

The air-sea difference terms are ΔT and Δq. These are given by

$$\Delta T = T_s - T_a \tag{24}$$

$$\Delta q = q_s - q\,. \tag{25}$$

The saturation specific humidity at the surface, q_s, is calculated based on the sea surface temperature. The value is decreased by 2% to compensate for the lower evaporation rate of salt water: $q_s = 0.98 q_{satur.}(T_s)$. The specific humidity, q, is calculated based on the air temperature and therefore valid at the height of the observation platform. The other humidity terms, relative humidity (rh) and vapor pressure (e) are also valid at the height of the observation platform.

7 Computation of monthly statistics and objective analysis

The raw monthly fields are computed from the individual observations in the following manner:

1. The world oceans are divided into boxes with constant grid spacing in latitude and longitude. The grid we consider here is 1-degree latitude by 1-degree longitude (the same as Levitus [1982] and da Silva *et al.* [1994]).

2. All available (quality controlled) observations are averaged in each box for each month during the 4 year period, and the standard deviation and number of observations recorded. Bias corrections, if applicable, are made to each individual observation before averaging.

The raw monthly mean fields are then objectively analyzed to filter out spatial noise and interpolate to gridpoints where data are missing. The objective analysis scheme used is identical to that used in da Silva *et al.* (1994), which is essentially the same scheme described by Levitus (1982). This is an iterative difference-correction scheme (Cressman 1959) with a weight function developed by Barnes (1964). The procedure can be summarized as follows:

1. Determine a first guess F (see below).

2. Compute the difference between the raw observed data (O) and the first guess (F),

$$Q_{ij} = O_{ij} - F_{ij},$$

at grid point (i, j).

3. Compute the smoothed analysis increments

$$C_{ij} = \frac{\sum_{s=1}^{n} W_s Q_{i_s,j_s}}{\sum_{s=1}^{n} W_s} \tag{26}$$

where W_s is the Barnes weight function: $W_s = \exp(-4r^2\mathcal{R}^{-2})$ for $r \leq \mathcal{R}$ where r is the distance between the sth gridpoint (i_s, j_s) and the analysis gridpoint (i, j). The sum on the RHS is over the region of influence, i.e., those points that are at a distance less than $\mathcal{R}$, the radius of influence.

4. Update the first guess

$$F_{ij} := F_{ij} + C_{ij}\,. \tag{27}$$

5. Apply a 5–point nonlinear median filter to F_{ij} (Beaton and Tukey 1974; Rabiner *et al.* 1975) followed by two passes of a 5–point linear filter (Shapiro 1970). It was found that this combination effectively filters out noise with scales of the mesh-size. The two filters are applied as follows:

   (a) Non-linear. The smoothed value at the grid point (i, j) is simply the *median* value of the nine grid points in the 3 by 3 box centered at the grid point (i, j). The filter is not applied to grid points located over or adjacent to land. The median filter is used to remove noise from the data while preserving sharp gradients (Reynolds 1988; Rabiner *et al.* 1975).

(b) Linear. The smoothed value S_{ij} at grid point (i, j) of a grid G is

$$S_{ij} = G_{ij} + \frac{\alpha}{4}(G_{i-1,j} + G_{i+1,j} + G_{i,j-1} + G_{i,j+1} - 4G_{ij})$$

where α is a smoothing parameter. Two passes of the Shapiro filter are performed with $\alpha = 0.5$ for the first pass and $\alpha = -0.5$ for the second pass. The second pass is intended to restore the amplitude of the large scales which were slightly damped in the first pass (Shapiro 1970). The filter is not applied to the grid point if it is located over land or if any of the four adjacent grid points (north, south, east, and west) are located over land.

6. Repeat steps 2–5 with a different radius of influence R.

The radius of influence is decreased with each pass in order to analyze smaller scale features with each successive iteration (Cressman 1959). In practice, the smallest wavelengths are noisy. Therefore, the smallest radius of influence needs to be at least seven to eight times the average separation distance (Levitus 1982). The smallest radius of influence we use, 771 km, is over seven times the average separation distance of a 1- by 1-degree grid.

For anomalies, 4 passes of the analysis scheme are performed with radii of influence equal to 1541 km, 1211 km, 881 km, and 771 km, as in Levitus (1982). These radii correspond to 14°, 11°, 8°, and 7° in latitude and longitude at the Equator. At 60° latitude North or South, the radii correspond to 28°, 22°, 16°, and 14° longitude. South of 40°S only the first two passes of the analysis are used in an effort to smooth the noisy data in these latitudes.

The response function of an analysis is defined as the ratio between the magnitude of an analyzed wave and that of the unanalyzed wave. The response function for the objective analysis using four passes with radii of 1541, 1211, 881, and 771 km, but without any linear or nonlinear filter, is given in the second column of Table 7 (from Levitus 1982). As expected, the short wavelengths are damped severely while the intermediate and longer wavelengths receive moderate and little damping, respectively. Table 7 also shows the response function of the analysis including the linear filter, for both four passes and two passes of the analysis. Notice that the damping is much greater for all but the smallest wavelengths with two passes of the analysis compared to that with four passes. For extremely long wavelengths (not shown), the damping from two passes of the analysis is nearly identical to the damping from four passes.

Table 6: Monthly air temperature correction coefficients (from Dorman and Bourke 1978). Temperature should be given in Celsius.

	a	b	c
Jan	0.973	0.0469	0.00382
Feb	0.941	0.0412	0.00207
Mar	0.804	0.0404	0.000129
Apr	0.720	0.0603	0.000042
May	0.489	0.0678	0.000012
Jun	0.726	-0.1030	0.008885
Jul	1.734	-0.2362	0.011943
Aug	1.115	-0.1217	0.008146
Sep	0.548	0.0060	0.005140
Oct	0.671	0.0421	0.002934
Nov	0.896	0.0701	0.001350
Dec	0.985	0.0662	0.001148

Table 7: Response function for objective analysis with and without linear Shapiro filter.

wavelength	no filter	with filter	
(km)	4 passes	4 passes	2 passes
3300	1.00	1.01	0.90
2640	0.99	1.00	0.77
2200	0.97	0.98	0.65
1980	0.95	0.95	0.56
1650	0.87	0.88	0.36
1320	0.70	0.69	0.14
1100	0.49	0.49	0.07
990	0.37	0.36	0.04
880	0.23	0.22	0.01
660	0.05	0.05	0.01
550	0.02	0.02	0.01

Using four passes and two passes of the analysis on different parts of the same field produces slight inconsistencies at the boundary. The level of inconsistency is of approximately the same order as noise south of 40° S, so that the final result is less noticeable in climatology fields, but more noticeable in anomaly fields.

In the UWM/COADS Extended data set we calculate only anomalies. From the observed raw monthly mean fields, the 1945-89 monthly mean analyzed climatology is subtracted to produce observed *raw* anomalies. A zero field is used as first guess F in the analysis scheme.

Finally, fields derived from component fluxes (i.e. constrained fluxes) are calculated from the analyzed climatology and anomaly fields. Observation density cannot be calculated for the constrained fluxes as their component fluxes have differing observation densities. Therefore, we do not show observation density maps for either of the constrained fluxes. If necessary, observation density may be generalized by looking at the observation densities of the components of the constrained flux.

Because we wished to maintain the utility of the UWM/COADS analysis, we did not compute anomalies from a 1945–93 climatology. The differences between the 1945-89 and 1945–93 climatologies are small on an annual basis. Sea surface temperature annual climatologies differ by a maximum of about 0.1° C. Annual wind speed climatologies differ by about 0.1 m/s or less. Latent heat flux annual climatologies differ by about 2.5 W/m^2 or less. Differences between the 1945–89 and 1945-93 climatologies for individual months, of course, are larger. Those interested in climatology differences in specific variables, areas or months may calculate a good approximation using the analyzed anomalies for 1990–93. While the differences in climatologies may not be extraordinary, users of the supplementary data should be aware of one point. If including the 1990-93 anomalies with those during the 1945–89 period, be aware that the mean anomaly is no longer zero. Trends will exist in the last four years. Modelers might find an unwelcome drift in their simulations if these anomalies are included.

8 Fine tuning of heat and fresh water fluxes

One of the applications of surface marine fluxes is the study of the heat and fresh water balances of the world oceans. Similar calculations based on surface marine data have been performed by many authors (Budyko 1956, Baumgartner and Reichel 1975, Esbensen and Kushnir 1981, Hastenrath 1982, Hsiung 1985, Oberhuber 1988, Isemer *et al.* 1989, among others.) As an example, consider the vertically integrated heat budget equation for the oceans

$$\frac{\partial H}{\partial t} + \nabla \cdot \mathcal{H} = Q_{net} \tag{28}$$

where

$$H = \text{oceanic heat content} \tag{29}$$

$$\mathcal{H} = \text{vertically integrated oceanic heat transport} = (\mathcal{H}_x, \mathcal{H}_y) \tag{30}$$

$$Q_{net} = \text{net heat flux at the surface} = R_S - (R_L + Q_L + Q_S)\,. \tag{31}$$

Integrating (28) for a sufficiently long period of time the storage term $\partial H/\partial t$ can be neglected, resulting in the balance equation

$$\nabla \cdot \overline{\mathcal{H}} = \overline{Q_{net}} \tag{32}$$

which relates the surface net heat flux to the divergence of the mean vertically integrated oceanic transport. If this equation is integrated over the globe, the left hand side vanishes, as the heat exchange with the continents is negligibly small. This imposes a consistency condition on the net heat fluxes:

$$\int\int_{Globe} \overline{Q_{net}}\, dx\, dy = 0\,. \tag{33}$$

As can be seen from (31), Q_{net} is computed as a residual from large, uncertain terms and the condition (33) is not guaranteed to be met. In fact, the mean annual net heat flux calculated from our estimates of R_S, R_L, Q_L, and Q_S climatologies (1945–89) does not satisfy this condition. Likewise, there are imbalances between our estimates of evaporation and precipitation that cannot be accounted for by the Baumgartner and Reichel (1975) estimates of river runoff (not included in this data set).

There are two main sources of errors in estimates of surface marine fluxes from historical data. First, there are observational errors associated with instrument bias (section 5) and sampling problems associated with the uneven and inadequate data coverage of the world oceans. Second, even in the presence of perfect surface marine data, one needs to rely on bulk parameterizations which are somewhat simplified representations of complex air-sea interaction processes. The individual components that make up the net heat flux are affected by all these uncertainties. Since Q_{net} is a small residual from heat gain (incoming solar radiation) and heat loss (primarily due to evaporation) terms, its relative error is much larger than the relative error for each of the individual components.

In section 5 we have documented our attempts to reduce some of the observational biases in COADS. We also derive an additional set of corrections aimed at producing physically consistent (in the sense of approximately satisfying eq. (33) or independent oceanic measurements) surface heat and fresh water fluxes over the global oceans. To accomplish this, we perform a simple linear inverse calculation to derive small corrections for some of the bulk formula parameters, thereby producing a more physically consistent net heat flux. The technique is standard in geophysics and the development is similar to Isemer *et al.* (1989). A summary of the results follows; details of the calculation can be found in Volume 1 of da Silva *et al.* (1994).

8.1 Producing fine tuned fluxes

The need to adjust the flux based on measurements for a particular application will undoubtedly require users to produce their own fine tuning of the heat and fresh water fluxes. To this end, we provide users of UWM/COADS with *sensitivity fields* associated with each of the six tuning parameters p discussed in this section. In the short wave parameterization, the tuning parameter p_{T_r} is roughly associated with the transmission coefficient and water vapor absorption coefficient; p_c is related to the cloud cover coefficient. In the long wave radiation formula, p_e is associated with the parameterized water vapor effect, and p_χ with the tuning parameter for the cloud cover correction. In the latent and sensible heat flux parameterizations, we have specified a single tuning parameter for each formula (p_L and p_S), representing primarily the uncertainties in the transfer coefficients. Subsequently, the net heat flux can be written as

$$Q_{net}(p_{T_r}, p_c, p_e, p_\chi, p_L, p_S) = R_S(p_{T_r}, p_c) - R_L(p_e, p_\chi) - Q_L(p_L) - Q_S(p_S) \quad (34)$$

The corresponding sensitivity fields are

$$\mathcal{A}_{T_r} = \frac{\partial R_S}{\partial p_{T_r}} = \frac{\partial Q_{net}}{\partial p_{T_r}} \quad (35)$$

$$= R_S^* \quad (36)$$

$$\mathcal{A}_c = \frac{\partial R_S}{\partial p_c} = \frac{\partial Q_{net}}{\partial p_c} \quad (37)$$

$$= R_{\text{clear}}(1-\alpha)(-0.62c) \quad (38)$$

$$\mathcal{A}_e = \frac{\partial R_L}{\partial p_e} = -\frac{\partial Q_{net}}{\partial p_e} \quad (39)$$

$$= -\epsilon\sigma T_s^4 \left(0.39 - 0.05\sqrt{e}\right)\left(1 - \chi c^2\right) \quad (40)$$

$$\mathcal{A}_\chi = \frac{\partial R_L}{\partial p_\chi} = -\frac{\partial Q_{net}}{\partial p_\chi} \quad (41)$$

$$= \epsilon\sigma T_s^4 \left(0.39 - 0.05\sqrt{e}\right)\left(-\chi c^2\right) \quad (42)$$

$$\mathcal{A}_L = \frac{\partial Q_L}{\partial p_{L,E}} = -\frac{\partial Q_{net}}{\partial p_{L,E}} \quad (43)$$

$$= Q_L^* \quad (44)$$

$$\mathcal{A}_S = \frac{\partial Q_S}{\partial p_S} = -\frac{\partial Q_{net}}{\partial p_S} \quad (45)$$

$$= Q_S^* . \quad (46)$$

The sensitivity fields $\mathcal{A}_{T_r}$, $\mathcal{A}_L$ and $\mathcal{A}_S$ are equal to the full unconstrained fields ($R_S^* = R_S$, $Q_L^* = Q_L$ and $Q_S^* = Q_S$) already included in UWM/COADS. The other sensitivity fields are computed either from individual observations with climatology and anomalies analyzed the same way as the other UWM/COADS fields ($\mathcal{A}_e$ and $\mathcal{A}_\chi$), or derived from analyzed fields ($\mathcal{A}_c$).

In order to produce constrained estimates of the individual heat flux components, one can calculate

$$R_S = R_S^* + (p_{T_r} - 1)\mathcal{A}_{T_r} + (p_c - 1)\mathcal{A}_c$$

$$= p_{T_r} R_S^* + (p_c - 1)\mathcal{A}_c \quad (47)$$

$$R_L = R_L^* + (p_e - 1)\mathcal{A}_e + (p_\chi - 1)\mathcal{A}_\chi \quad (48)$$

$$Q_L = p_{L,E} Q_L^* \quad (49)$$

$$Q_S = p_S Q_L^* \quad (50)$$

where $(\ )^*$ denotes the unconstrained estimate of the heat flux component as included in UWM/COADS. Likewise, constrained evaporation and precipitation fields can be computed from

$$E = p_{L,E} E^* \quad (51)$$

$$P = p_P P^* \quad (52)$$

where $p_{L,E}$ is the tuning parameter related to the uncertainties in the transfer coefficient (C_E), and p_P reflects the uncertainties in the bulk formulation of precipitation. The values of the parameters p in Table 8 can be used to produce several versions of the constrained heat and fresh water fluxes. In addition, new values for the tuning parameters can also be calculated. Details are given in Volume 1 of da Silva *et al.* (1994).

8.2 Constrained fluxes in UWM/COADS

The individual heat flux components, evaporation and precipitation provided in the UWM/COADS Extended data set are not tuned in any way. It is left to the user to choose a particular set of tuning parameters most suitable to the application at hand. However, the net heat flux and evaporation minus precipitation fields included in the data set have been constrained using the global balance requirement given in the first row of Table 8. These constrained fluxes have been computed using analyzed component fluxes.

Table 8: Parameters from the simultaneous tuning of heat and fresh water fluxes. Imposed constraints on the meridional heat transport (H) and meridional fresh water transport (F) listed in the first column, with resulting transports at 25° N in the Atlantic appearing in the last column. The constraint for heat flux is taken from the global balance requirement. Constraints for fresh water flux are chosen as follows: 0.06 Sv at 65° S, Peixoto and Oort (1992); 0.27 Sv at 65° S, Stommel (1980). The other fresh water constraints are chosen between the unconstrained value and the value obtained when the Peixoto and Oort (1992) constraint is applied.

Imposed Constraints	Tuning Parameters								Transport 25° N
	p_{T_r}	p_c	p_e	p_χ	$p_{L,E}$	p_S	p_P	p_R	
(H) 0. PW 65°S Global	0.92	1.04	1.02	0.99	1.13	1.02	1.12	1.01	0.95 PW
(F) 0.06 Sv 65°S Global									-0.95 Sv
(H) 0. PW 65°S Global	0.92	1.04	1.02	0.99	1.14	1.01	1.10	1.01	0.95 PW
(F) 0.27 Sv 65°S Global									-0.90 Sv
(H) 0. PW 65°S Global	0.92	1.04	1.02	0.99	1.14	1.01	1.09	1.01	0.95 PW
(F) 0.5 Sv 65°S Global									-0.89 Sv
(H) 0. PW 65°S Global	0.93	1.04	1.02	0.99	1.14	1.01	1.05	1.00	0.95 PW
(F) 1. Sv 65°S Global									-0.86 Sv
(H) 0. PW 65°S Global	0.93	1.04	1.02	0.99	1.15	1.01	1.01	1.00	0.95 PW
(F) 1.5 Sv 65°S Global									-0.82 Sv

The constrained climatology and anomaly fields are computed as follows: For each component of Q_{net} or E–P, we compute the monthly mean by adding the analyzed anomaly field for each month and year to the analyzed climatology for that month. The monthly mean fields are then multiplied by the tuning coefficient and added/subtracted to form constrained monthly mean fields of Q_{net} or E–P. Constrained monthly climatology fields are formed from the constrained monthly mean fields. Constrained monthly anomalies are then formed by subtracting the constrained monthly climatology from each constrained monthly mean field.

The zonally integrated meridional heat transport is shown in Fig. 1. In agreement with previous studies, our constrained heat flux climatologies for 1945–89 produce a northward meridional heat transport throughout the Atlantic and a southward transport in the Indian ocean. In the Atlantic our estimate is within the error bars for Wunsch's (1984) measurement at the equator, and Hall and Bryden's (1982) measurement at 25° N. Our estimated transport at 32° N is about half the measurement of Rago and Rossby (1987) who admit their measurement is rather large. Our estimate for the southward transport in the South Pacific is somewhat smaller than previous estimates by Hsiung (1985) and Hastenrath (1982).

Figure 2 shows the fresh water transport calculated with our constrained fluxes. We use initial transports at the northern boundary after Coachman and Aagaard (1988) and Wijffels *et al.* (1992). In the Atlantic, our constrained zonally integrated meridional fresh water transport is directed southward over the entire range of latitude. Our values are generally larger than Schmitt *et al.* 's (1989) throughout the North Atlantic (when Schmitt *et al.* (1989) is adjusted for the Wijffels *et al.* (1992) initial transport value). At 25° N our estimate gives a southward transport of 0.95 Sv which is larger than Hall and Bryden's (1982) measured value of −0.78 Sv[1], but conceivably within their error bars. In the Northern Hemisphere, our Atlantic transport is comparable to that of Wijffels *et al.* (1992), but larger in the Southern Hemisphere. Our Pacific transport, like that of Wijffels *et al.* (1992), shows northward transport in the Pacific, although our Pacific transport is greater in magnitude — as much as 0.5 Sv greater at the equator and 0.9 Sv greater at 40° S.

While the results above suggest that our choice of tuning parameters (first row of Table 8) produces reasonable estimates of heat and fresh water fluxes, it is important to keep in mind that this choice does not produce a balanced net heat flux. When regions poleward of 65° are considered, a small imbalance (−0.06 PW) remains. It is also important to note that our choice of tuning parameters is very likely non-optimal for specific applications. We strongly encourage users to experiment with other choices of parameters.

[1] We have adjusted Hall and Bryden's (1982) value of −0.03 Sv using Coachman and Aagaard's (1988) updated value for transport through the Bering Strait.

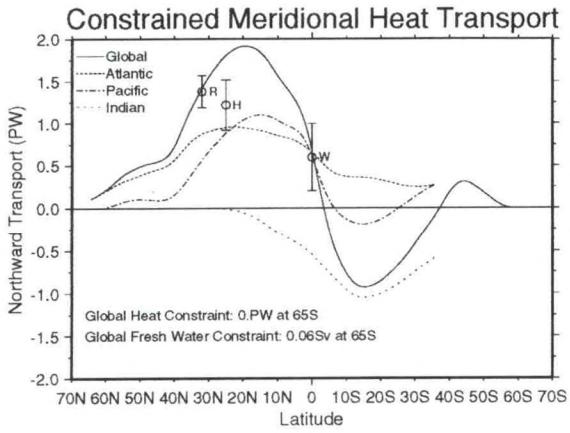

Figure 1: Meridional heat transport (1 PW = 10^{15}W) calculated from constrained net heat flux. Heat flux is constrained so that the global meridional heat transport at the southern boundary is zero and the fresh water transport at the southern boundary is 0.06 Sv. Three oceanographic measurements for Atlantic heat transport are shown with error bars: (R) Rago and Rossby [1987], (H) Hall and Bryden [1982], (W) Wunsch [1984].

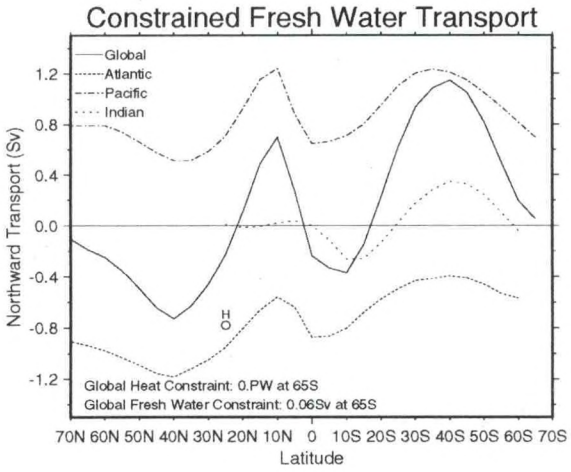

Figure 2: Meridional fresh water flux (in Sv) calculated from constrained fresh water flux. Heat flux is constrained as in the previous figure. One oceanographic measurement for Atlantic fresh water transport is shown: (H) Hall and Bryden [1982] adjusted using the Coachman and Aagaard [1988] Bering Strait transport.

9 Results

Table 9 lists the twenty-two quantities presented in this supplement. Although all the analyses have been performed globally, in order to conserve space we only present maps from 40°S to 80°N, eliminating the less observed and noisier Southern and Arctic oceans. For each quantity[2] the following information is displayed:

Seasonal density of observations:
These maps document the average data coverage for each season in the period 1990-93. The density of observations η is defined as the mean number of observations per month per $1° \times 1°$ box. The size of each black square is related to the mean value of η in each 5° box (see scale on top of page). Units are observations per month per 1°box.

Seasonal climatology:
Computed from monthly mean analyzed 1945–89 climatology (from da Silva *et al.* [1994]). Units are given in Table 9.

Seasonal anomalies:
Computed from analyzed monthly mean anomalies. The anomalies are computed from the analyzed 1945–89 climatology for each month. Units are given in Table 9.

The contour interval ("ci" for short) along with units and season information (DJF for December-January-February, MAM for March-April-May, etc.) are displayed in a box on the continent of Asia for each map.

A detailed exposition of the spatial and temporal structure of the anomaly fields is beyond the scope of this atlas. Several projects are in progress to document the decadal/interannual variability of the atmosphere-ocean system which in turn will provide guidance regarding the quality of the data set and hopefully point to ways to improve it in future releases. The maps presented here are intended to serve as a reference for researchers engaged in observational or modeling studies using our revised data sets.

10 Limitations and shortcomings of the data sets

A description of surface marine data sets could not be complete without a discussion of the remaining problems and limitations for which solutions may never be found. Because ship and buoy reports are probably the only comprehensive observational record available of the surface marine climate, this data source will undoubtedly continue to be used in studies of the ocean-atmosphere system. As large uncertainties are present, it is imperative that researchers remember that an analysis of surface marine data is an evolving

[2] Constrained net heat flux and E–P are derived from analyzed component fluxes and therefore lack figures for observation density. We do not display maps for A_c, A_χ, or A_e.

Table 9: Quantities presented in this atlas supplement. Quantities marked with † are derived from analyzed component quantities; observation density maps are therefore not available.

Parameter	Description	Units
sst	sea surface temperature	°C
sat	air temperature	°C
q	specific humidity	g/kg
c	fractional cloud cover	none
slp	sea level pressure	hPa
u	20 m zonal wind speed	m/s
v	20 m meridional wind speed	m/s
w	20 m wind speed	m/s
taux	zonal wind stress	N/m^2
tauy	meridional wind stress	N/m^2
Rs	net short wave radiation	W/m^2
Rl	net long wave radiation	W/m^2
Ql	latent heat flux	W/m^2
Qs	sensible heat flux	W/m^2
Qnet†	constrained net heat flux	W/m^2
E	evaporation rate	mm/(3 hr)
P	precipitation rate	mm/(3 hr)
E-P†	constrained E minus P rate	mm/(3 hr)
dT	sea minus air temperature	°C
dq	qs minus q	g/kg
e	vapor pressure	hPa

process. Continual improvement will be necessary as more data or metadata become available, physical parameterizations are improved, and advances in data assimilation techniques become available. The corrections we have reported here are, at best, a step in the right direction, but much remains to be done. In the remainder of this section, we discuss some of the remaining problems. This list is by no means exhaustive.

The first, and most uncontrollable errors exist in the ship reports themselves. Marine and atmospheric measurement techniques and the recording of these observations are not perfect. Some errors are introduced through poor instrumentation. Surface air temperature can be biased due to heating of a ship's superstructure during the day and inadequate shelter ventilation (Isemer and Hasse 1987; Ramage 1984; Kent *et al.* 1993a,b). Sea surface temperature observations taken via ship intake will be biased compared to those taken by insulated bucket or hull sensors.

Many of the biases are impossible to correct due to the lack of instrumentation information as discussed in section 3. A proper homogenization of the measured wind speeds requires the knowledge of the precise anemometer height information which is not included in COADS1a at the present time; an average anemometer height of 20 m has been assumed for ships and 5 m for buoys in our calculations. In addition, the flag WI in COADS1a/LMRF, which allows the discrimination between measured and estimated winds, may not be reliable (Slutz *et al.* 1985, Cardone *et al.* 1990). Our wind speed bias correction procedure takes the WI flag at face value and consequently is affected by this uncertainty. Any systematic bias in the anemometer winds remains to be evaluated.

Even when an observation is considered accurate and unbiased, the recording stage may result in errors (Slutz *et al.* 1985). Some observations are taken in different units (such as Fahrenheit vs. Celsius) without documentation. Coding practices change but are not implemented by all observers on the same date. Ship positions may be erroneous. The transfer of written records to digital form can also introduce error. Dew point temperatures in deck 927 are known to be biased during January–May, 1988 due to a keying error. Some recording errors were repaired by the compilers of COADS, but some miscoded errors undoubtedly remain. The tendency for ships to avoid stormy weather also introduces a fair weather bias into the observations when considered as a whole, although this bias is less problematic in the tropics.

Trimming flags exist in COADS so that erroneous data may be omitted from an analysis. Our usage of the relatively strict 3.5σ limit for trimming introduces error by eliminating or reducing the intensity

of extreme events, such as the 1982–83 El Niño. Although the more relaxed 4.5σ trimming limits were available for the 1980–93 data, they were not used at this time, awaiting our full reanalysis.

After we deal with the correctable biases and calculate raw fields, error can be introduced by the analysis scheme as well. One problem with the successive correction method used in our analysis is the introduction of unrealistic features (Levitus 1982). Objective analysis of the sort used here fills in the gaps by interpolating/extrapolating smoothed data from remote regions, but cannot compensate entirely for poor sampling. This effect is particularly troublesome in the tropics and southern oceans where observations are clumped along ship tracks with data void areas in between. As a result, bull's eye type features often remain in analyzed fields, particularly in anomaly fields. More observations were available for the 1980's in COADS1a, but we did not compute a reanalysis of the 1980's at this time.

The analysis of anomaly values rather than the observed data can result in spurious extrema. For example, the analysis has problems handling positive definite quantities such as fractional cloud cover which only take values between 0 and 1. The analysis procedure can produce full field values (climatology plus anomalies) less than 0 in broad clear areas or values greater than 1 in broad overcast regions. The climatology fields in the data set have been corrected so that positive definite quantities (cloudiness, relative and specific humidity, vapor pressure, precipitation, etc.) have a minimum value of zero. Maximum limits have not been applied to the climatology, however, nor have the full field values been corrected to their valid ranges. The only additional correction made to the anomaly fields was to force the 45-year mean monthly anomaly to equal zero at each grid point. The 1990-93 anomalies, however, were not adjusted in any way.

It should always be kept in mind that although the analyzed fields are given on a $1^\circ \times 1^\circ$ grid, only features with wavelength greater than 770 km (1300 km or greater for regions south of 40°S and for standard deviation fields) are retained. The reader is referred to Levitus (1982) or Daley (1991) for additional discussions of the limitations of the objective analysis technique. A higher resolution climatological analysis has been performed on a half-degree by half-degree grid where features with wavelength greater than 386 km are retained. These results will be presented elsewhere.

In contrast to our analysis method, modern data assimilation techniques are assisted by some sort of dynamic constraint: a model is used to provide a first guess for the analysis or to ensure a proper balance of the analyzed fields (Daley 1991). In this first version of our analysis, we concentrated on bias corrections and calculations from individual observations, using a successive correction method to grid the data. Current four dimensional atmospheric reanalysis efforts (Schubert *et al.* 1993; Kalnay and Jenne 1991; Bengtsson and Shukla 1988) will provide several estimates of surface marine fields which would prove useful to validate and assess the limitations of our approach. We are also making available the raw, unanalyzed fields to allow researchers to develop their own objective analyses/data assimilation system from the monthly mean data.

11 Summary and plans for future work

We have described the results of a collaborative project between the Department of Geosciences of the University of Wisconsin-Milwaukee and the National Oceanographic Data Center to produce high resolution analyses of surface marine fields for climate variability studies. Our work is based on individual surface marine reports prepared by the COADS project (Slutz *et al.* 1985, Woodruff *et al.* 1993). We have corrected wind speed and cloudiness biases in the original COADS reports and produced monthly means and other statistics on 1° boxes over the global oceans. Although we have attempted to create objectively analyzed fields that can be used as is, we have documented several shortcomings and limitations of the data sets which we hope will be taken into consideration by the careful researcher. Analyzed fields of this sort are estimates of the *true* surface marine climate, and we hope to improve these estimates by inclusion of additional data/metadata and overall improvements in our analysis system.

An immediate improvement concerns the use of COADS Release 1a (COADS1a) which was not available at the time of our initial calculations (da Silva *et al.* 1994). For the 1980's, our analysis was based on the so-called *interim* product. The UWM/COADS Extended data set provides anomalies from 1990 through 1993, but does not take advantage of all the additional metadata in COADS1a. We use the same techniques as used in da Silva *et al.* (1994) in order to provide a consistent data set. In the future we intend to use the additional data and metadata in COADS1a to improve our analysis in the 1980's and 1990's. By the end of 1996, Release 1b, covering 1950–79, and an extension to Release 1a, covering 1994–95, are scheduled to be completed (S. Worley, personal communication). We will conduct our intended reanalysis on the data in COADS Releases 1a, 1b, and any avail-

able extensions beginning in 1997. The COADS releases covering at least 1950 through 1995 will include more observations than Release 1, better duplicate elimination, correction of various data set errors (e.g. 1980's relative humidity), better quality control, and the more flexible 4.5σ trimming limits. In our analysis of this improved data source, we will apply the 4.5σ trimming limit, the dew point and air temperature corrections proposed by Kent *et al.* (1993a,b), an improved wind speed correction scheme using actual anemometer height, an updated ice mask, an improved objective analysis, and possibly an improved technique to estimate precipitation.

Ultimately, the use of these data to address scientific issues in the dynamics of the ocean-atmosphere climate system will establish the strengths and weaknesses of the data sets and hopefully provide clues for further improvements. For this reason, and to ensure the widest possible distribution, the objective analyses as well as the raw monthly means on which they are based are being made available internationally, without restriction, on magnetic media as well as CD-ROM.

12 FORTRAN access software for UWM/COADS netCDF files

This section presents FORTRAN access software to read the analyzed UWM/COADS Extended netCDF files. This is an enhanced version (original version is in Volume 1 of da Silva *et al.* [1994]) which is able to read the anomaly-only files of the 1990–93 Extended set without returning error conditions. This software is included with the data and current versions can be obtained from the anonymous ftp site `niteroi.gsfc.nasa.gov`. The file `uwmcdf.f` can be found in the directory `pub/uwm_coads/1x1/software/analyzed/`.

Tables 10–11 list `UWREAD`, a routine to read analyzed UWM/COADS netCDF files. On input the user only needs to specify the desired month and year along with the name of the file (see Table 1 for a list of the Extended file names). On output, the array `X(360,180)` contains the desired gridded data. Climatological data are obtained by supplying the climatology-only or anomaly-climatology file name and specifying `year = 0`. Notice that the UWM/COADS analyses are available only over the oceans, a special land-value (by default -10^{10}) is used to indicate those grid-points over land. Once a file is opened by `UWREAD` it remains opened for subsequent reading. All file pointers and other necessary parameters needed to access the data are handled internally and are transparent to the user. By default, `UWREAD` can open a maximum of 10 files. This number can be increased by changing parameter `NMAX` in the include file `uwmcdf.h` (Table 11). In order to close all netCDF files opened by `UWREAD` the user needs to call `UWCFIL`. Consult Table 10 for a complete list of I/O parameters.

Unanalyzed data in the Extended set are stored in the same manner as the raw data in UWM/COADS. The software to read the unanalyzed data can be found in Volume 1 of da Silva *et al.* (1994).

The subroutines above rely on the netCDF FORTRAN Library which is described in Volume 1 of da Silva *et al.* (1994) (see also Rew *et al.* 1993). The structure of the anomaly-only files of the Extended data set is identical to the anomaly-climatology files of UWM/COADS, but with one difference. Files in the Extended data set do not contain any information related to climatology (e.g. data, valid range, add offset, etc.). For a full description of the structure of the UWM/COADS netCDF files see Volume 1 of da Silva *et al.* (1994).

Table 10: File uwmcdf.f: FORTRAN subroutines to read UWM/COADS and UWM/COADS Extended netCDF analyzed files.

```
* uwmcdf.f - last change: 11/21/95 (ccy/ams)
*
*     Access routines to the netCDF UWM/COADS data sets and extended sets.
*

*.....................................................................


      subroutine UWREAD (ier, x, idim, jdim, label, mon, year, filen)

      integer       idim, jdim, mon, year, ier
      real          x(idim,jdim)
      character*80  label, filen

*
*     This routine reads grids from the netCDF UWM/COADS files.
*
*     On input:
*        idim, jdim  - dimensions of output array (usually 360x180)
*        mon         - desired month (jan=1, feb=2, etc.)
*        year        - desired year.  If 'year' is between 1945
*                      and 1993, the corresponding anomalies are
*                      returned.  The climatology for month
*                      'mon' is returned if year = 0.
*        filen       - full file name (including path) for the
*                      input netCDF file. End file name with '$'.
*                      Files containing anomalies after 1989 have
*                      the suffix of 'nc2', instead of 'nc'.
*                      Example:  filen = '/data/cdf/sst.nc$'
*                      post-1989:  filen = '/data/cdf/sst.nc2$'
*
*
*     On output:
*        x      array containing the grid over the globe.  Land
*               points receive the special value -1.0E+10.
*      label    informational label about the data just read.
*               This can used for the title of a plot.
*        ier    error code:
*                0  -   no error
*               <0  -   netCDF error code (-errcod)
*                1  -   not enough work space.
*                2  -   too many files open
*                3  -   incompatible dimensions
```

```
*     NOTE:  For the 1 degree x 1 degree data products (360x180
*            arrays) the zonal and meridional grids are as follows:
*
*     longitude(i) = 0.5 + (i-1),  for i = 1,...,360
*     latitude(j) = -89.5 + (j-1), for j = 1,...,180
*

*     Land value
*     ----------
      real ALAND
      parameter ( ALAND = -1.0E+10 )

      include 'netcdf.inc'
      include 'uwmcdf.h'

      integer      errcod, idlat, idlon
      character    pname*10, chyr*4, shorti*80
      character*3  chmon(12)

      logical      strcmp

      integer      cst(2), clen(2), ast(3), alen(3)
      save         cst, clen, ast, alen

      data chmon / 'jan', 'feb', 'mar', 'apr', 'may', 'jun', 'jul',
     .             'aug', 'sep', 'oct', 'nov', 'dec' /
      data cst / 1, 1 /, clen / npmax, 1 /
      data ast / 1, 1, 1 /, alen / npmax, 1, 1 /


*     Initialize error parameter
*     --------------------------
      ier = 0
      errcod = 0

      lf = index(filen,'$') - 1
      if ( lf .le. 0 ) lf = 80

      iyear = year
      if ( year .ne. 0 .and. year .lt. 1900 ) iyear = 1900+year

*     Try to fix the name
*     -------------------
      if (year .ge. 1990 .and. lf .ne. 80) then
         if ( filen(lf:lf) .ne. '2') then
            filen = filen(1:lf) // '2$'
            lf = lf + 1
         end if
      end if
```

```
*     Do if this is the first call
*     ----------------------------
      if ( icount .eq. 0 ) then
         icount = icount + 1
         nfile = icount
         files(icount) = filen
         call NCPOPT ( NCVERBOS )

*        open netcdf file
*        ----------------
         idfile(icount) = NCOPN ( filen(1:lf), NCNOWRIT, errcod )
         if ( errcod .ne. 0 ) go to 999

*        determine if resolution is compatible
*        -------------------------------------
         idnpt = NCDID ( idfile(icount), 'npoint', errcod )
         if ( errcod .ne. 0 ) go to 999
         call NCDINQ ( idfile(icount), idnpt, pname, npoint, errcod )
         if ( errcod .ne. 0 ) go to 999
         if ( npoint .gt. npmax ) then
            ier = 1
            return
         end if
         alen(1) = npoint
         clen(1) = npoint

*        get id numbers for lat and lon
*        ------------------------------
         idlat = NCVID ( idfile(icount), 'lat', errcod )
         if ( errcod .ne. 0 ) go to 999
         idlon = NCVID ( idfile(icount), 'lon', errcod )
         if ( errcod .ne. 0 ) go to 999

*        read in lat and lon data
*        ------------------------
         call NCVGT ( idfile(icount), idlat, 1, npoint, lat, errcod )
         if ( errcod .ne. 0 ) go to 999
         call NCVGT ( idfile(icount), idlon, 1, npoint, lon, errcod )
         if ( errcod .ne. 0 ) go to 999

*        Get climatology attributes
*        --------------------------
         if ( iyear .le. 1989 ) then
            idclm(icount) = NCVID ( idfile(icount), 'clm', errcod )
            if ( errcod .ne. 0 ) go to 999
            call NCAGT ( idfile(icount), idclm(icount), 'add_offset',
     .                   offclm(icount), errcod )
            if ( errcod .ne. 0 ) go to 999
            call NCAGT ( idfile(icount), idclm(icount), 'scale_factor',
     .                   sclclm(icount), errcod )
            if ( errcod .ne. 0 ) go to 999
         end if
```

```
*        get anomaly attributes
*        ----------------------
         idanm(icount) = NCVID ( idfile(icount), 'anom', errcod )
         if ( errcod .eq. 0 ) then
          call NCAGT ( idfile(icount), idanm(icount), 'add_offset',
     .                 offanm(icount), errcod )
          if ( errcod .ne. 0 ) go to 999
          call NCAGT ( idfile(icount), idanm(icount), 'scale_factor',
     .                 sclanm(icount), errcod )
          if ( errcod .ne. 0 ) go to 999
         end if

         isopen = 1

*     Otherwise check to see if it is a new file
*     ------------------------------------------
      else

         isopen = 0
         do 10 i = 1, icount
            if ( STRCMP ( filen, files(i), '$' ) ) then
               nfile = i
               isopen = 1
            end if
 10      continue

      end if


*     Do only if a new file
*     ---------------------
      if ( isopen .ne. 1 ) then
         icount = icount + 1
         if ( icount .gt. nmax ) then
            ier = 2
            return
         end if
         files(icount) = filen
         nfile = icount

*        open netcdf file
*        ----------------
         idfile(nfile) = NCOPN ( filen(1:lf), NCNOWRIT, errcod )
         if ( errcod .ne. 0 ) go to 999
```

```
*       determine if resolution is compatible
*       -------------------------------------
        idnpt = NCDID ( idfile(nfile), 'npoint', errcod )
        if ( errcod .ne. 0 ) go to 999
        call NCDINQ ( idfile(nfile), idnpt, pname, npts, errcod )
        if ( errcod .ne. 0 ) go to 999
        if ( npts .ne. npoint ) then
           ier = 3
           return
        end if

*       Get climatology attributes
*       --------------------------
        if ( iyear .le. 1989 ) then
           idclm(nfile) = NCVID ( idfile(nfile), 'clm', errcod )
           if ( errcod .ne. 0 ) go to 999
           call NCAGT ( idfile(nfile), idclm(nfile), 'add_offset',
     .                  offclm(nfile), errcod )
           if ( errcod .ne. 0 ) go to 999
           call NCAGT ( idfile(nfile), idclm(nfile), 'scale_factor',
     .                  sclclm(nfile), errcod )
           if ( errcod .ne. 0 ) go to 999
        end if

*       Get anomaly attributes
*       ----------------------
        idanm(nfile) = ncvid( idfile(nfile), 'anom', errcod )
        if ( errcod .eq. 0 ) then
         call NCAGT ( idfile(nfile), idanm(nfile), 'add_offset',
     .                offanm(nfile), errcod )
         if ( errcod .ne. 0 ) go to 999
         call NCAGT ( idfile(nfile), idanm(nfile), 'scale_factor',
     .                sclanm(nfile), errcod )
         if ( errcod .ne. 0 ) go to 999
       end if

      end if

*     Do every time:  acquire the global attribute 'source'
*     -----------------------------------------------------
      call NCAGTC ( idfile(nfile),
     .              NCGLOBAL, 'source', uwmver, 80, errcod )
      if ( errcod .ne. 0 ) go to 999
      call NCAGTC ( idfile(nfile), NCGLOBAL,
     .              'title', shorti, 80, errcod )
      if ( errcod .ne. 0 ) go to 999
```

```
*     fill in land values in x array
*     ------------------------------
      if ( iaccum .eq. 0 ) then
         do 100 j = 1, jdim
            do 100 i = 1, idim
 100           x(i,j) = ALAND
      end if

*     Get climatology or anomaly data
*     -------------------------------
      if ( iyear .eq. 0 ) then
         cst(2) = mon
         call NCVGT ( idfile(nfile), idclm(nfile), cst, clen, var,
     .                errcod )
         if ( errcod .ne. 0 ) go to 999
         vscal = sclclm(nfile)
         voffst = offclm(nfile)
      else
         ast(2) = mon
         if ( iyear .le. 1989 ) then
            ast(3) = iyear-1944
         else
            ast(3) = iyear-1989
         end if
         call NCVGT ( idfile(nfile), idanm(nfile), ast, alen, var,
     .                errcod )
         vscal = sclanm(nfile)
         voffst = offanm(nfile)
      end if

*     uncondense field
*     ----------------
      if ( iaccum .eq. 1 ) then
         do 200 k = 1, npoint
            i = lon(k)
            j = lat(k)
            xvar = var(k)
            x(i,j) =  x(i,j) + xvar * vscal + voffst
 200     continue
      else
         do 300 k = 1, npoint
            i = lon(k)
            j = lat(k)
            xvar = var(k)
            x(i,j) =  xvar * vscal + voffst
 300     continue
      end if
```

```
*     create an informative label
*     ---------------------------
      lf = index( shorti, '$' ) - 1

      if ( iyear .eq. 0 ) then
         label = '/' // shorti(1:lf) // ' climatology for '
     .              // chmon(mon) // '$'

      else
         write( chyr, '(i4)' ) iyear
         label = '/' // shorti(1:lf) // ' anomaly for ' // chmon(mon)
     .              // ' ' // chyr // '$'
      end if


*     Normal end
*     ----------
      ier = 0

      return


*     Abnormal end: error on return from netCDF
*     -----------------------------------------
 999  continue
      if ( errcod .eq. -1 ) then
         ier = -999
      else
         ier = - errcod
      end if

      return

      end
```

```
*.....................................................................

      logical function STRCMP ( str1, str2, del )

      character*(*) str1, str2
      character*1   del

*
*     Returns TRUE if strings are the same.
*

      STRCMP = .false.

      l1 = index ( str1, del ) - 1
      l2 = index ( str2, del ) - 1

      if ( l1 .le. 0 .or. l2 .le. 0 .or. l1 .ne. l2 ) return

      STRCMP = .true.
      do 10 i = 1, l1
         if ( str1(i:i) .ne. str2(i:i) ) STRCMP = .false.
 10   continue

      return
      end
```

```
*.....................................................................

      subroutine UWCFIL ( ier )

*
*     Close all netCDF files in use.
*
      include 'uwmcdf.h'
      integer errcod

      do 10 i = 1, icount
         call NCCLOS ( idfile(i), errcod )
         if ( errcod .ne. 0 ) go to 999
 10   continue

*     Reset counter
*     -------------
      icount = 0

*     Normal end
*     ----------
      return

*     Abnormal end
*     ------------
 999  continue
      if ( errcod .eq. -1 ) then
         ier = -999
      else
         ier = - errcod
      end if


      return
      end

*.....................................................................

      Block Data UWMCDF

      include 'uwmcdf.h'

      data icount / 0 /
      data iaccum / 0 /

      end
```

Table 11: File uwmcdf.h: include file for uwmcdf.f.

```
************************************************************
* uwmcdf.h - last change: 6/23/92 (ams)                    *
*                                                          *
*     Include file for netCDF UWM/COADS I/O programs.      *
*                                                          *
************************************************************

*     Arrays to hold lat/lon and packed grid
*     --------------------------------------
      parameter ( npmax = 42164 )
      integer    npoint
      integer*2  lat(npmax), lon(npmax), var(npmax)

*     Info. about files previously open
*     ---------------------------------
      parameter ( nmax = 10 )
      integer  icount, idfile(nmax), idclm(nmax), idanm(nmax)

      real   offclm(nmax), sclclm(nmax)
      real   offanm(nmax), sclanm(nmax)

      character*80 uwmver, files(nmax)

      common / uwcdf1 / npoint, lat, lon, var
      common / uwcdf2 / icount, idfile, idclm, idanm
      common / uwcdf3 / offclm, sclclm, offanm, sclanm
      common / uwcdf4 / uwmver, files
      common / uwcdf5 / iaccum
```

References

Alexander, R., and R. Mobley, 1976: Monthly average sea-surface temperature and ice-pack limits on a 1°global grid. *Mon. Wea. Rev.*, **104**, 143–148.

Arkin, P. A., and B. N. Meisner, 1987: The relationship between large-scale convective rainfall and cloud cover over the western hemisphere during 1982–84. *Mon. Wea. Rev.*, **115**, 51–74.

Barnes, S. L., 1964: A technique for maximizing details in numerical weather map analysis. *J. Appl. Meteor.*, **3**, 396–409.

Baron, M. S., 1994: The new code and other news. *Mariners Wea. Log*, **38**:3, 67–68.

Baumgartner, A., and E. Reichel, 1975: *The World Water Balance.* Elsevier, 179 pp.

Beaton, A. E., and J. W. Tukey, 1974: The fitting of power series, meaning polynomials, illustrated on band-spectroscopic data. *Technometrics*, **16**, 147–185.

Bengtsson, L., and J. Shukla, 1988: Integration of space and in situ observations to study global climate change. *Bull. Amer. Meteor. Soc.*, **69**, 1130–1143.

Bottomley, M., C. K. Follund, J. Hsiung, R. E. Newell and D. E. Parker, 1990: *Global Ocean Surface Temperature Atlas.* Joint Meteorol. Off./Mass. Inst. Techno. Proj., supported by U. S. Dept. of Energy, U. S. Natl. Sci. Found., and U. S. Off. of Nav. Res., funded by U. K. Depts. of Energy and Environ., Her Majesty's Stationery Office, London, 20 pp., 313 plates.

Budyko, M. I., 1956: *The Heat Balance of the Earth's Surface*, translated by N. A. Stepanova, 1958. U. S. Dept. of Commerce, Washington D. C., 259 pp.

Budyko, M. I., 1974: *Climate and Life.* Academic Press, 508 pp.

Bunker, A. F., 1976: Computations of surface energy flux and annual air-sea interaction cycles of the North Atlantic Ocean. *Mon. Wea. Rev.*, **104**, 1122–1140.

Brunt, D., 1932: Notes on radiation in the atmosphere. *Q. J. Royal Meteor. Soc.*, **58**, 389-420.

Cardone, V. J., 1969: Specification of the wind distribution in the marine boundary layer for wave forecasting. Report TR69-1, New York University, New York, NY, 131 pp. [NTIS AD 702 490].

Cardone, V. J., J. G. Greenwood and M. Cane, 1990: On trends in historical marine wind data. *J. Climate*, **3**, 113–127.

Coachman, L. K., and K. Aagaard, 1988: Transports through Bering Strait: Annual and interannual variability. *J. Geophys. Res.*, **93**, 15 535–15 539.

Cressman, G. P., 1959: An operational objective analysis scheme. *Mon. Wea. Rev.*, **87**, 329–340.

Daley, R., 1991: *Atmospheric Data Analysis.* Cambridge University Press, Cambridge, 457 pp.

Dorman, C. E., and R. H. Bourke, 1978: A temperature correction for Tucker's ocean rainfall estimates. *Q. J. Royal Meteor. Soc.*, **104**, 765–773.

Esbensen, S. K. and J. Kushnir, 1981: The heat budget of the global oceans: An atlas based on estimates from marine surface observations. Oregon State University Climate Research Institute Rep. No. 29, 27 pp.

Esbensen, S. K., and R. Reynolds, 1981: Estimating monthly averaged air–sea transfers of heat and momentum using the bulk aerodynamic method. *J. Phys. Oceanogr.*, **11**, 457–465.

Farmer, G., T. M. L. Wigley, P. D. Jones and M. Salmon, 1989: Documenting and explaining recent global-mean temperature changes. *Final Report to Natural Environment Research Council.*, Climate Research Unit, University of East Anglia, U. K.

Folland, C. K., 1991: Sea temperature bucket models used to correct historical SST data in the Meteorological Office. Climate Research Technical Note No. 14, British Meteorological Office, England.

Folland, C. K., and J. Hsiung, 1986: Correction of seasonally varying biases in uninsulated bucket sea surface temperature data using a physical model. Met. Office Synoptic Climatology Branch Memo No. 154.

Folland, C. K., D. E. Parker and F. E. Kates, 1984: World wide marine temperature fluctuations 1856–1981. *Nature*, **310**, 670–673.

Hahn, C. J., S. G. Warren and J. London, 1992: The use of COADS ship observations in cloud climatologies. *Proceedings of the International COADS Workshop, Boulder, Colorado, 13–15 January*, U. S. Dept. of Commerce NOAA/ERL, 271–280.

Hall, M. M., and H. L. Bryden, 1982: Direct estimates and mechanisms of ocean heat transport. *Deep–Sea Res.*, **29**, 339–359.

Halpern, D., 1988: Moored surface wind observations at four sites along the Pacific Equator between 140° and 95° W. *J. Climate*, **1**, 1251-1260.

Hastenrath, S., 1982: On meridional heat transports in the world ocean. *J. Phys. Oceanogr.*, **10**, 159-170.

Hsiung, J., 1985: Estimates of global oceanic meridional heat transport. *J. Phys. Oceanogr.*, **15**, 1405–1413.

Hsiung, J., 1986: Mean surface energy fluxes over the global ocean. *J. Geophys. Res.*, **91**, 10 585–10 606.

Isemer, H.–J. and L. Hasse, 1987: *The Bunker Atlas of the North Atlantic Ocean. Vol. 2: Air–sea interactions.* Springer Verlag, 252 pp.

———, 1991: The scientific Beaufort equivalent scale: Effects on wind statistics and climatological air–sea flux estimates in the North Atlantic ocean. *J. Climate*, **4**, 819–836.

Isemer, H.–J., J. Willebrand and L. Hasse, 1989: Fine adjustment of large air-sea energy flux parameterizations by direct estimates of ocean heat transport. *J. Climate*, **2**, 1173–1184.

Kalnay, E., and R. Jenne, 1991: Summary of the NMC/NCAR reanalysis workshop of April 1991. *Bull. Amer. Meteor. Soc.*, **72**, 1897–1904.

Kaufeld, L., 1981: The development of a new Beaufort equivalent scale. *Meteor. Rundsch.*, **34**, 17–23.

Kent, E. C. and P. K. Taylor, 1991: Ships observing marine climate: a catalogue of the Voluntary Observing Ships Participating in the VSOP-NA. *Marine and Oceanographic Activities Report 25*, WMO, Geneva, 123 pp.

Kent, E. C. and P. K. Taylor, 1995: A comparison of sensible and latent heat flux estimates for the North Atlantic ocean. *J. Phys. Oceanogr.*, **25**, 1530–1549.

Kent, E. C., P. K. Taylor, B. S. Truscott and J. S. Hopkins, 1993a: The accuracy of voluntary observing ships' meteorological observations – Results of the VSOP-NA. *J. Atmos. & Oceanic Tech.*, **10**, 591–608.

Kent, E. C., R. J. Tiddy and P. K. Taylor, 1993b: Correction of marine daytime air temperature observations for radiation effects. *J. Atmos. & Oceanic Tech.*, **10**, 900–906.

Kushnir, Y., 1994: Interdecadal variations in North Atlantic sea surface temperature and associated atmospheric conditions. *J. Climate*, **7**, 141–157.

Large, W., and S. Pond, 1981: Open ocean momentum flux measurements in moderate to strong winds. *J. Phys. Oceanogr.*, **11**, 324–336.

Large, W., and S. Pond, 1982: Sensible and latent heat flux measurements over the ocean. *J. Phys. Oceanogr.*, **12**, 464–482.

Levitus, S., 1982: Climatological Atlas of the World Ocean, NOAA Prof. Paper No. 13, U. S. Government Printing Office, Washington D. C., 17 fiches, 173 pp.

List, R. J., 1958: *Smithsonian Meteorological Tables*, 6th Revised Ed. Smithsonian Institution Press, 527 pp.

Oberhuber, J. M., 1988: An Atlas Based on the COADS Data Set: The Budgets of Heat, Buoyancy, and Turbulent Kinetic Energy at the Surface of the Global Ocean. Report No. 15, Max-Planck Institut für Meteorology.

Payne, R. E., 1972: Albedo of the sea surface. *J. Atmos. Sci.*, **29**, 959–970.

Peixoto, J. P., and A. H. Oort, 1992: *Physics of Climate*. American Institute of Physics, 520 pp.

Petersen, P., 1927: Zur Bestimmung der Windstärke auf See. *Ann. Hydrogr.*, **55**, 69–72.

Rabiner, L. R., M. R. Sambur and C. E. Schmidt, 1975: Applications of a nonlinear smoothing algorithm to speech processing. *IEEE Transactions on Acoustics, Speech, and Signal Processing*, **ASSP–23**, 552–557.

Rago, T. T., and H. T. Rossby, 1987: Heat transport into the North Atlantic Ocean north of 27°N latitude. *J. Phys. Oceanogr.*, **17**, 854–871.

Ramage, C. S., 1984: Can shipboard measurements reveal secular changes in tropical air–sea heat flux? *J. Climate Appl. Meteor.*, **23**, 187–193.

Reed, R. K., 1977: On estimating insolation over the oceans. *J. Phys. Oceanogr.*, **7**, 482-485.

Rew, R., G. Davis and S. Emmerson, 1993: *NetCDF User's Guide, an Interface for Data Access*. Unidata Program Center, University Corporation for Atmospheric Research, Boulder, CO, 186 pp.

Reynolds, R. W., 1988: A real–time global sea surface temperature analysis. *J. Climate*, **1**, 75–86.

Riehl, H., 1947: Diurnal variation of cloudiness over the subtropical Atlantic ocean. *Bull. Amer. Meteor. Soc.*, **28**, 37–40.

Roll, H. U., 1965: *Physics of the Marine Atmosphere*. Int. Geophys. Ser., Vol. 7, 426 pp.

Rosati, A., and K. Miyakoda, 1988: A general circulation model for the upper ocean circulation. *J. Phys. Oceanogr.*, **18**, 1601–1626.

Schlatter, T. W., and D. V. Baker, 1981: Algorithms for thermodynamic calculations. NOAA/ERL PROFS Program Office, Boulder, CO, 34 pp.

Schmitt, R. W., P. S. Bogden and C. E. Dorman, 1989: Evaporation minus precipitation and density fluxes for the North Atlantic. *J. Phys. Oceanogr.*, **19**, 1208–1221.

Schneider, G., P. Paluzzi and J. P. Oliver, 1989: Systematic error in the synoptic sky cover record of the South Pole. *J. Climate*, **2**, 295–302.

Schubert, S. D., R. B. Rood and J. Pfaendtner, 1993: An assimilated dataset for earth sciences applications. *Bull. Amer. Meteor. Soc.*, **74**, 2331–2342.

Shapiro, R., 1970: Smoothing, filtering, and boundary effects. *Rev. of Geophys. and Space Phys.*, **8**, 359–387.

da Silva, A. M., C. C. Young and S. Levitus, 1994: *Atlas of Surface Marine Data 1994*. NOAA Atlas NESDIS 6–10, U. S. Government Printing Office, Washington, D.C., 5 volumes.

Simpson, G. C., 1906: The velocity equivalents of the Beaufort scale. Rep. of Director of Meteorological Office No. 180, London.

Simpson, J. J. and C. A. Paulson, 1979: Mid-ocean observations of atmospheric radiation. *Q. J. Royal Meteor. Soc.*, **105**, 487–502.

Slutz, R. J., S. J. Lubker, J. D. Hiscox, S. D. Woodruff, R. L. Jenne, D. H. Joseph, P. M. Steurer and J.

D. Elms, 1985: COADS, Comprehensive Ocean–Atmosphere Data Set, Release 1. Climate Research Program, Environmental Research Laboratory, Boulder, CO, 262 pp.

Stommel, H. 1980: Assymetry of interoceanic freshwater and heat fluxes. *Proc. Natl. Acad. Sci. USA*, **77**, 2377–2381.

Sverdrup, H. U., 1933: *The Norwegian North Polar Expedition with the "Maud", 1918–1925, Scientific Results*, Vol. II: Meteorology, Part I, Discussion, John Griegs, Bergen, 331 pp.

Trenberth, K. E., W. G. Large and J. G. Olson, 1990: The mean annual cycle in global ocean wind stress. *J. Phys. Oceanogr.*, **20**, 1742-1760.

Tucker, G. B., 1961: Precipitation over the North Atlantic Ocean. *Q. J. Royal Meteor. Soc.*, **87**, 147–158.

U. S. Government Printing Office, 1990: *Astronomical Almanac*. Nautical Almanac Office, United States Naval Observatory.

Wijffels, S. E., R. W. Schmitt, H. L. Bryden and A. Stigebrandt, 1992: Transport of freshwater by the oceans. *J. Phys. Oceanogr.*, **22**, 155–162.

Wolter, K. 1992: Sifting out erroneous observations in COADS — the trimming problem. *Proceedings of the International COADS Workshop, Boulder, Colorado, 13–15 January*, U. S. Dept. of Commerce NOAA/ERL, 91–101.

Woodruff, S. D., S. J. Lubker, K. Wolter, S. J. Worley and J. D. Elms, 1993: Comprehensive Ocean-Atmosphere Data Set (COADS) Release 1a: 1980-92. *Earth System Monitor*, **4**:1.

Woodruff, S. D., R. J. Slutz, R. L. Jenne and P. M. Steurer, 1987: A comprehensive ocean–atmosphere data set. *Bull. Amer. Meteor. Soc.*, **68**, 1239–1250.

World Meteorological Organization (WMO), 1970: Reports on marine science affairs. Rep. No. 3: The Beaufort scale of wind force. WMO, Geneva, Switzerland, 22 pp.

World Meteorological Organization (WMO), 1990: International list of selected, suplementary and auxiliary ships. *WMO Publ. No. 47*, World Meteorological Organization, Geneva.

Wunsch, C., 1984: An eclectic Atlantic Ocean circulation model. Part I: The meridional flux of heat. *J. Phys. Oceanogr.*, **14**, 1712–1733.

13 Seasonal maps

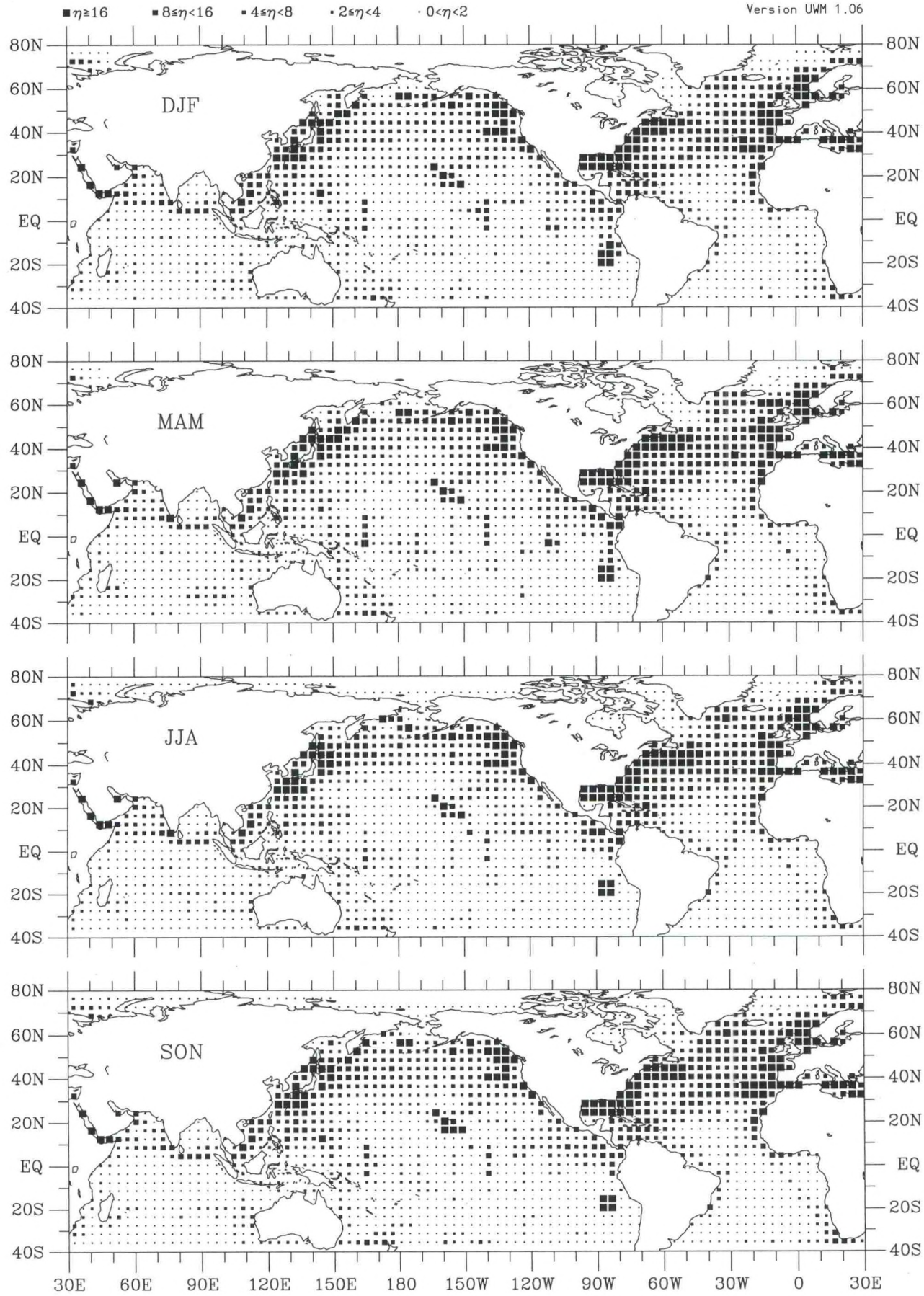

Figure sst-1. Sea surface temperature seasonal observation density (1990-93).

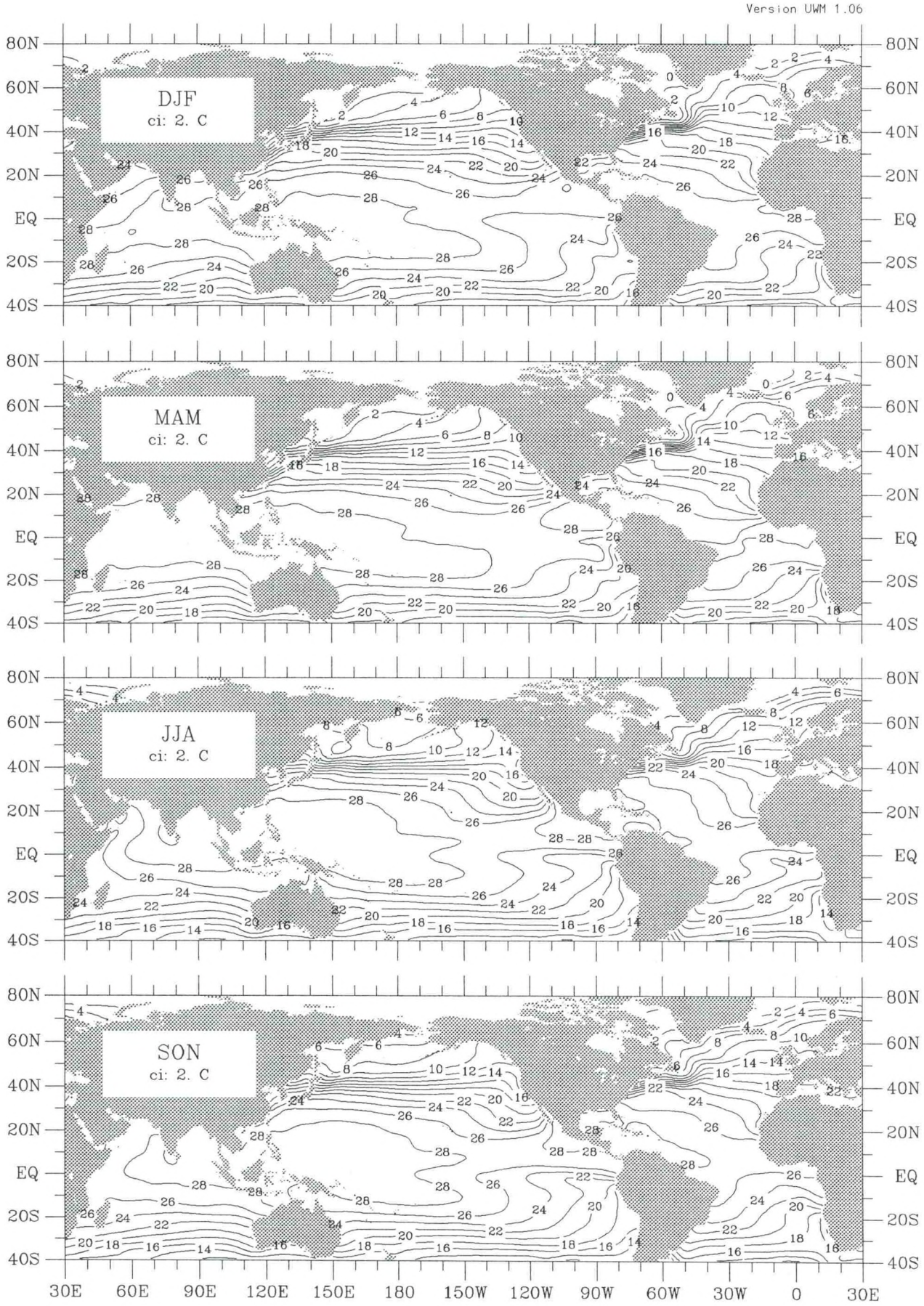

Figure sst–2. Sea surface temperature seasonal climatology (1945–89).

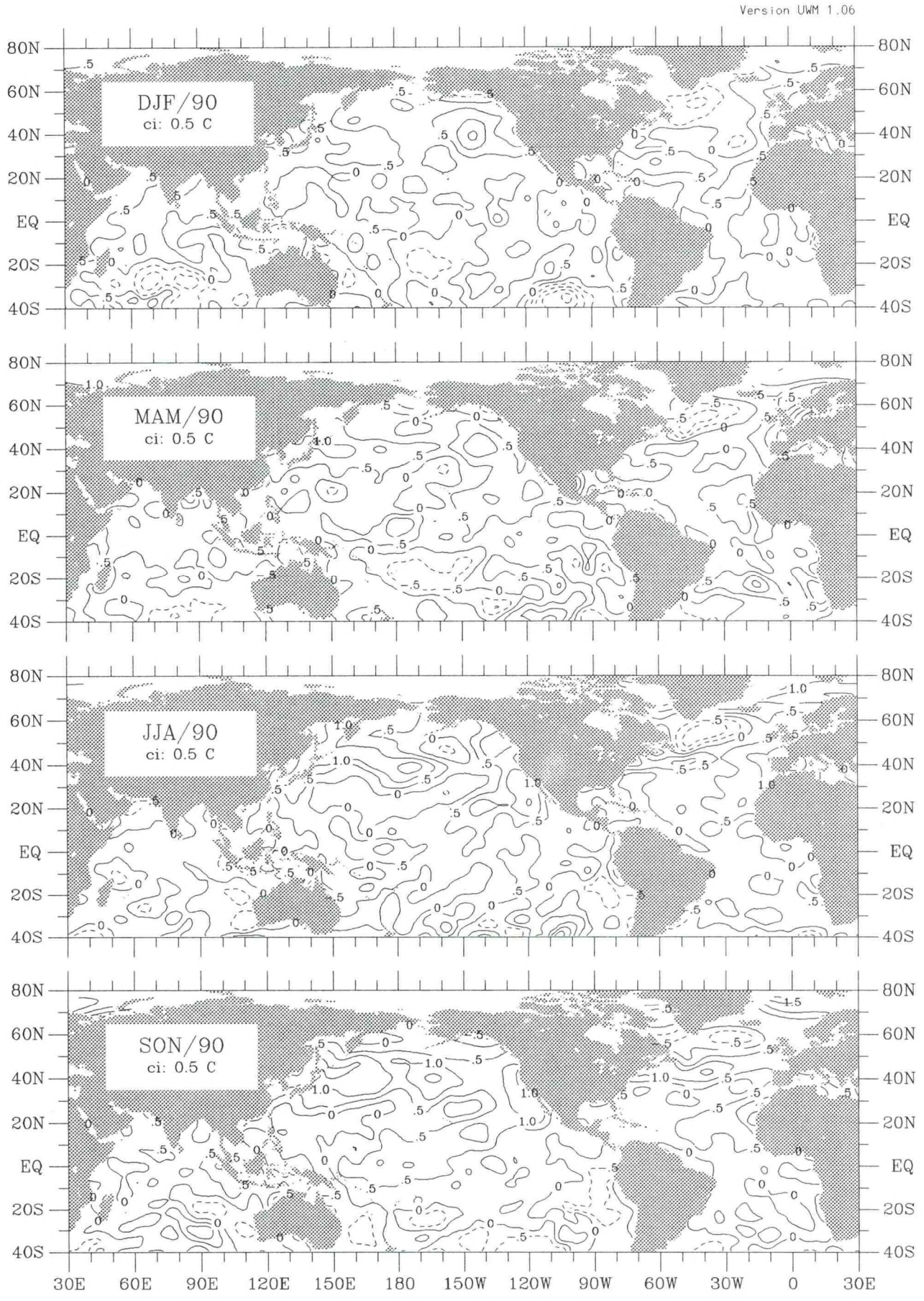

Figure sst-3. Sea surface temperature seasonal anomaly for 1990.

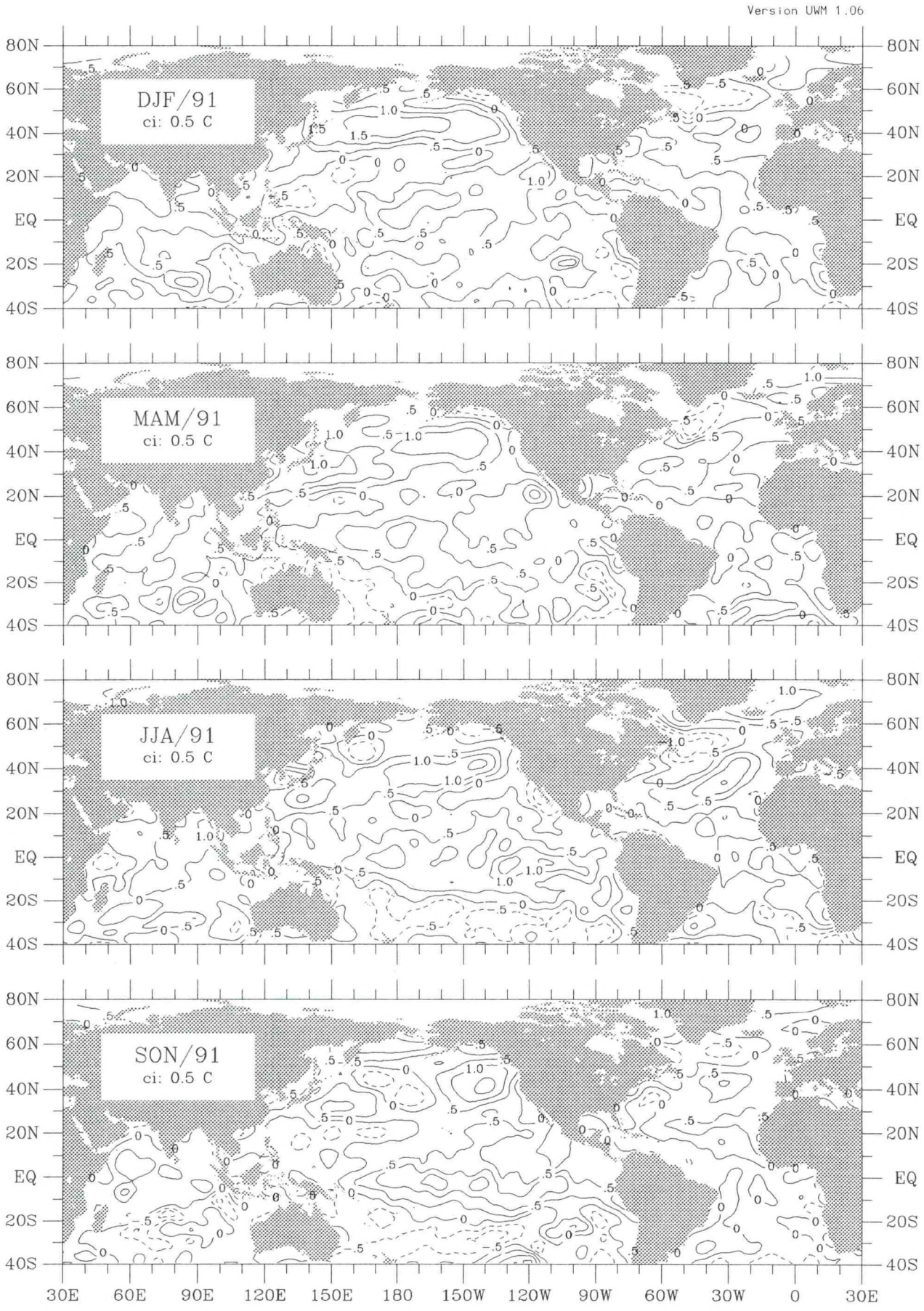

Figure sst-4. Sea surface temperature seasonal anomaly for 1991.

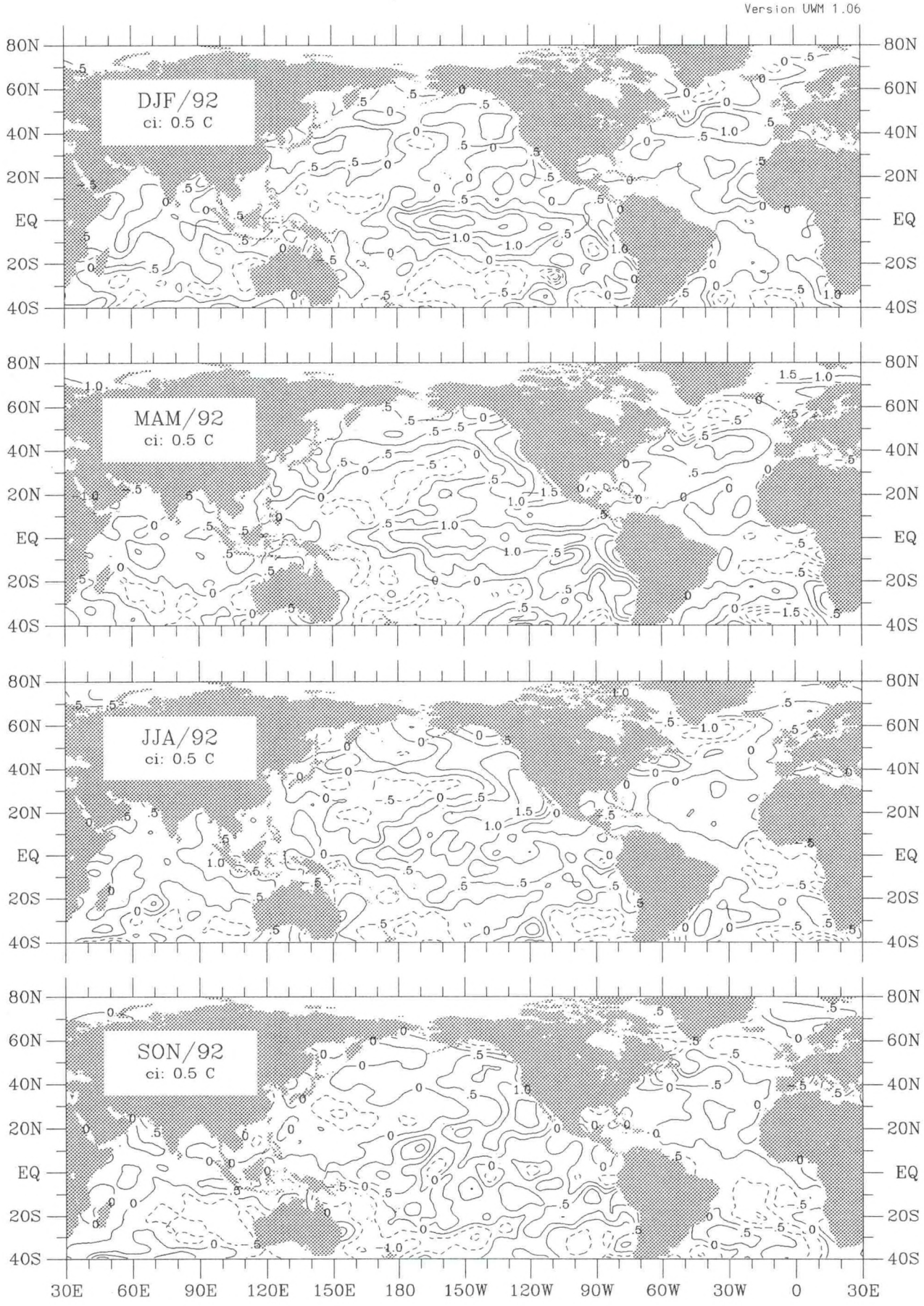

Figure sst–5. Sea surface temperature seasonal anomaly for 1992.

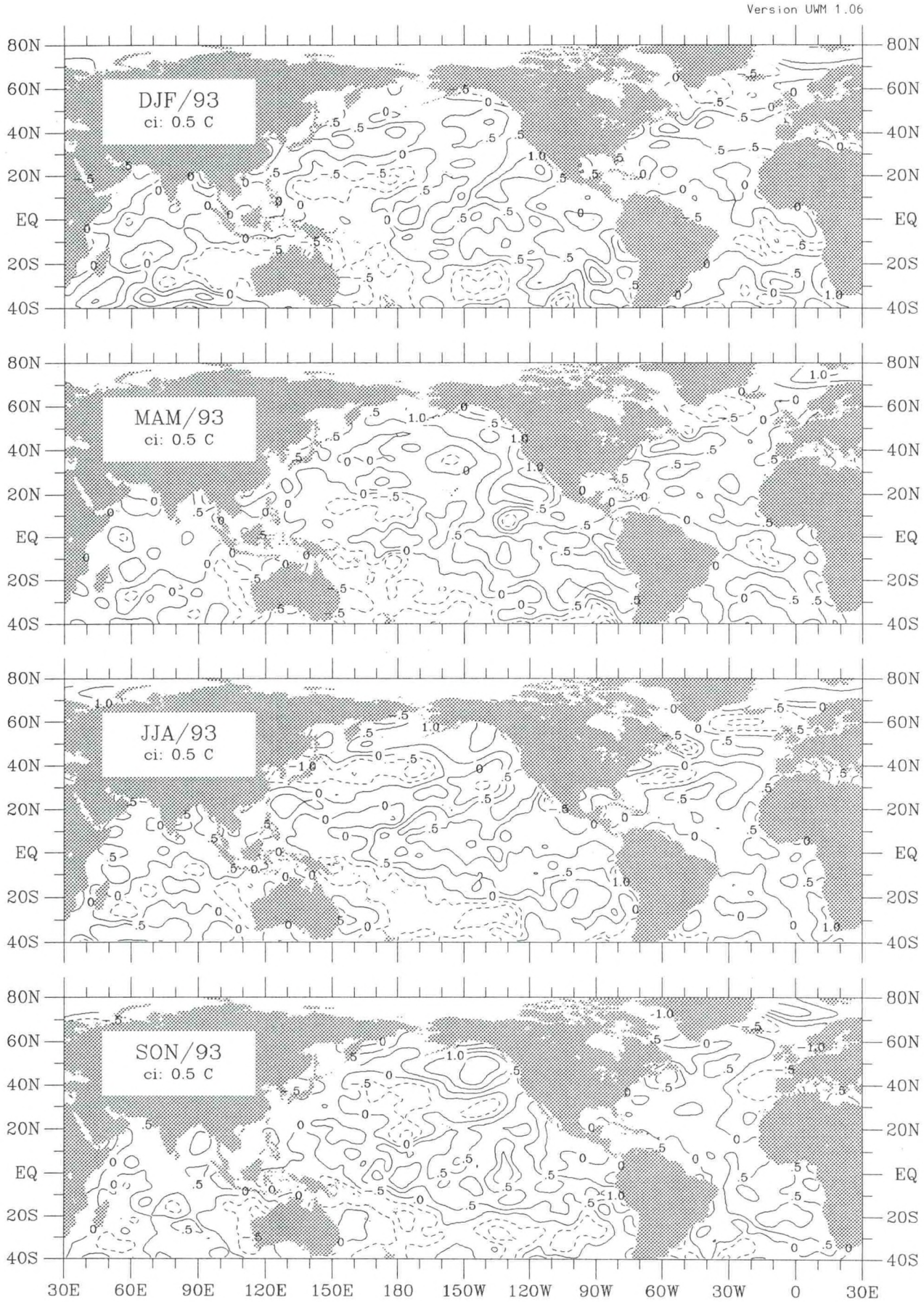

Figure sst-6. Sea surface temperature seasonal anomaly for 1993.

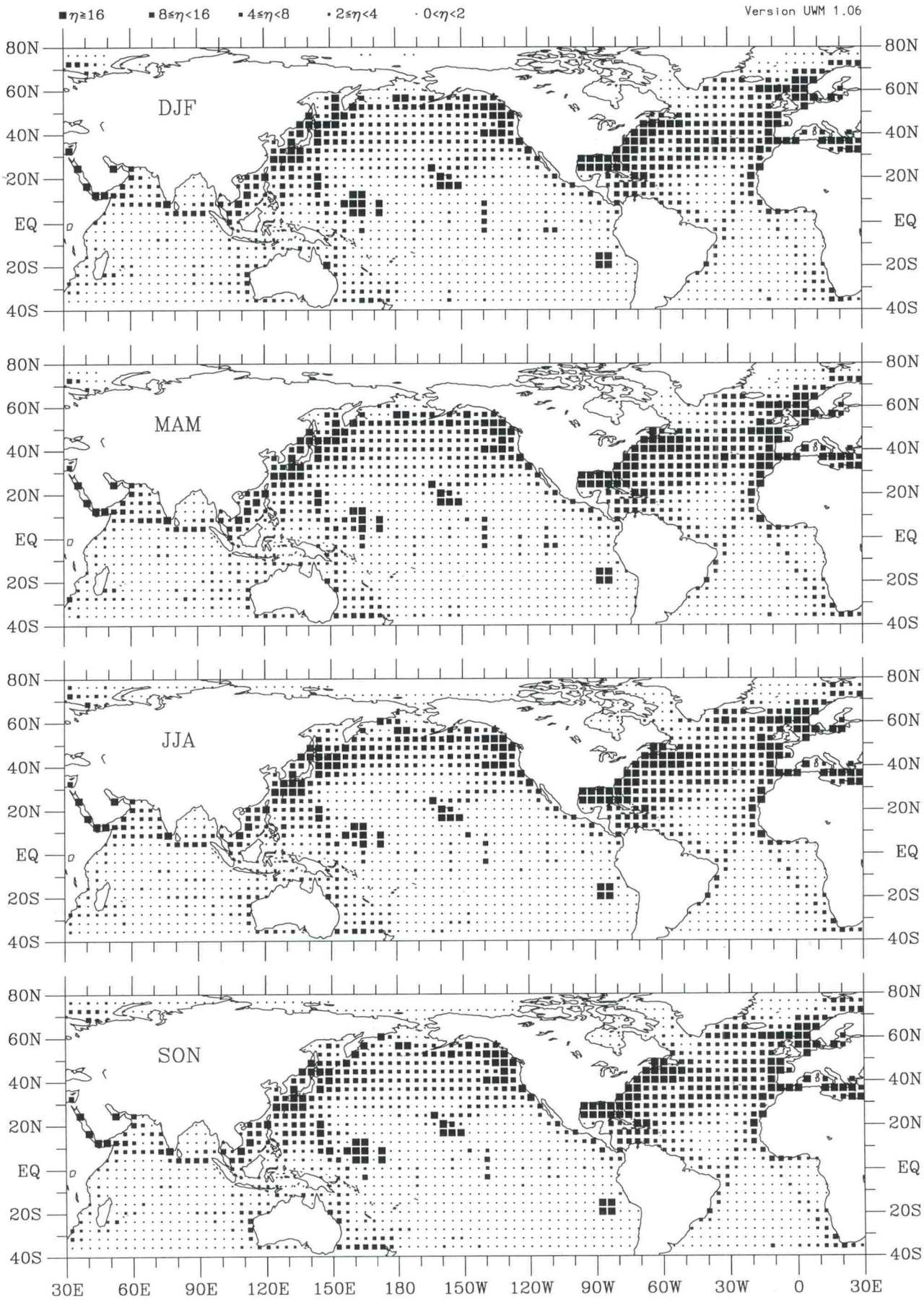

Figure sat−1. Air temperature seasonal observation density (1990−93).

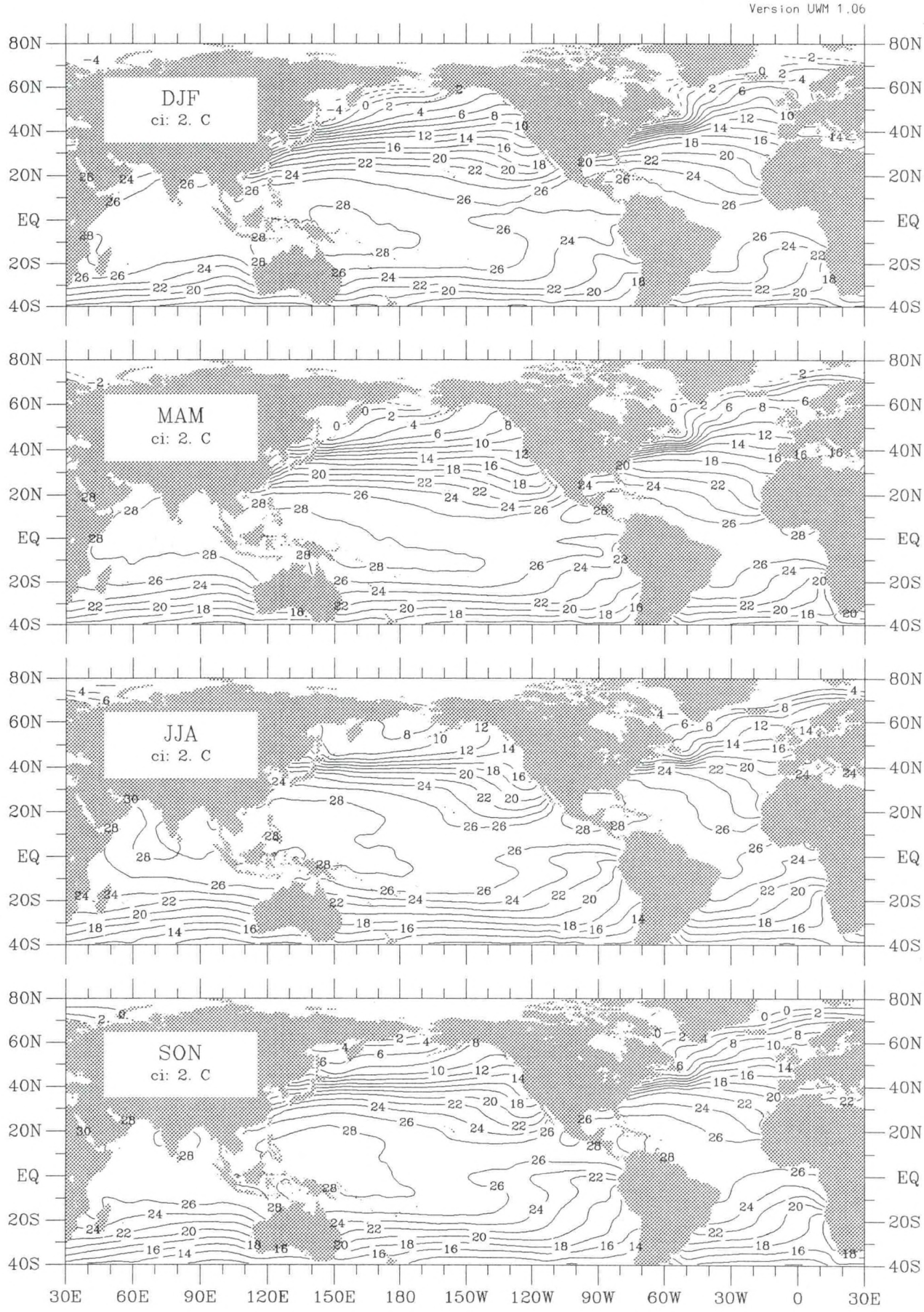

Figure sat-2. Air temperature seasonal climatology (1945-89).

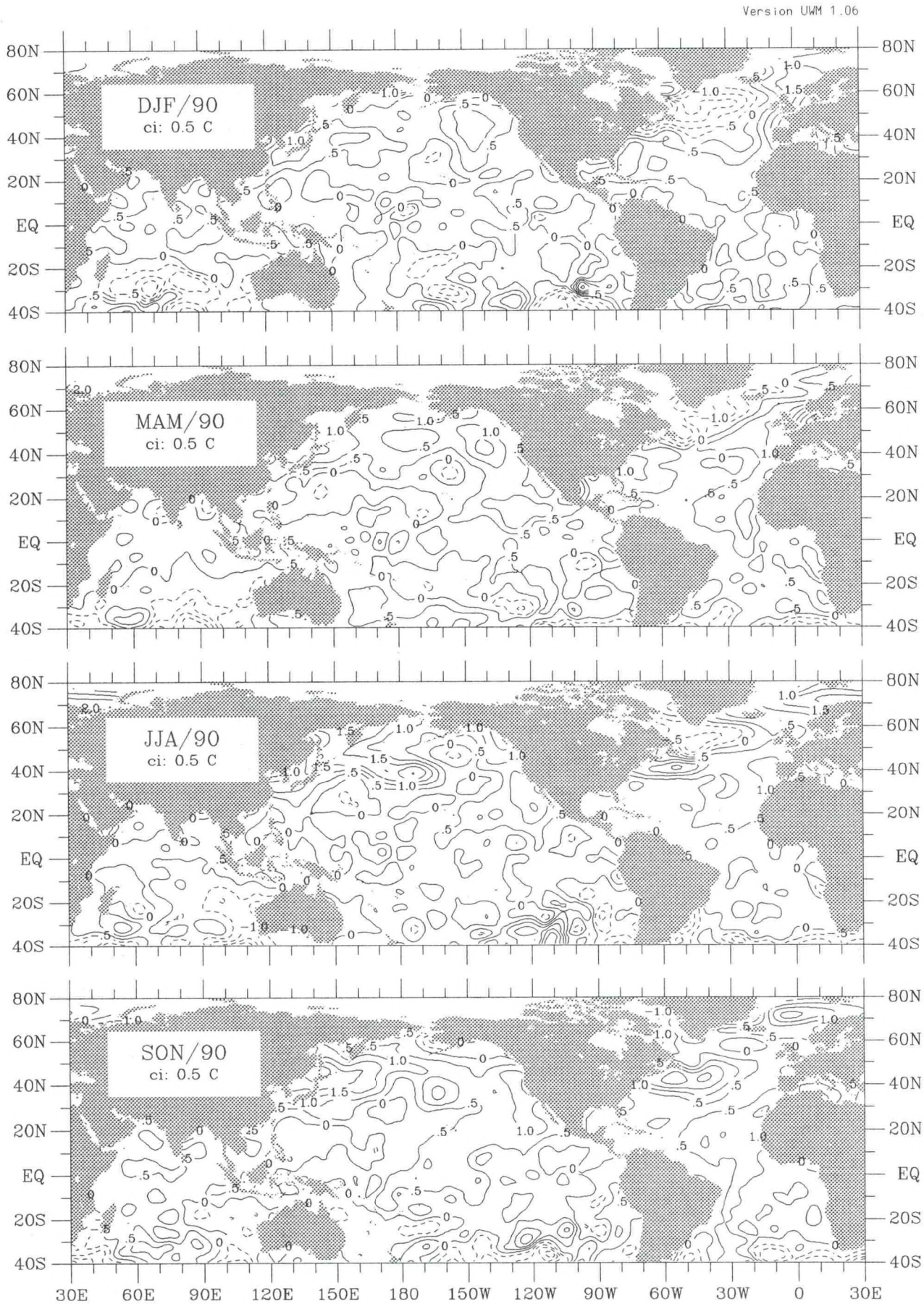

Figure sat-3. Air temperature seasonal anomaly for 1990.

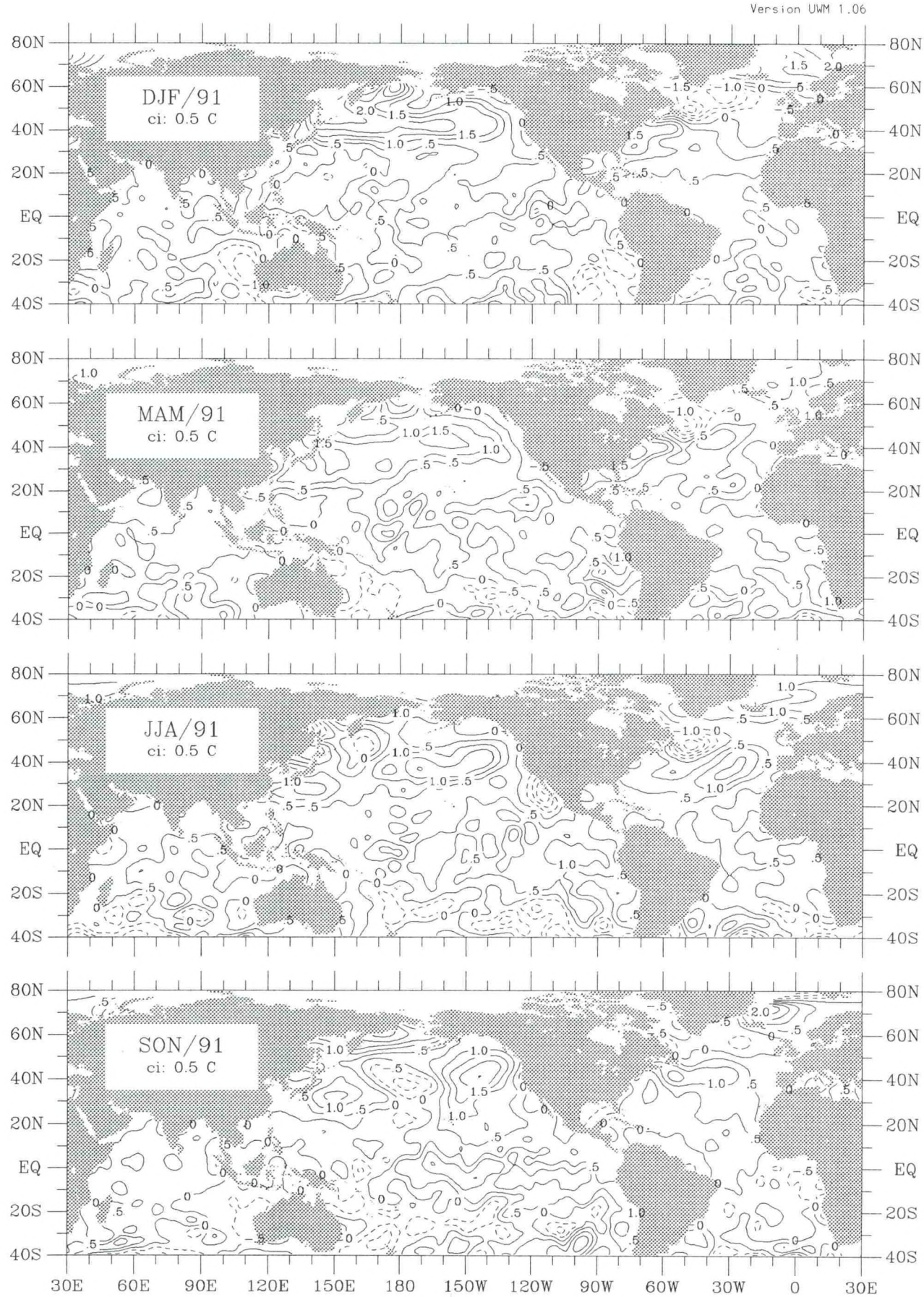

Figure sat-4. Air temperature seasonal anomaly for 1991.

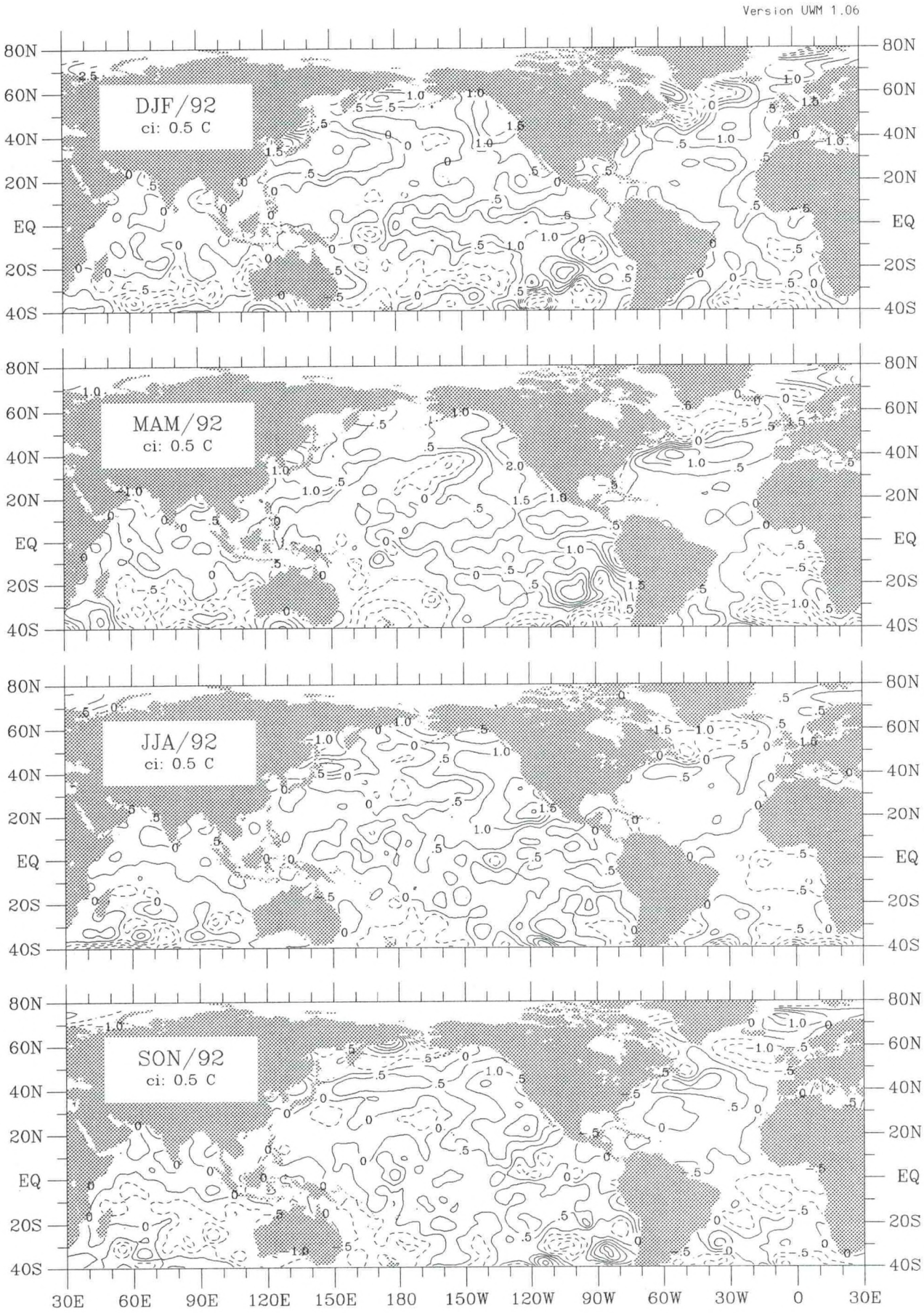

Figure sat-5. Air temperature seasonal anomaly for 1992.

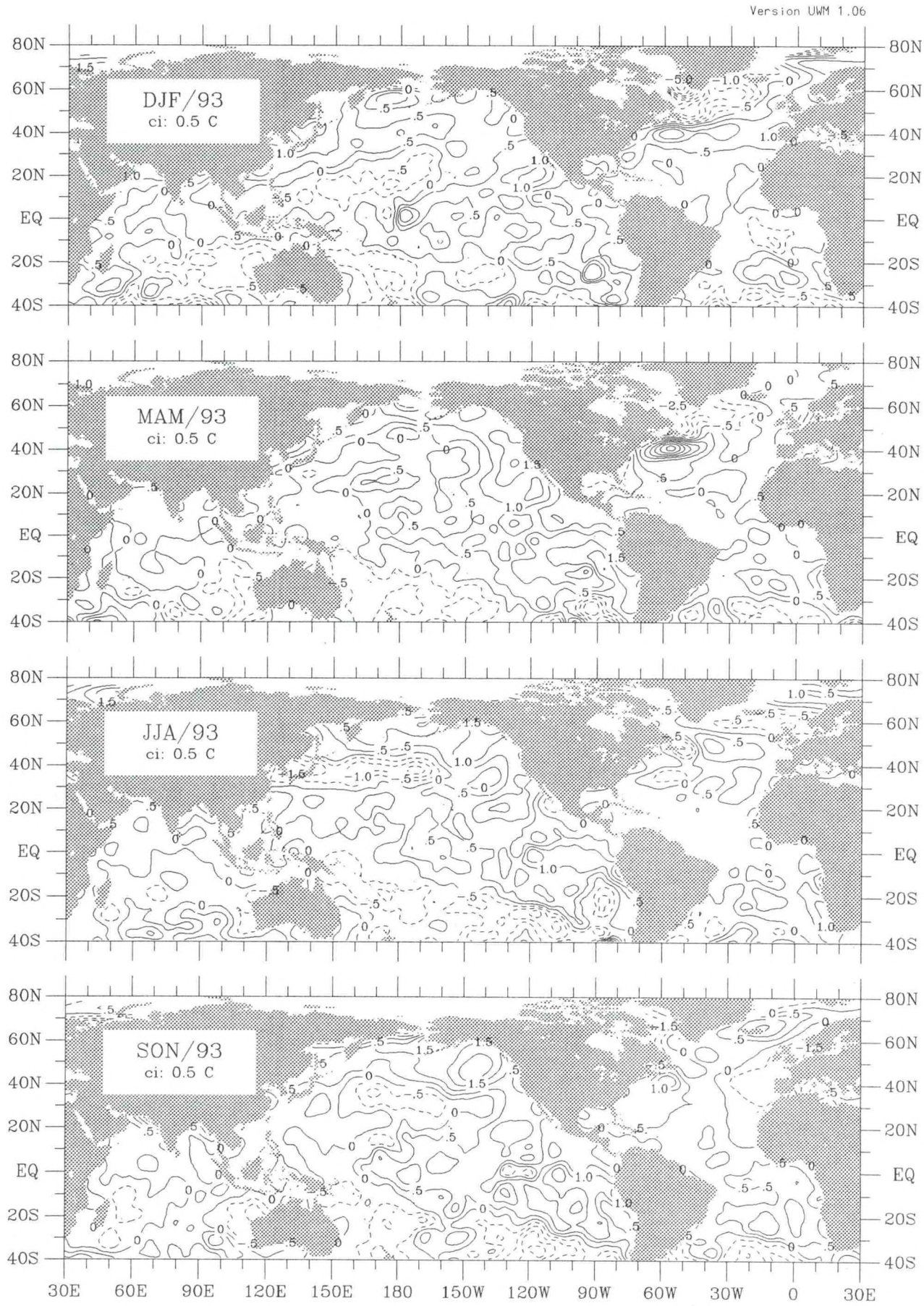

Figure sat-6. Air temperature seasonal anomaly for 1993.

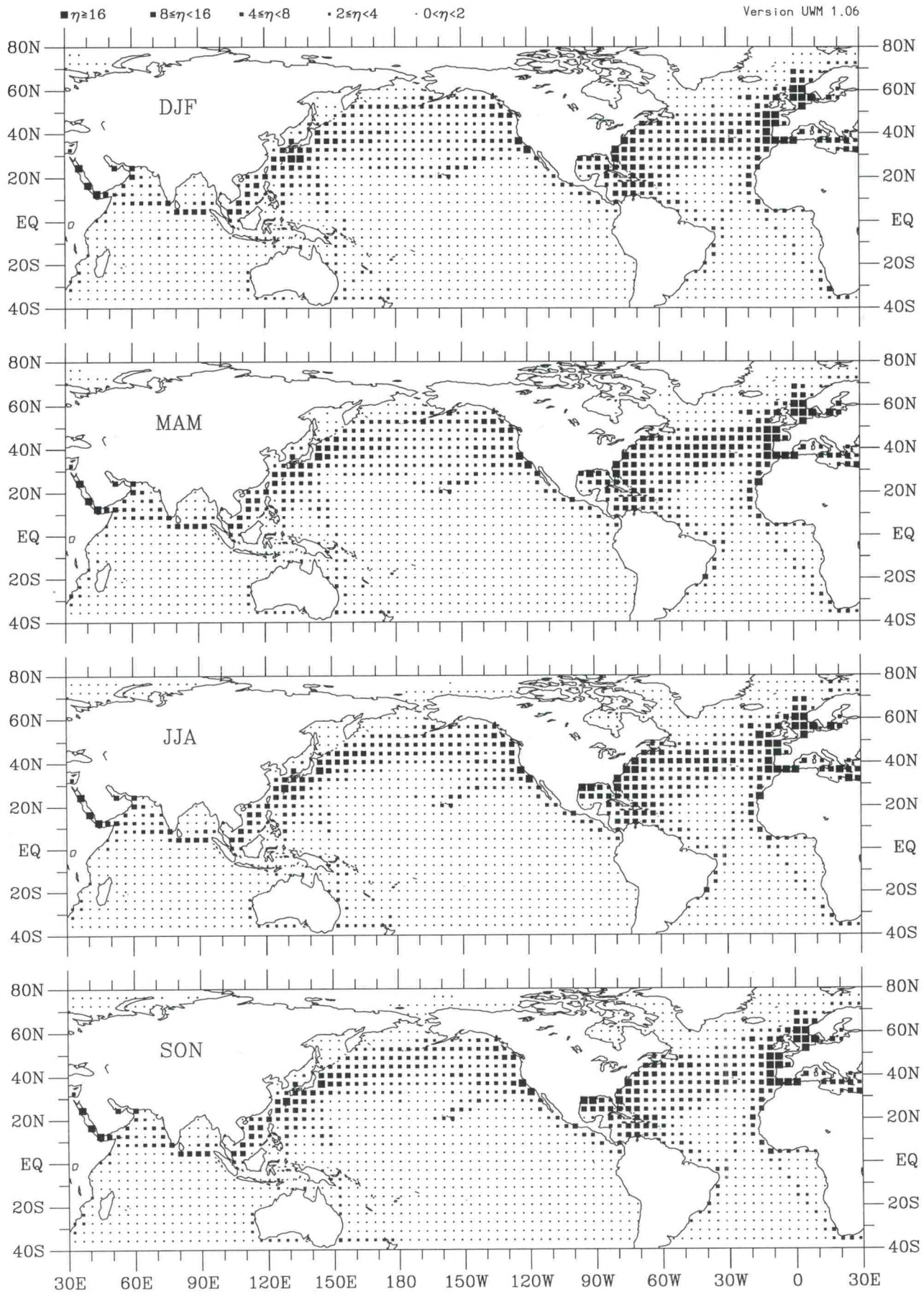

Figure q−1. Specific humidity seasonal observation density (1990−93).

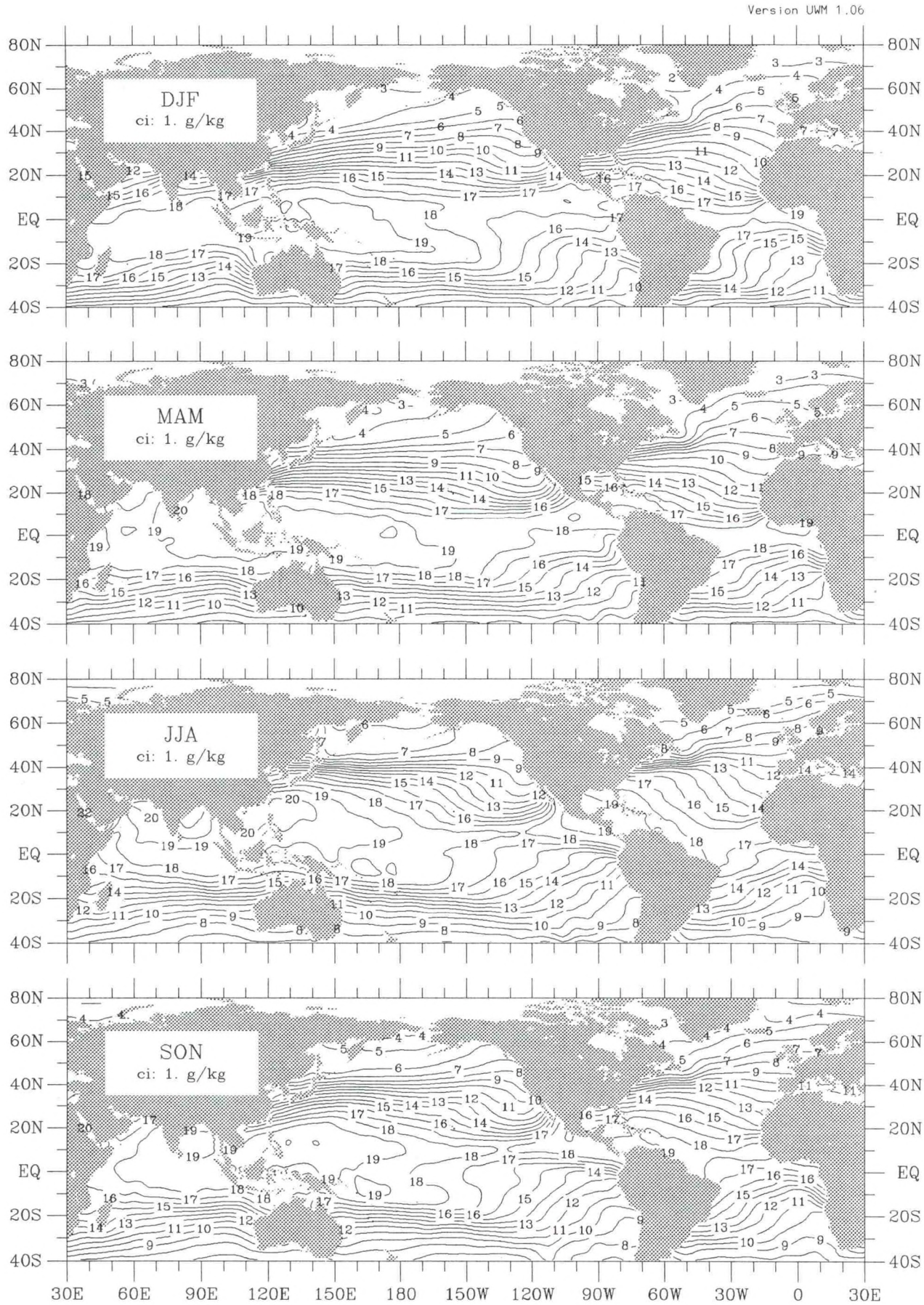

Figure q-2. Specific humidity seasonal climatology (1945-89).

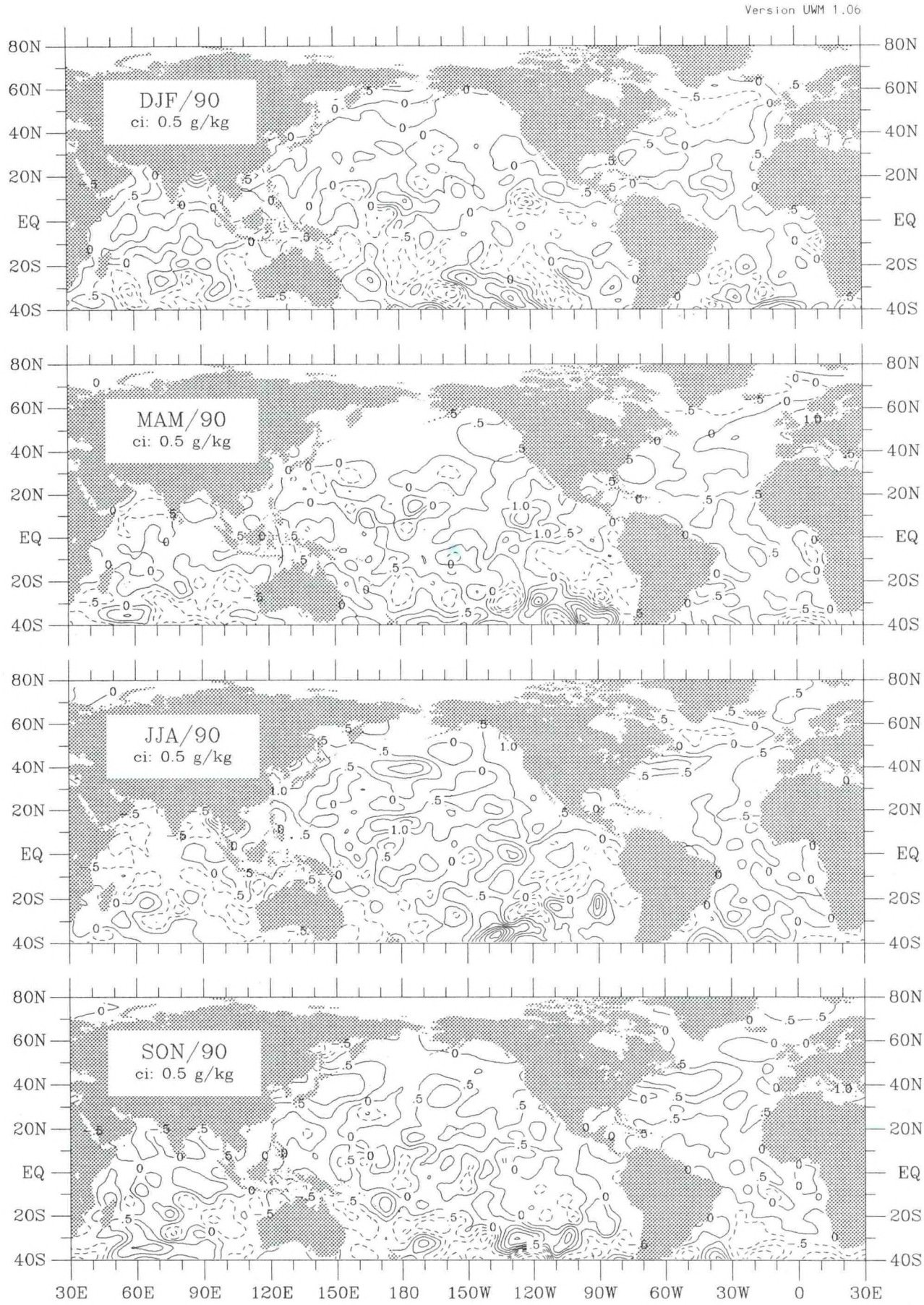

Figure q-3. Specific humidity seasonal anomaly for 1990.

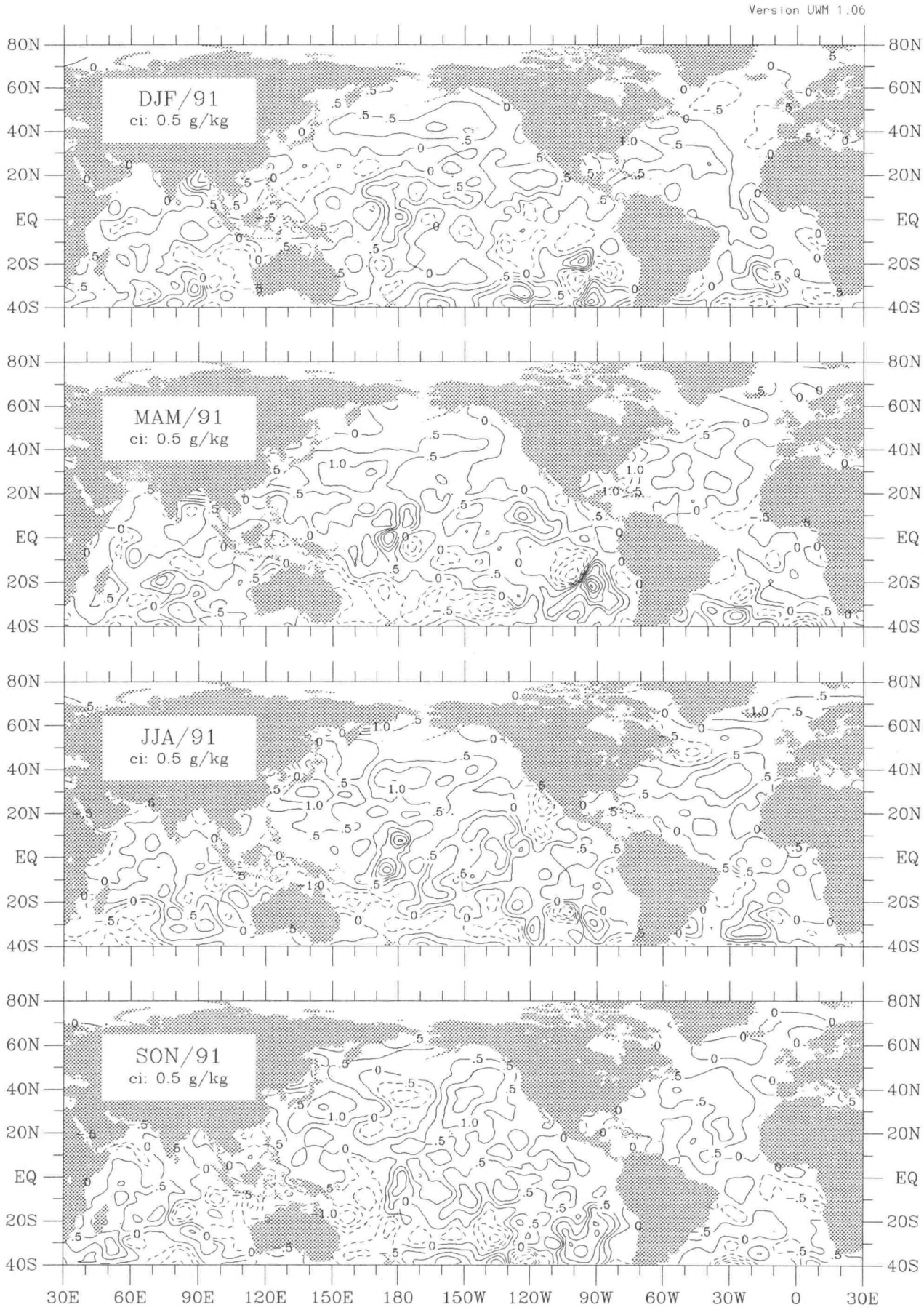

Figure q-4. Specific humidity seasonal anomaly for 1991.

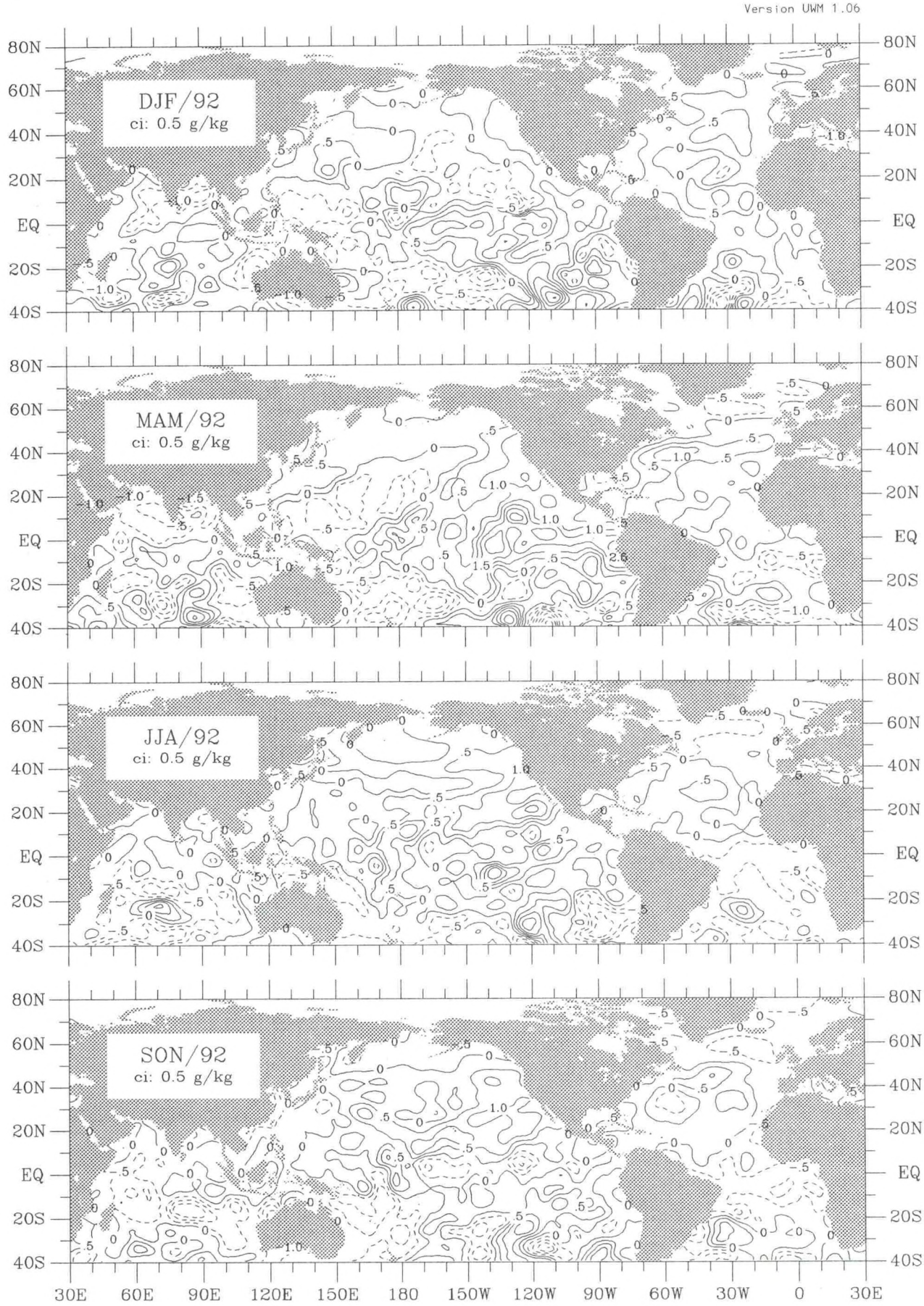

Figure q-5. Specific humidity seasonal anomaly for 1992.

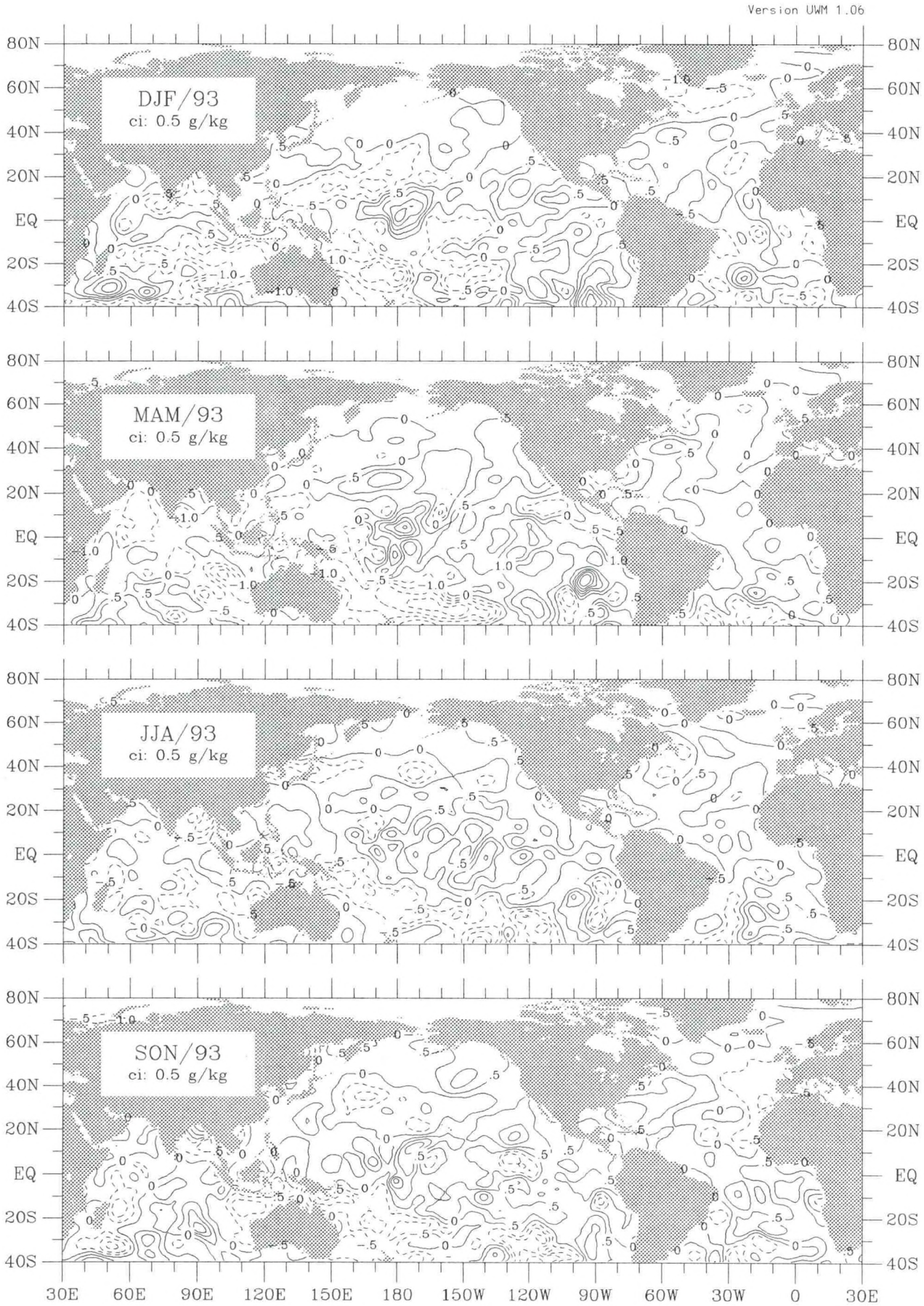

Figure q-6. Specific humidity seasonal anomaly for 1993.

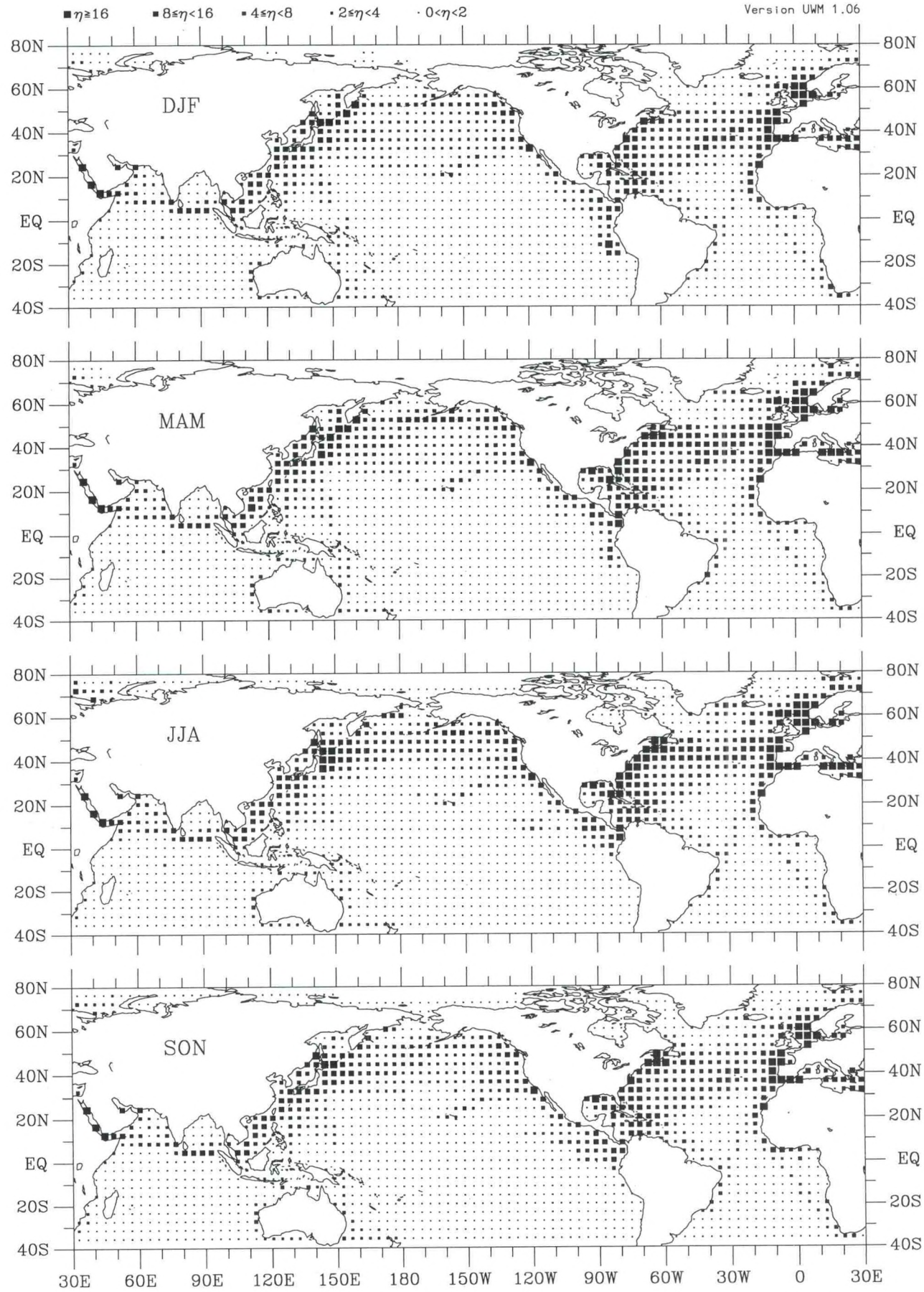

Figure c−1. Fractional cloud cover seasonal observation density (1990−93).

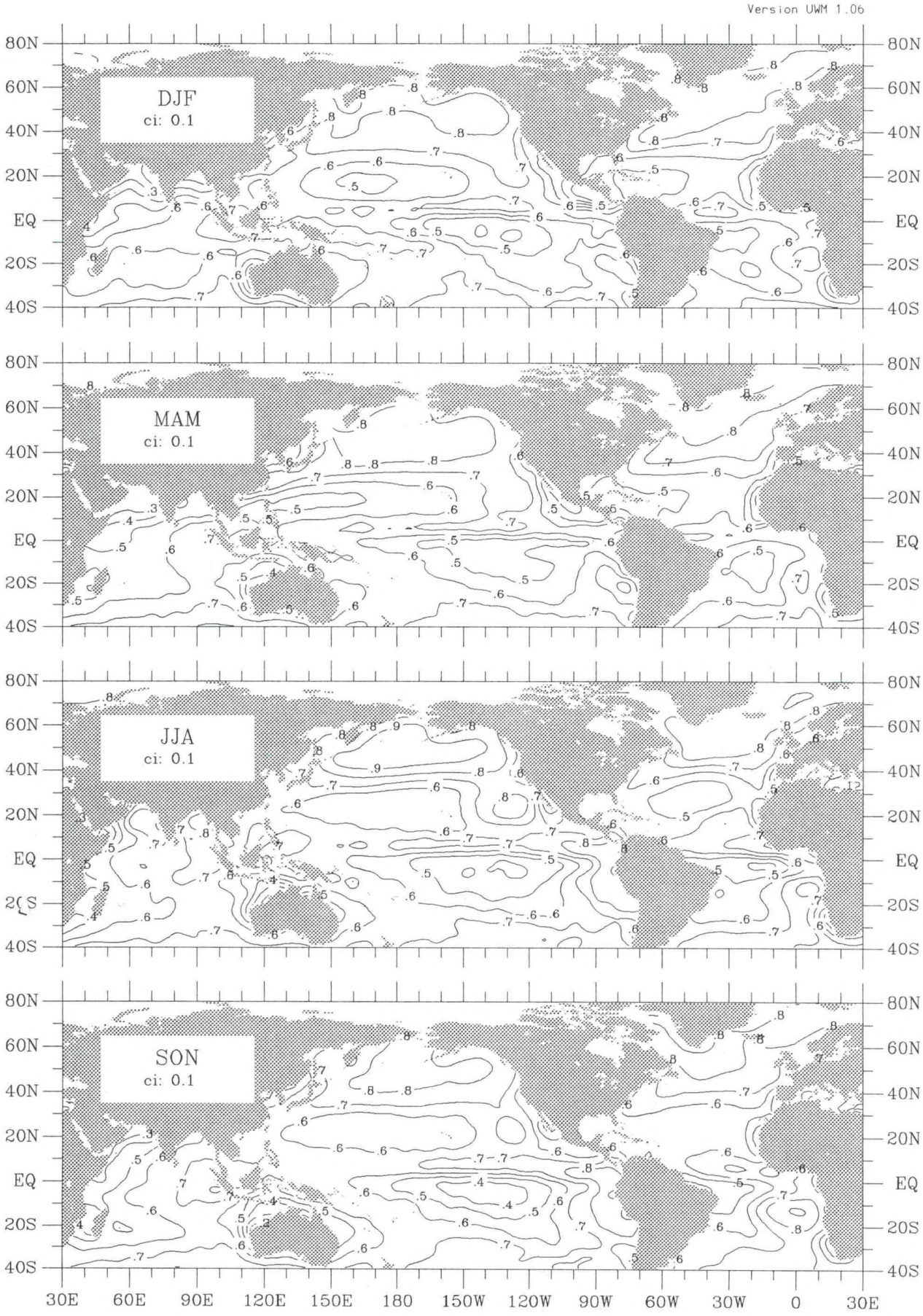

Figure c-2. Fractional cloud cover seasonal climatology (1945-89).

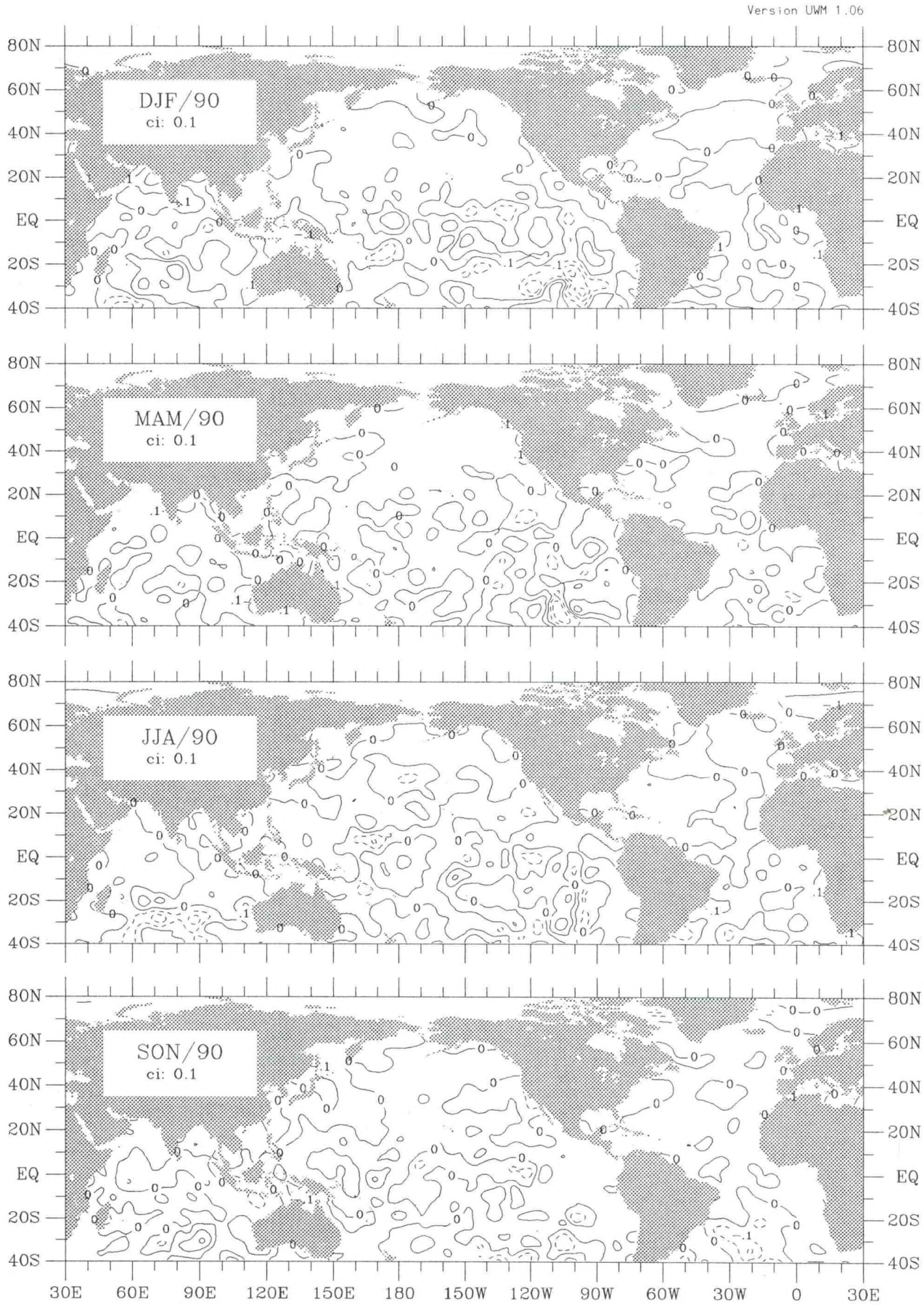

Figure c-3. Fractional cloud cover seasonal anomaly for 1990.

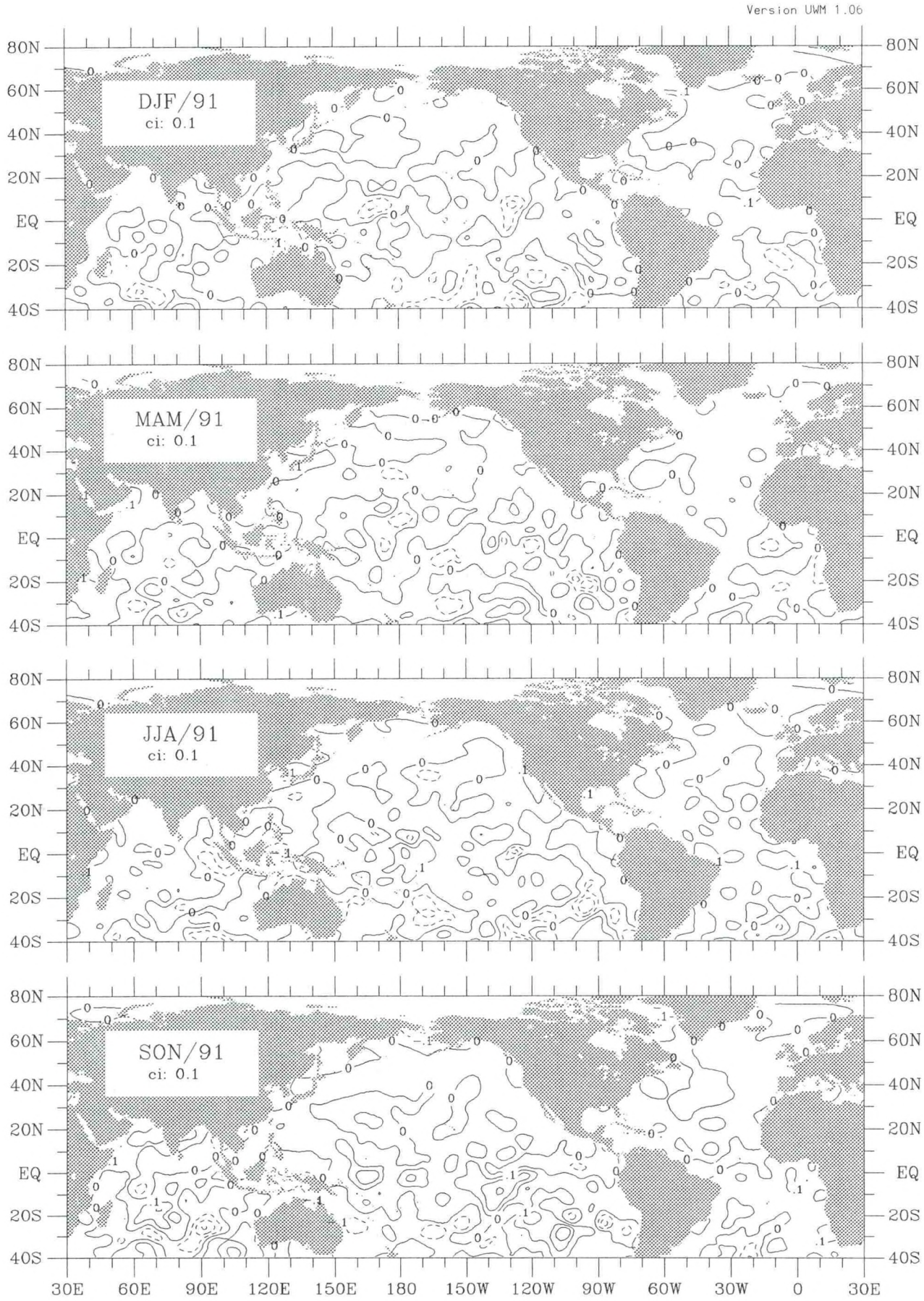

Figure c-4. Fractional cloud cover seasonal anomaly for 1991.

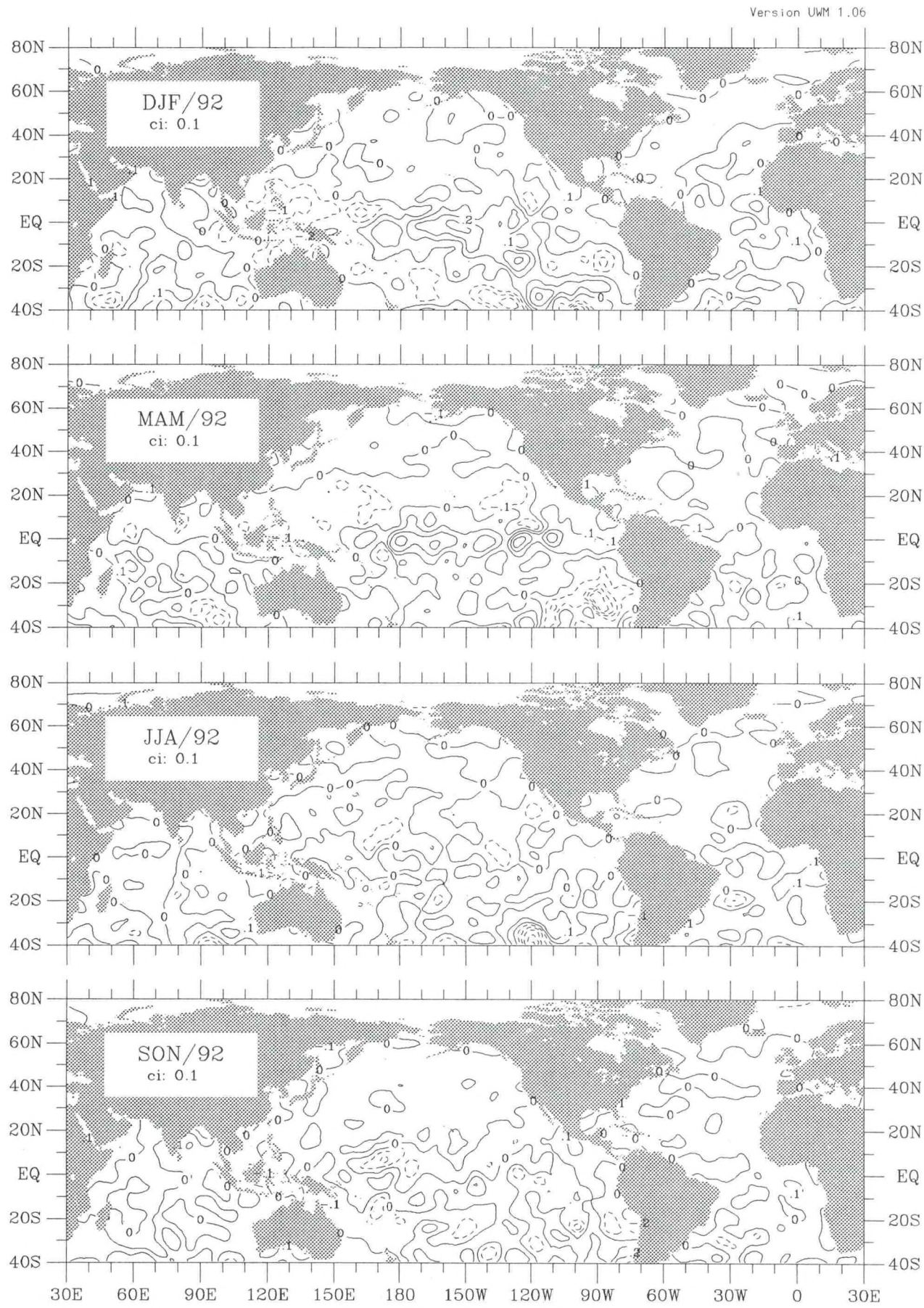

Figure c-5. Fractional cloud cover seasonal anomaly for 1992.

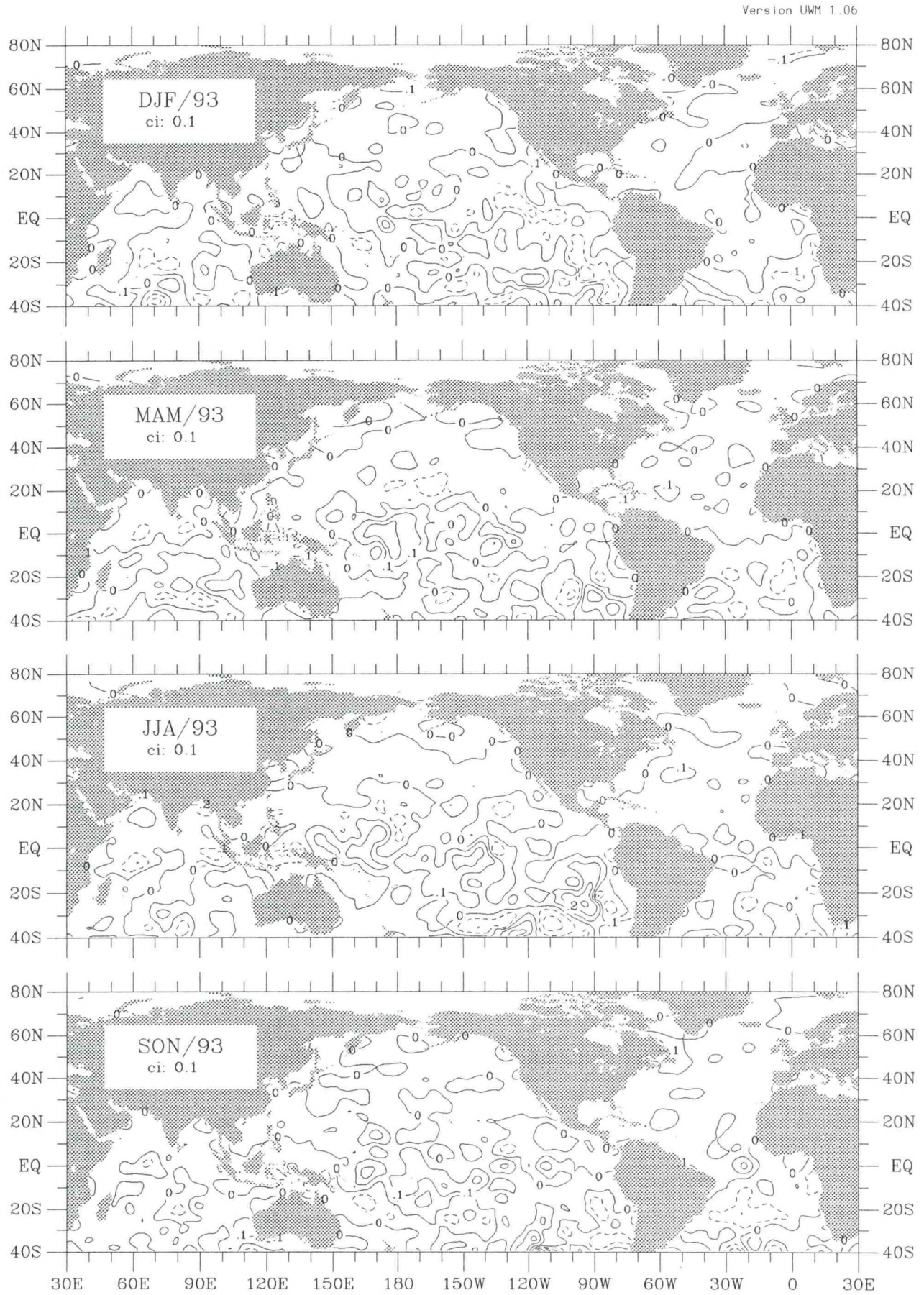

Figure c-6. Fractional cloud cover seasonal anomaly for 1993.

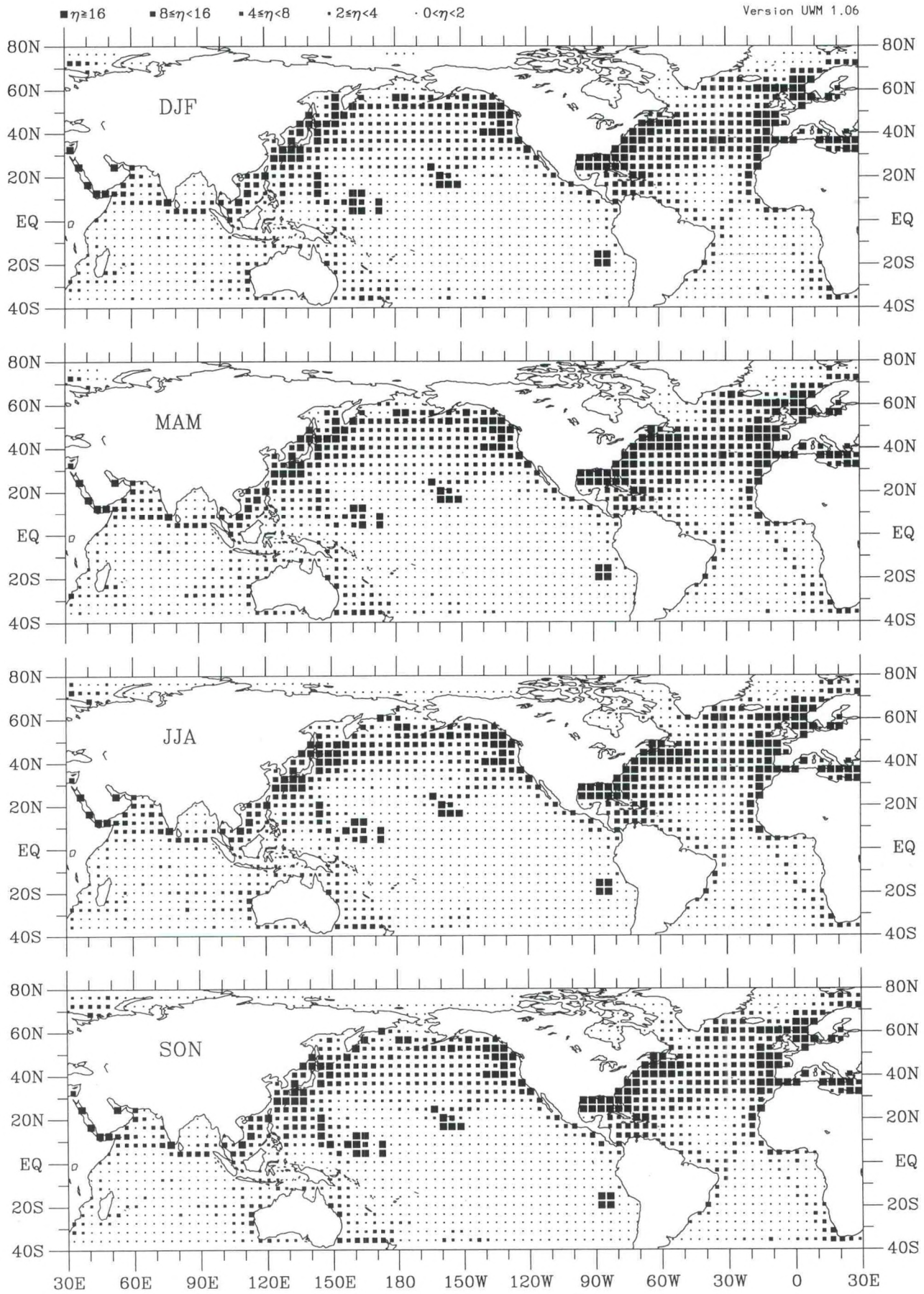

Figure slp−1. Sea level pressure seasonal observation density (1990−93).

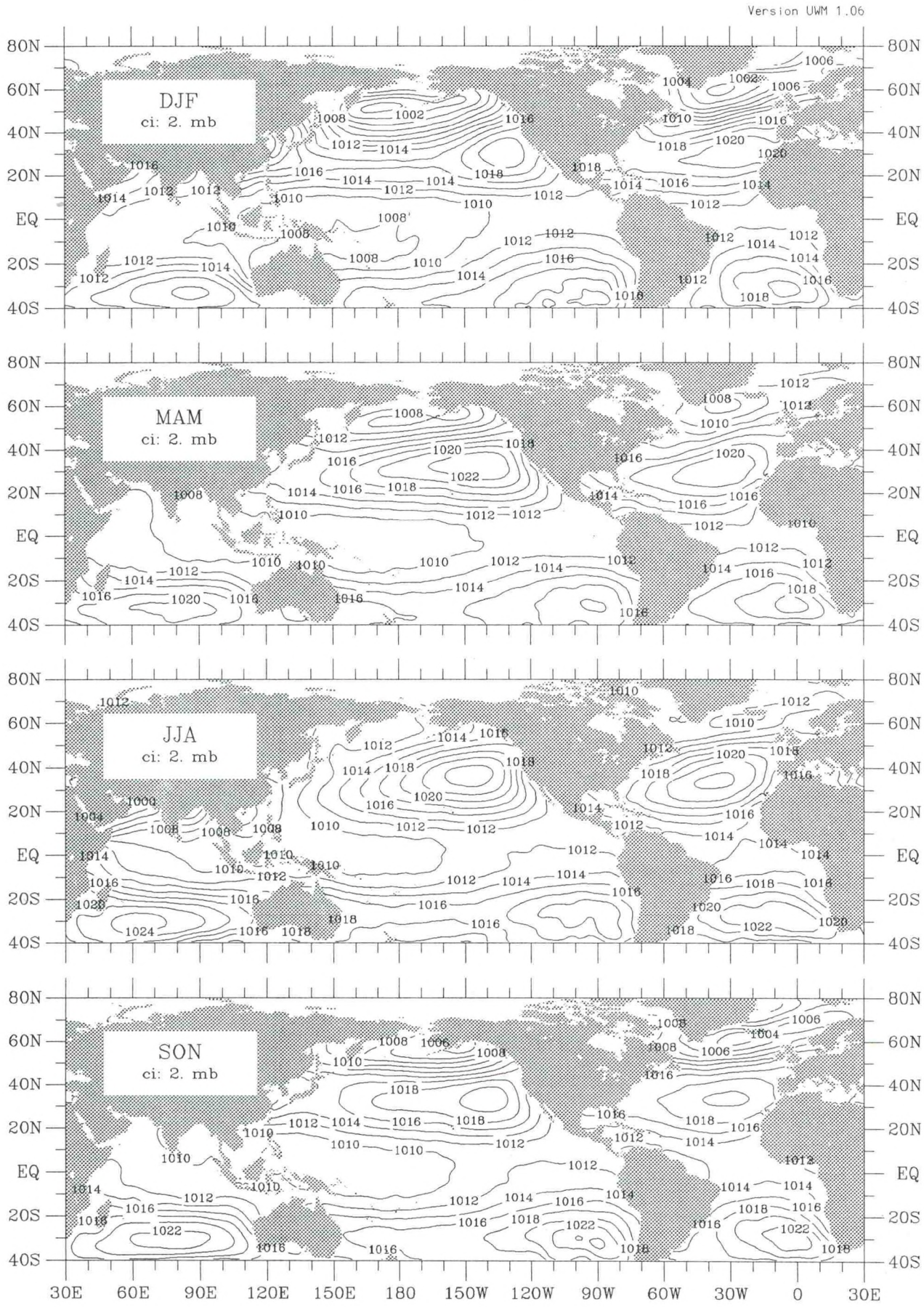

Figure slp-2. Sea level pressure seasonal climatology (1945-89).

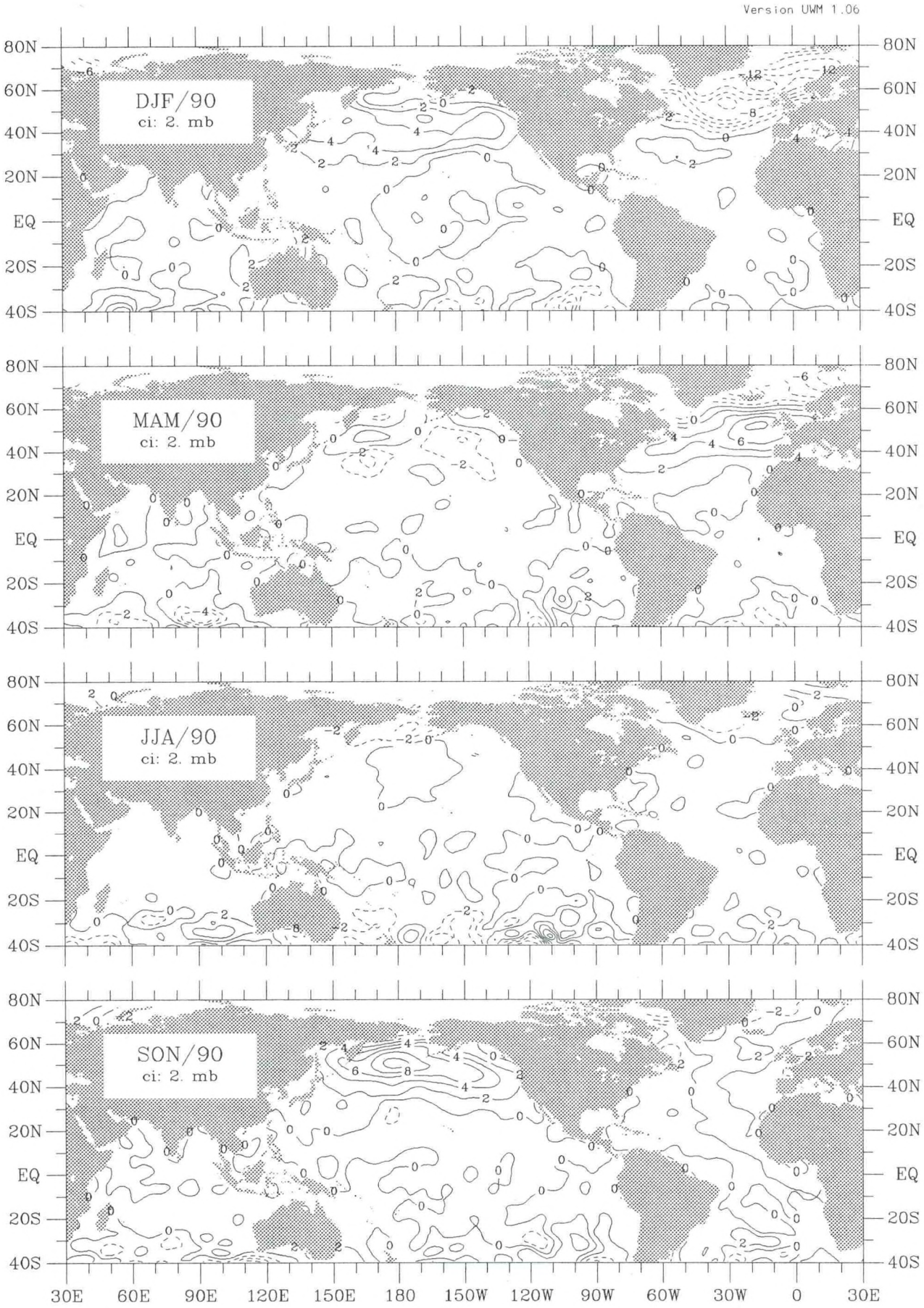

Figure slp-3. Sea level pressure seasonal anomaly for 1990.

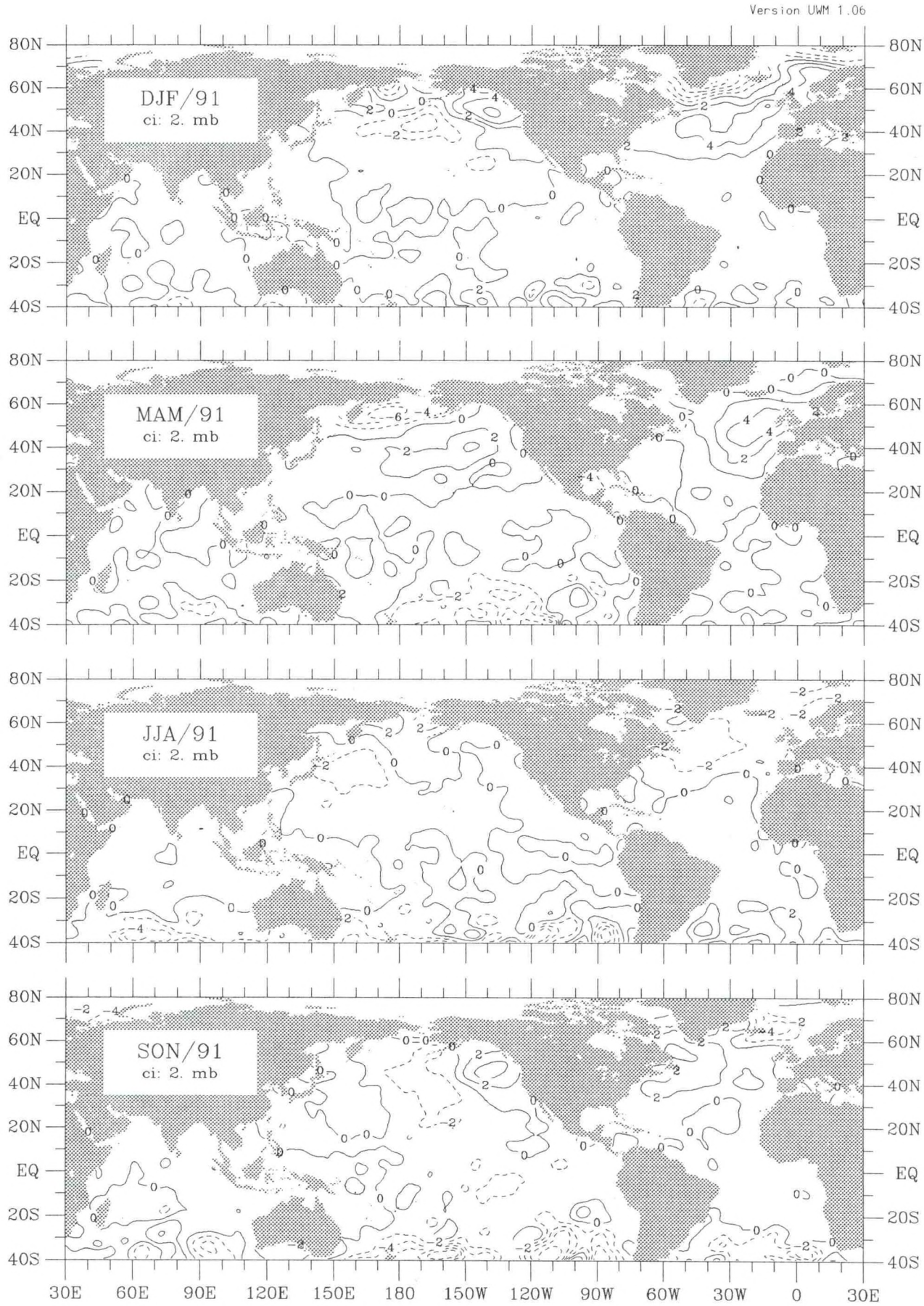

Figure slp-4. Sea level pressure seasonal anomaly for 1991.

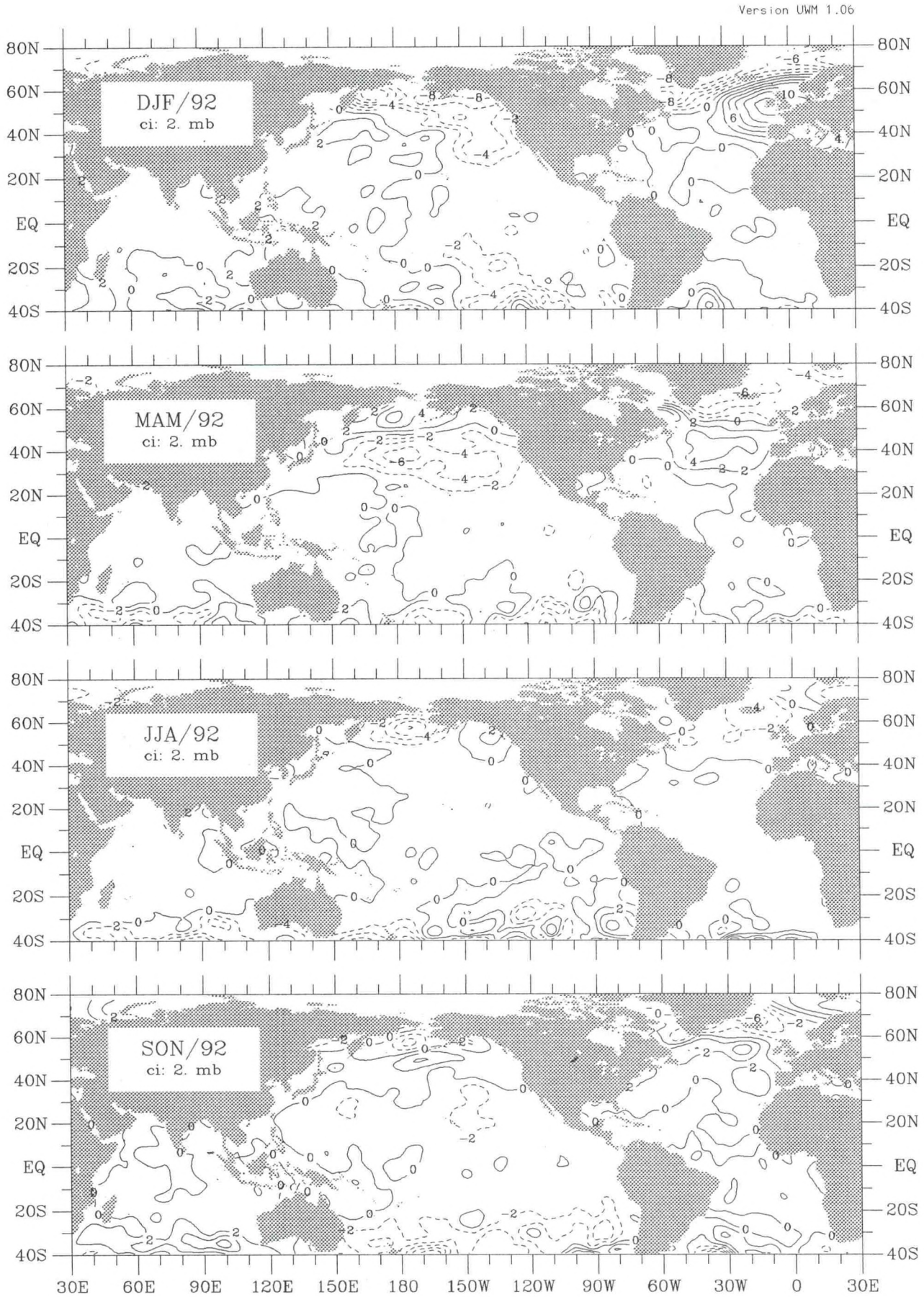

Figure slp-5. Sea level pressure seasonal anomaly for 1992.

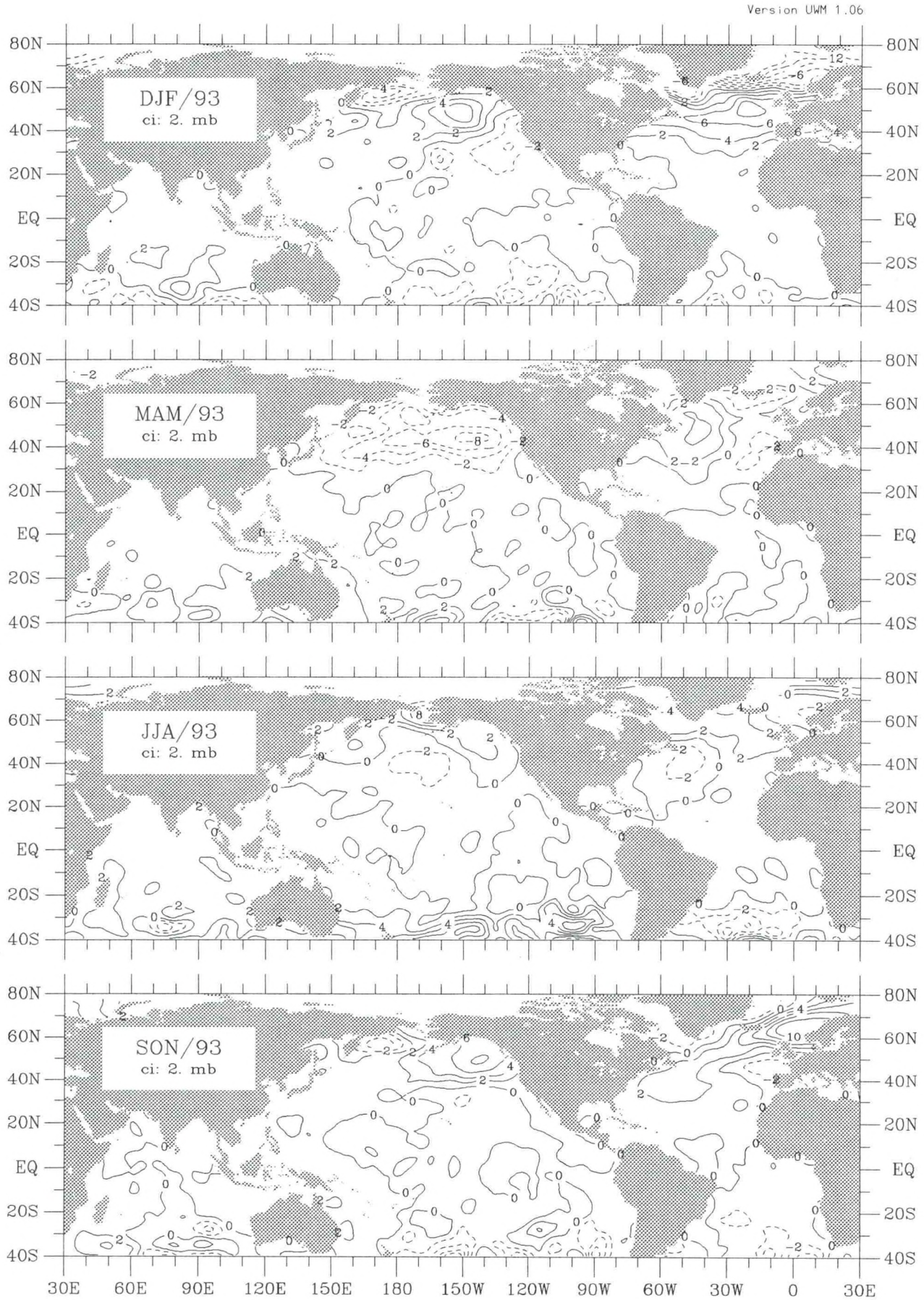

Figure slp-6. Sea level pressure seasonal anomaly for 1993.

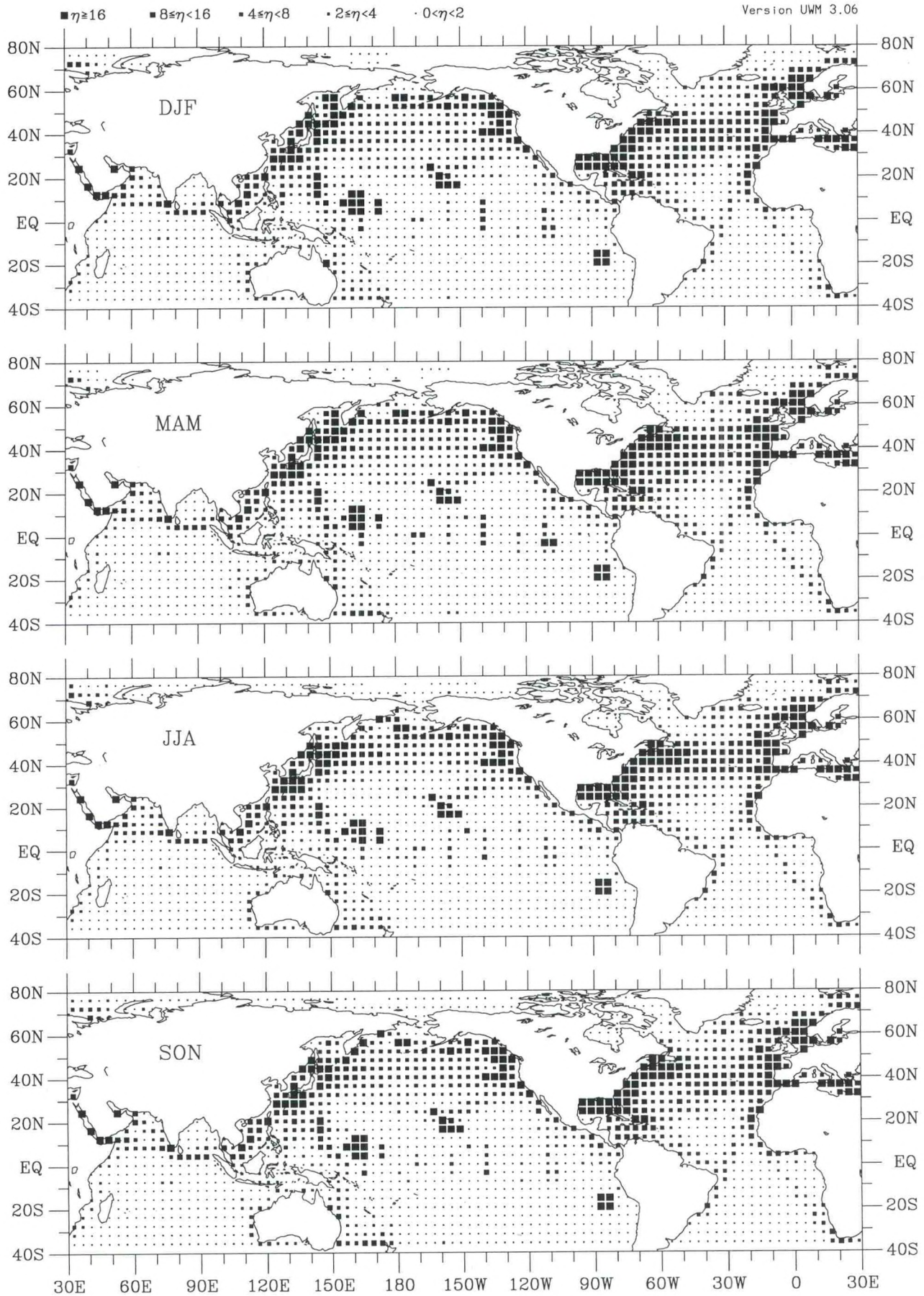

Figure u−1. 20m zonal wind seasonal observation density (1990−93).

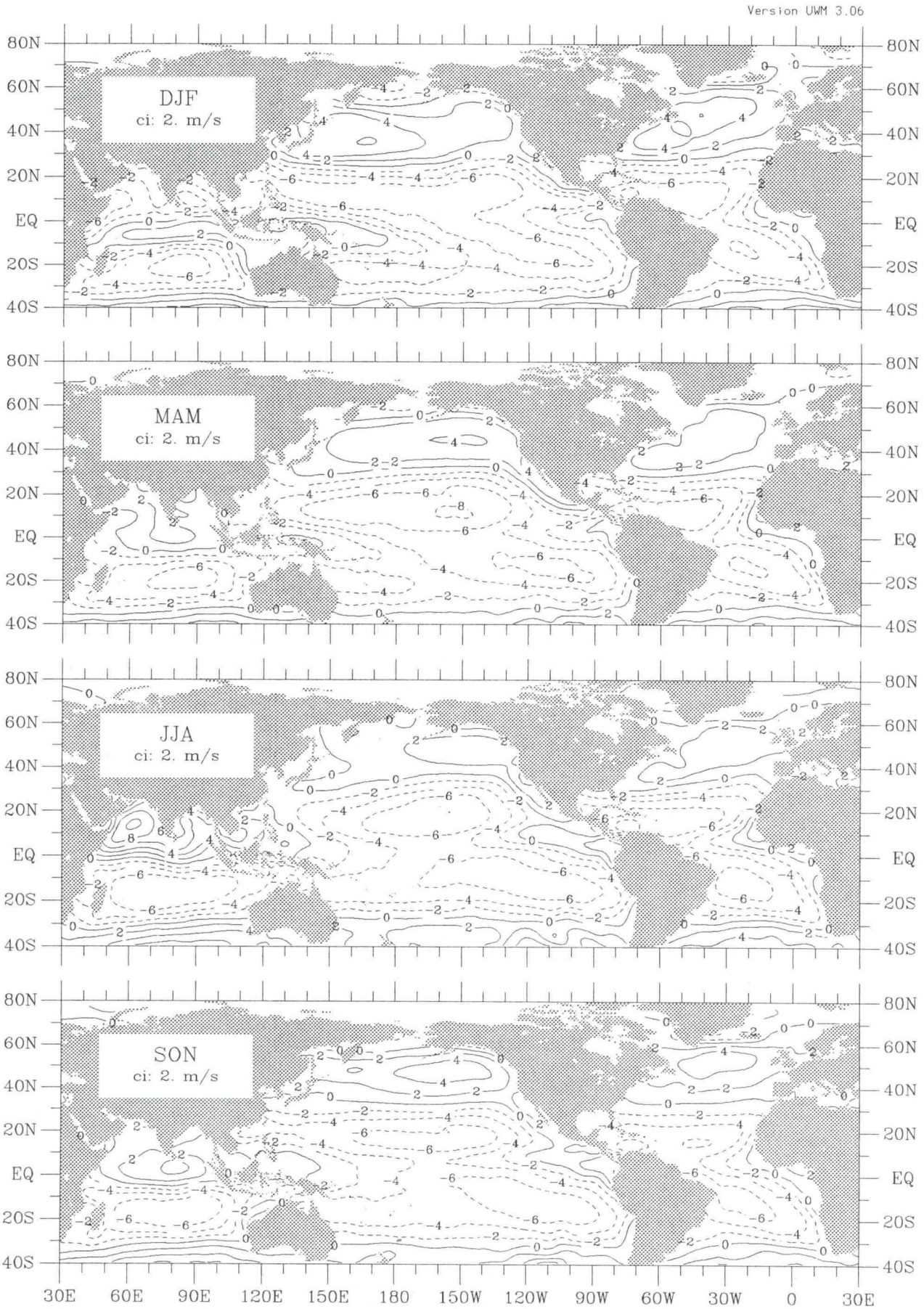

Figure u-2. 20m zonal wind seasonal climatology (1945-89).

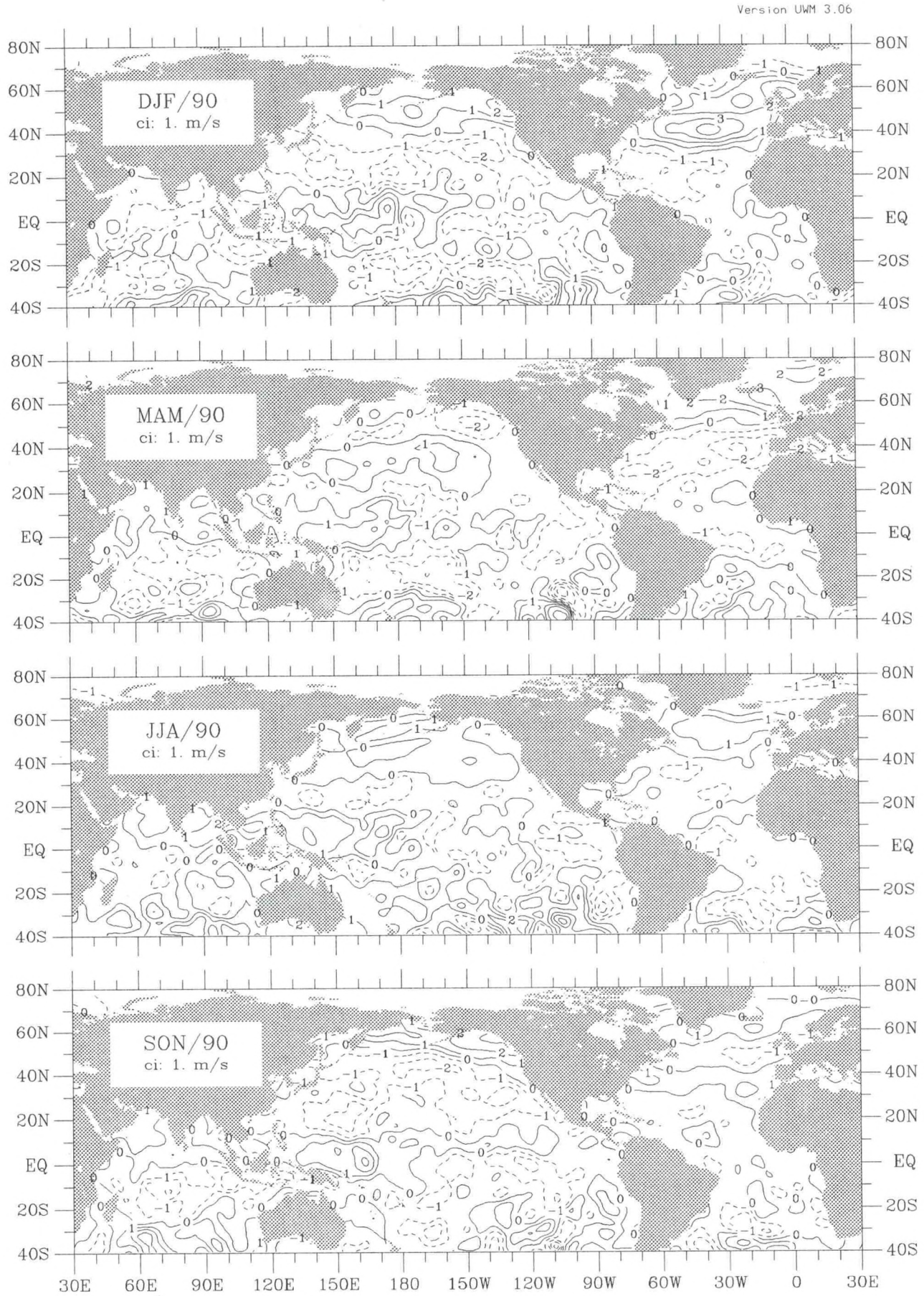

Figure u-3. 20m zonal wind seasonal anomaly for 1990.

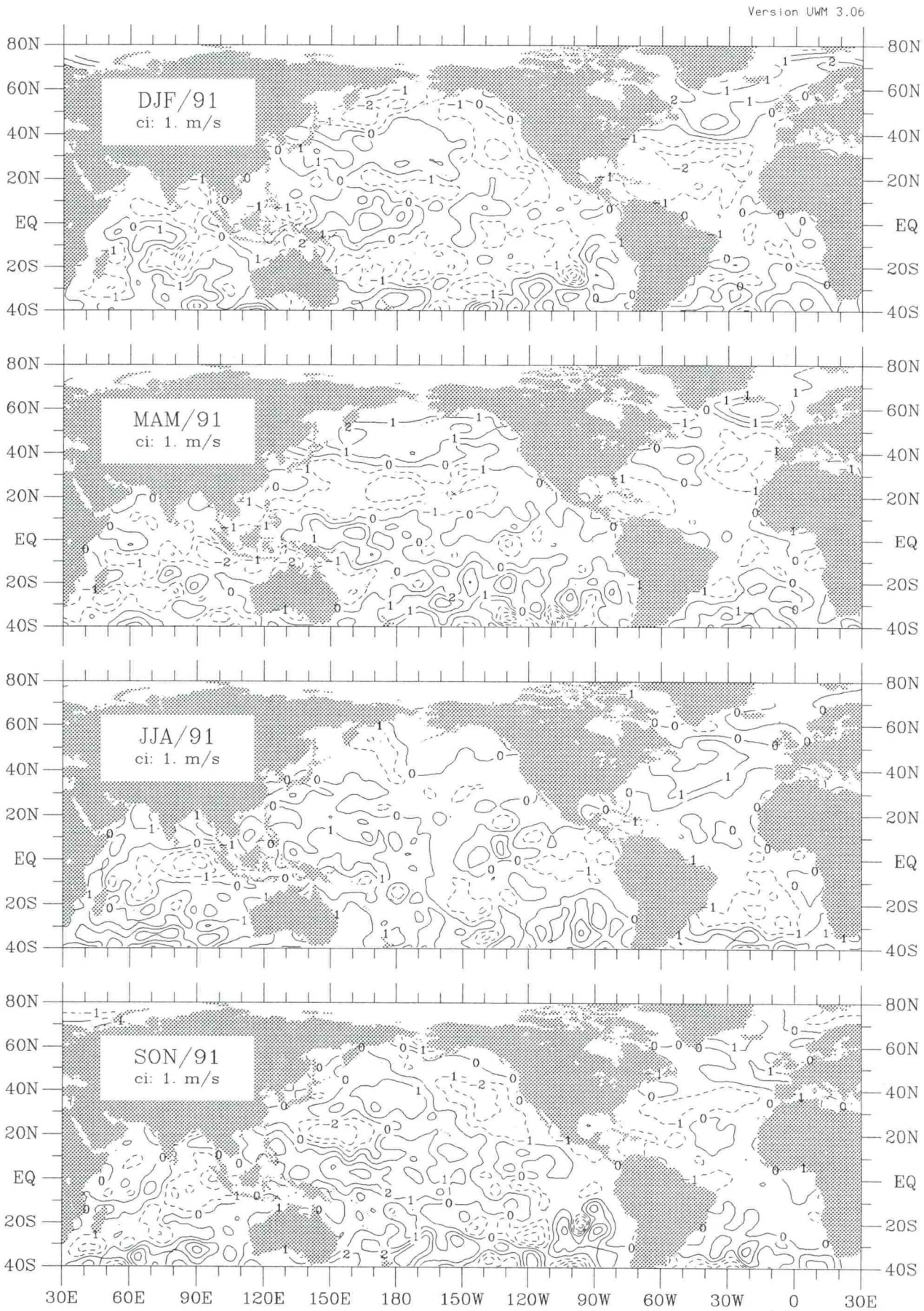

Figure u-4. 20m zonal wind seasonal anomaly for 1991.

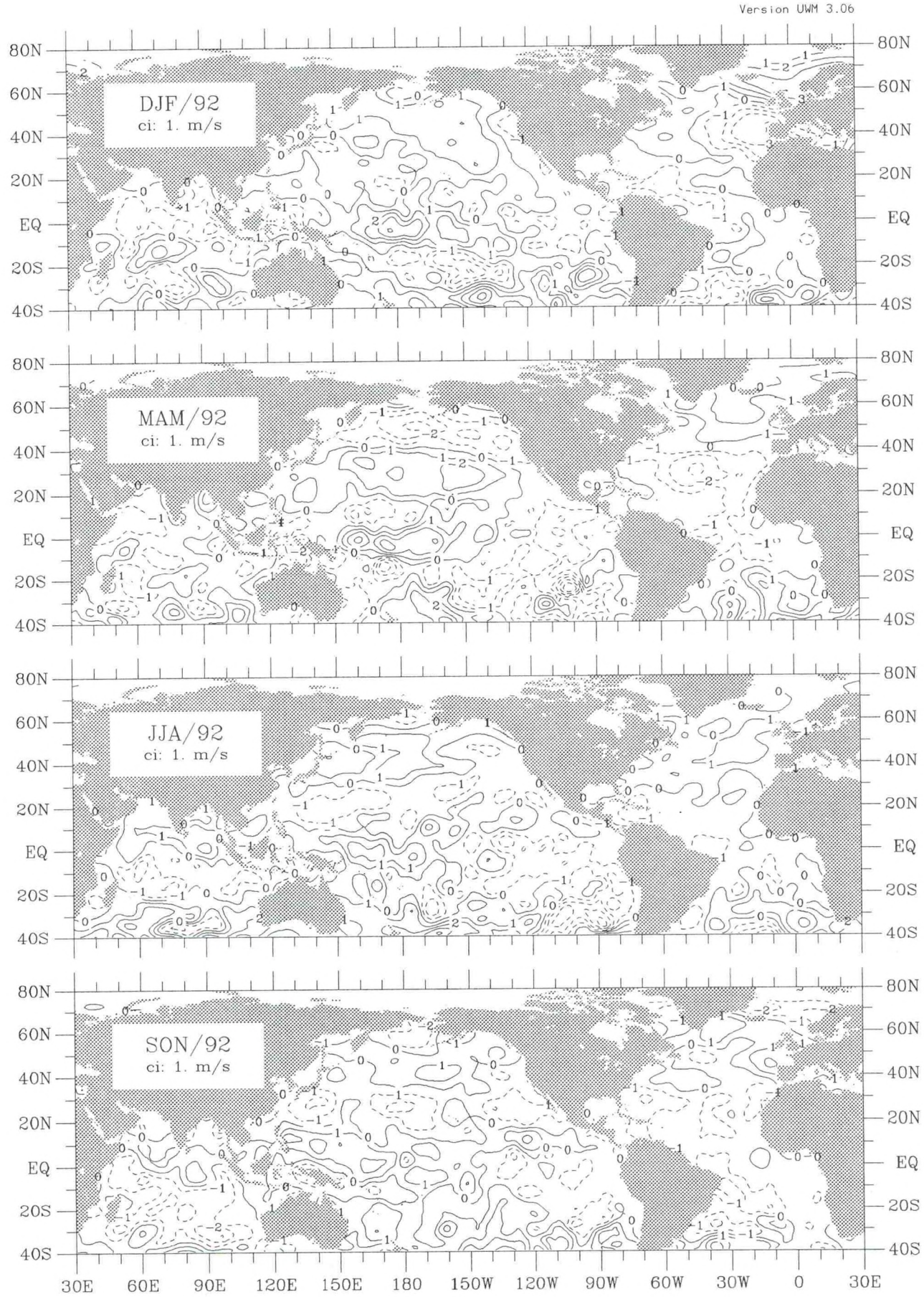

Figure u-5. 20m zonal wind seasonal anomaly for 1992.

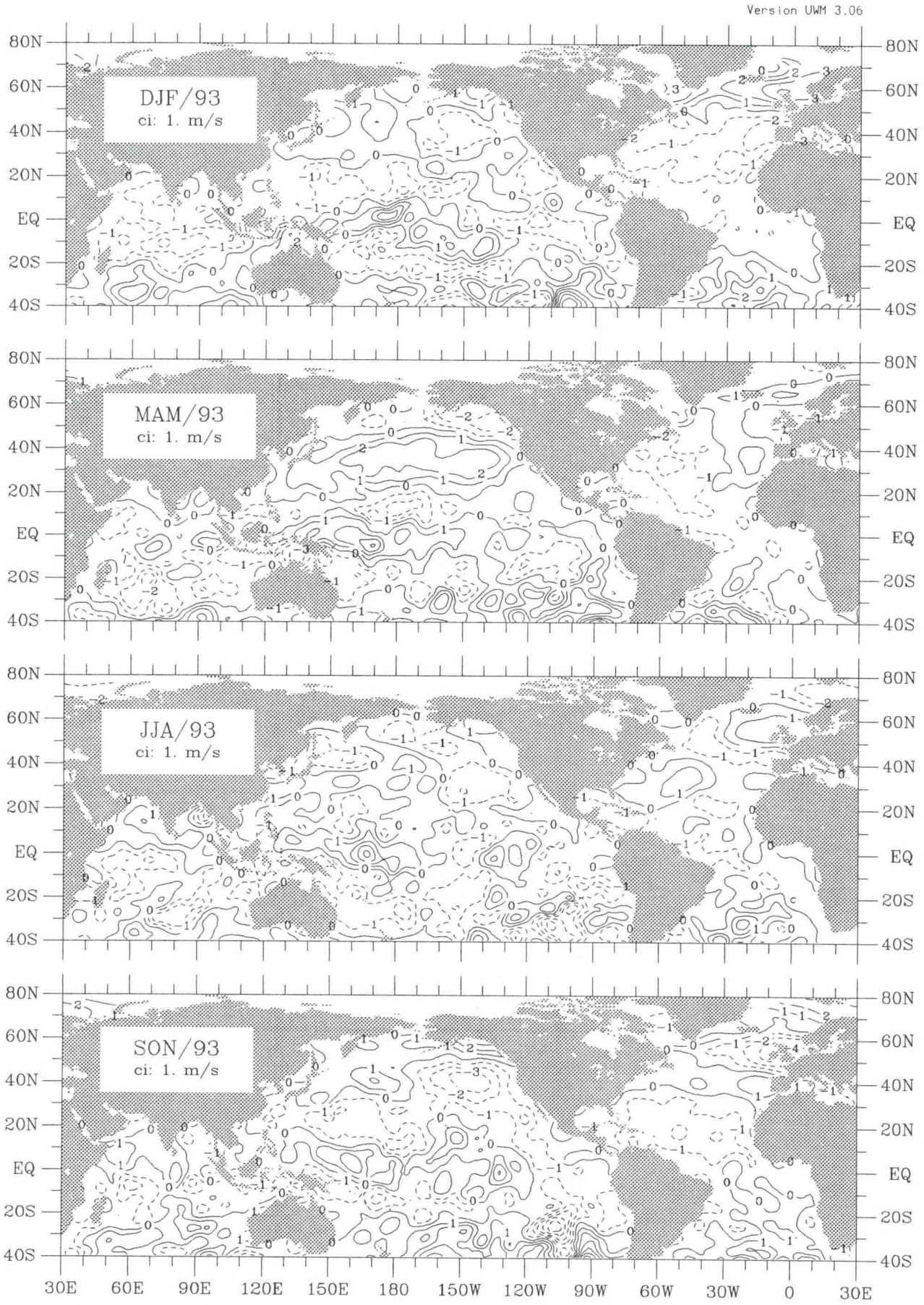

Figure u-6. 20m zonal wind seasonal anomaly for 1993.

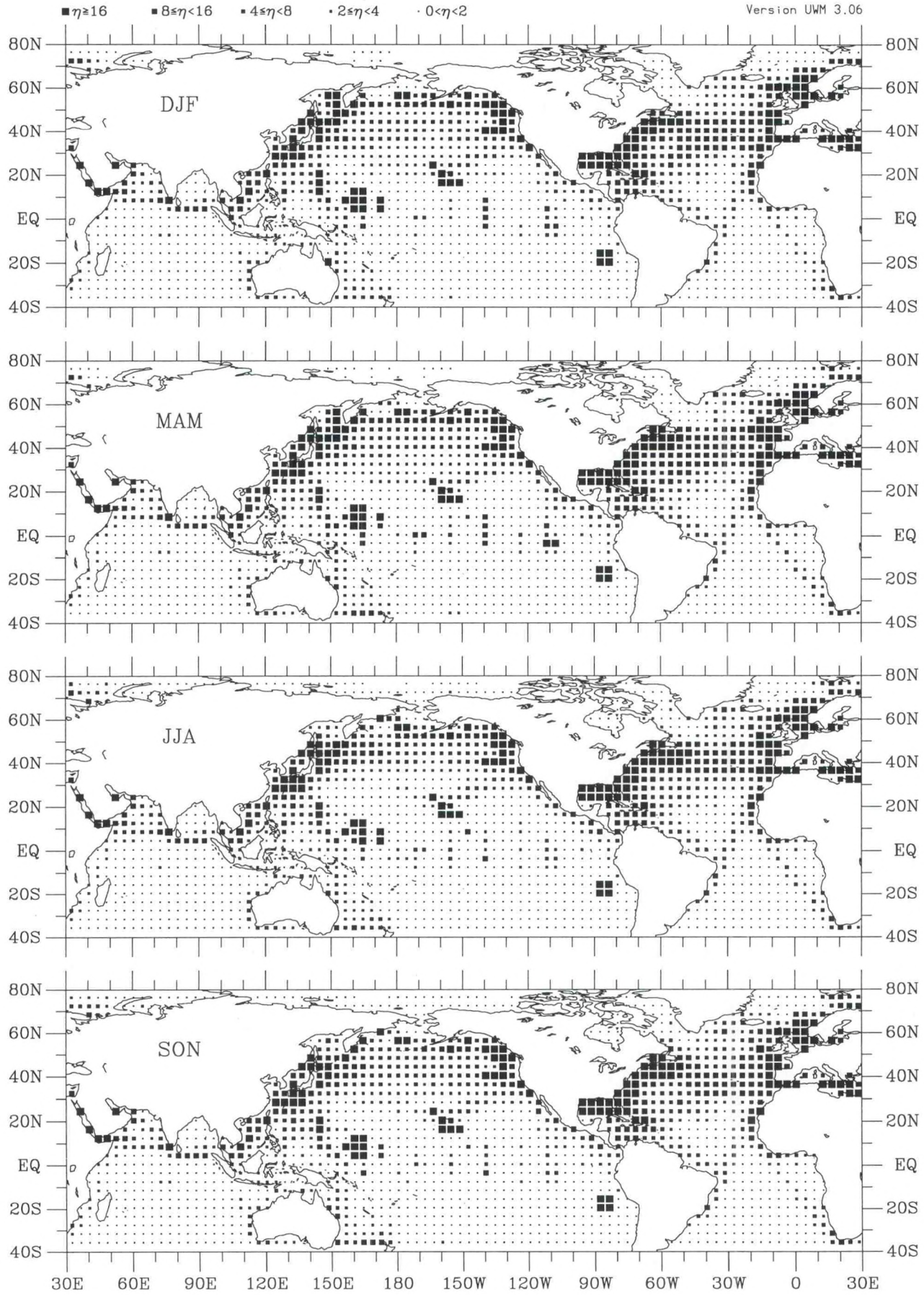

Figure v−1. 20m meridional wind seasonal observation density (1990−93).

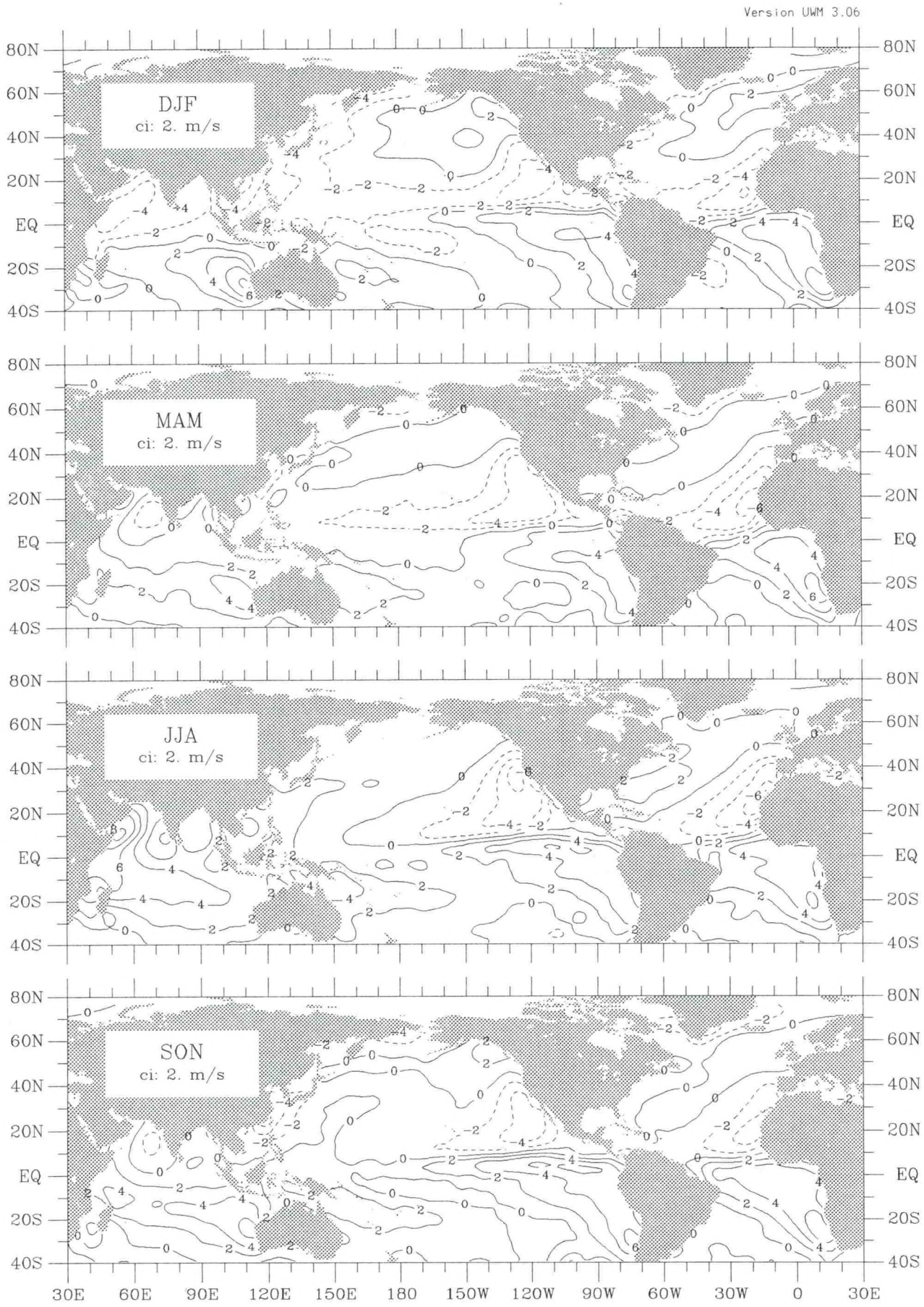

Figure v-2. 20m meridional wind seasonal climatology (1945-89).

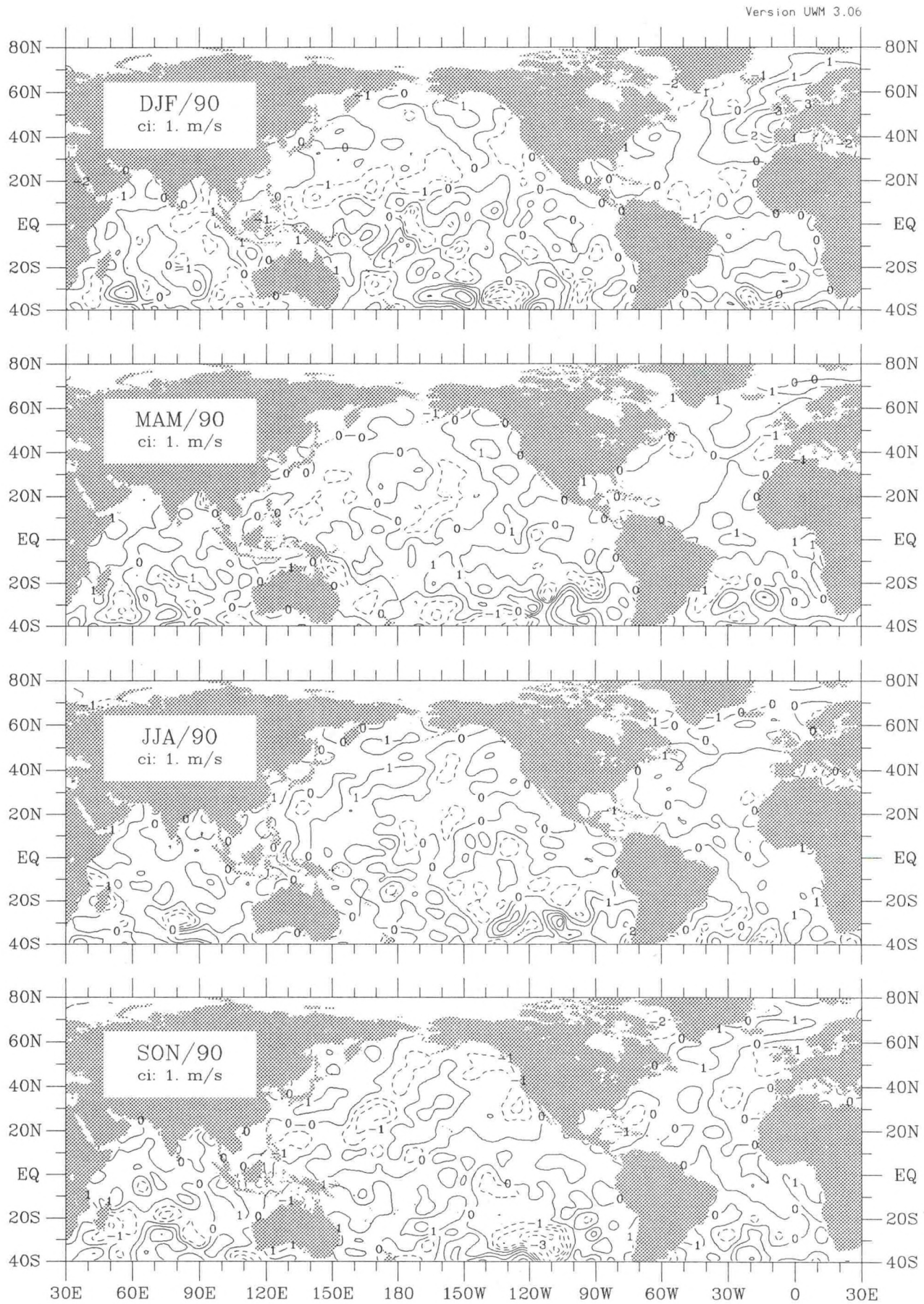

Figure v-3. 20m meridional wind seasonal anomaly for 1990.

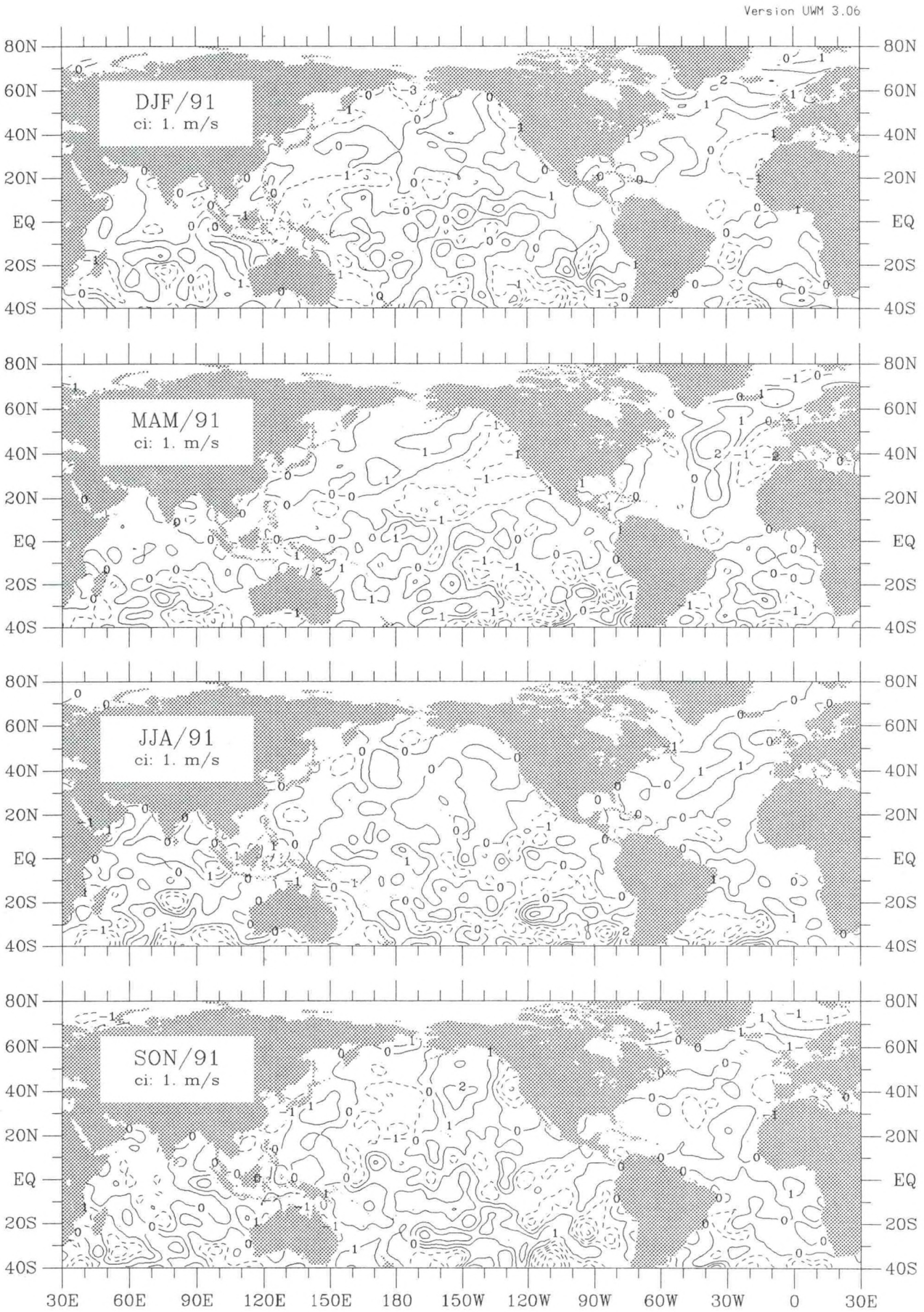

Figure v-4. 20m meridional wind seasonal anomaly for 1991.

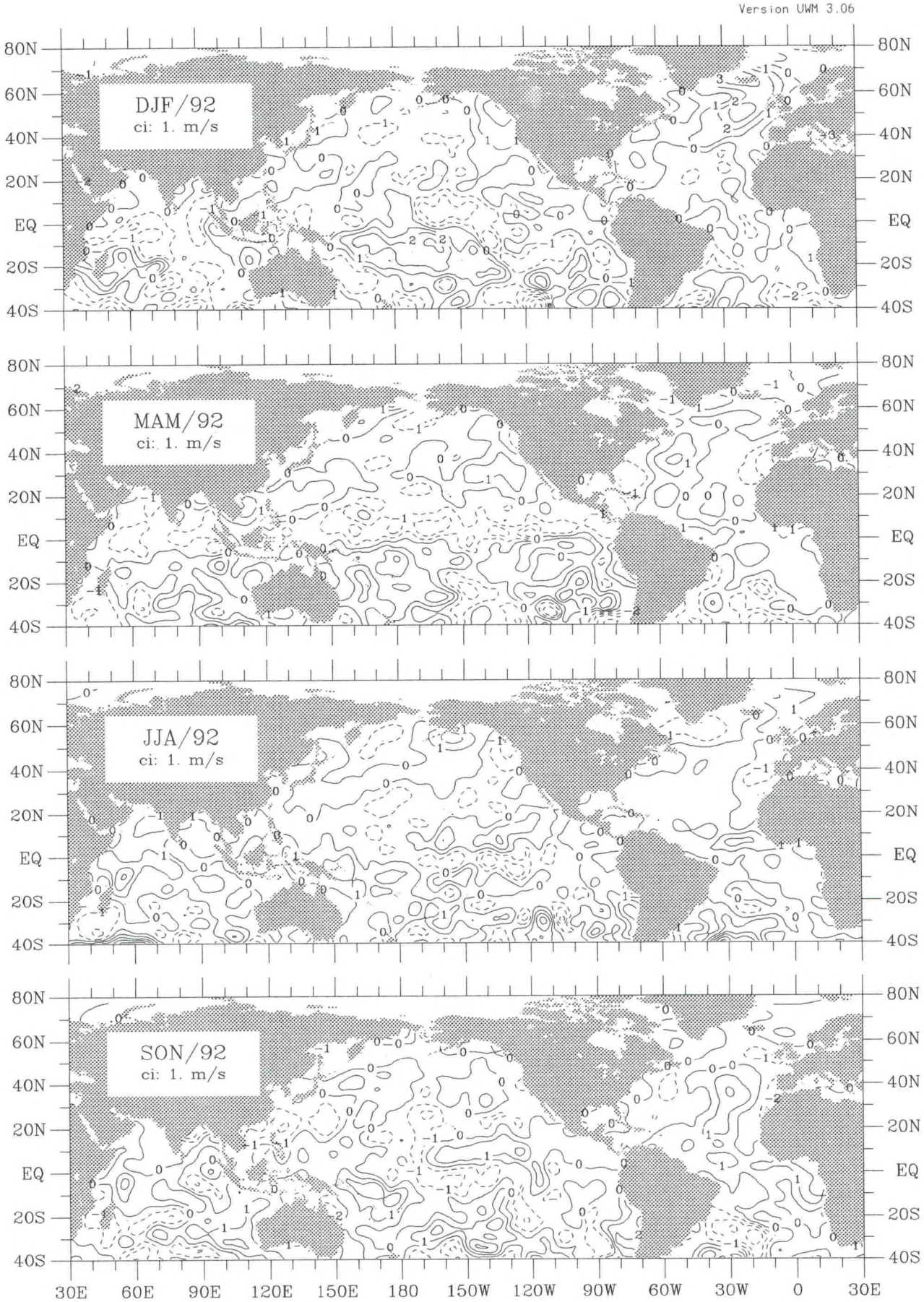

Figure v-5. 20m meridional wind seasonal anomaly for 1992.

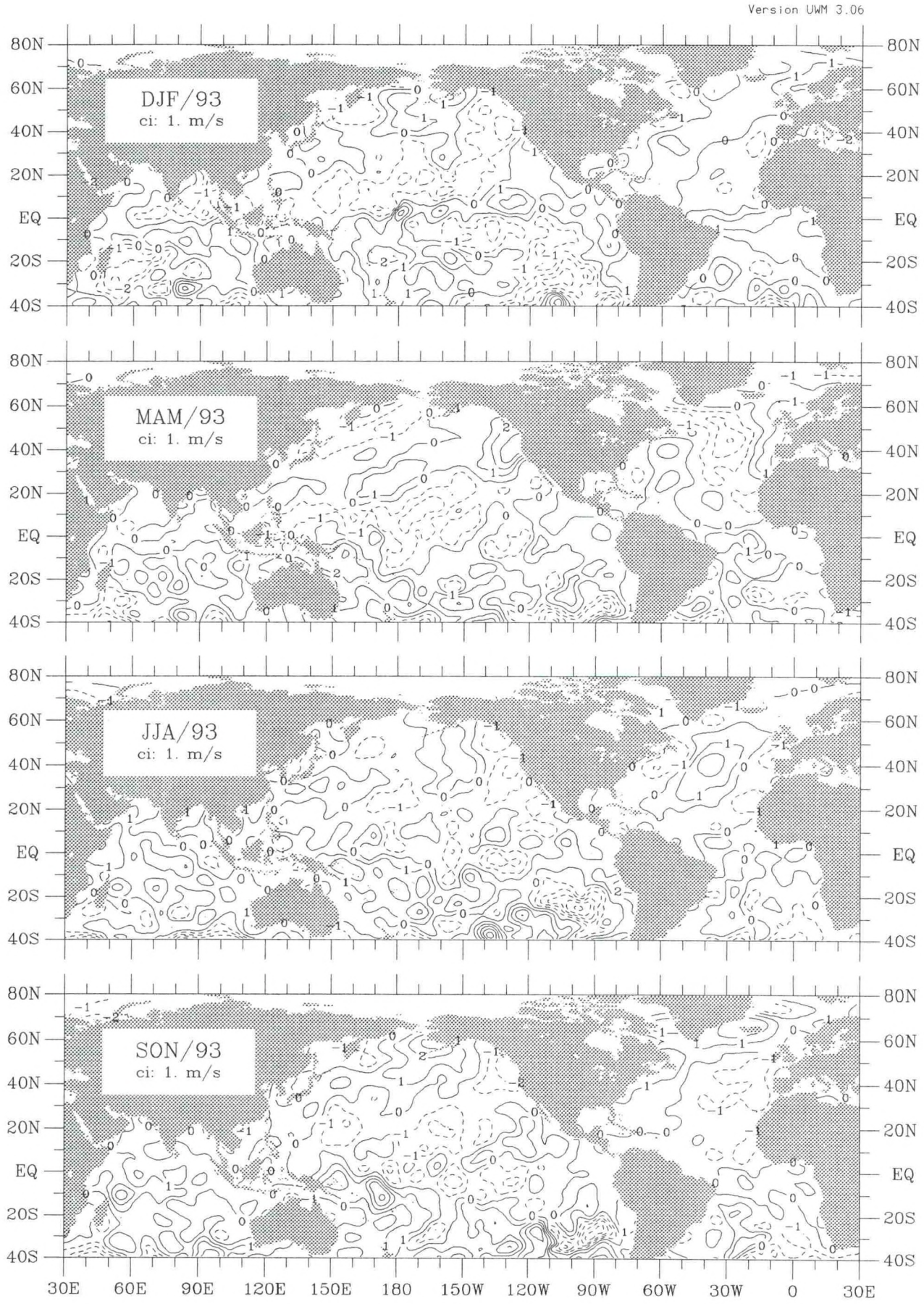

Figure v-6. 20m meridional wind seasonal anomaly for 1993.

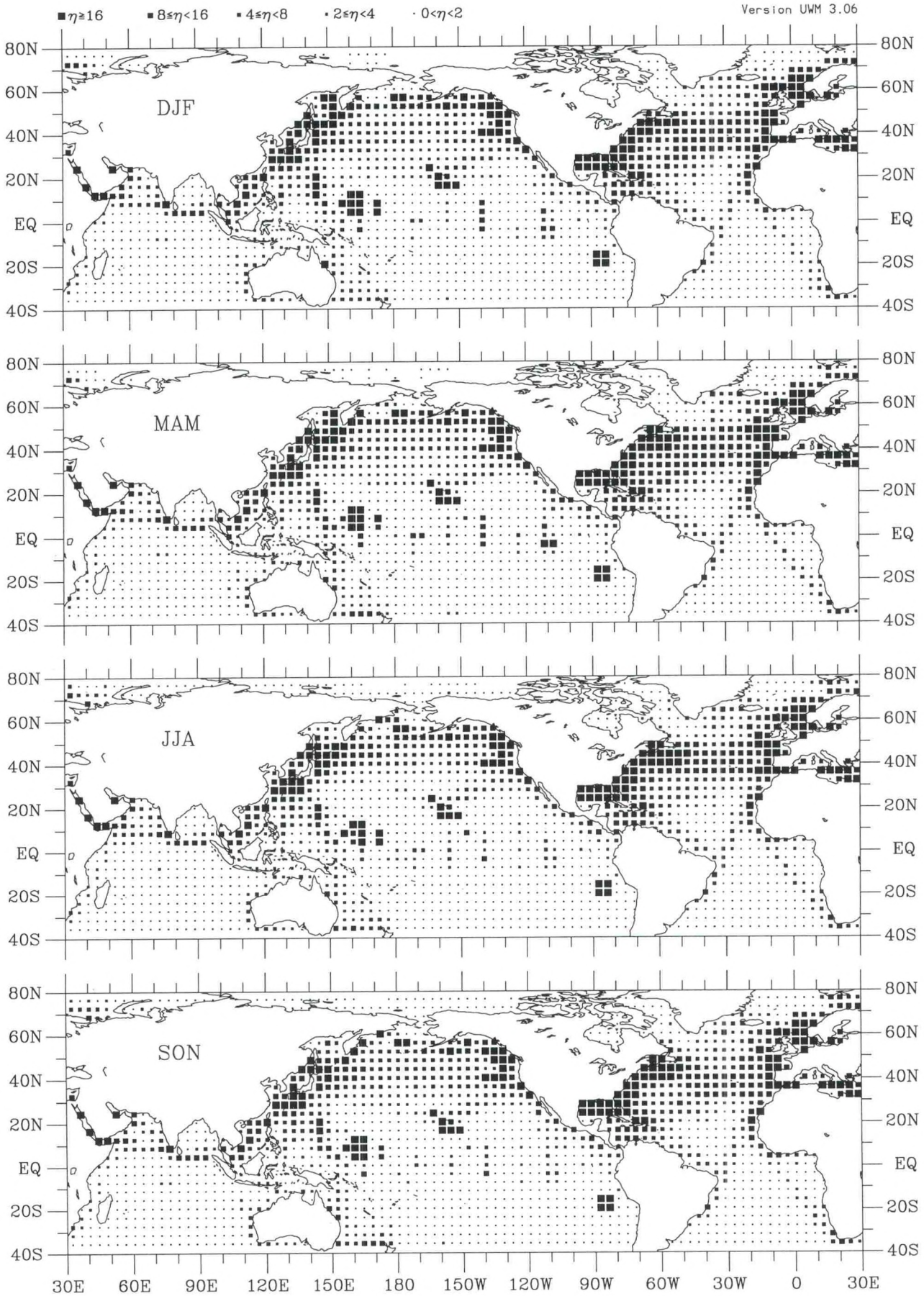

Figure w-1. 20m wind speed seasonal observation density (1990-93).

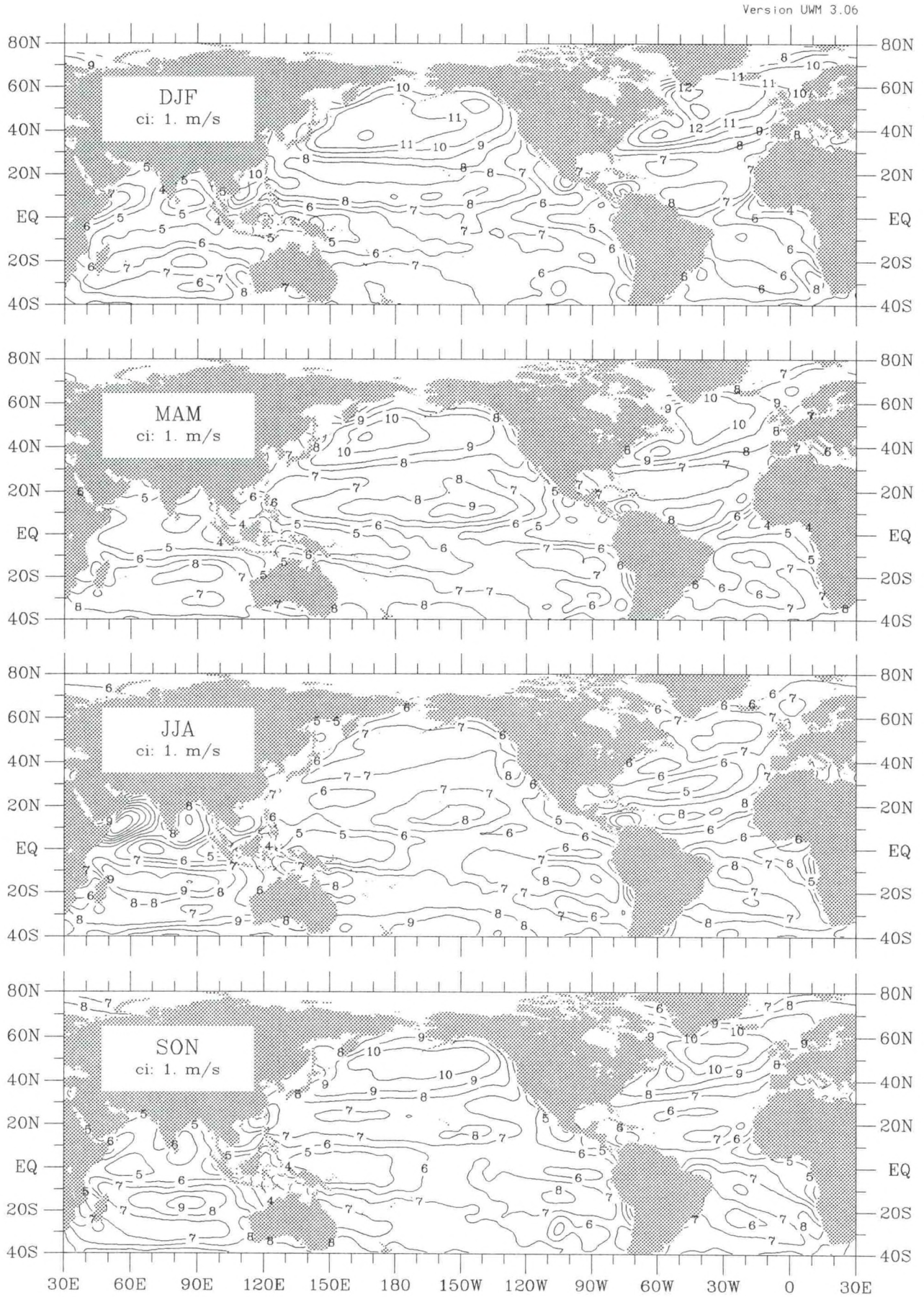

Figure w-2. 20m wind speed seasonal climatology (1945-89).

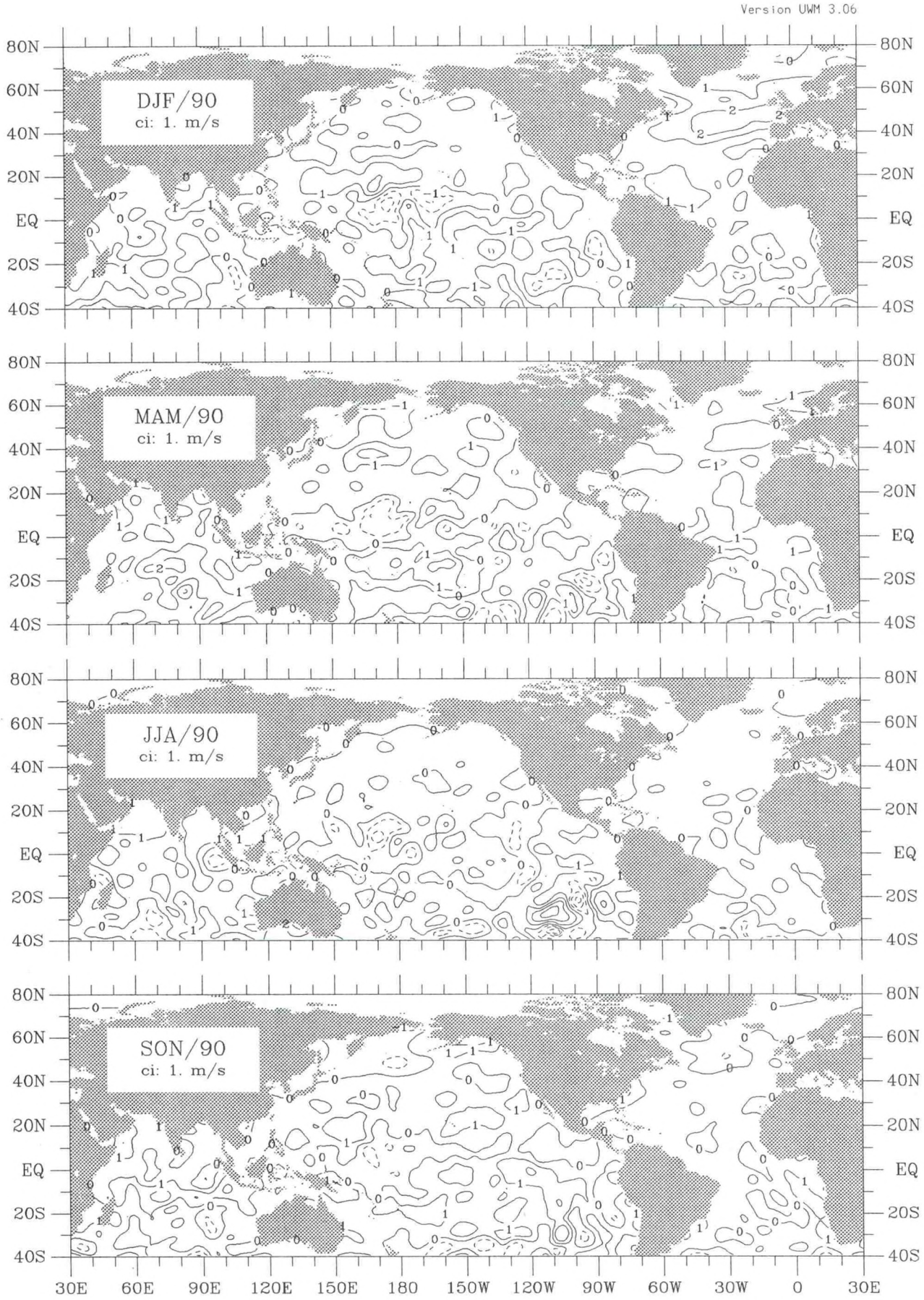

Figure w–3. 20m wind speed seasonal anomaly for 1990.

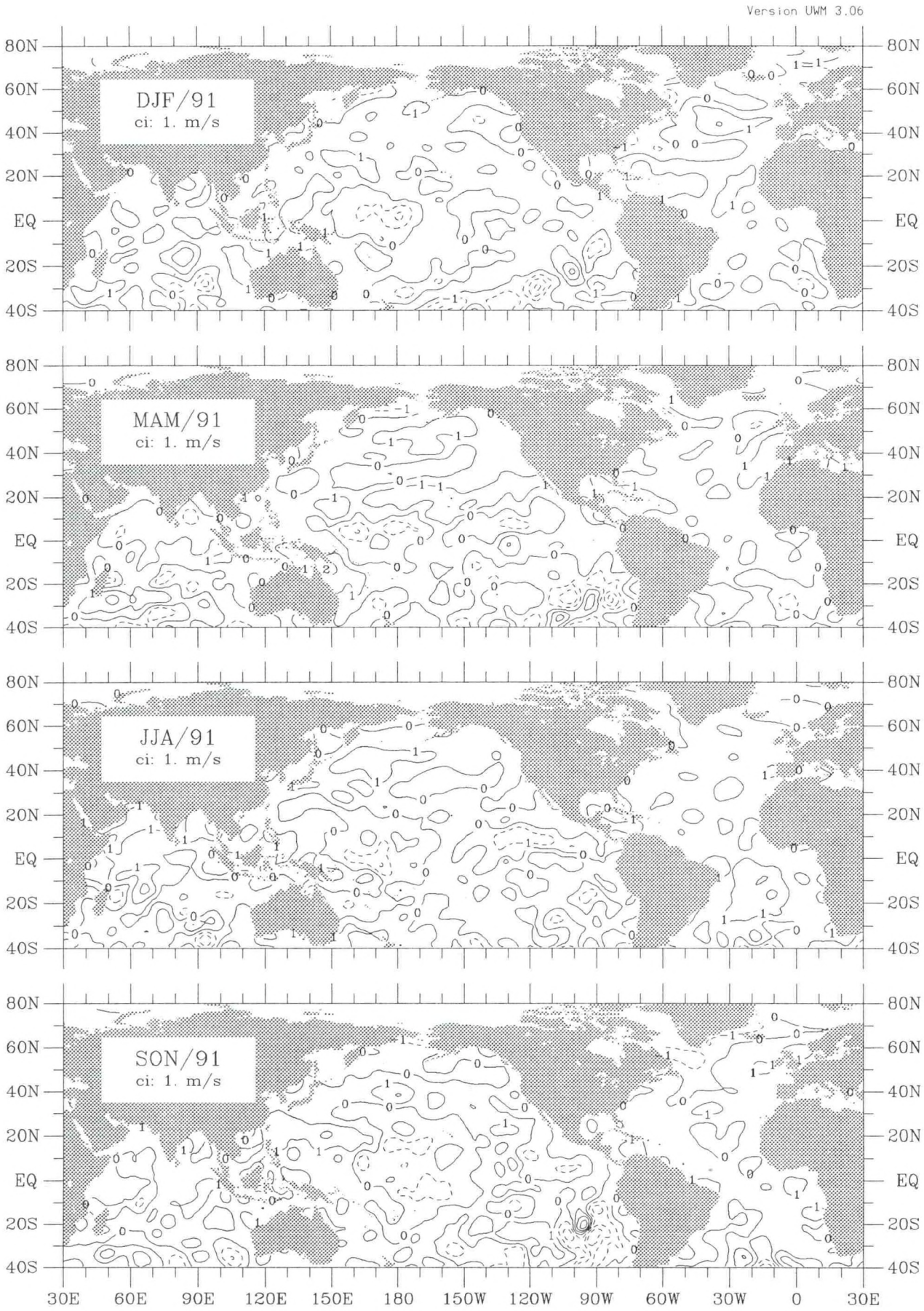

Figure w-4. 20m wind speed seasonal anomaly for 1991.

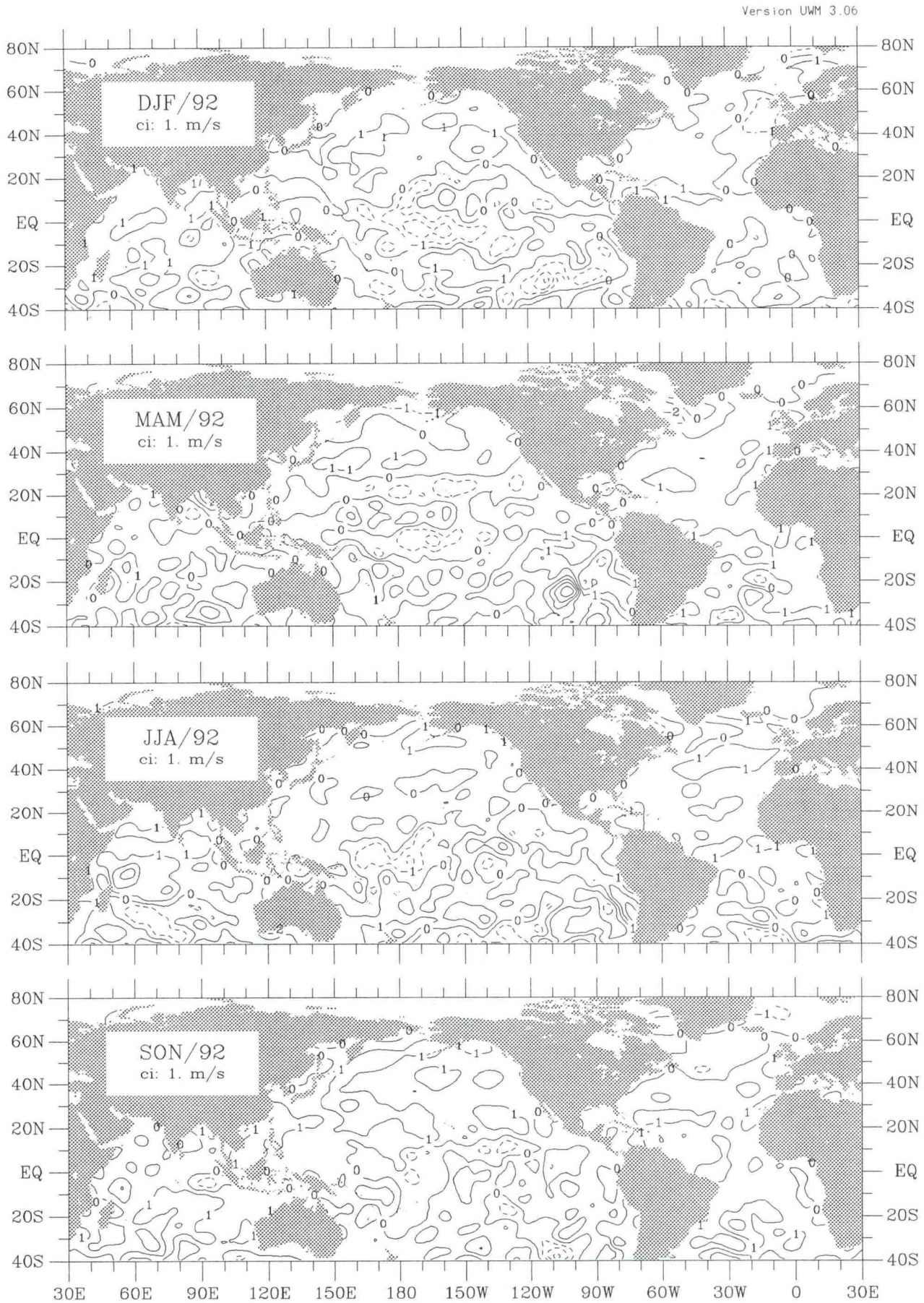

Figure w-5. 20m wind speed seasonal anomaly for 1992.

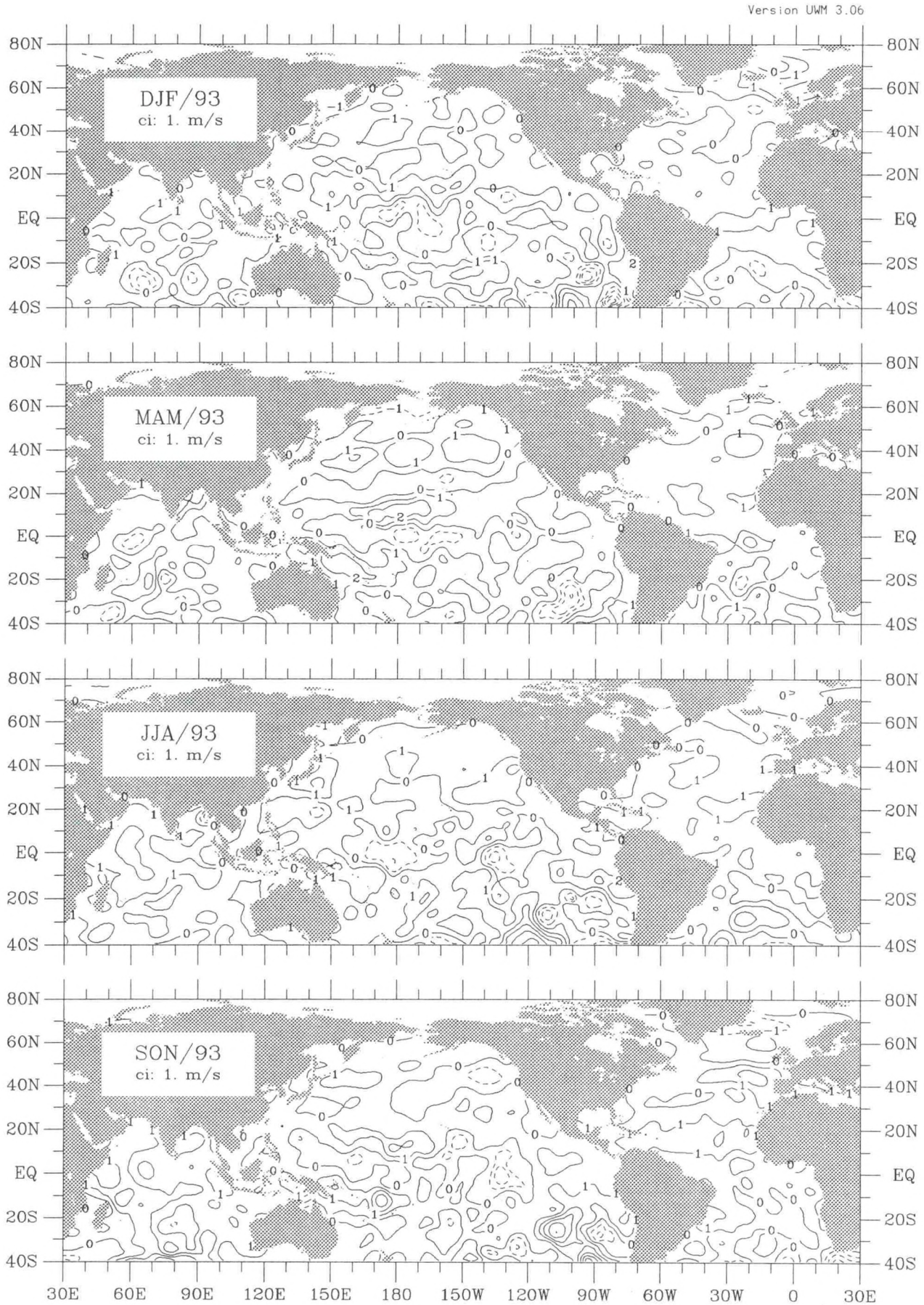

Figure w–6. 20m wind speed seasonal anomaly for 1993.

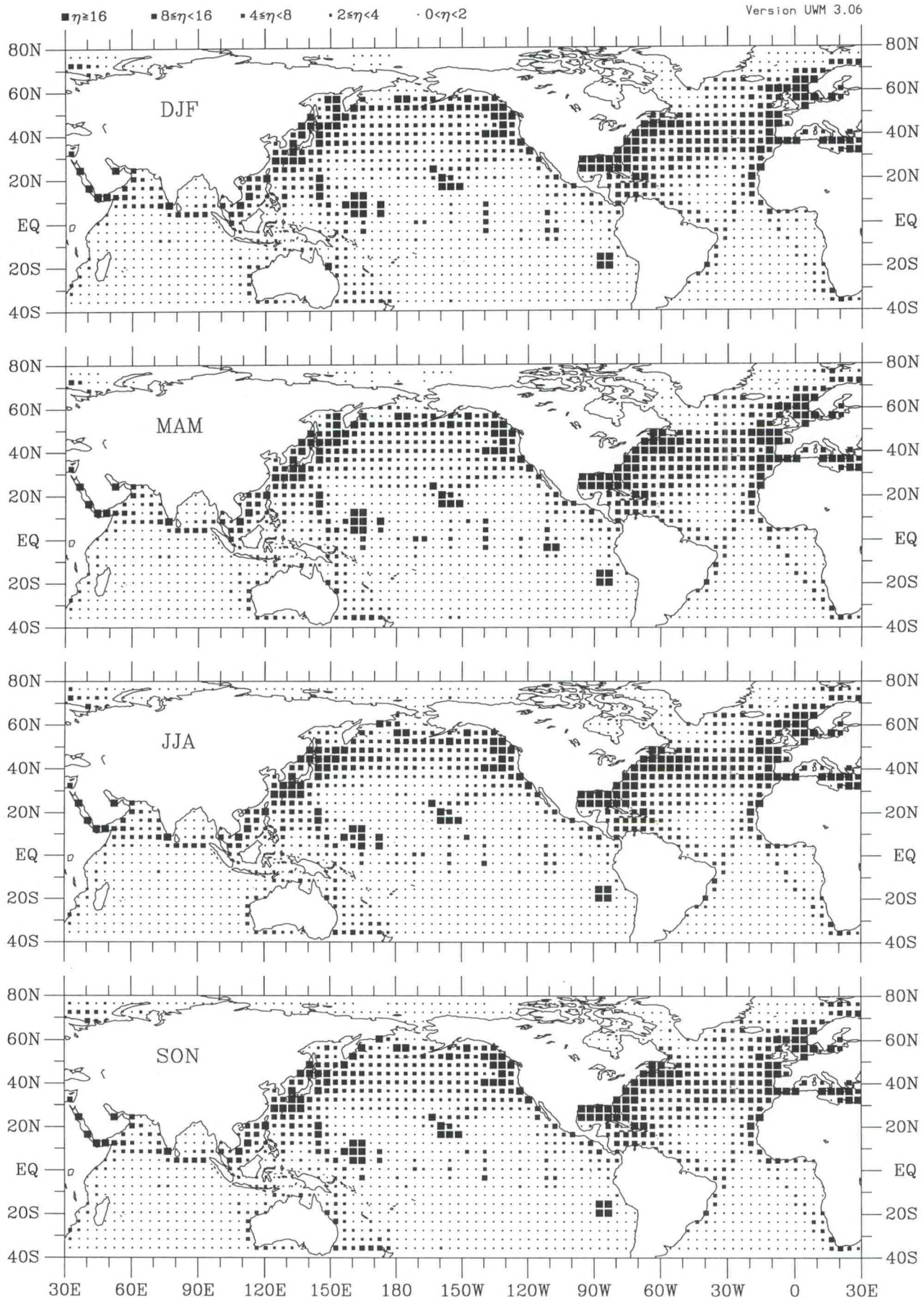

Figure taux−1. Zonal wind stress seasonal observation density (1990−93).

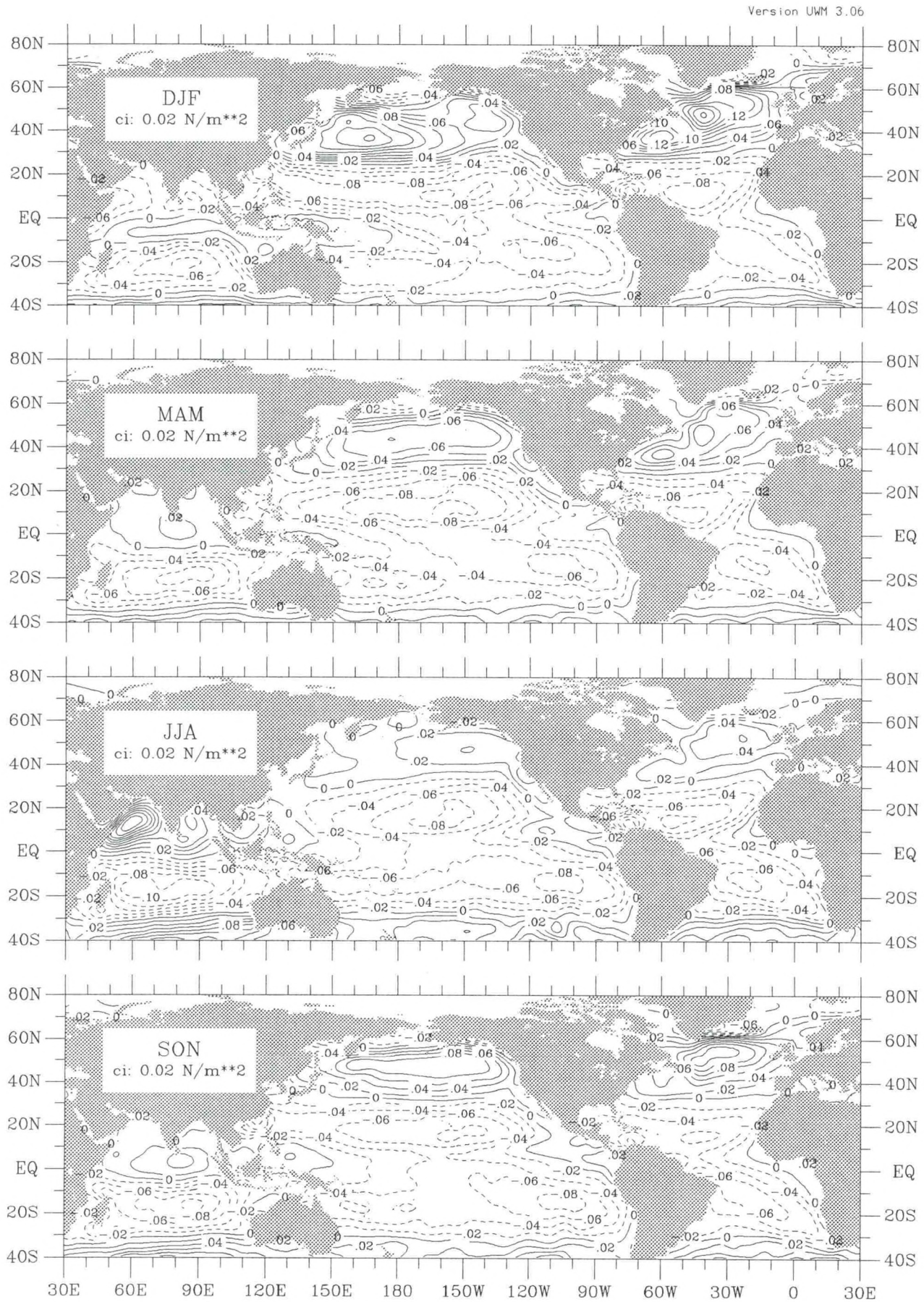

Figure taux-2. Zonal wind stress seasonal climatology (1945-89).

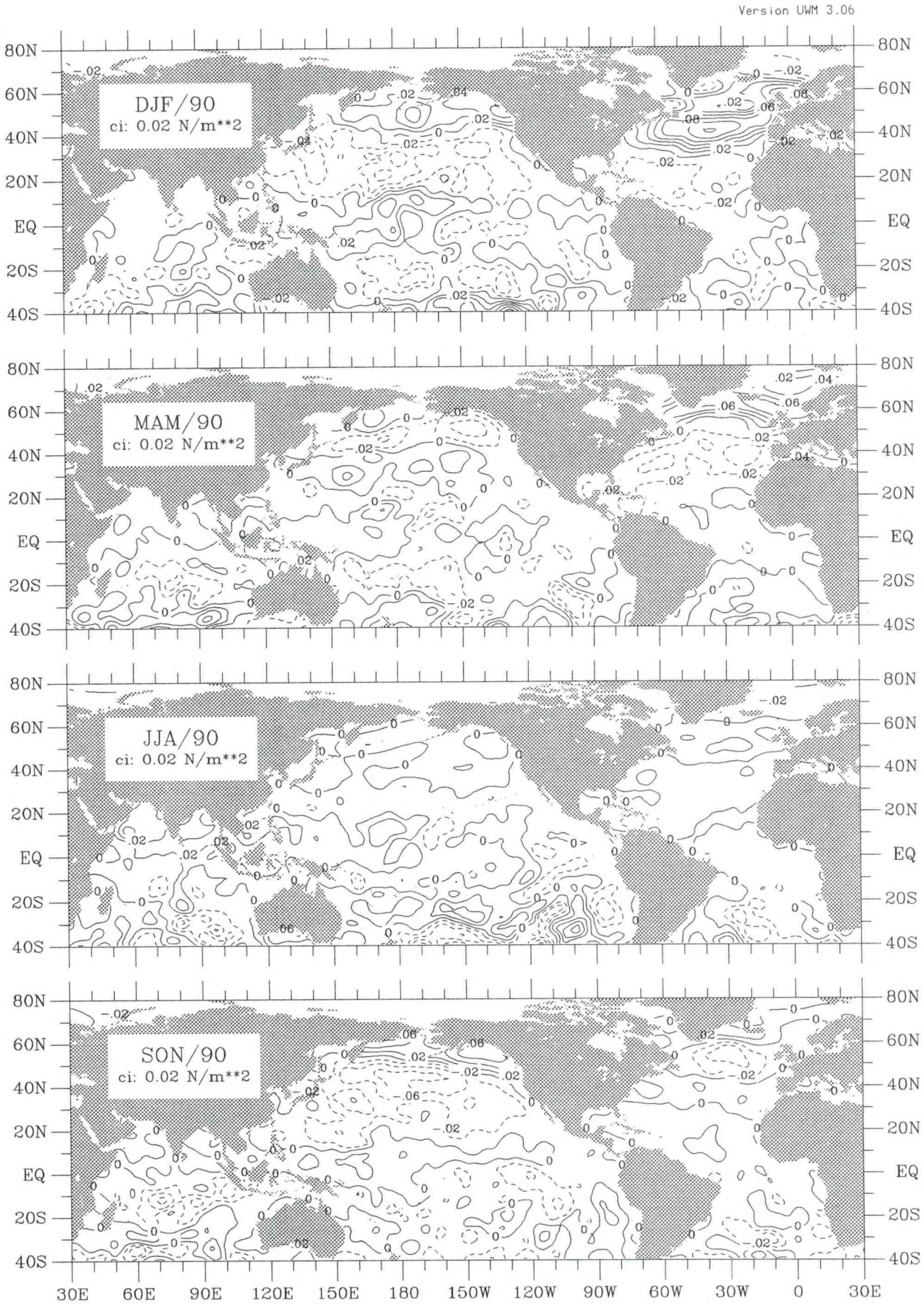

Figure taux-3. Zonal wind stress seasonal anomaly for 1990.

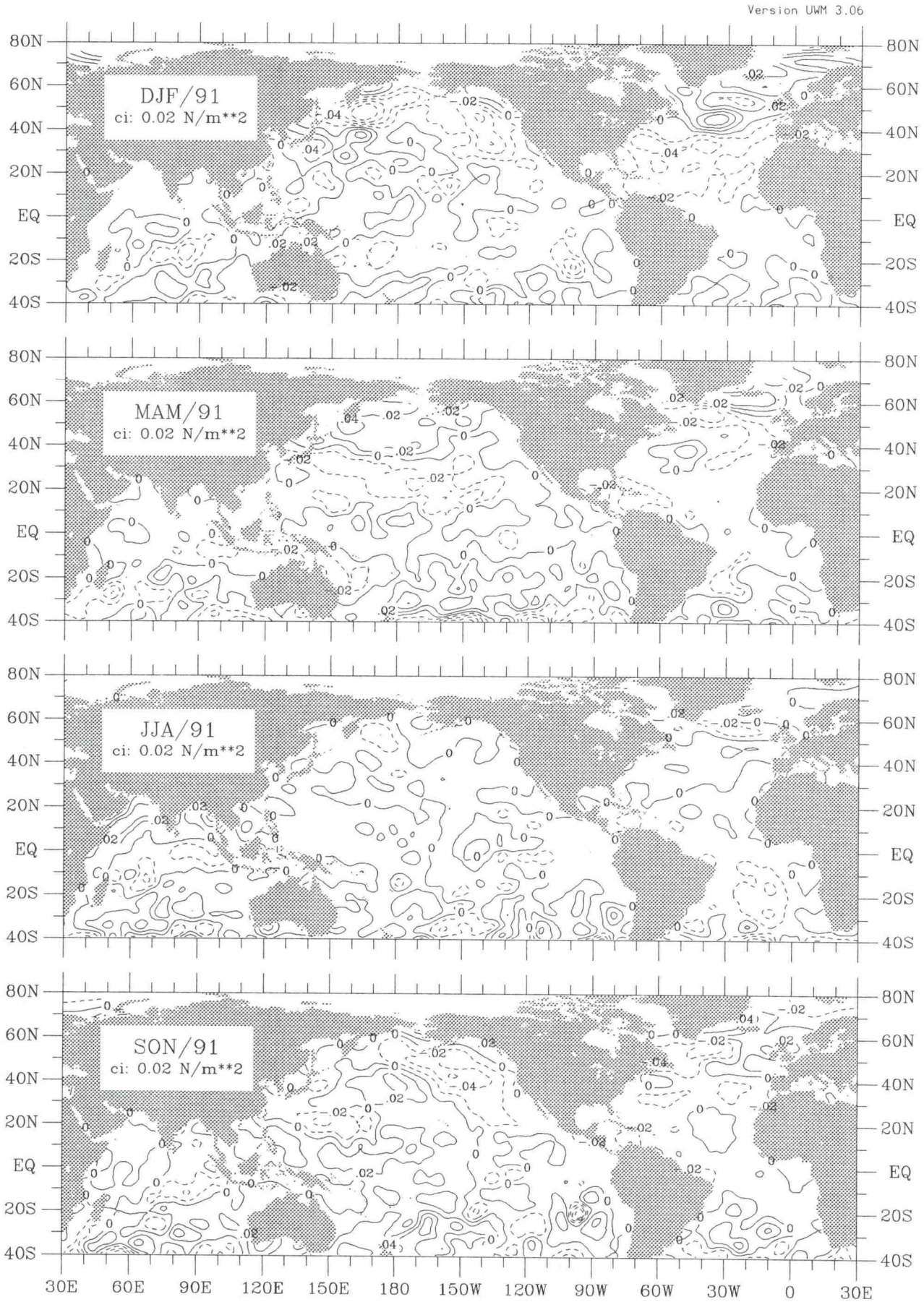

Figure taux-4. Zonal wind stress seasonal anomaly for 1991.

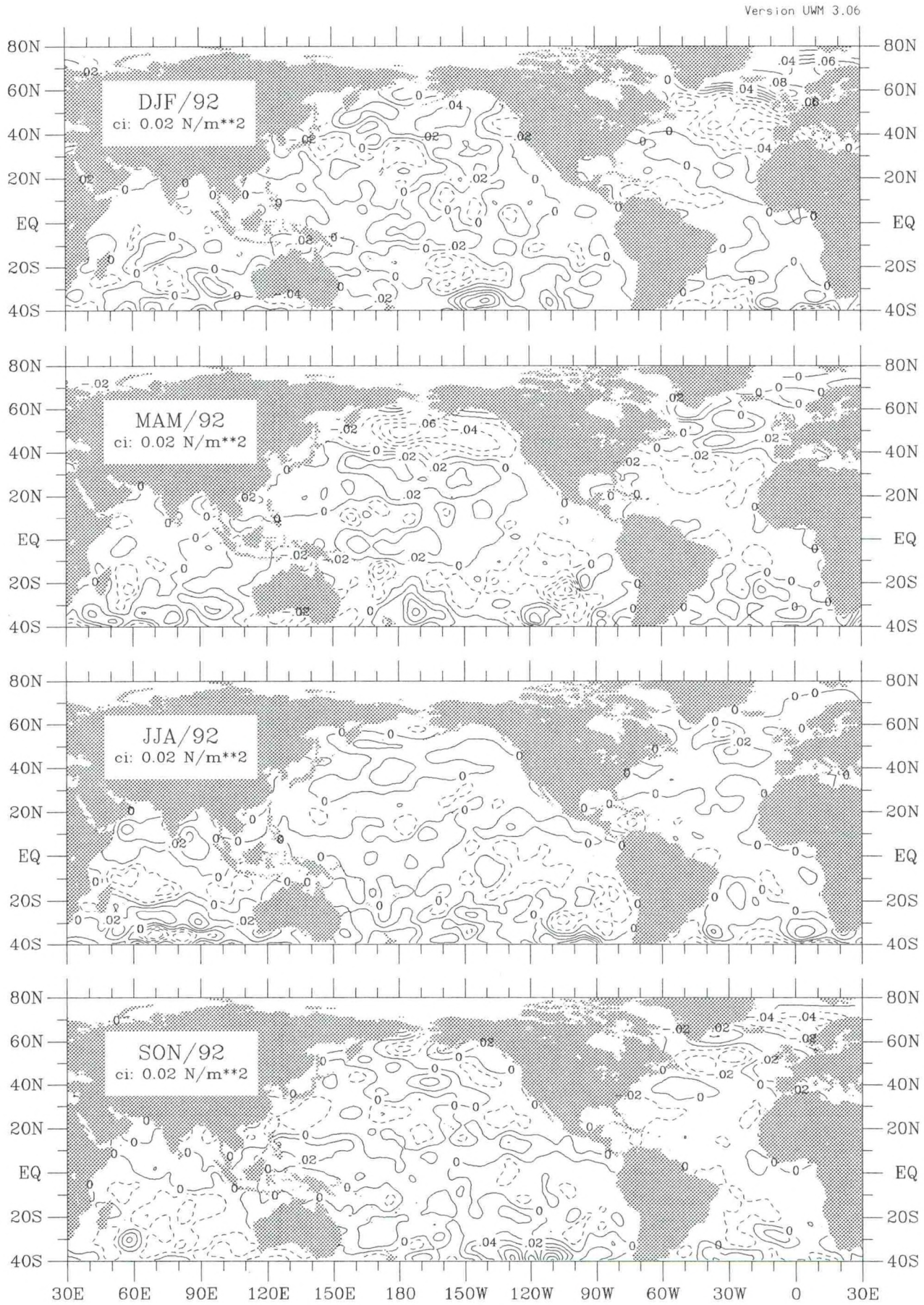

Figure taux-5. Zonal wind stress seasonal anomaly for 1992.

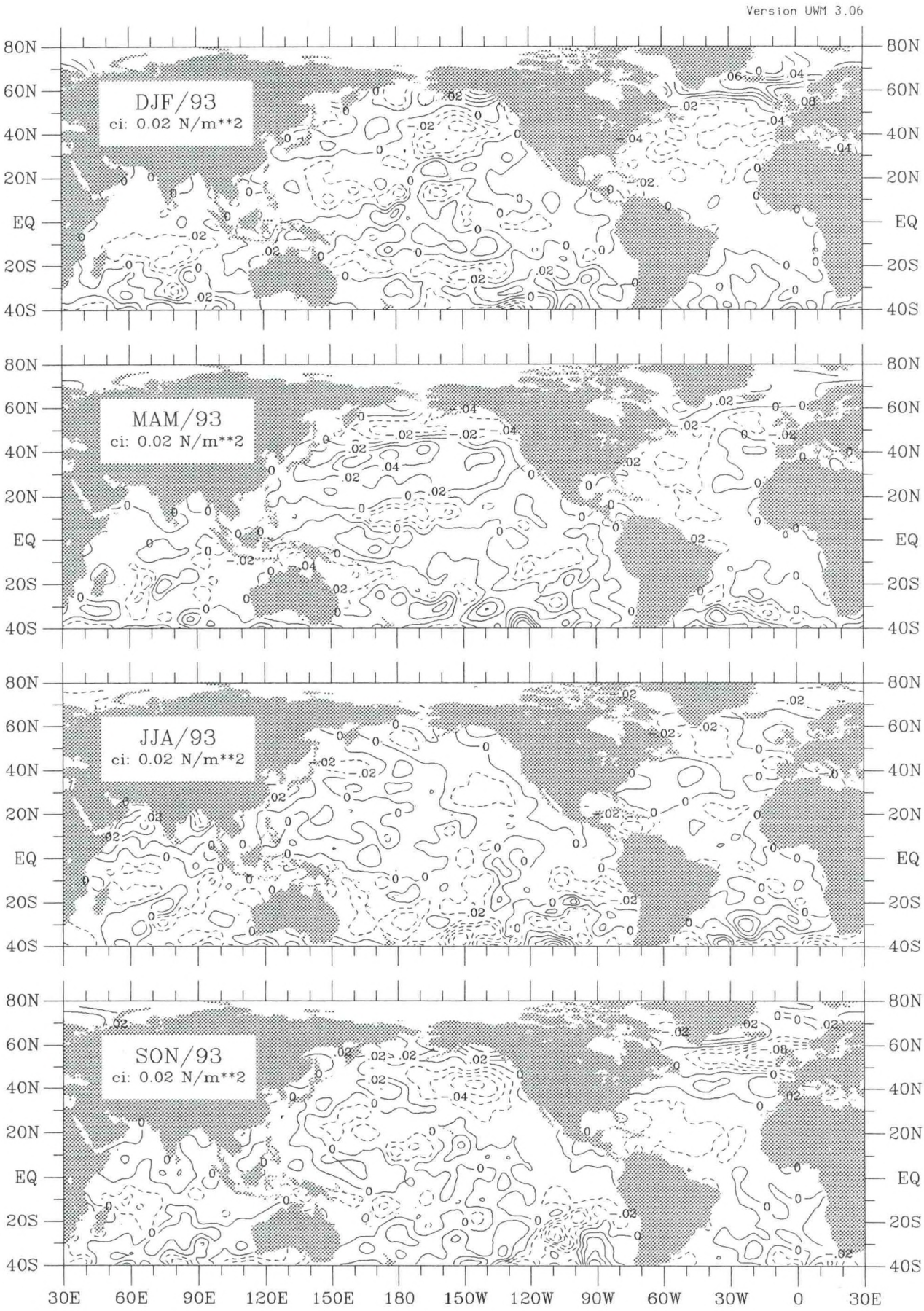

Figure taux-6. Zonal wind stress seasonal anomaly for 1993.

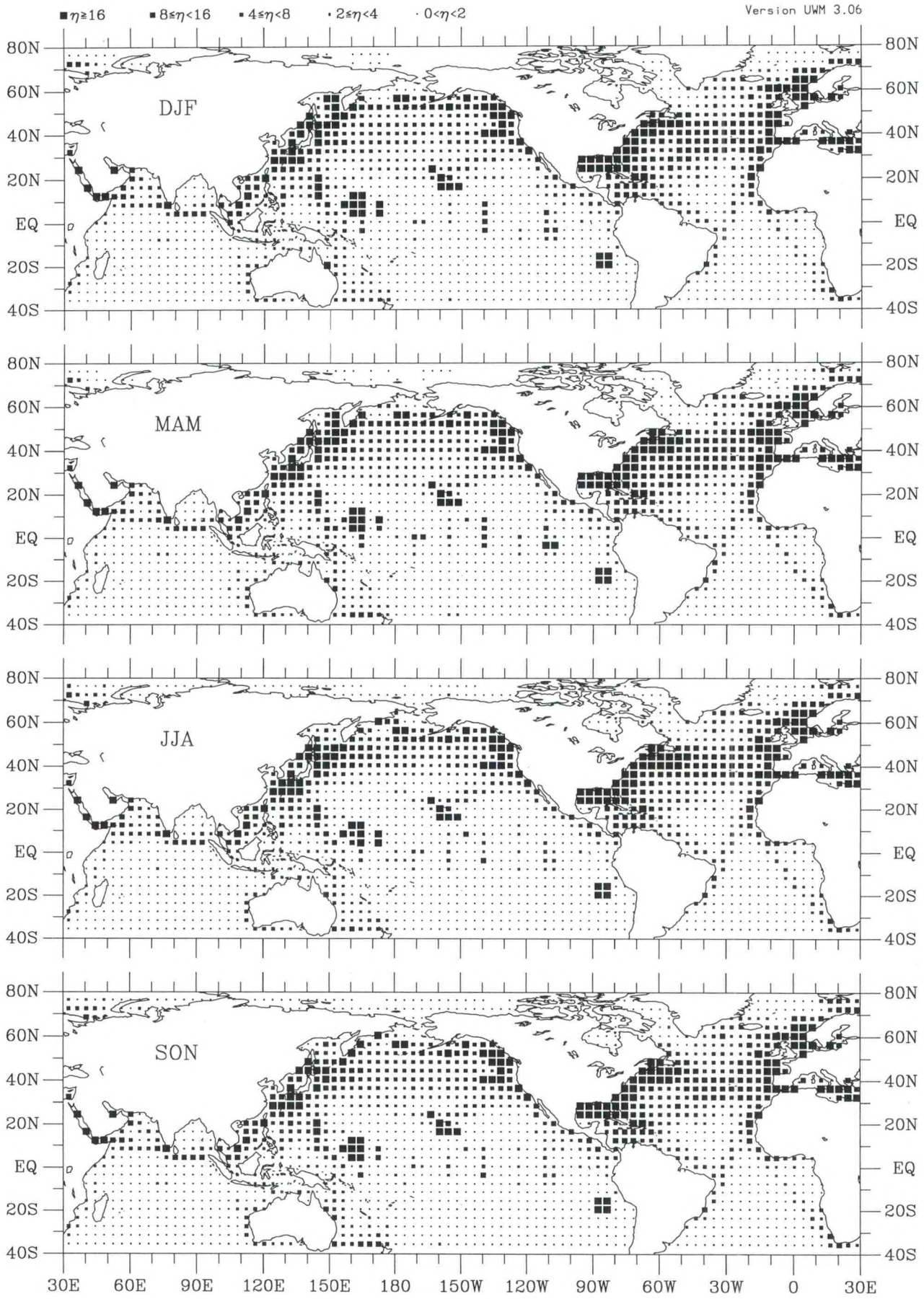

Figure tauy-1. Meridional wind stress seasonal observation density (1990-93).

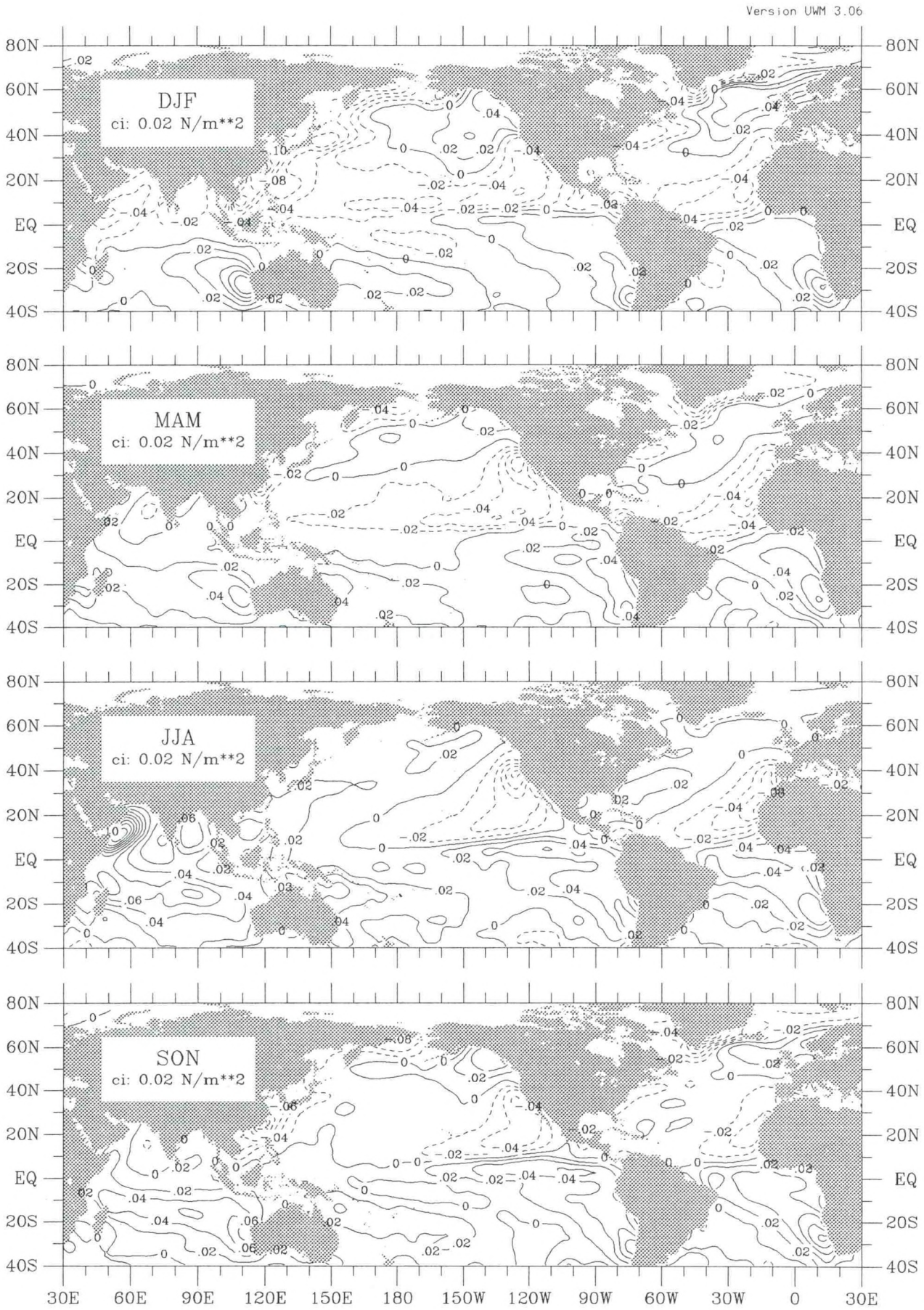

Figure tauy-2. Meridional wind stress seasonal climatology (1945-89).

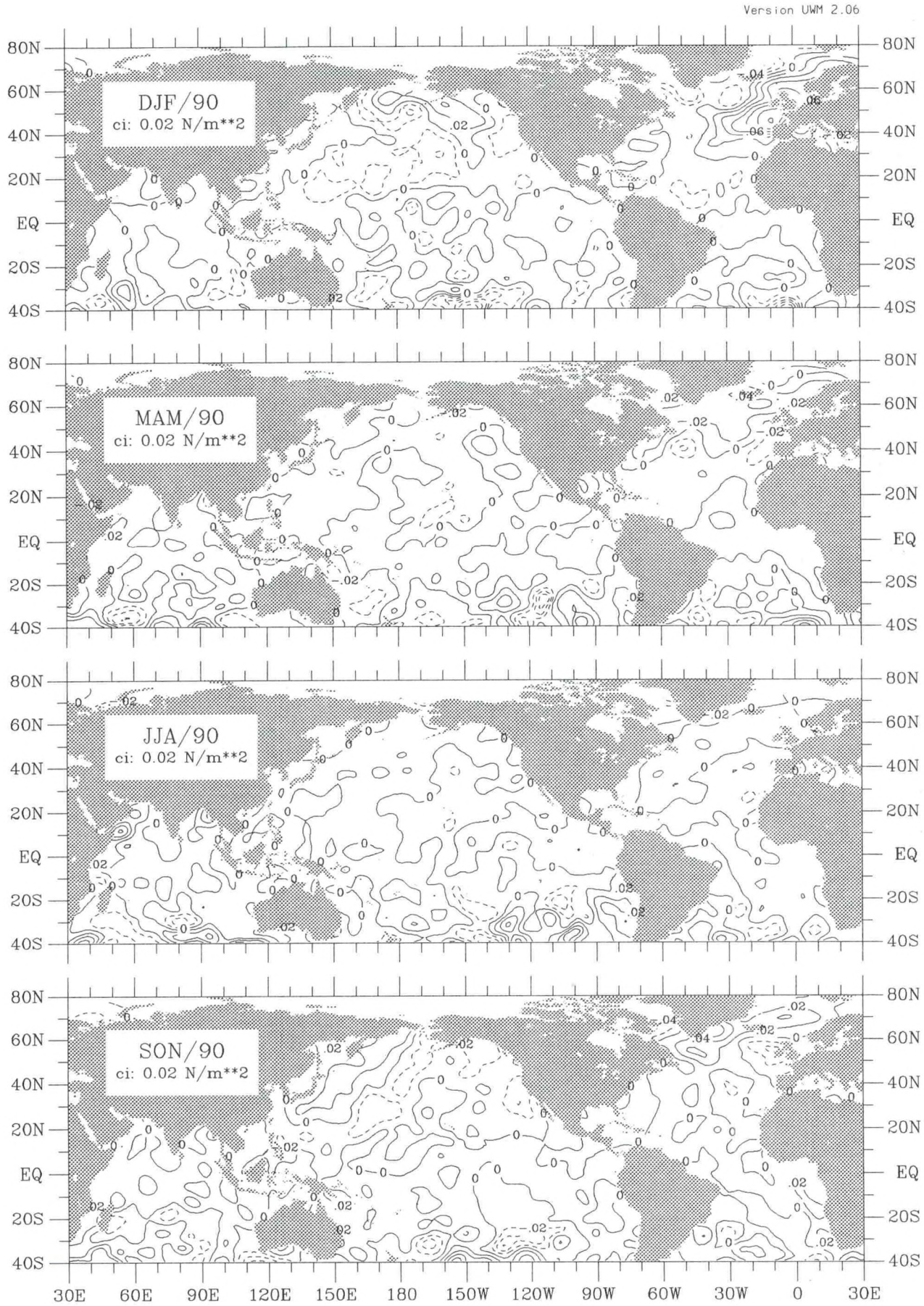

Figure tauy-3. Meridional wind stress seasonal anomaly for 1990.

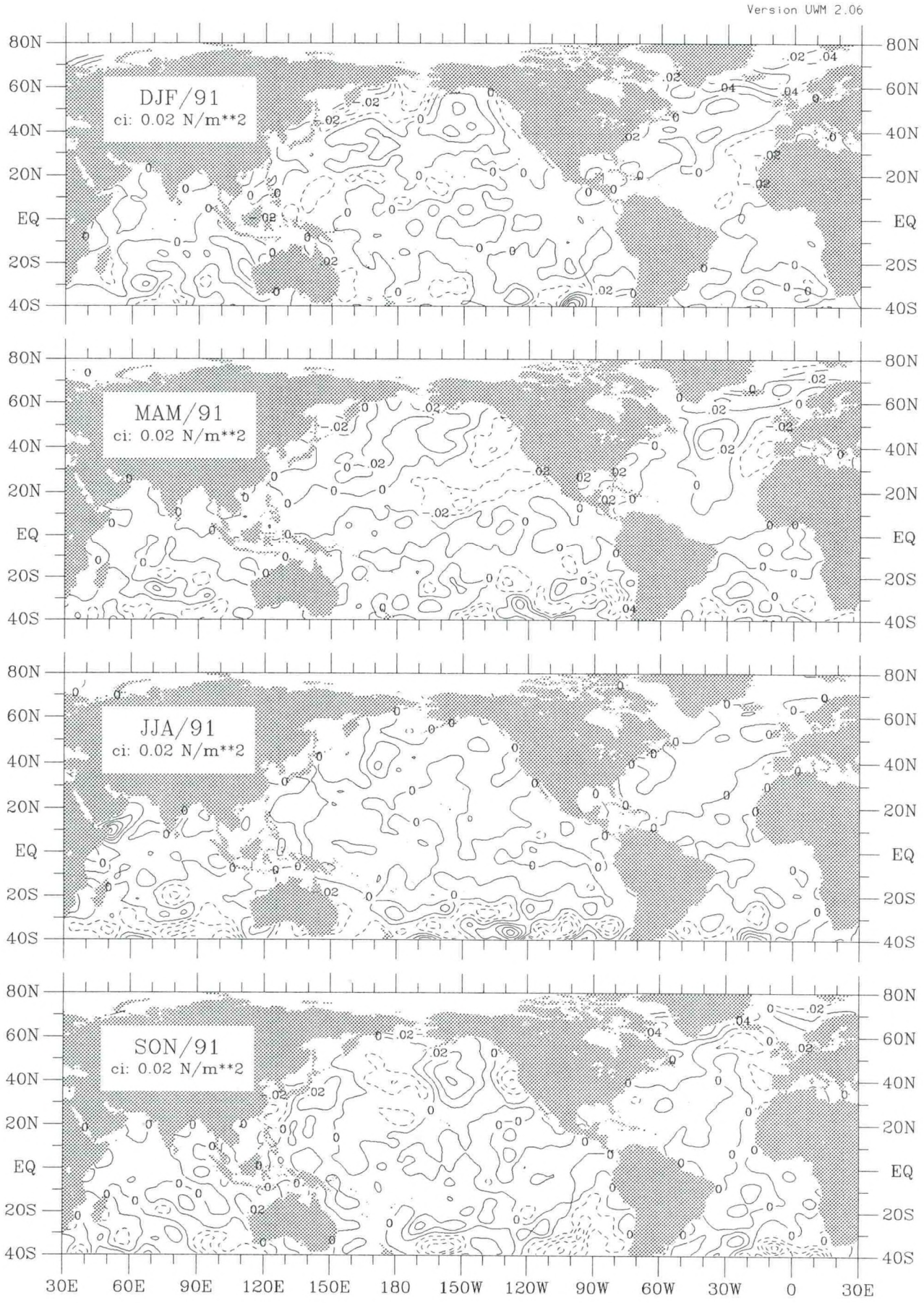

Figure tauy-4. Meridional wind stress seasonal anomaly for 1991.

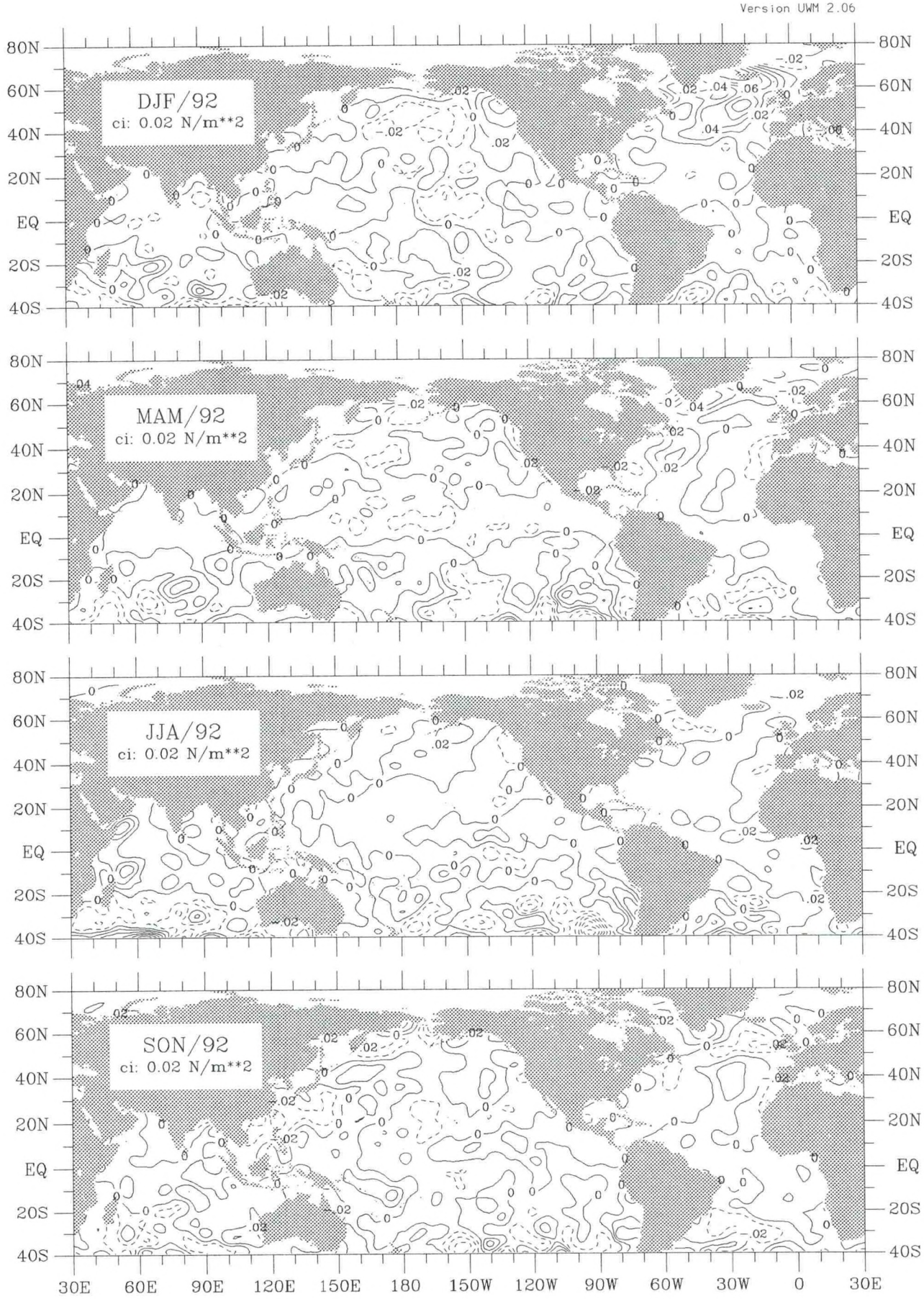

Figure tauy-5. Meridional wind stress seasonal anomaly for 1992.

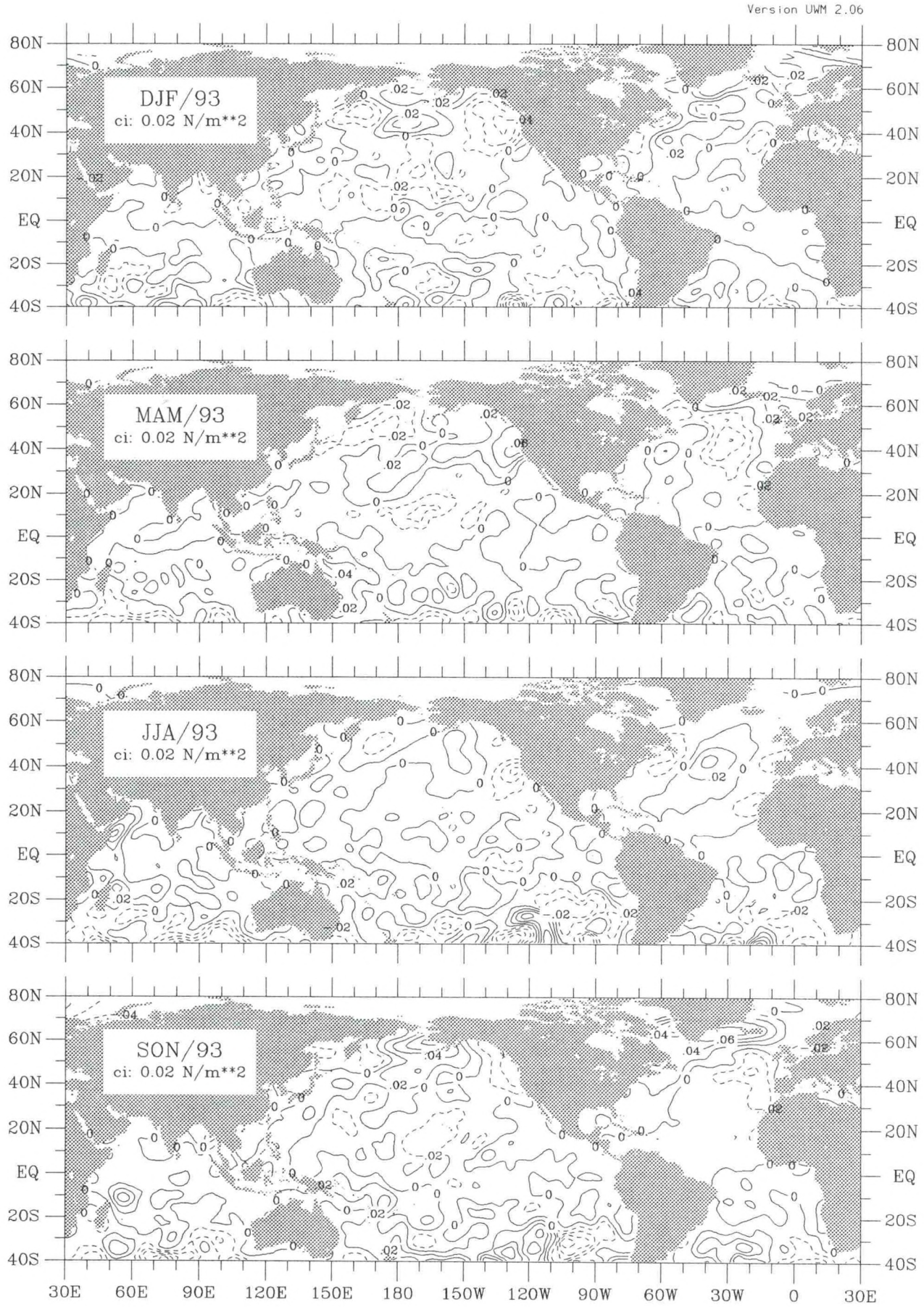

Figure tauy-6. Meridional wind stress seasonal anomaly for 1993.

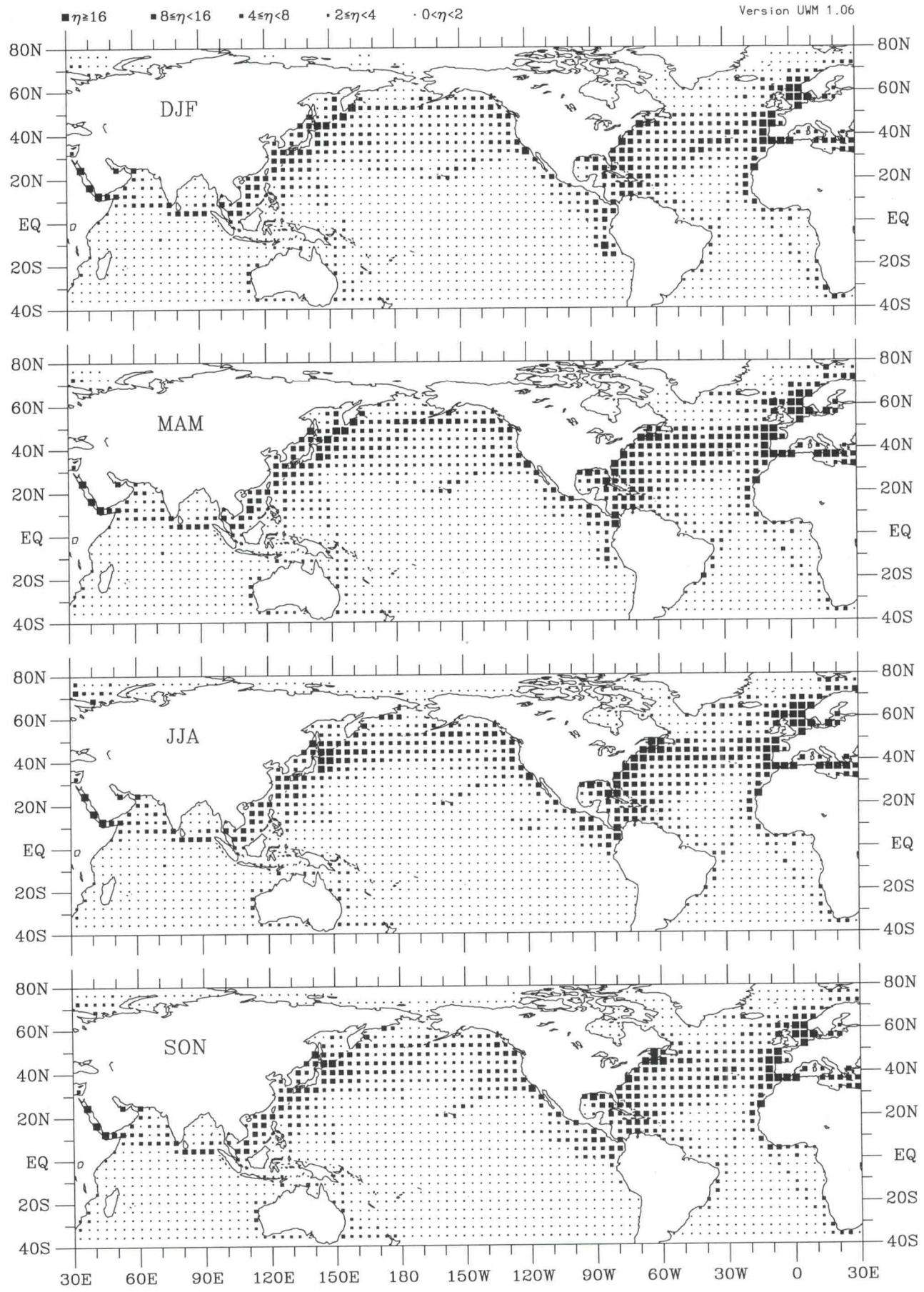

Figure Rs–1. Net short wave radiation seasonal observation density (1990–93).

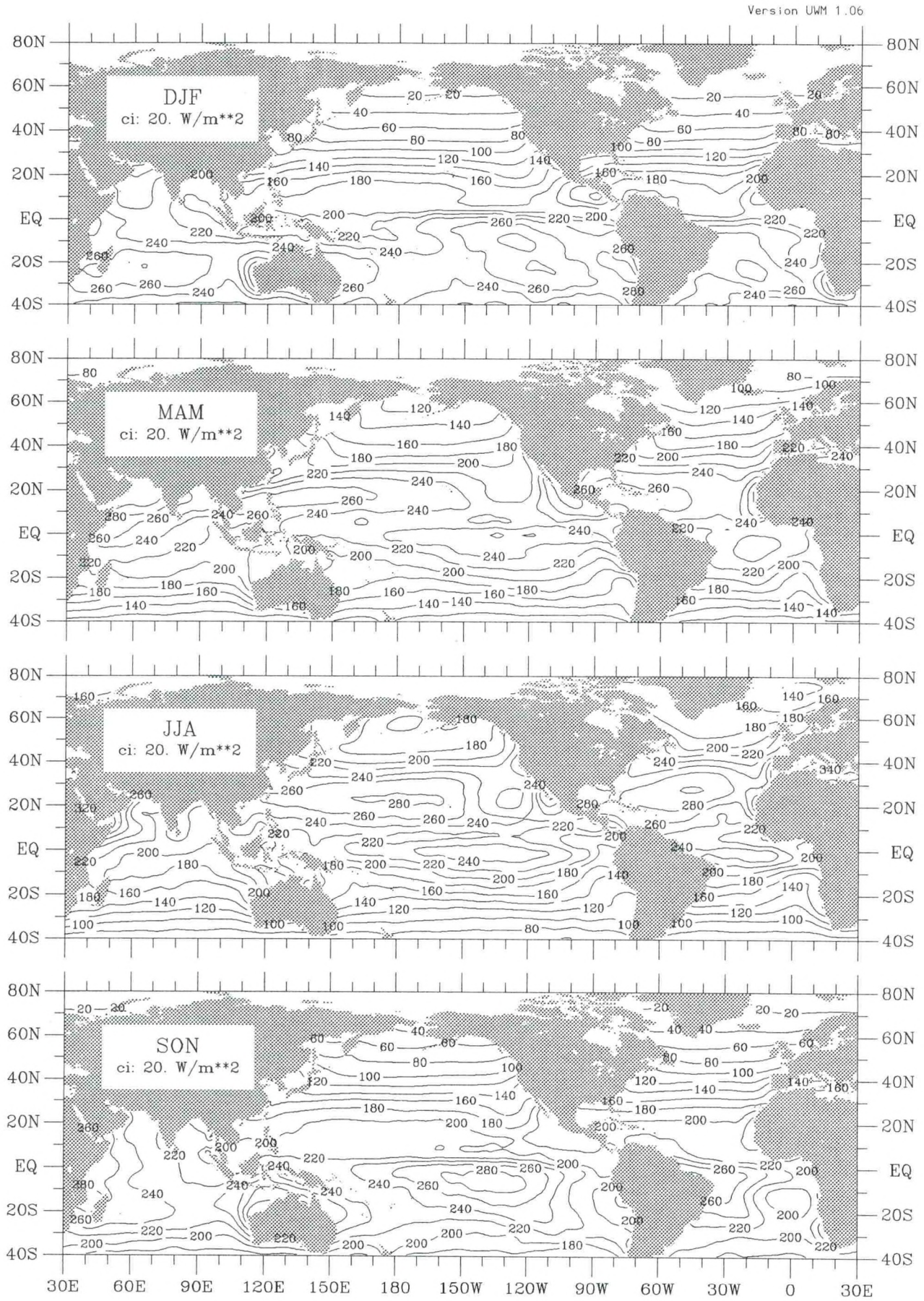

Figure Rs-2. Net short wave radiation seasonal climatology (1945-89).

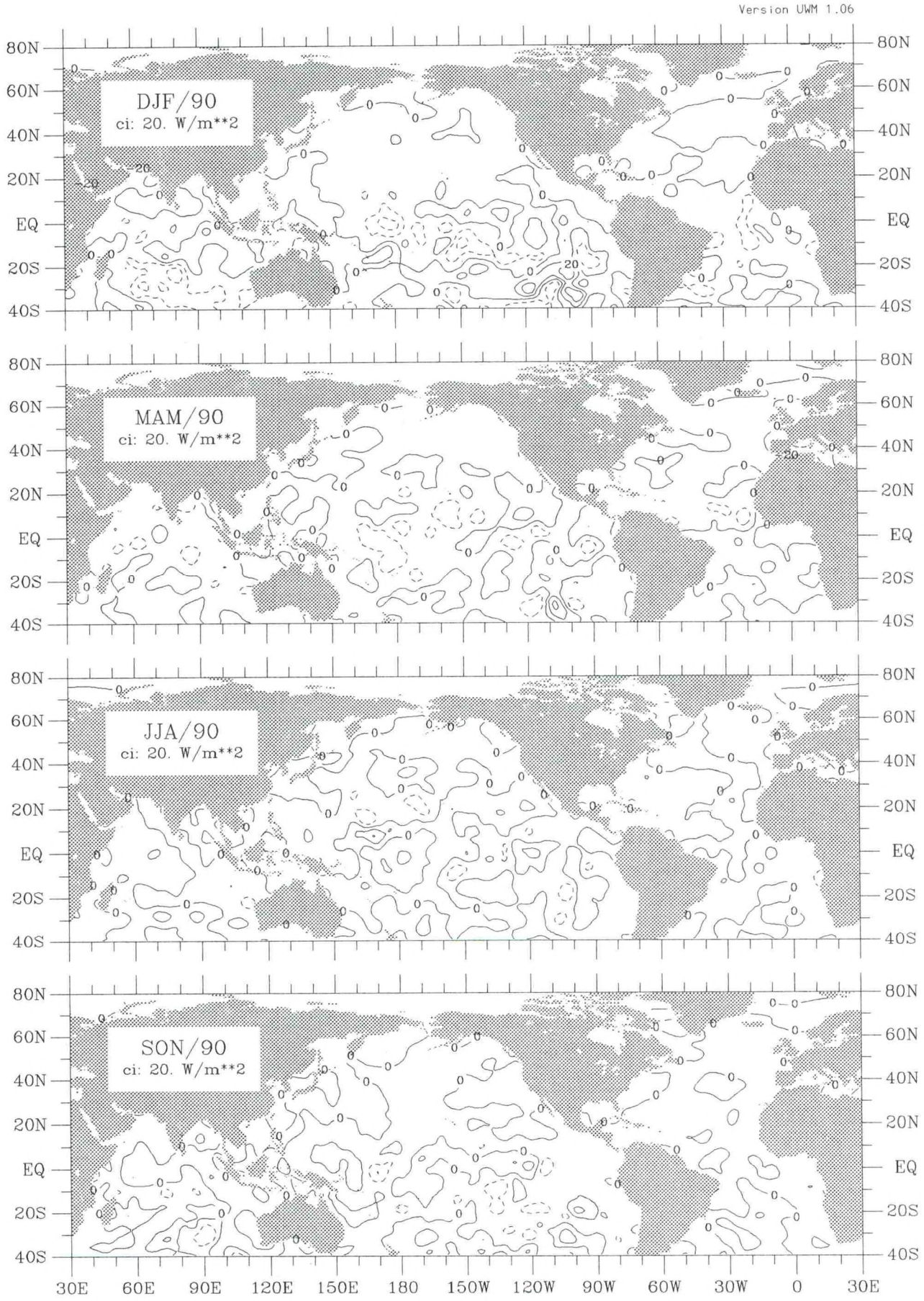

Figure Rs-3. Net short wave radiation seasonal anomaly for 1990.

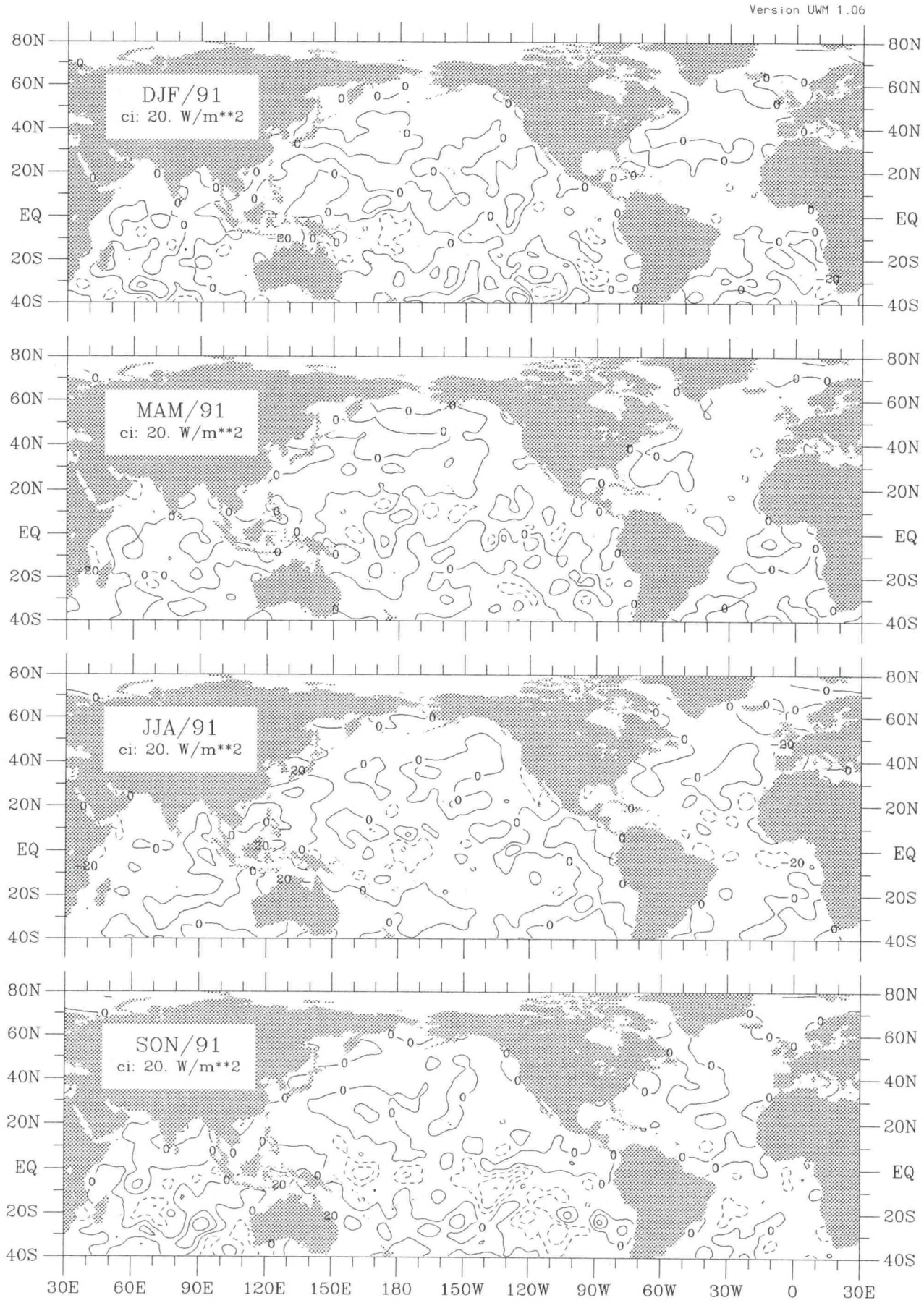

Figure Rs-4. Net short wave radiation seasonal anomaly for 1991.

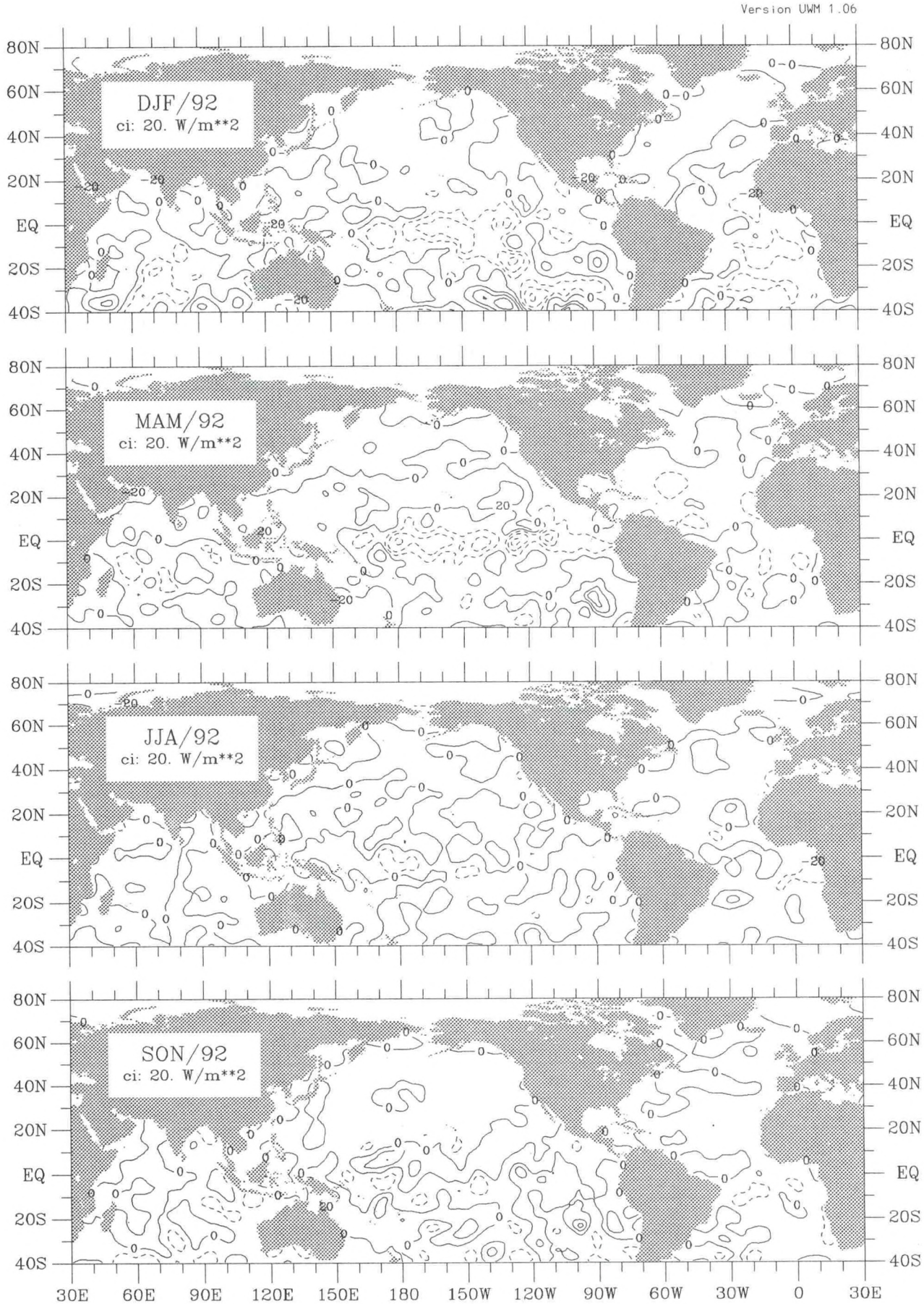

Figure Rs-5. Net short wave radiation seasonal anomaly for 1992.

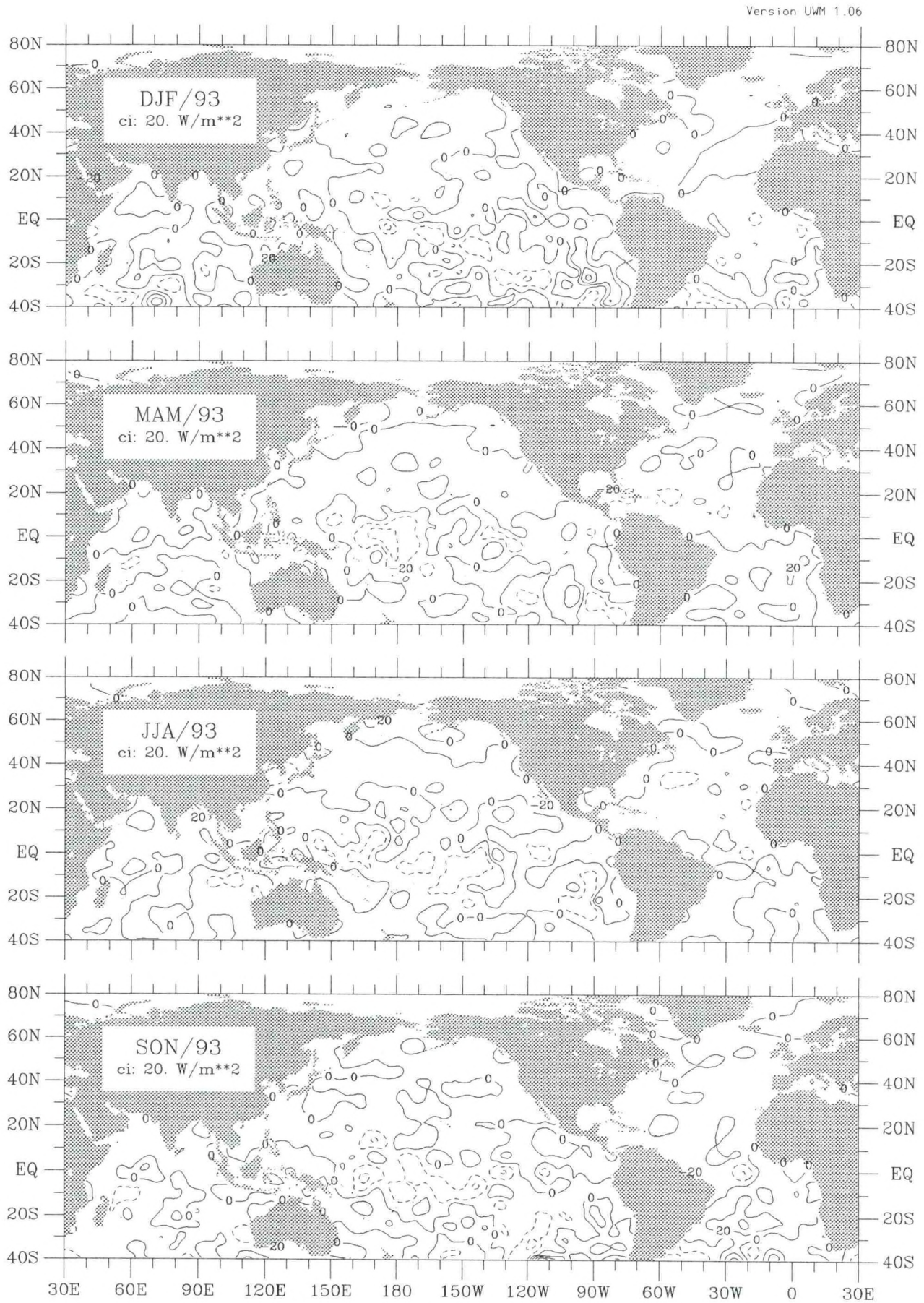

Figure Rs-6. Net short wave radiation seasonal anomaly for 1993.

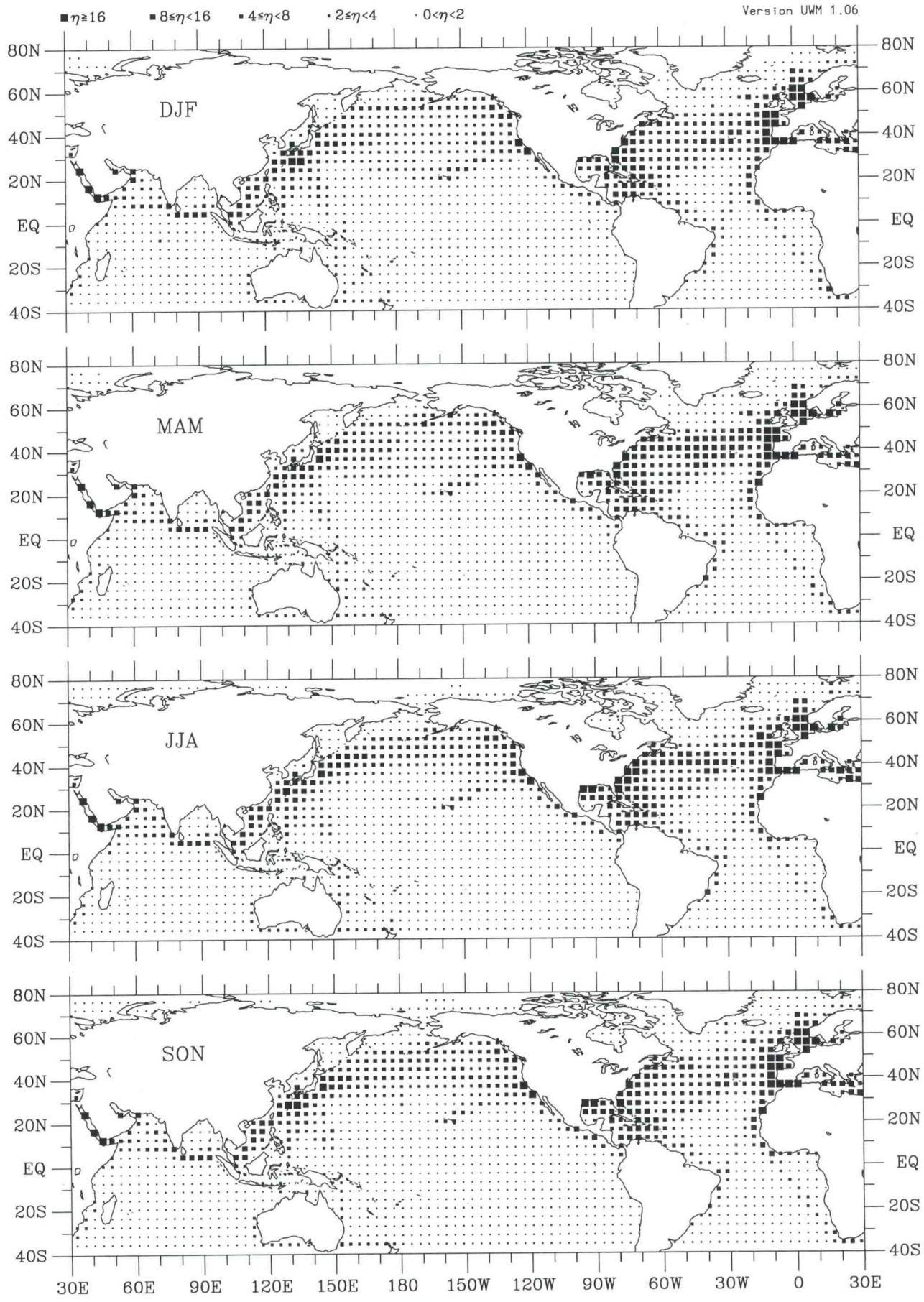

Figure Rl-1. Net long wave radiation seasonal observation density (1990-93).

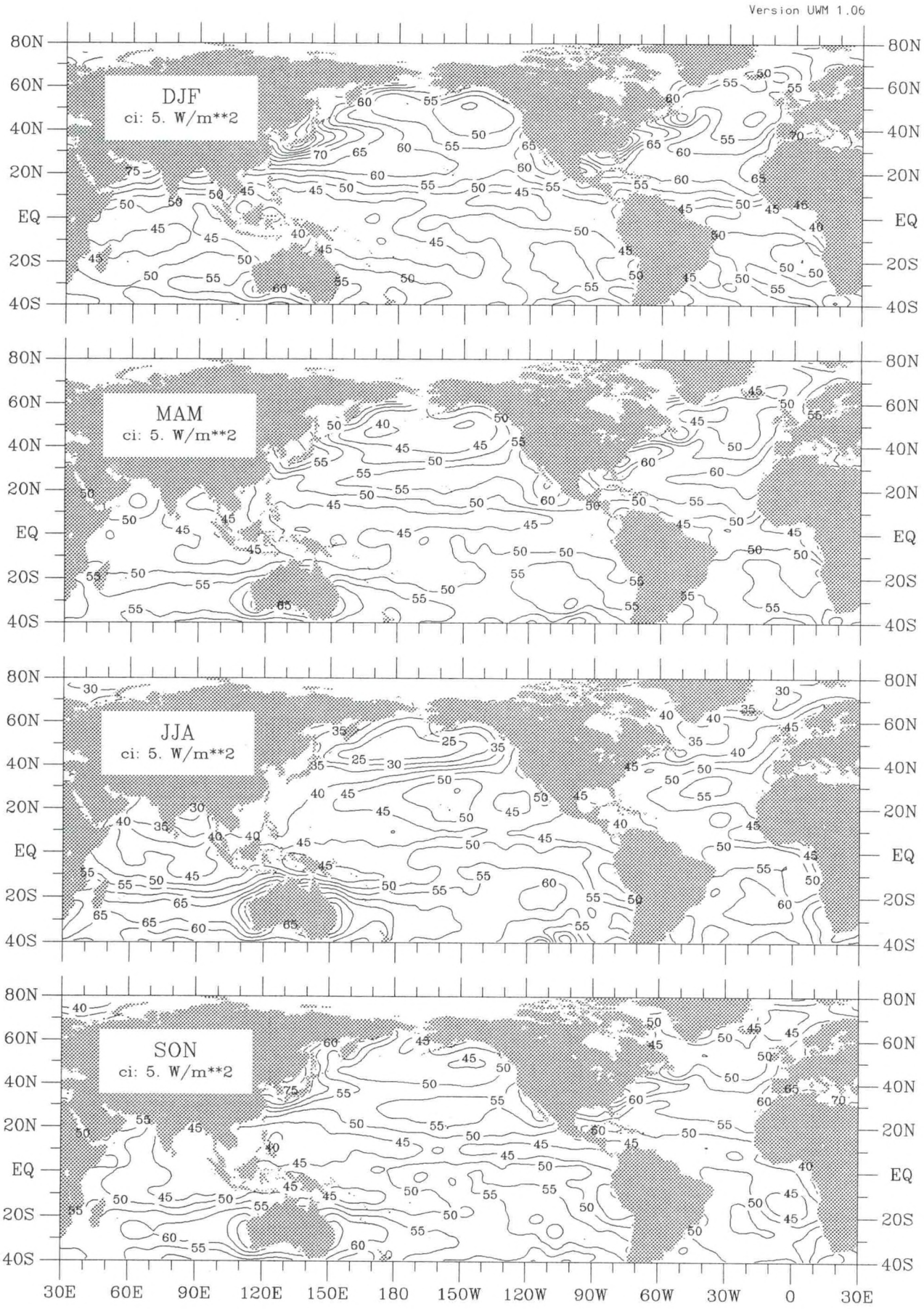

Figure Rl–2. Net longwave radiation seasonal climatology (1945–89).

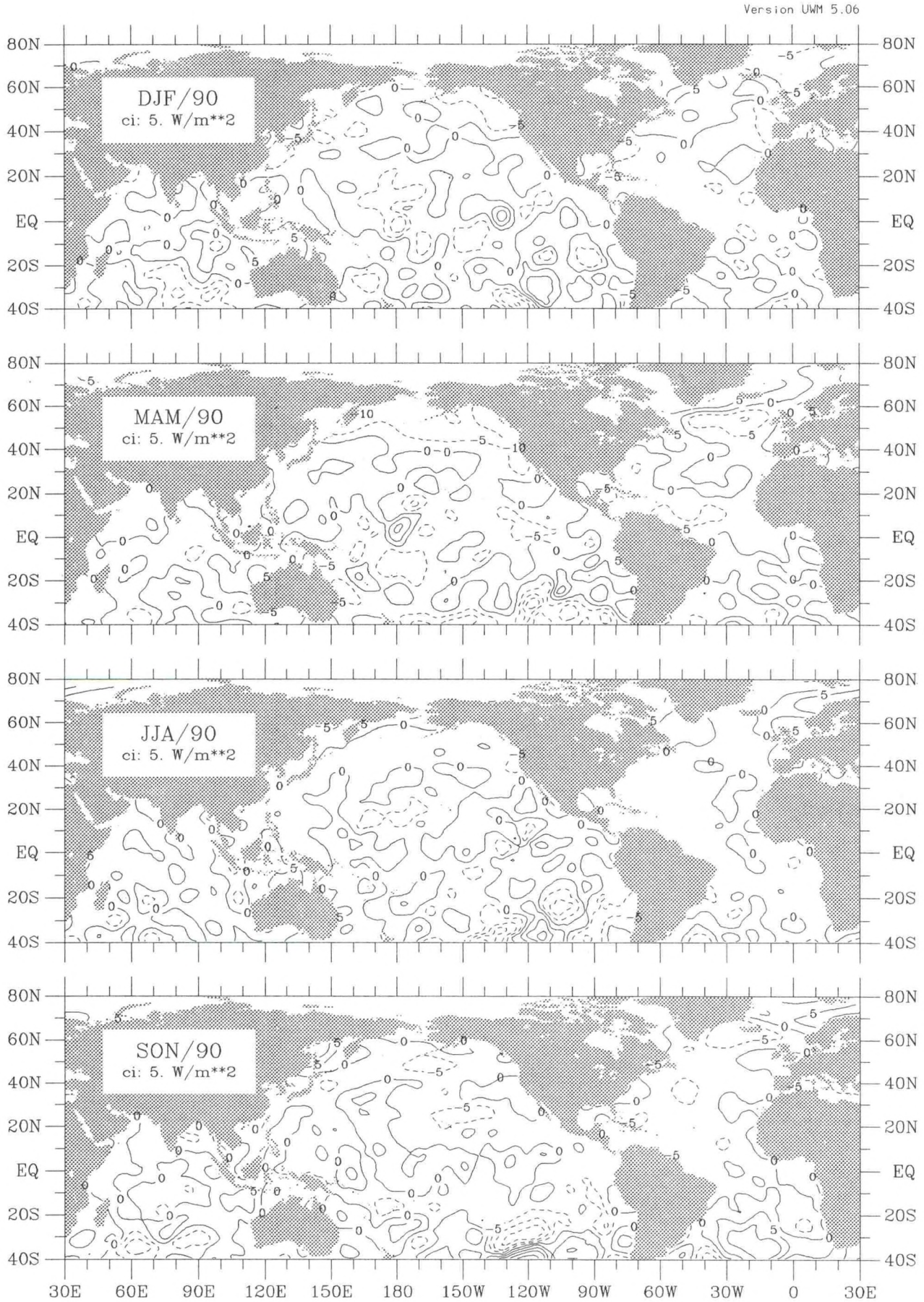

Figure R1-3. Net long wave radiation seasonal anomaly for 1990.

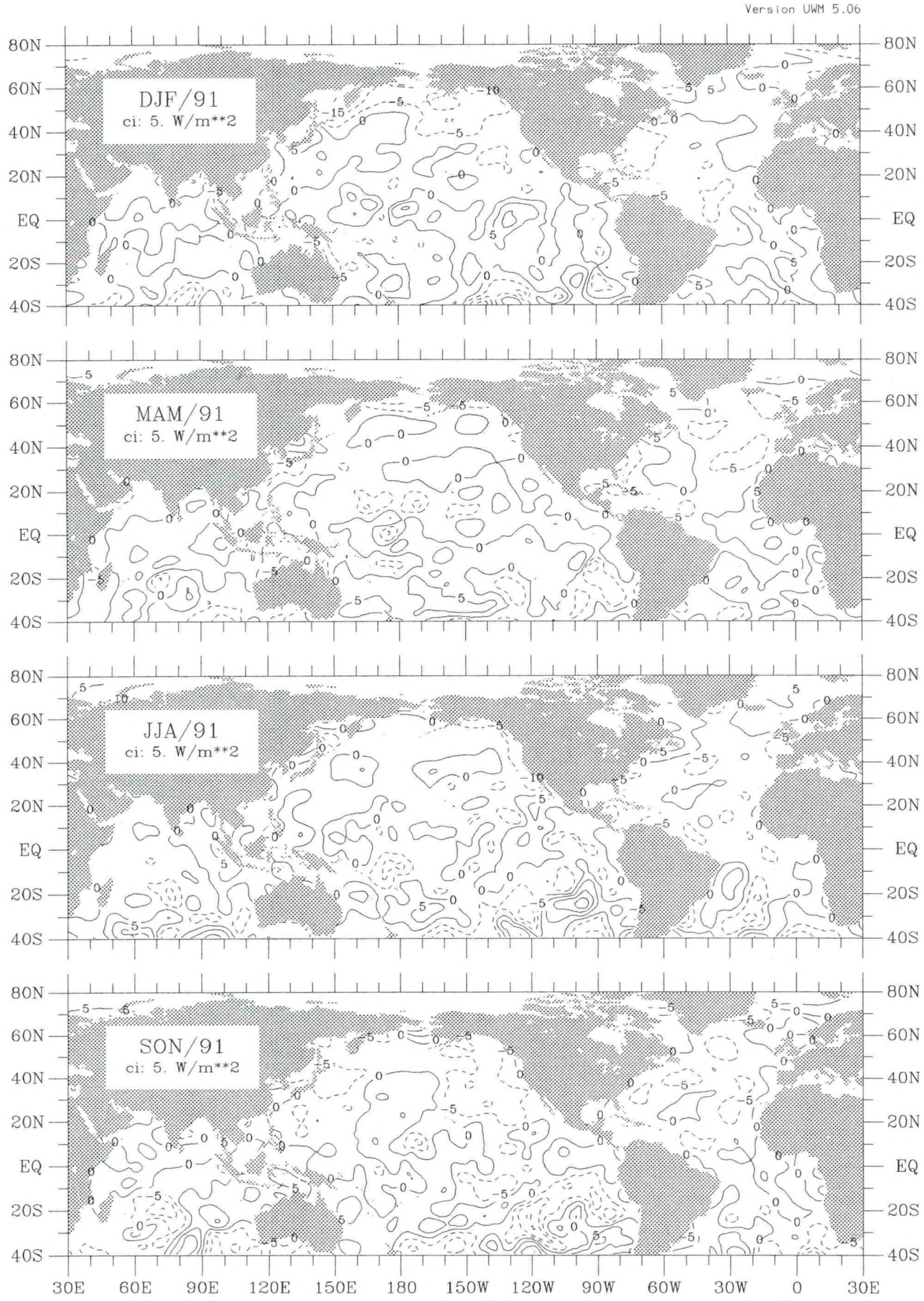

Figure Rl-4. Net long wave radiation seasonal anomaly for 1991.

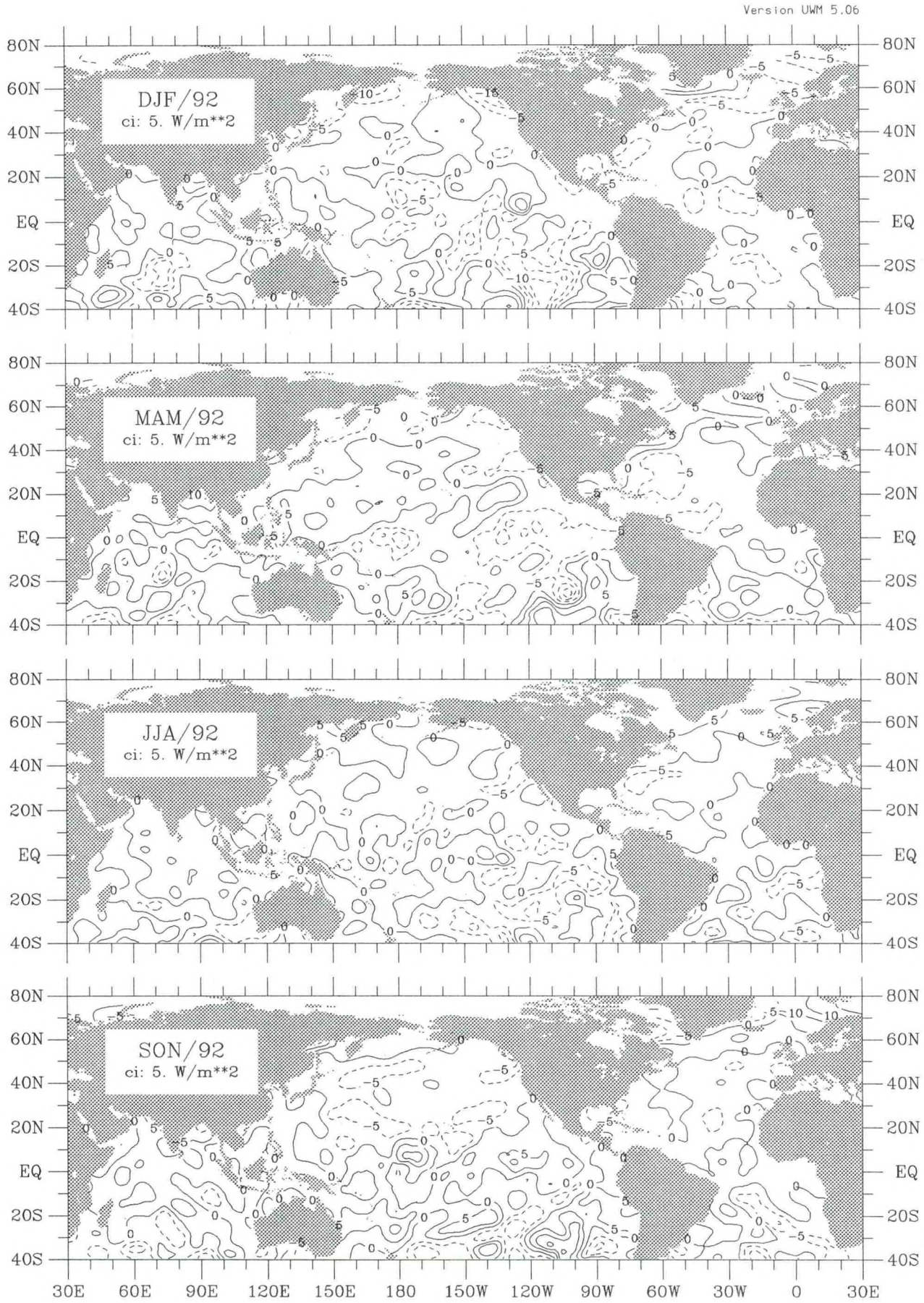

Figure Rl–5. Net long wave radiation seasonal anomaly for 1992.

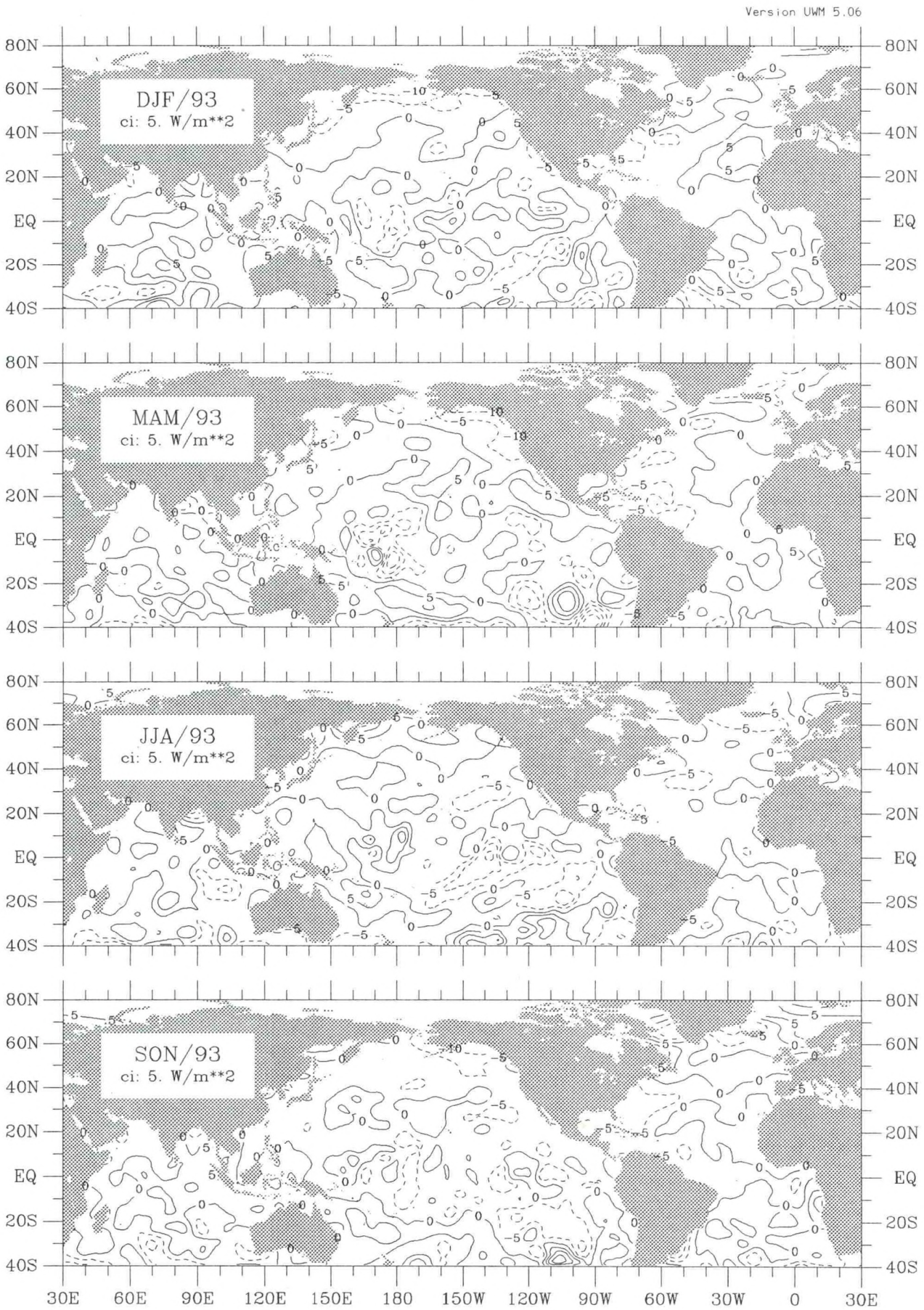

Figure Rl–6. Net long wave radiation seasonal anomaly for 1993.

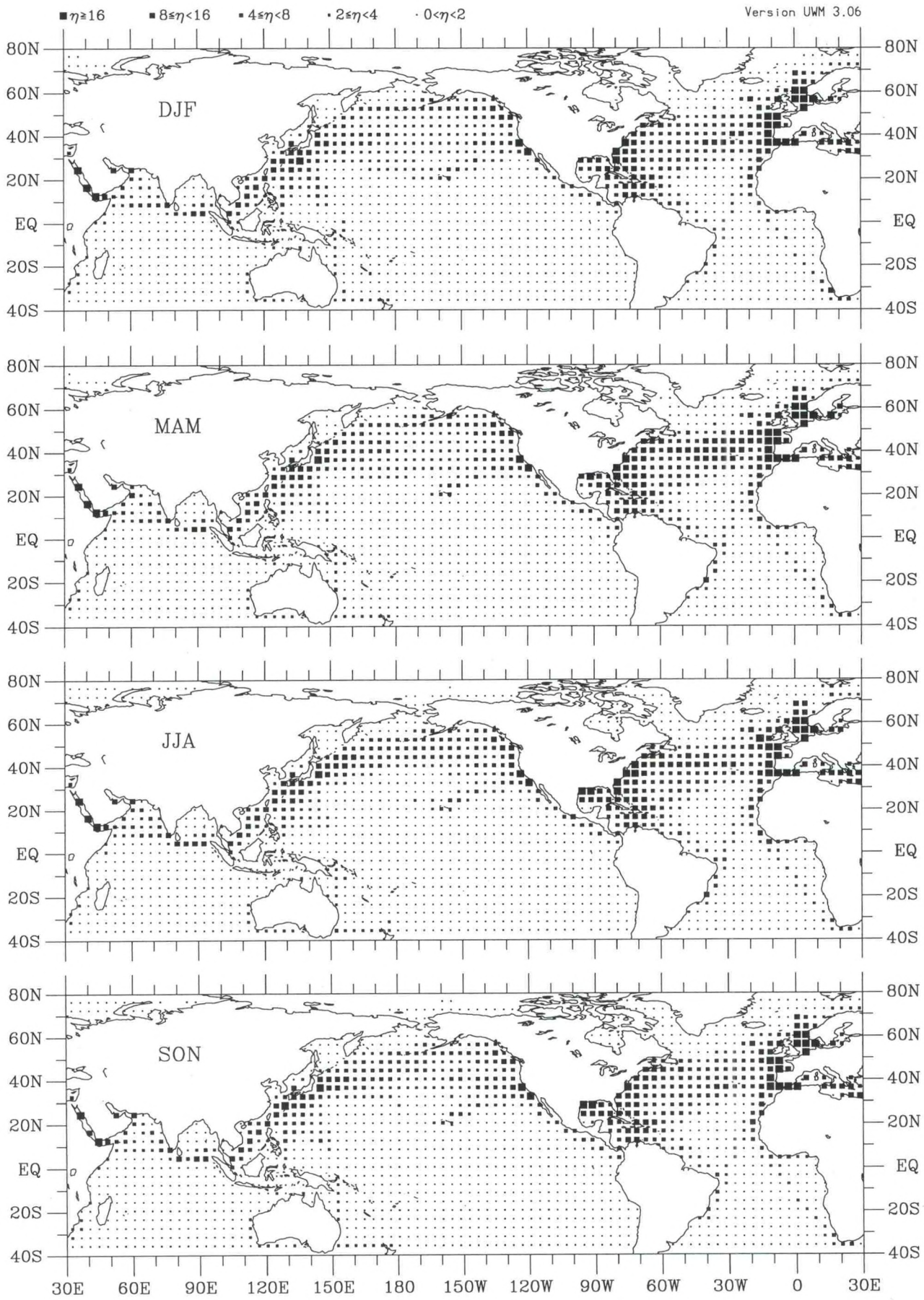

Figure Ql−1. Latent heat flux seasonal observation density (1990−93).

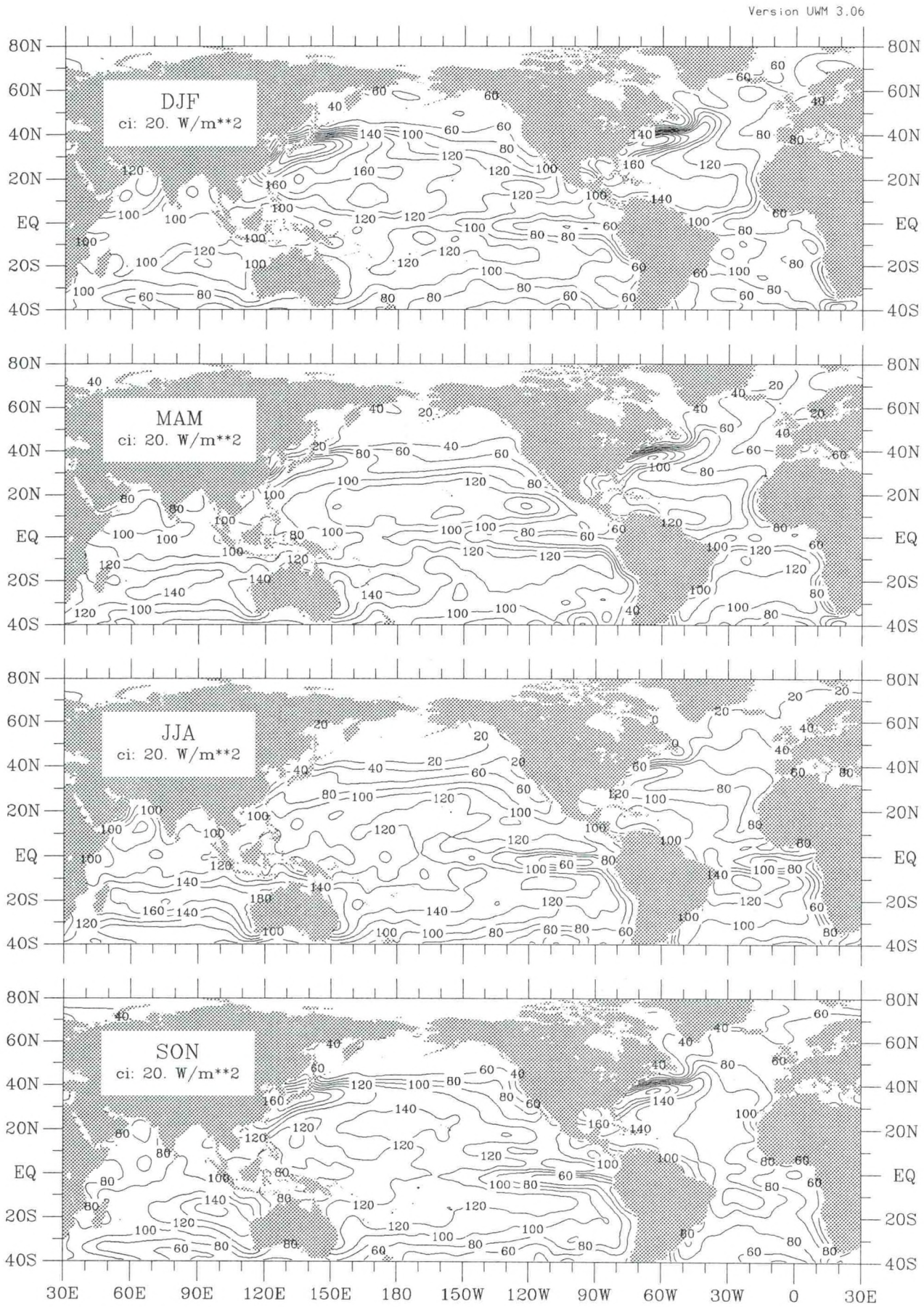

Figure Q1-2. Latent heat flux seasonal climatology (1945-89).

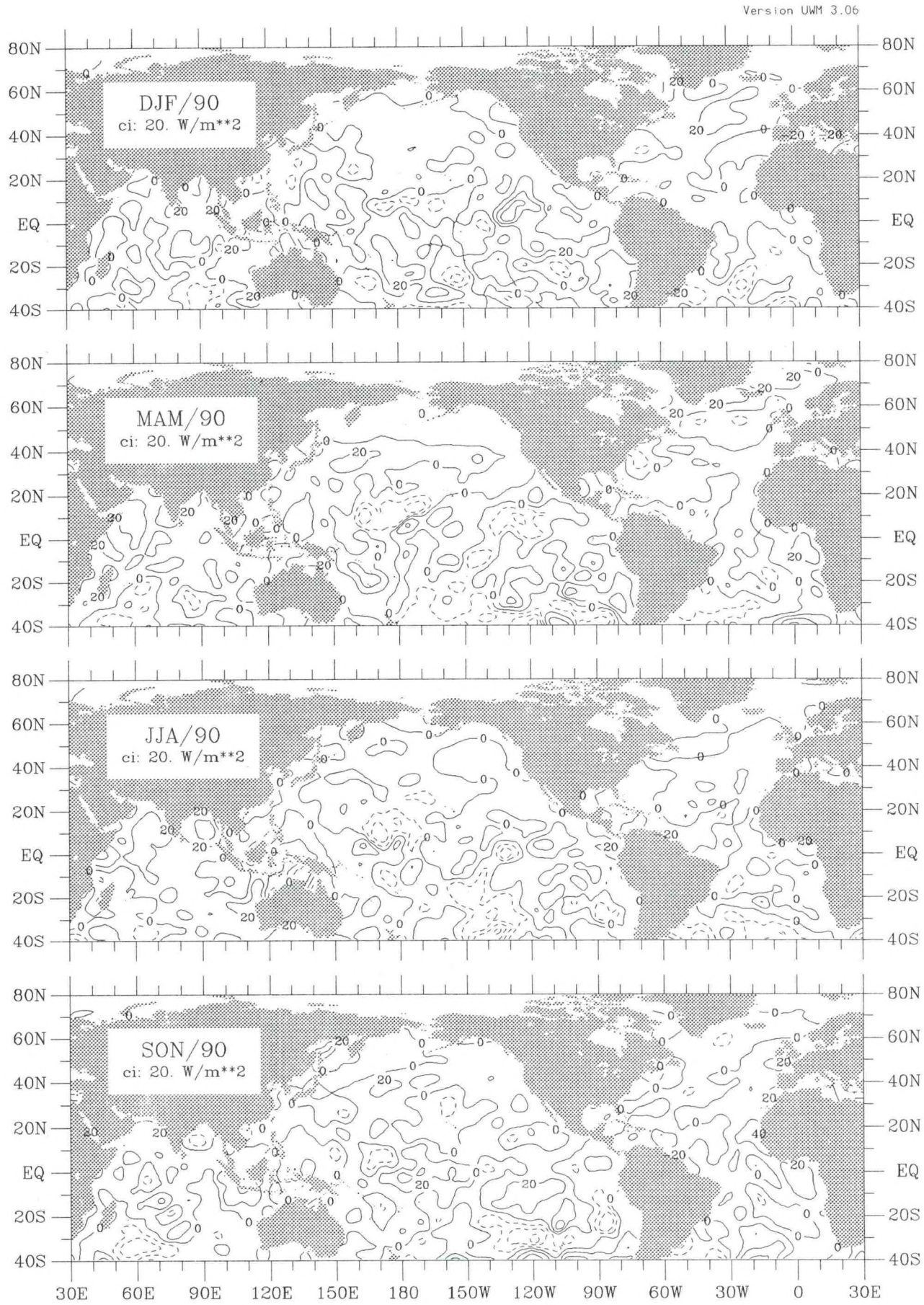

Figure Q1-3. Latent heat flux seasonal anomaly for 1990.

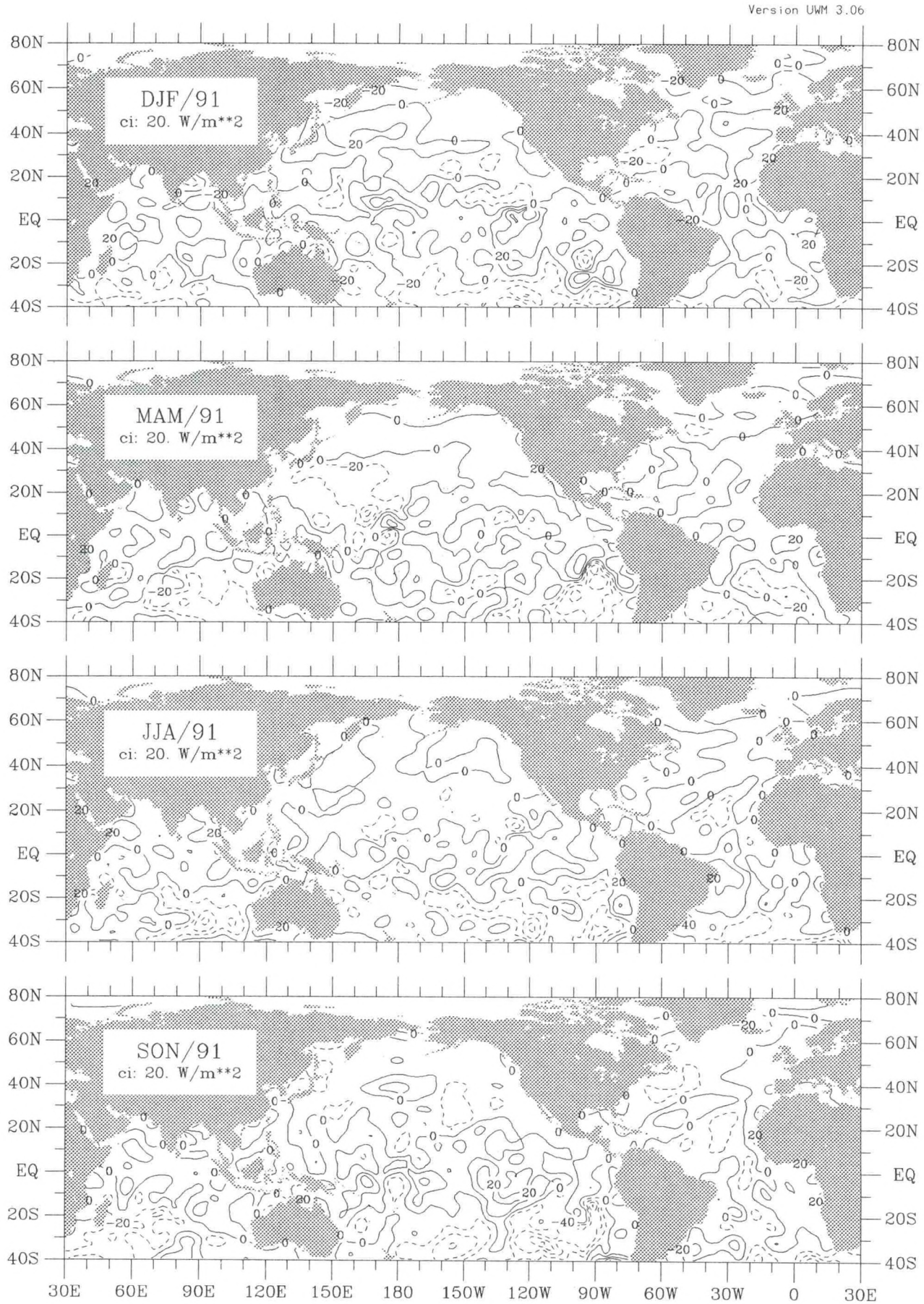

Figure Q1-4. Latent heat flux seasonal anomaly for 1991.

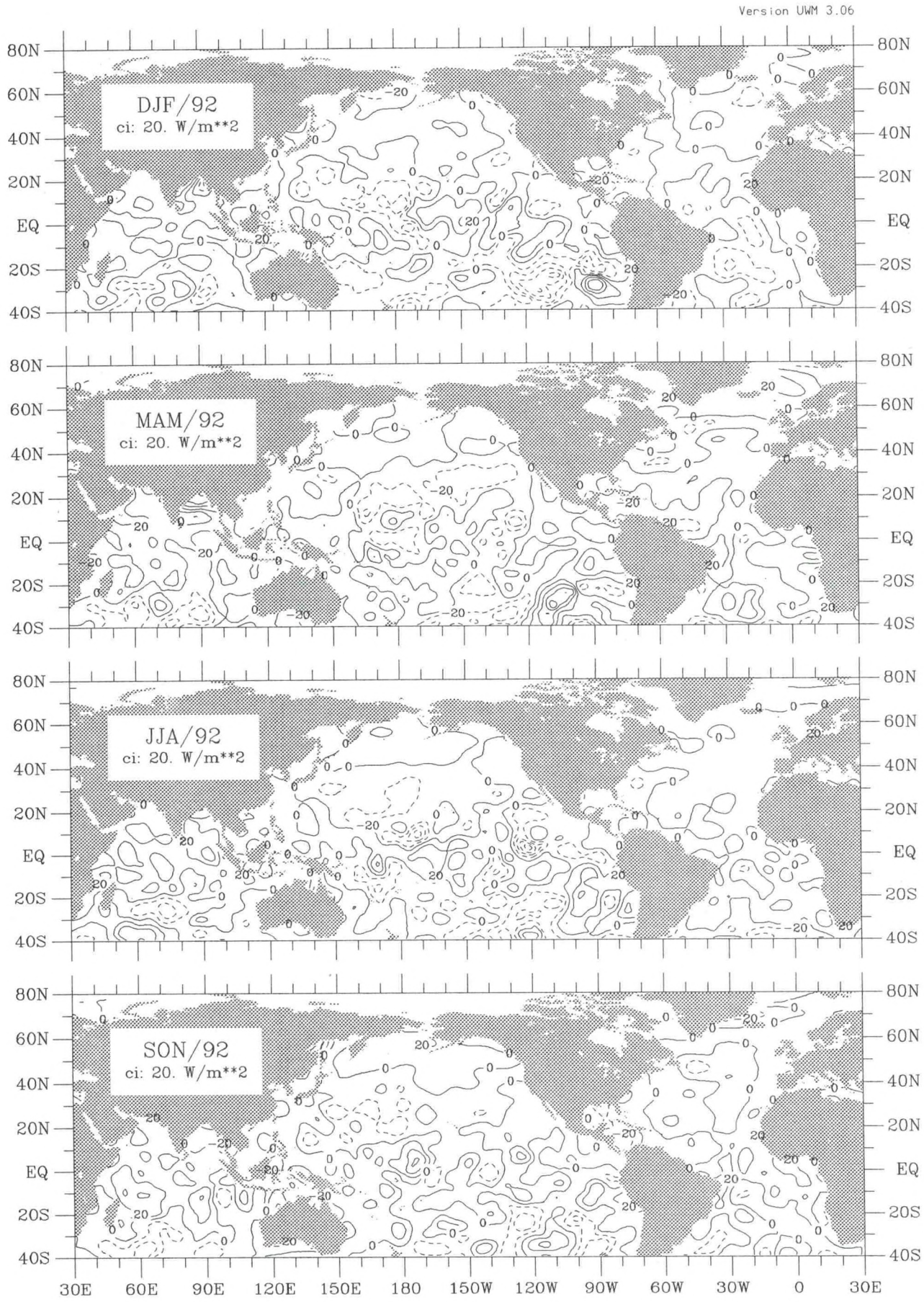

Figure Q1-5. Latent heat flux seasonal anomaly for 1992.

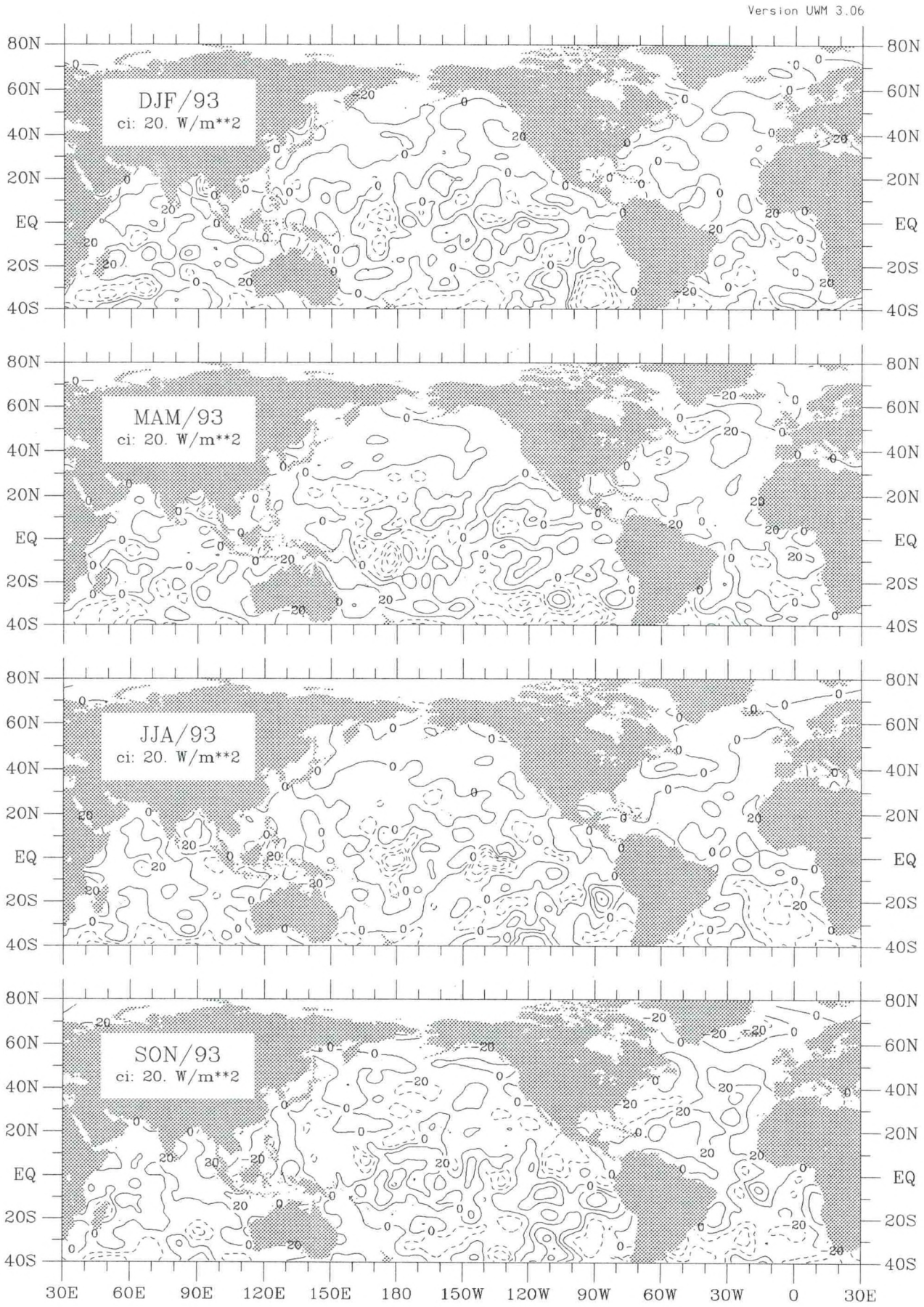

Figure Q1-6. Latent heat flux seasonal anomaly for 1993.

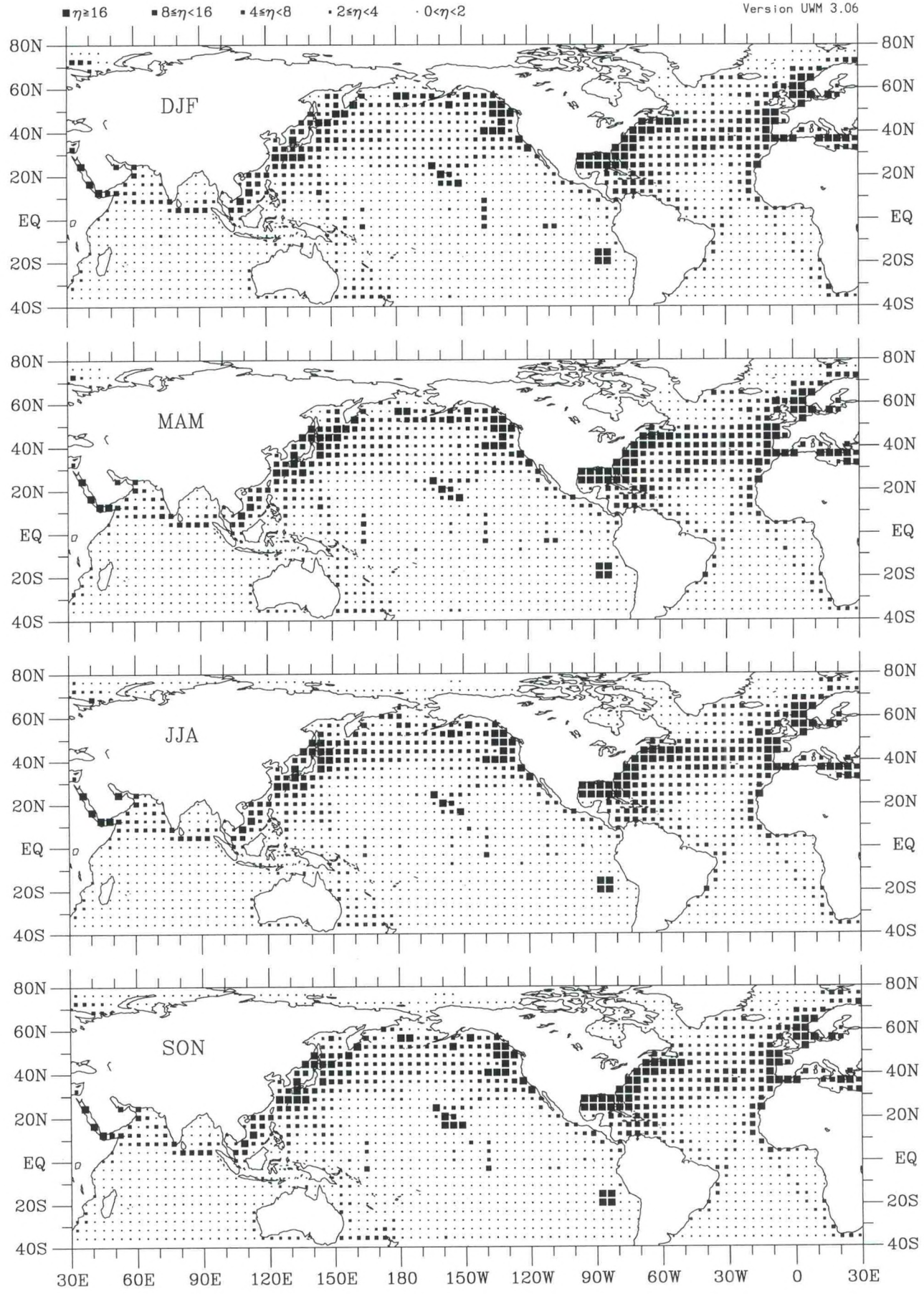

Figure Qs-1. Sensible heat flux seasonal observation density (1990-93).

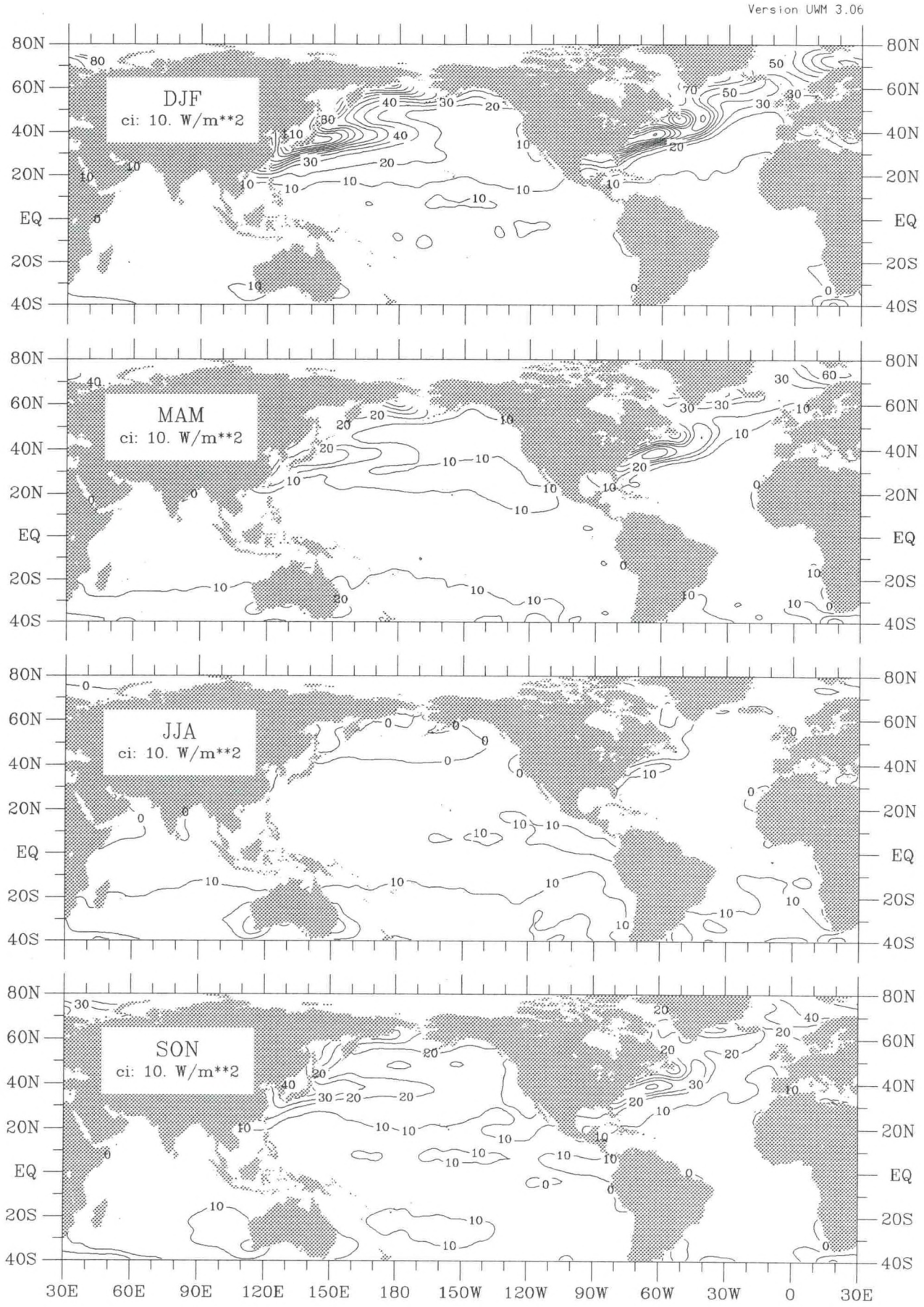

Figure Qs-2. Sensible heat flux seasonal climatology (1945-89).

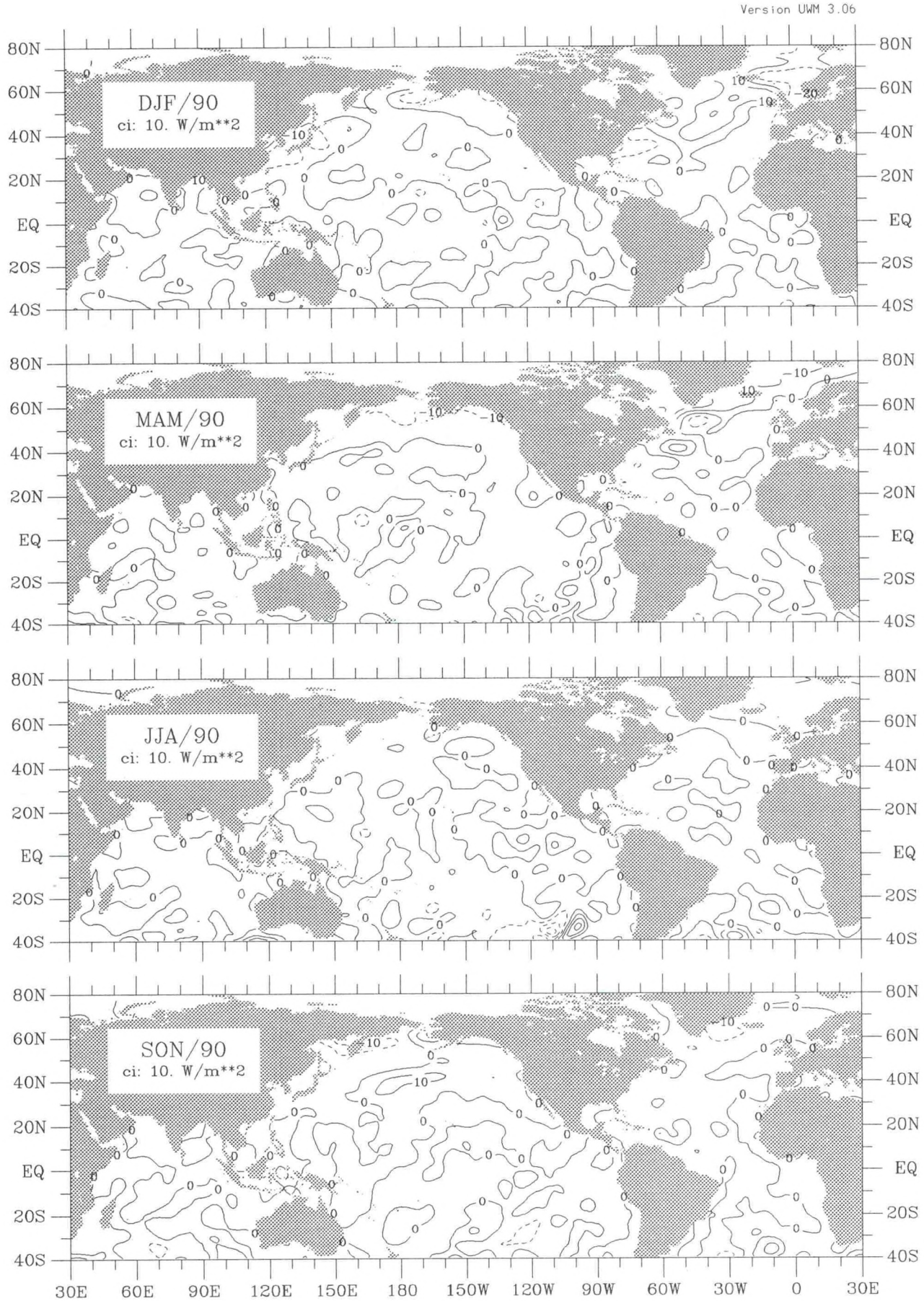

Figure Qs-3. Sensible heat flux seasonal anomaly for 1990.

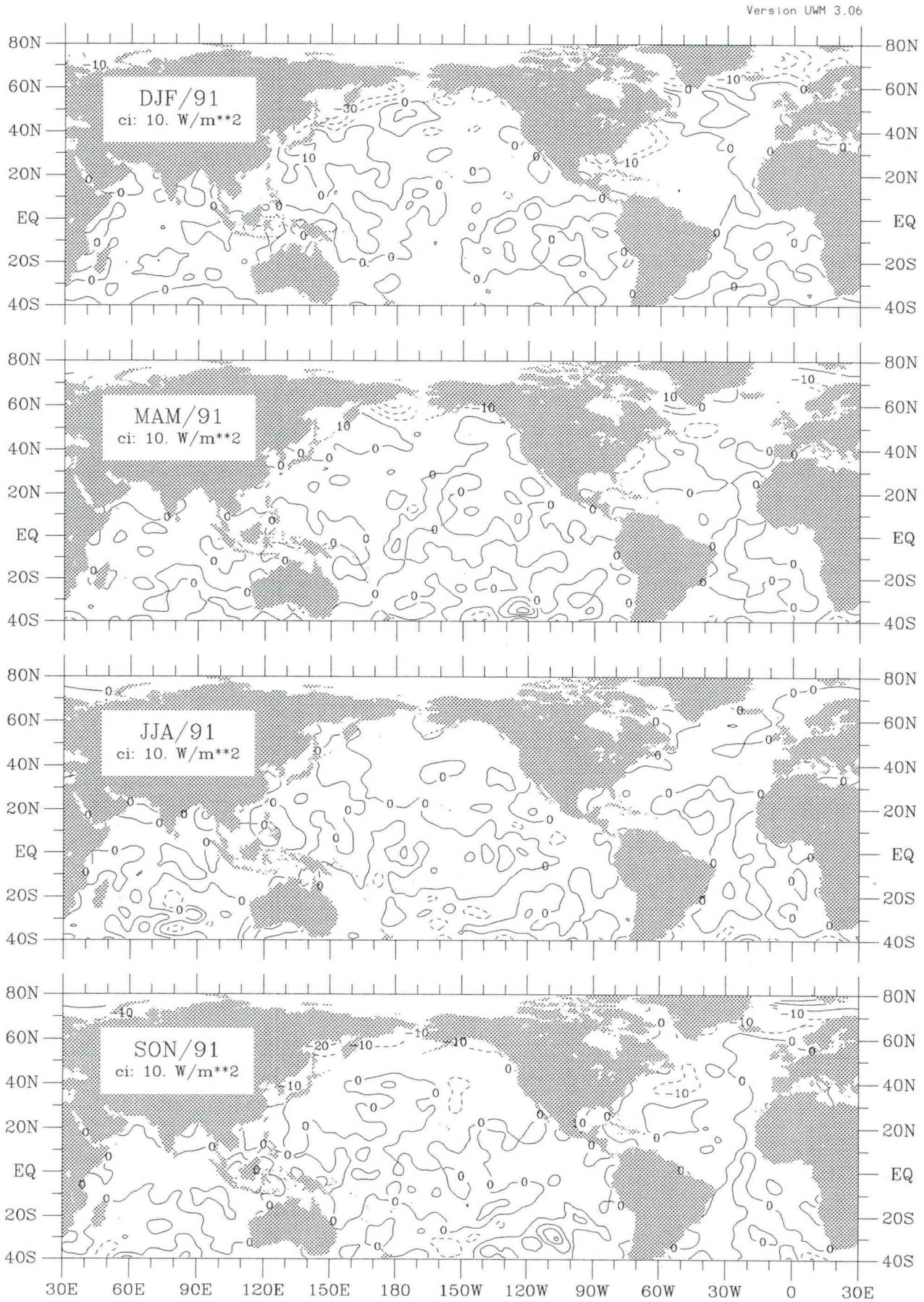

Figure Qs-4. Sensible heat flux seasonal anomaly for 1991.

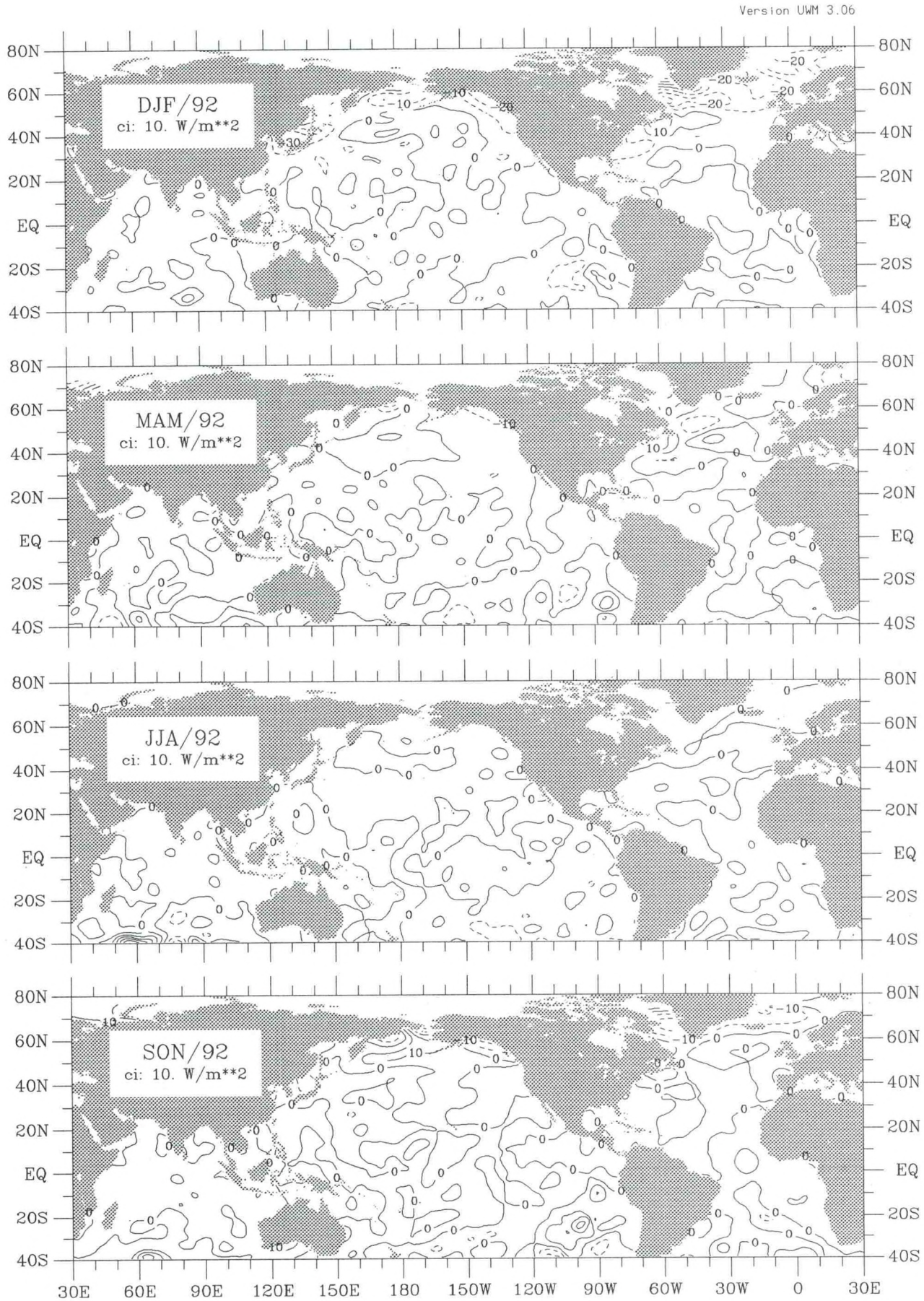

Figure Qs-5. Sensible heat flux seasonal anomaly for 1992.

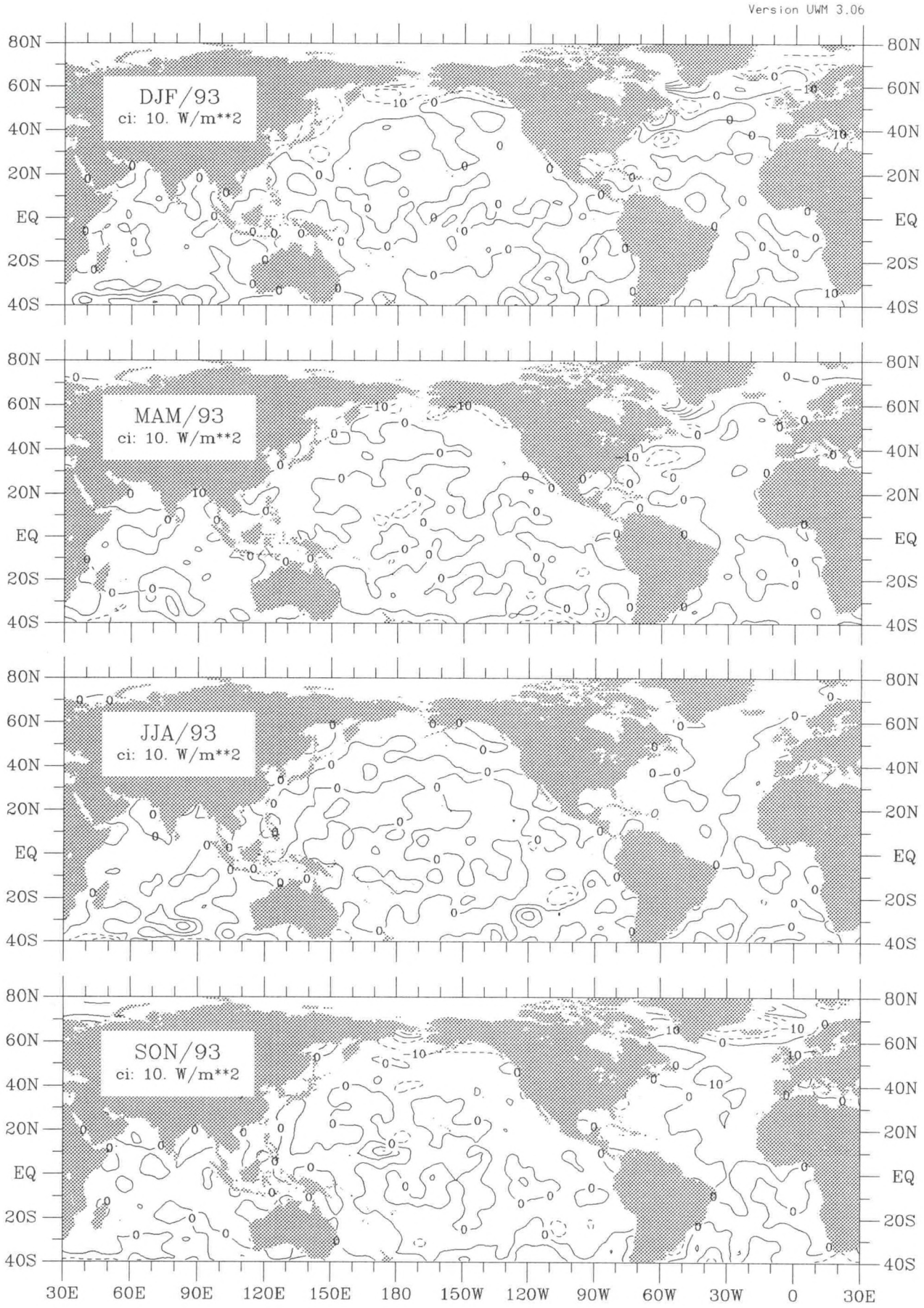

Figure Qs-6. Sensible heat flux seasonal anomaly for 1993.

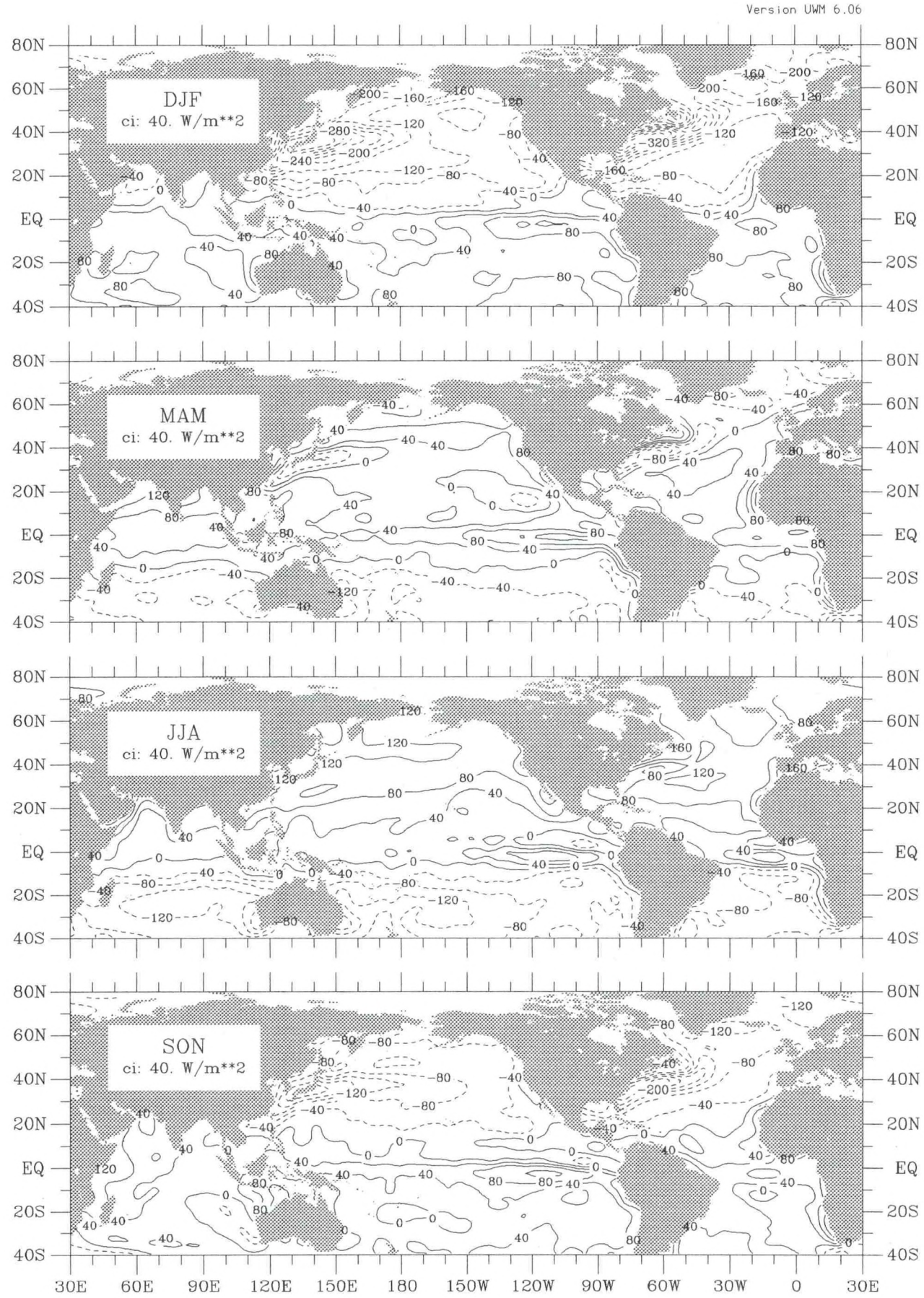

Figure Qnet-2. Constrained net heat flux seasonal climatology (1945-89).

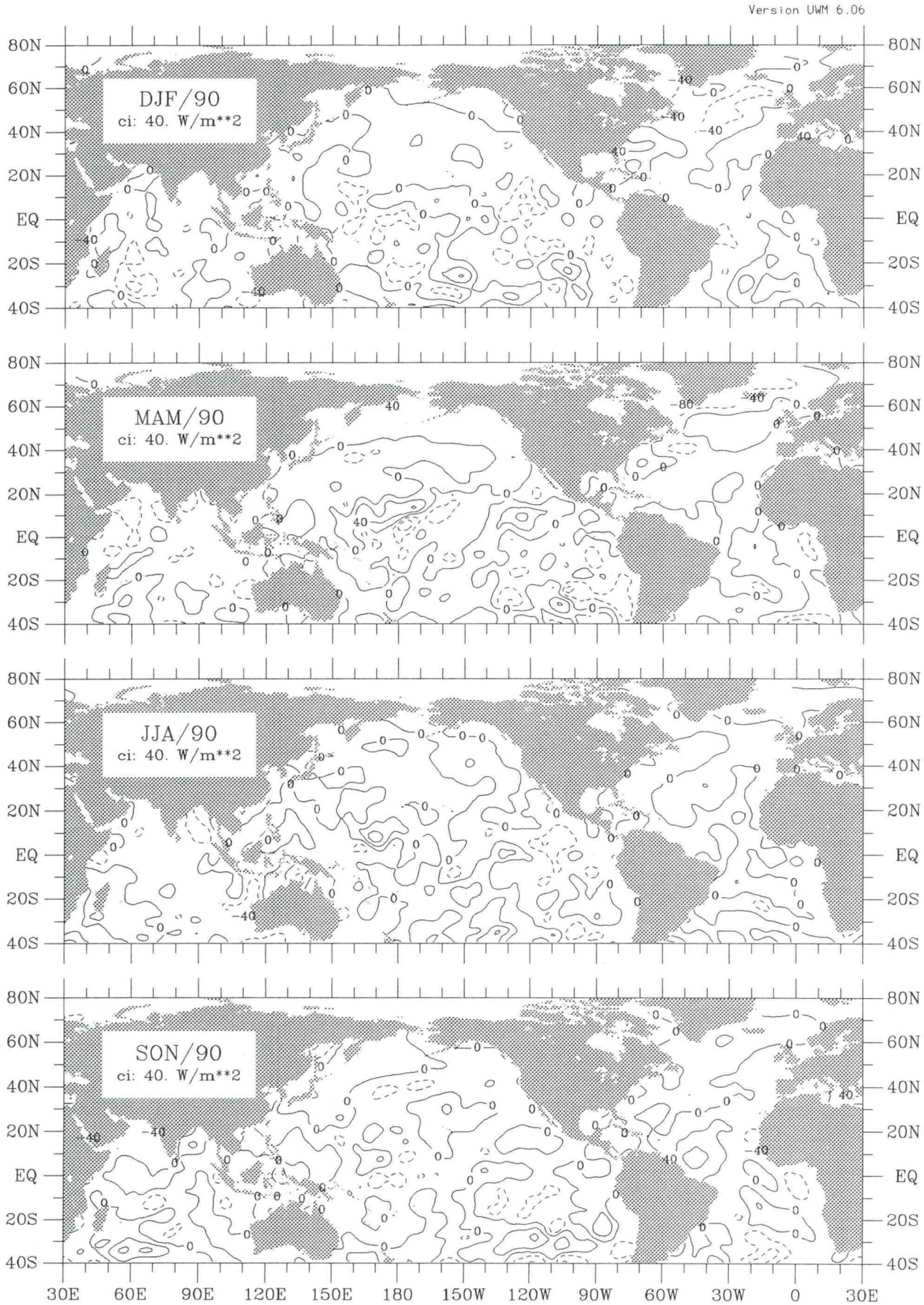

Figure Qnet-3. Constrained net heat flux seasonal anomaly for 1990.

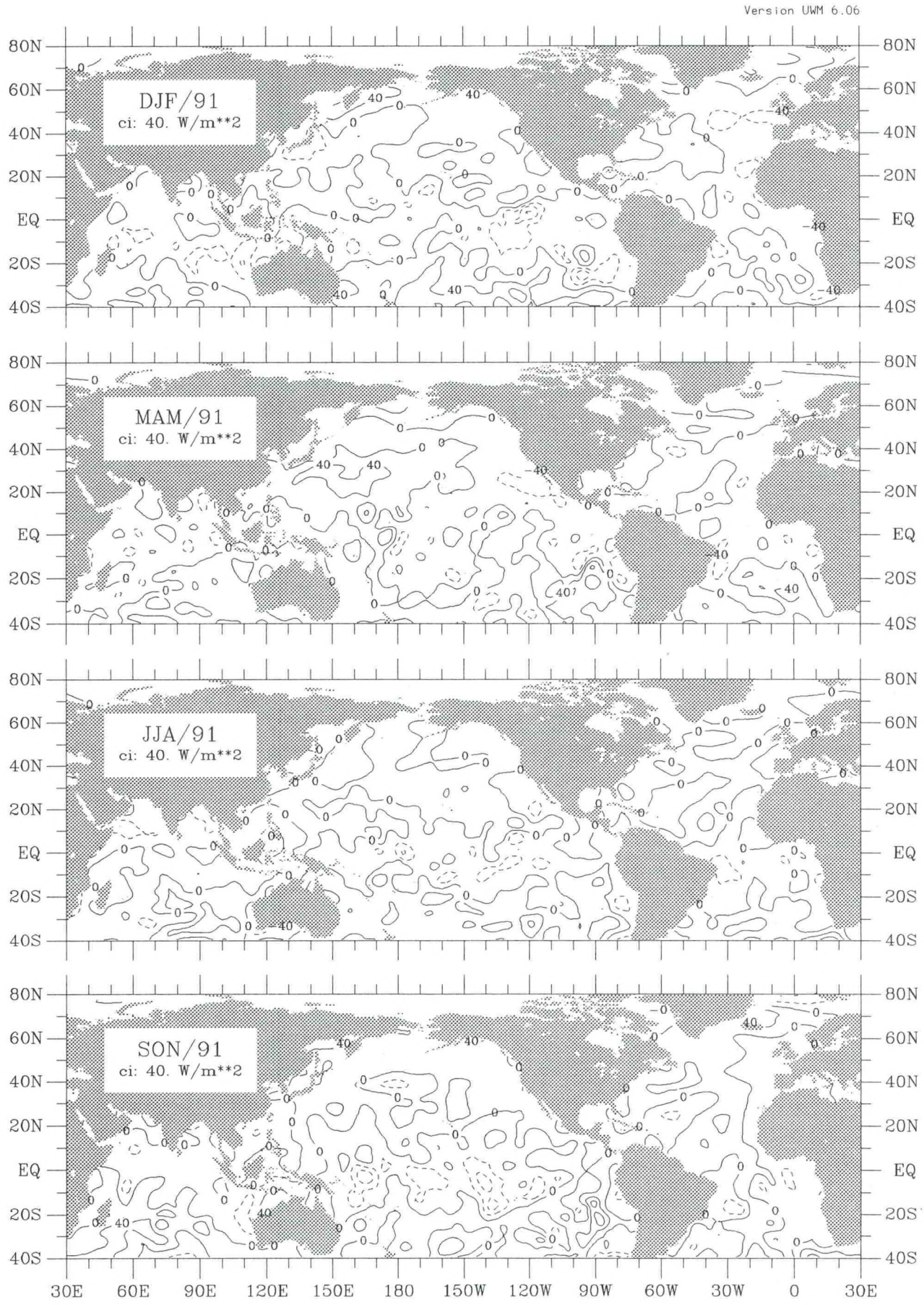

Figure Qnet-4. Constrained net heat flux seasonal anomaly for 1991.

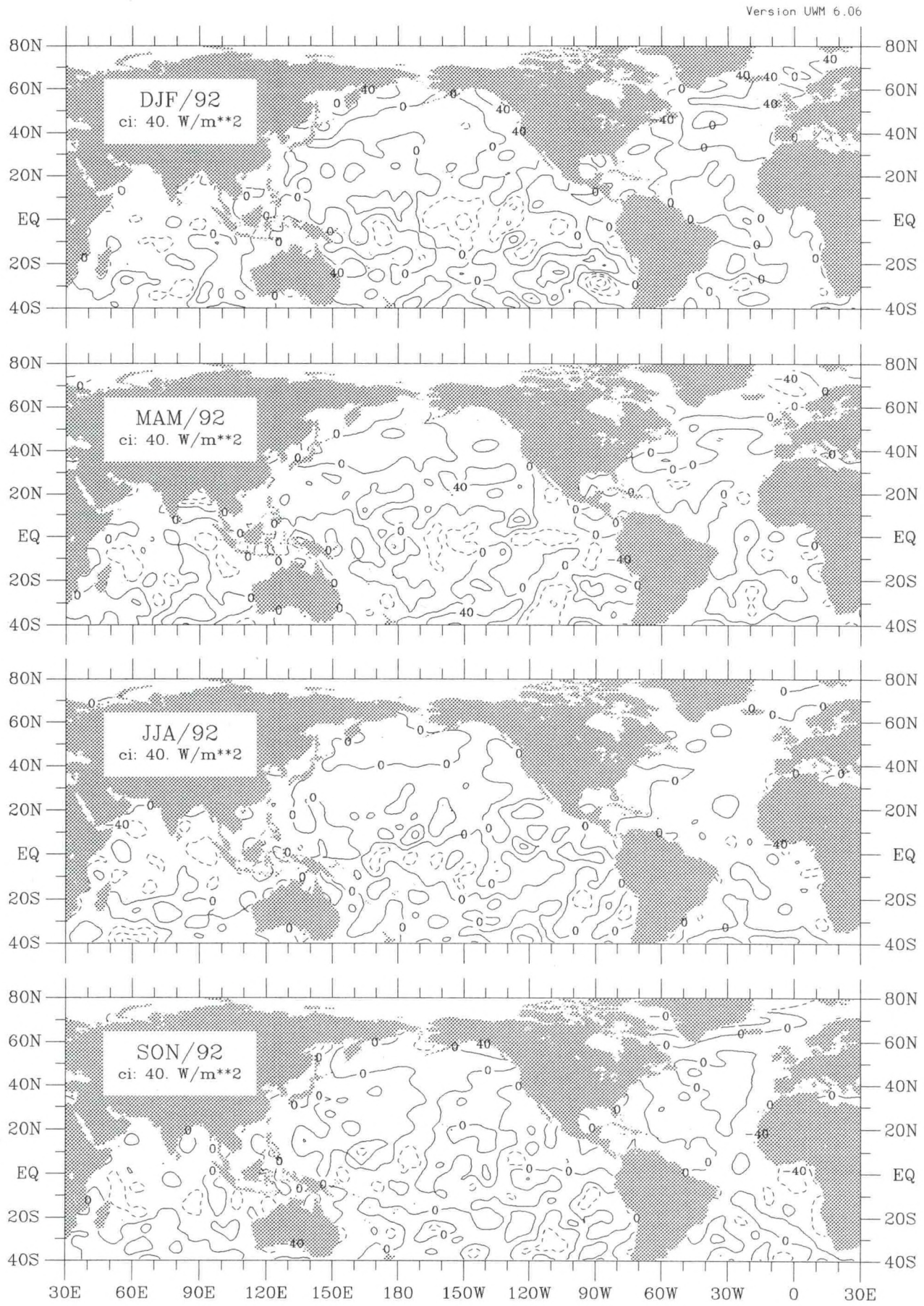

Figure Qnet-5. Constrained net heat flux seasonal anomaly for 1992.

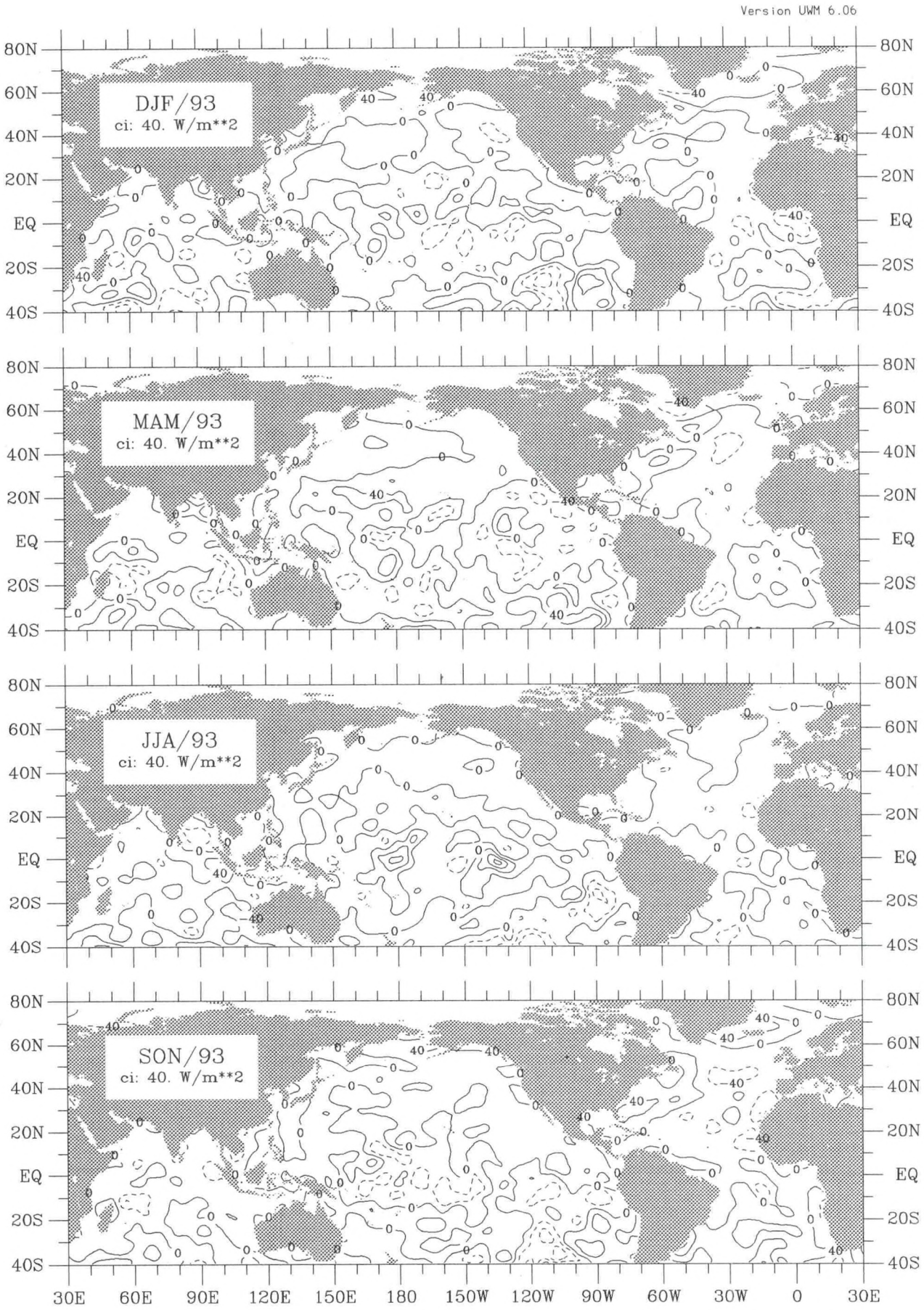

Figure Qnet-6. Constrained net heat flux seasonal anomaly for 1993.

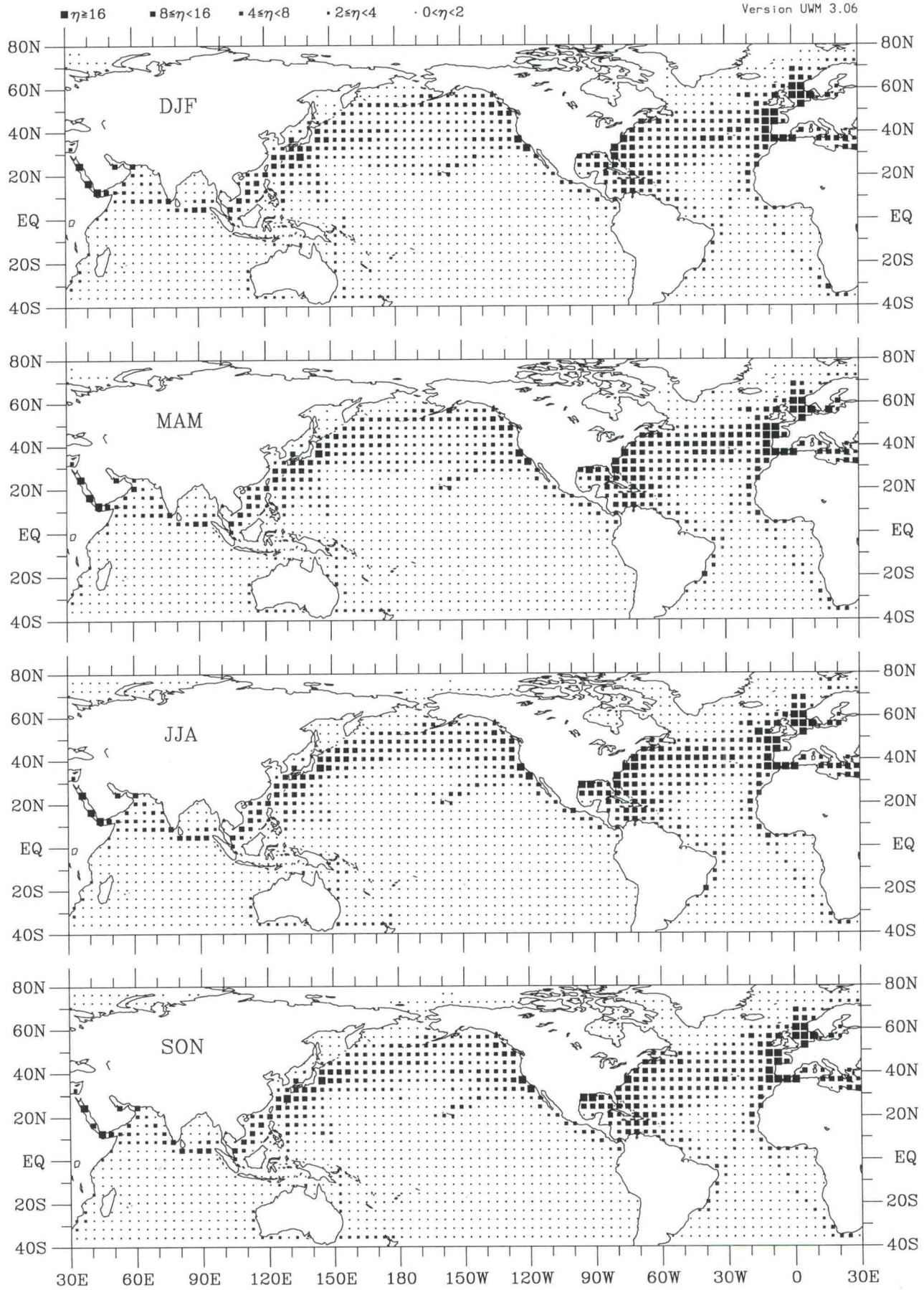

Figure E−1. Evaporation rate seasonal observation density (1990−93).

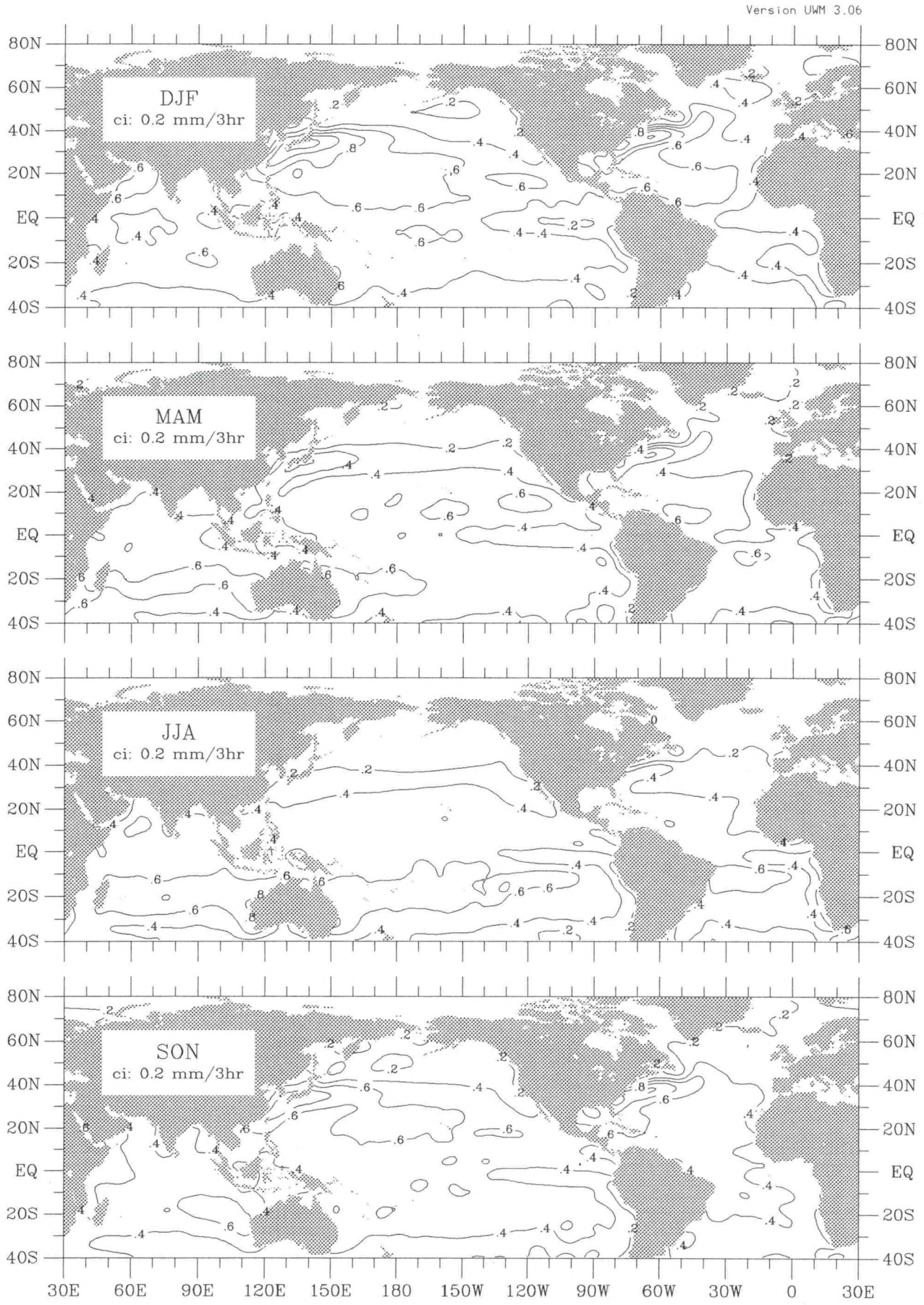

Figure E-2. Evaporation rate seasonal climatology (1945-89).

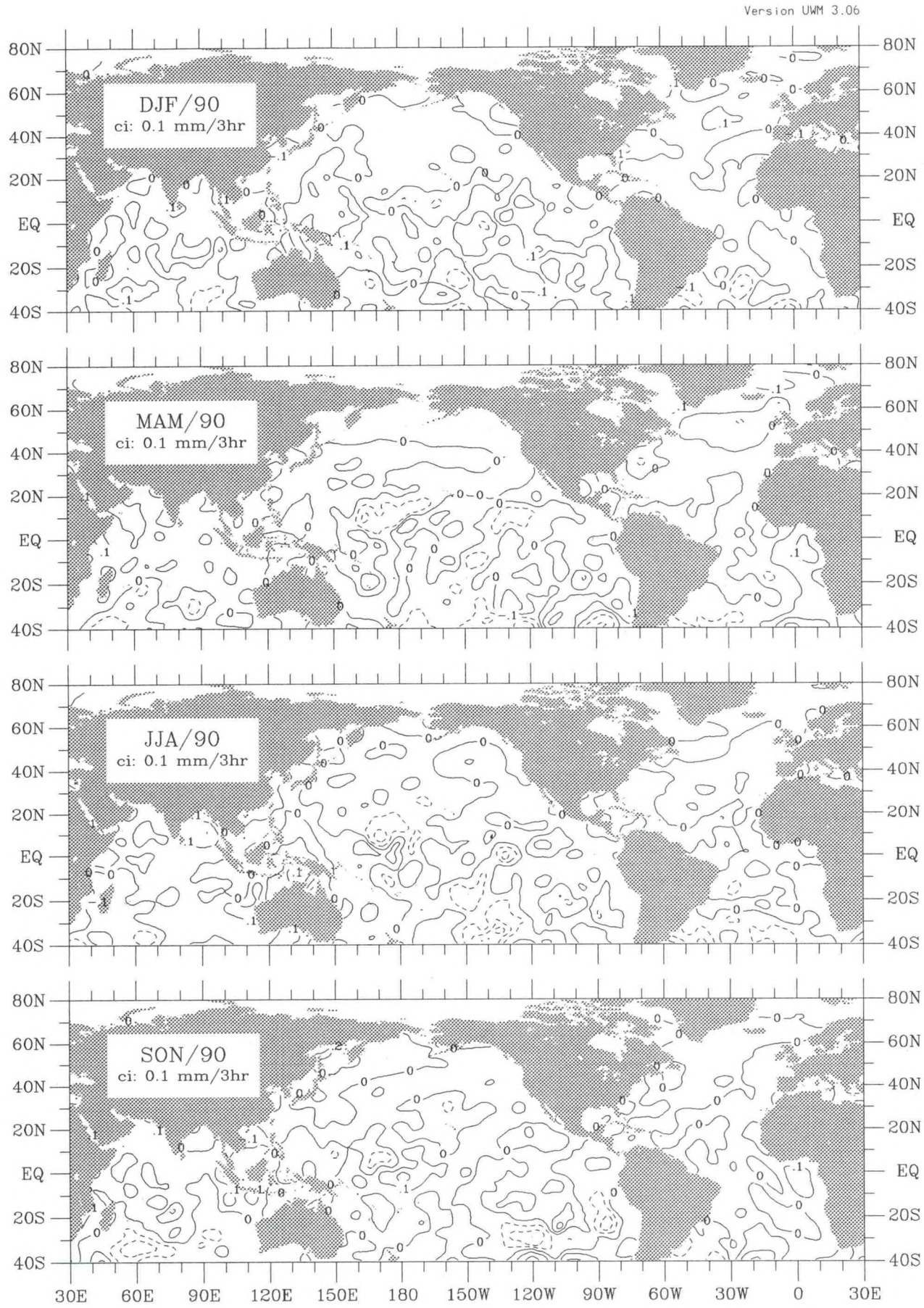

Figure E-3. Evaporation rate seasonal anomaly for 1990.

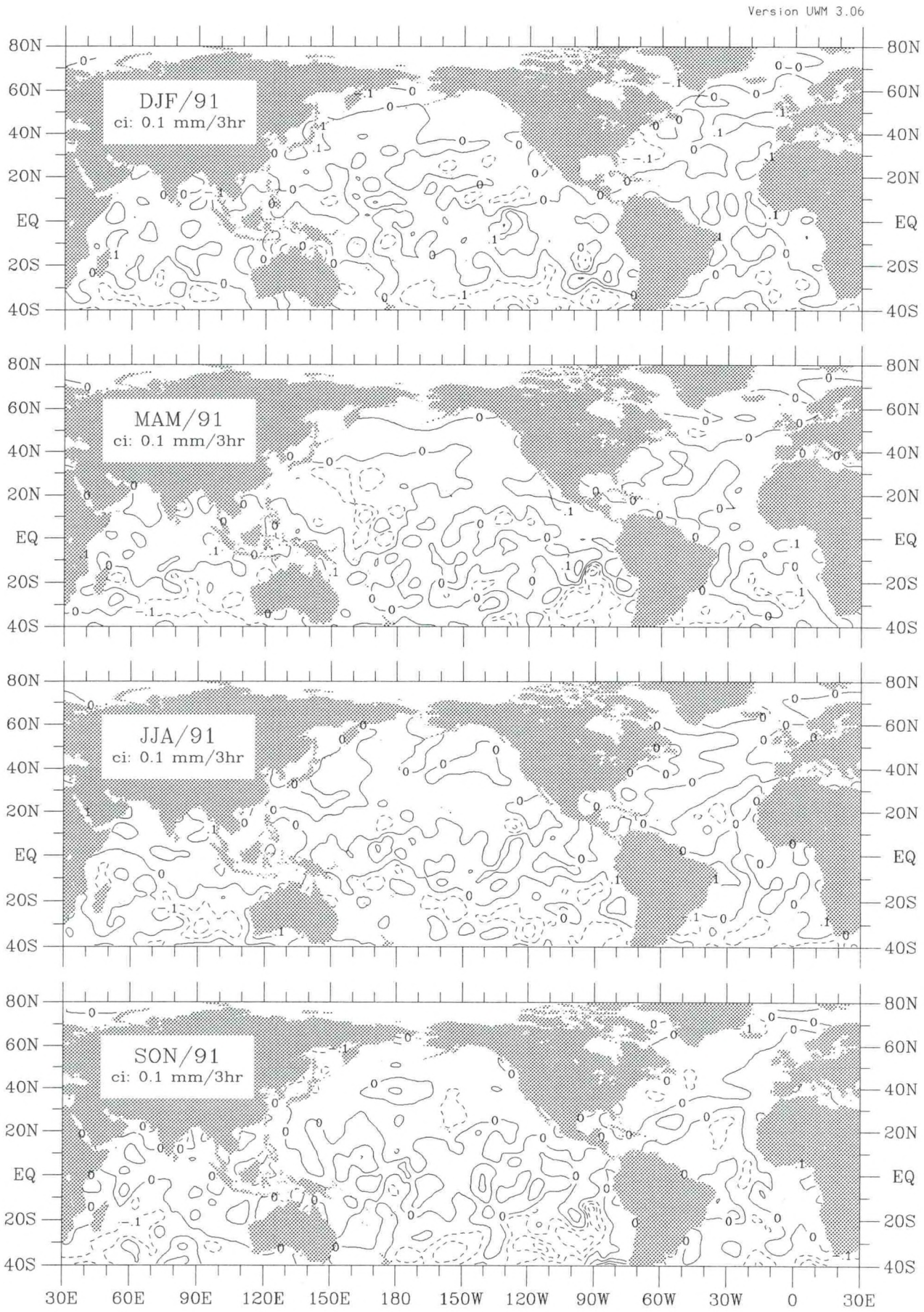

Figure E-4. Evaporation rate seasonal anomaly for 1991.

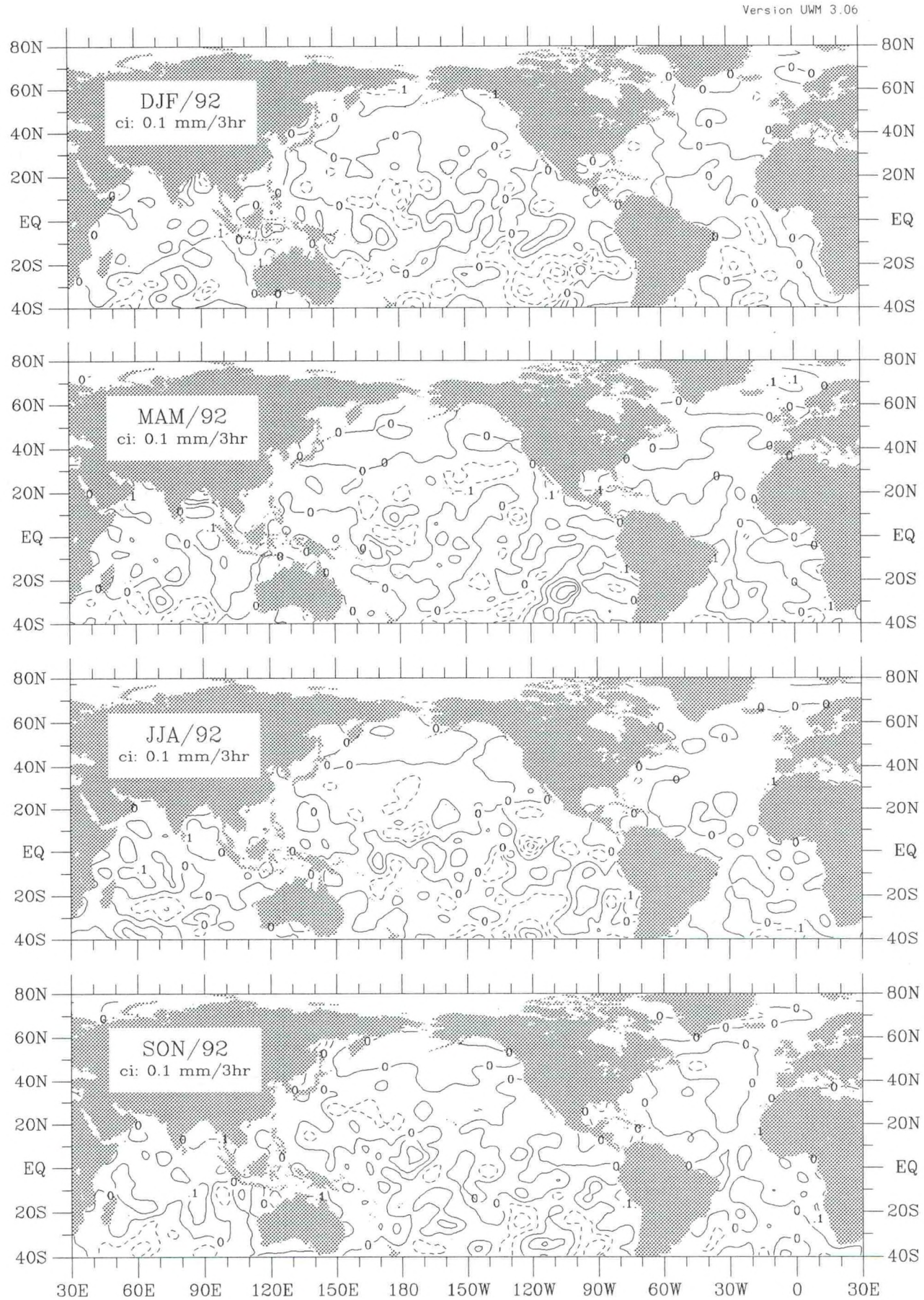

Figure E-5. Evaporation rate seasonal anomaly for 1992.

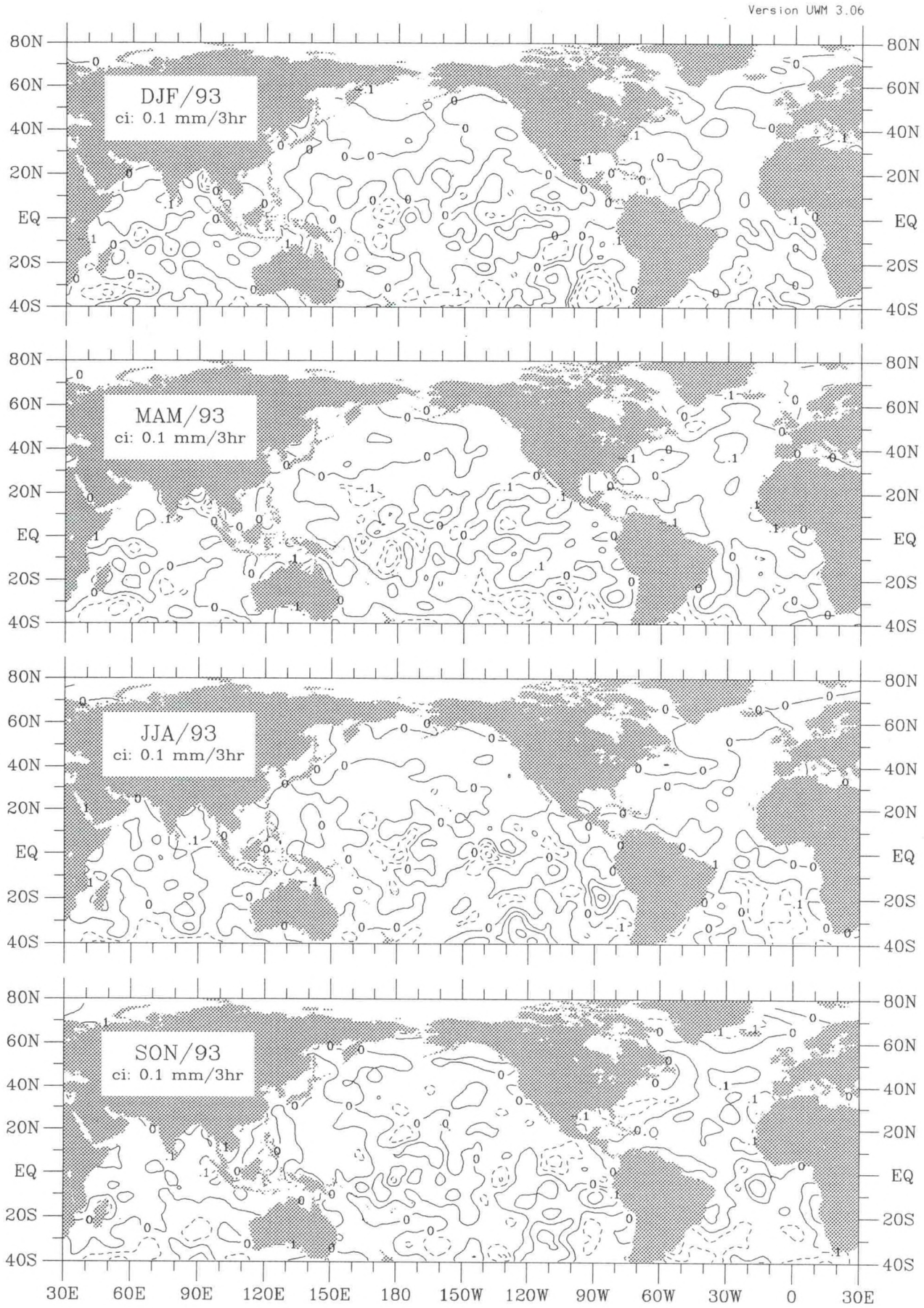

Figure E-6. Evaporation rate seasonal anomaly for 1993.

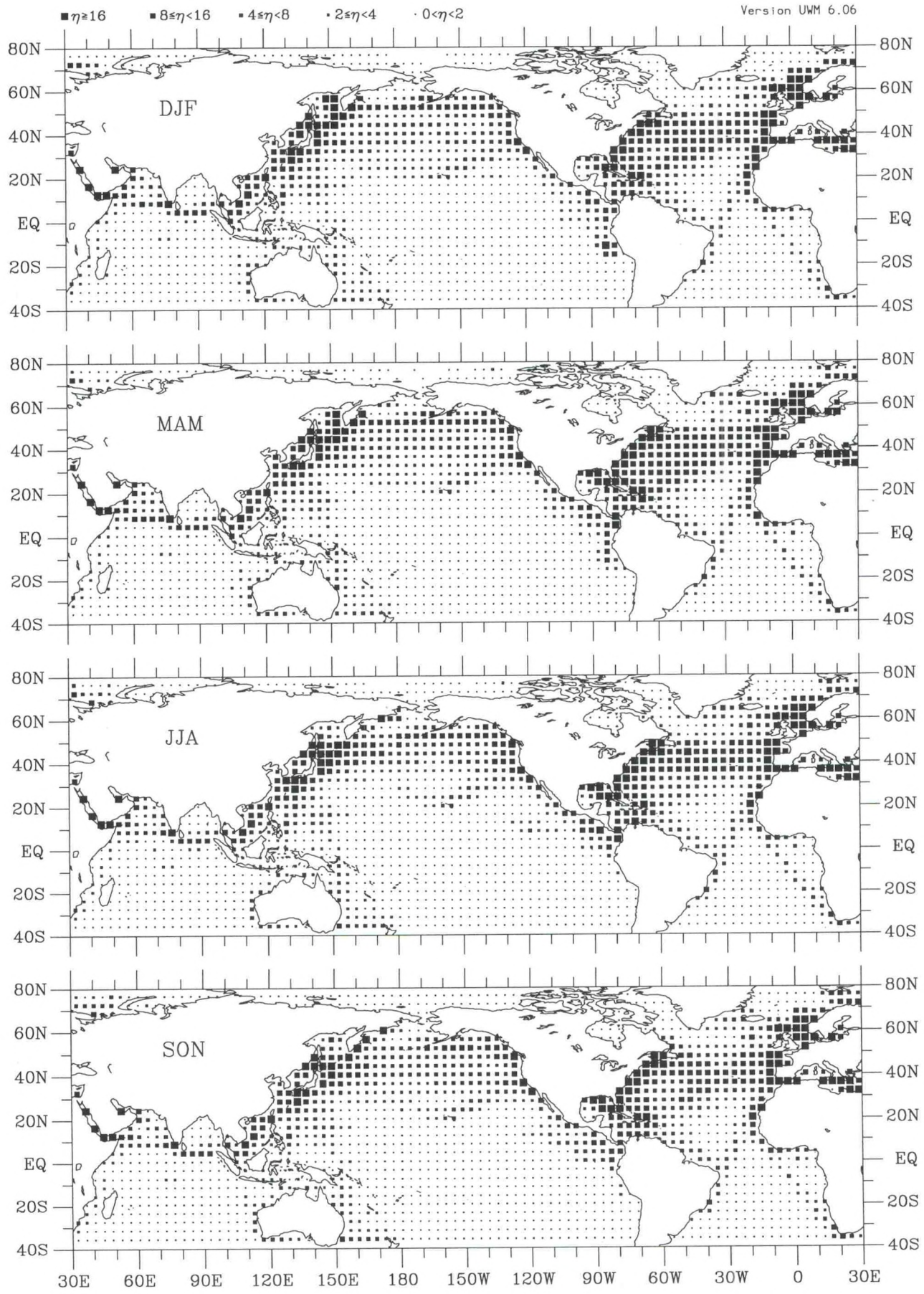

Figure P–1. Precipitation rate seasonal observation density (1990–93).

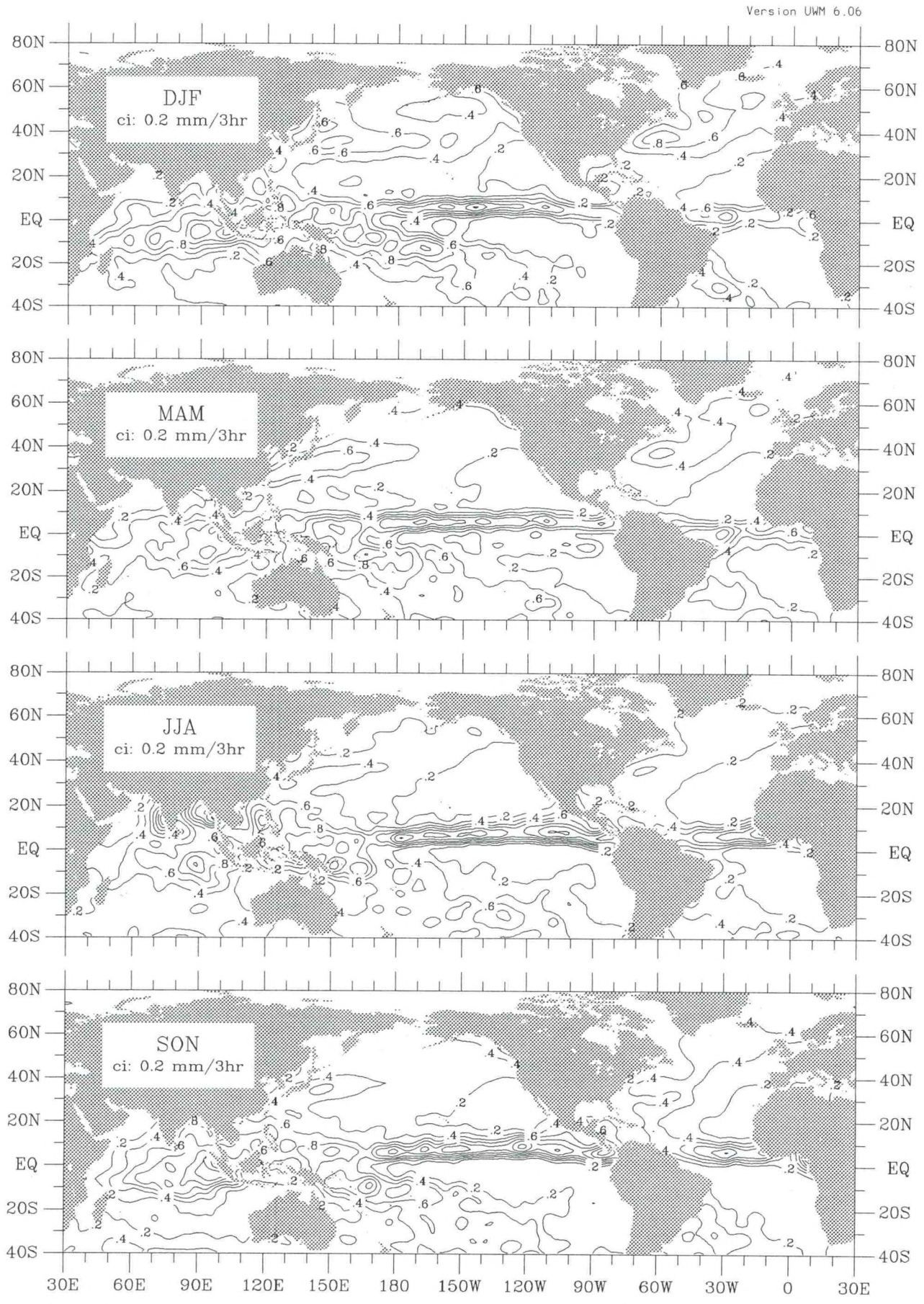

Figure P-2. Precipitation rate seasonal climatology (1945-89).

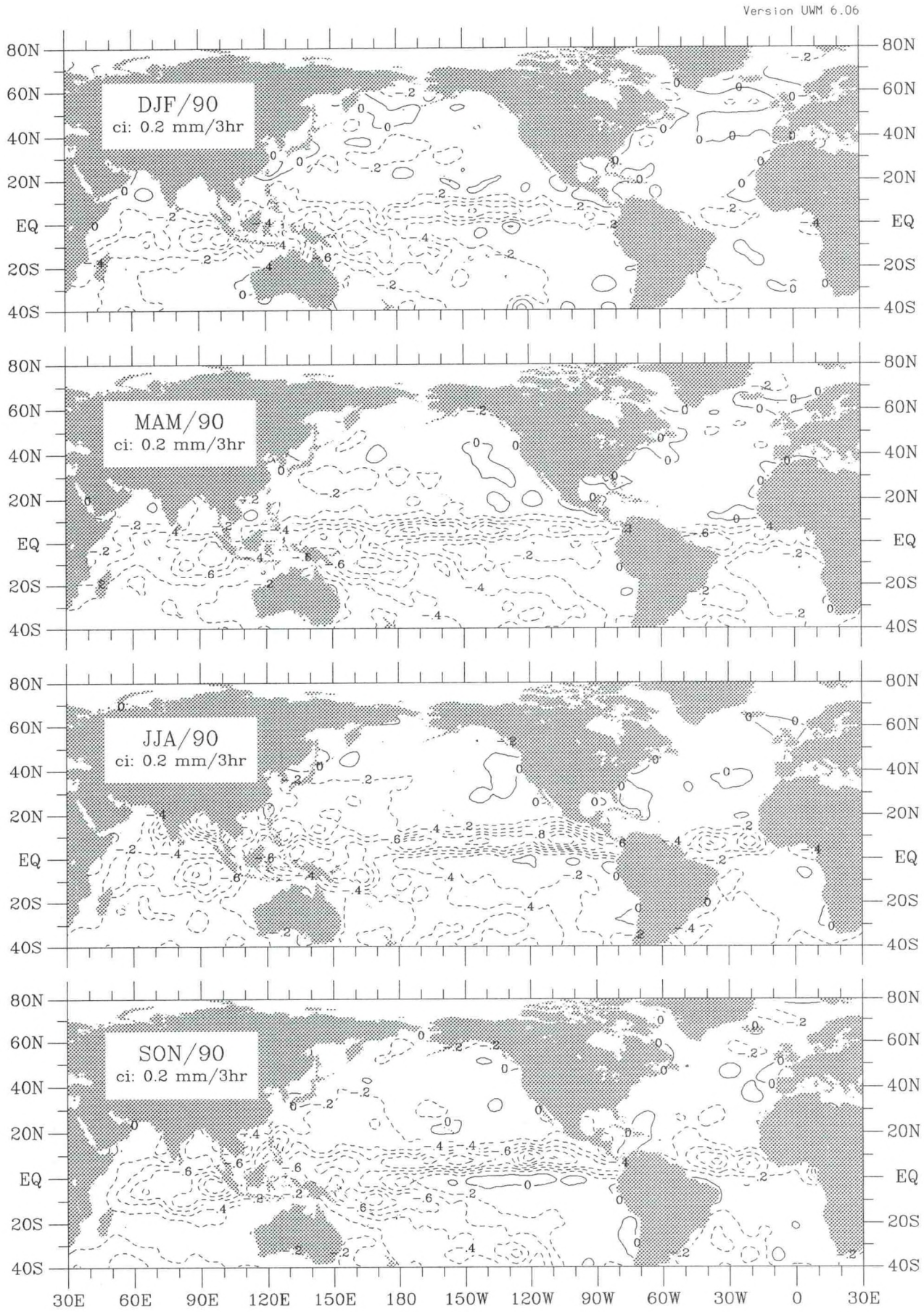

Figure P-3. Precipitation rate seasonal anomaly for 1990.

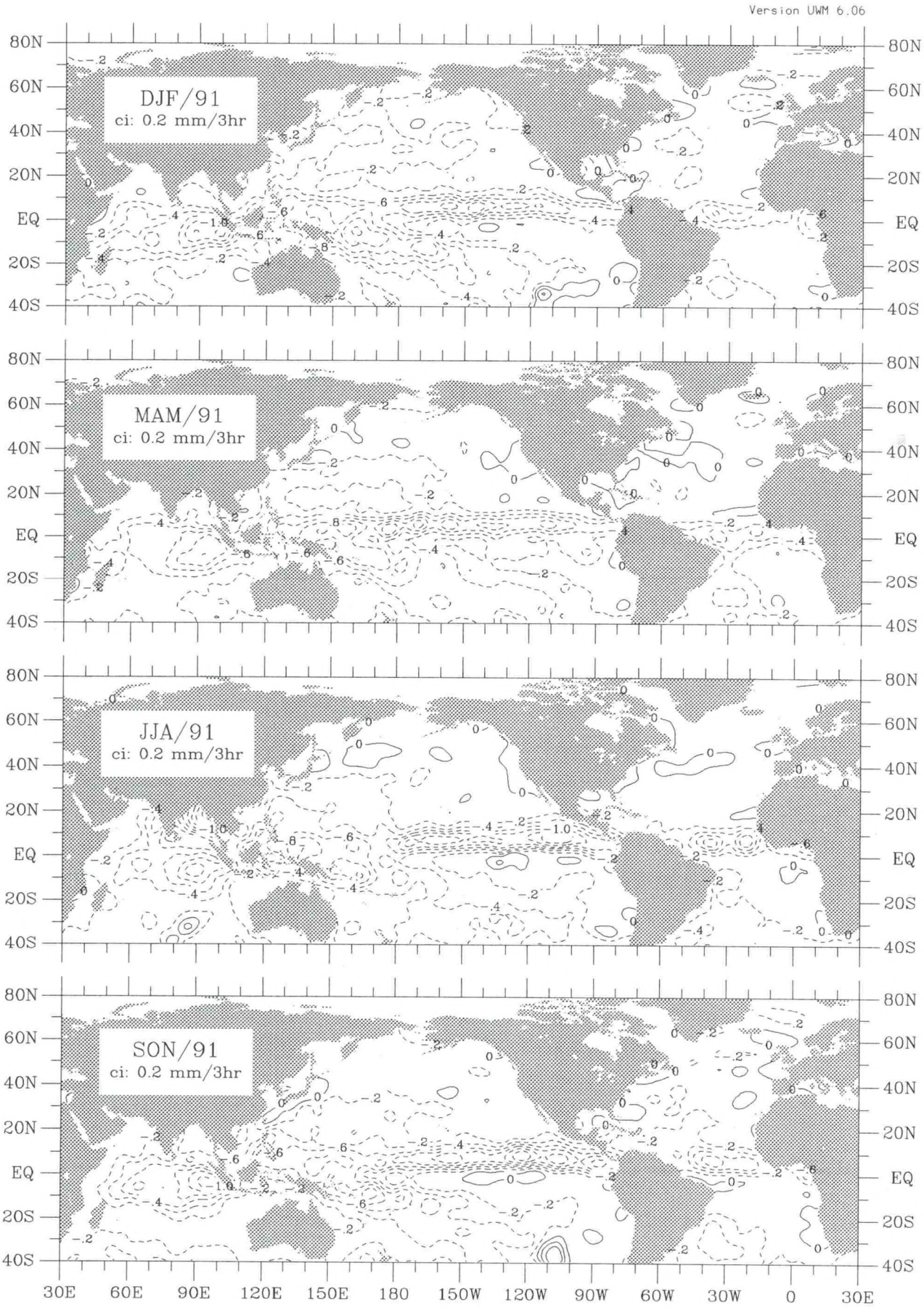

Figure P–4. Precipitation rate seasonal anomaly for 1991.

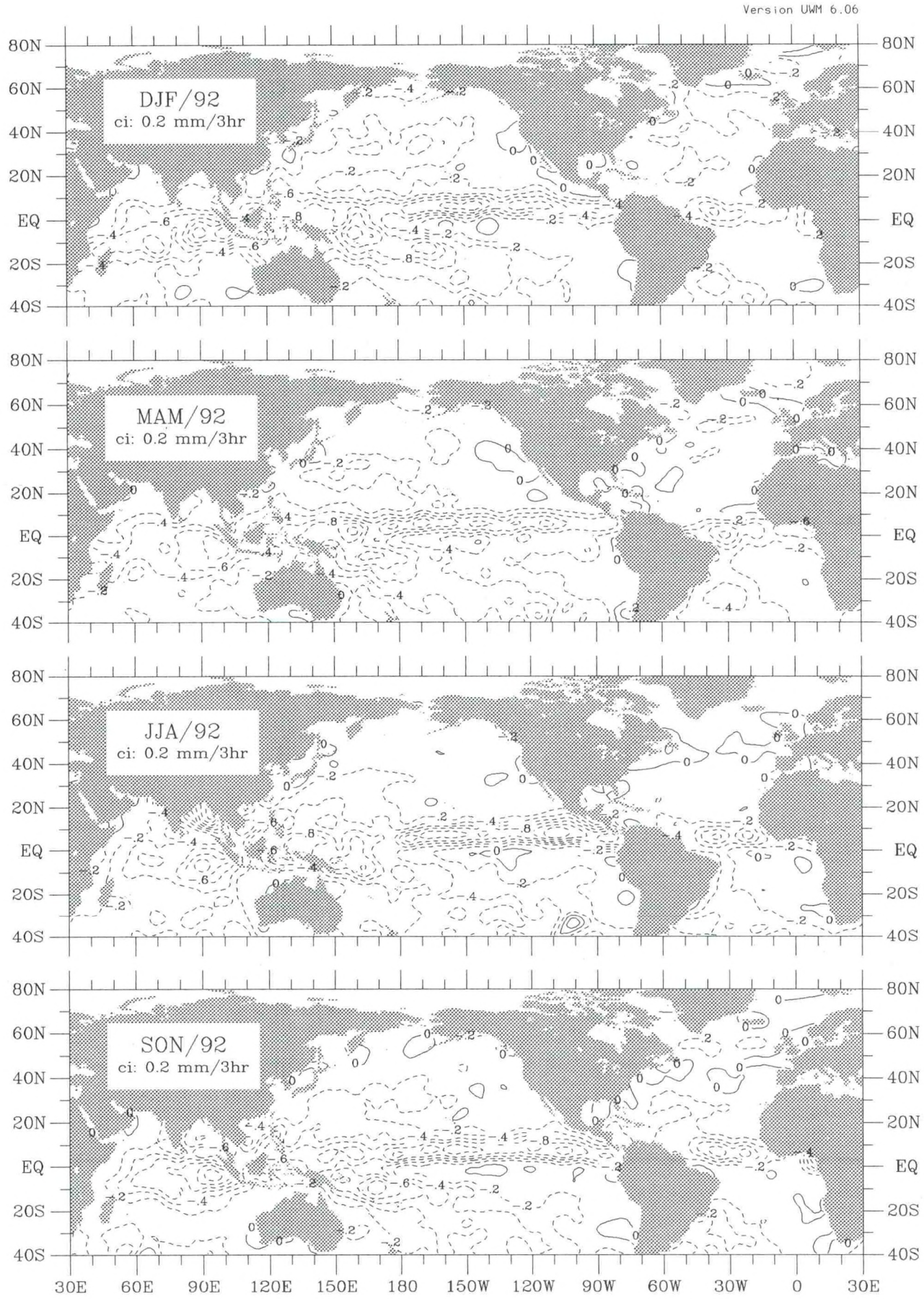

Figure P–5. Precipitation rate seasonal anomaly for 1992.

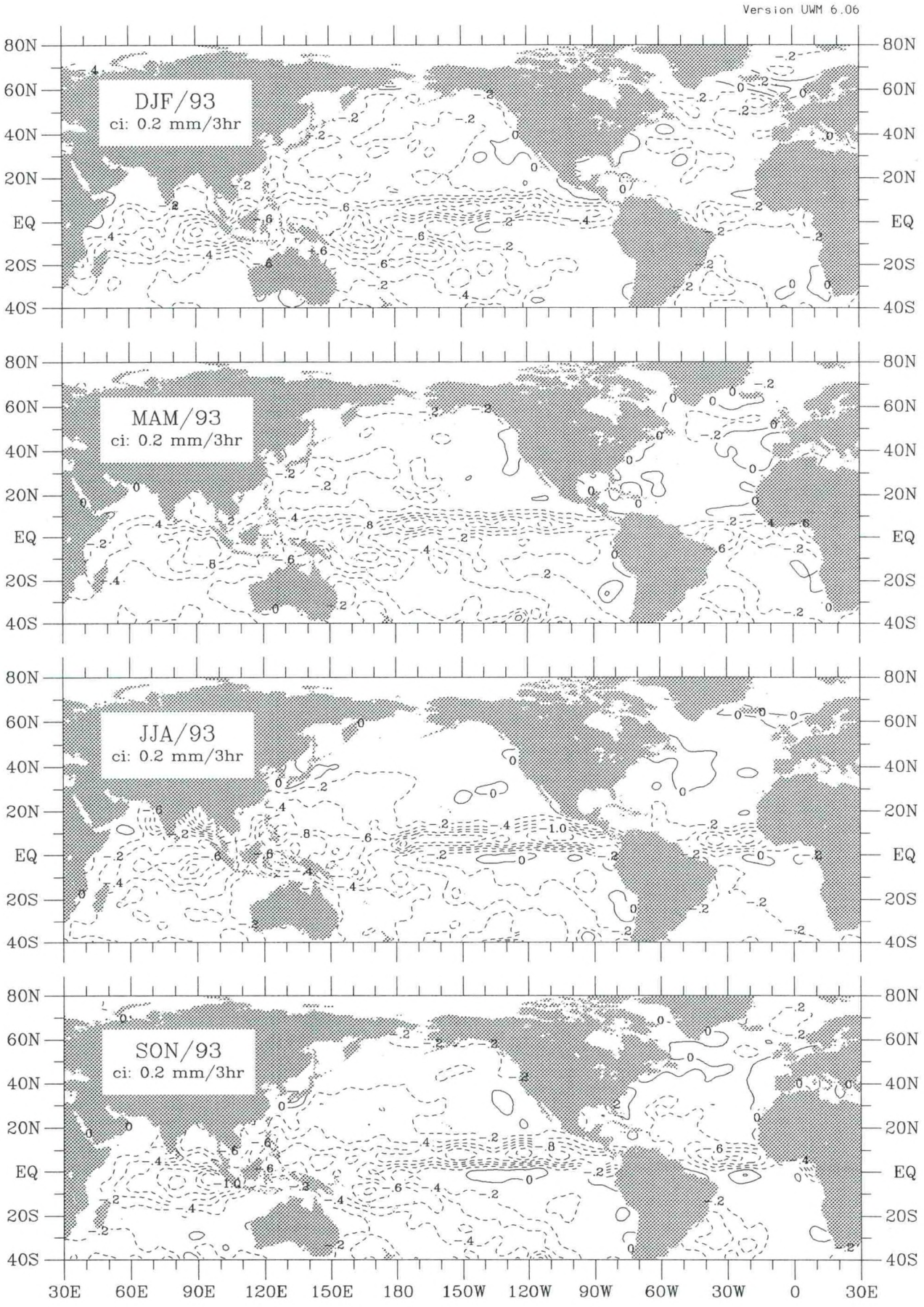

Figure P–6. Precipitation rate seasonal anomaly for 1993.

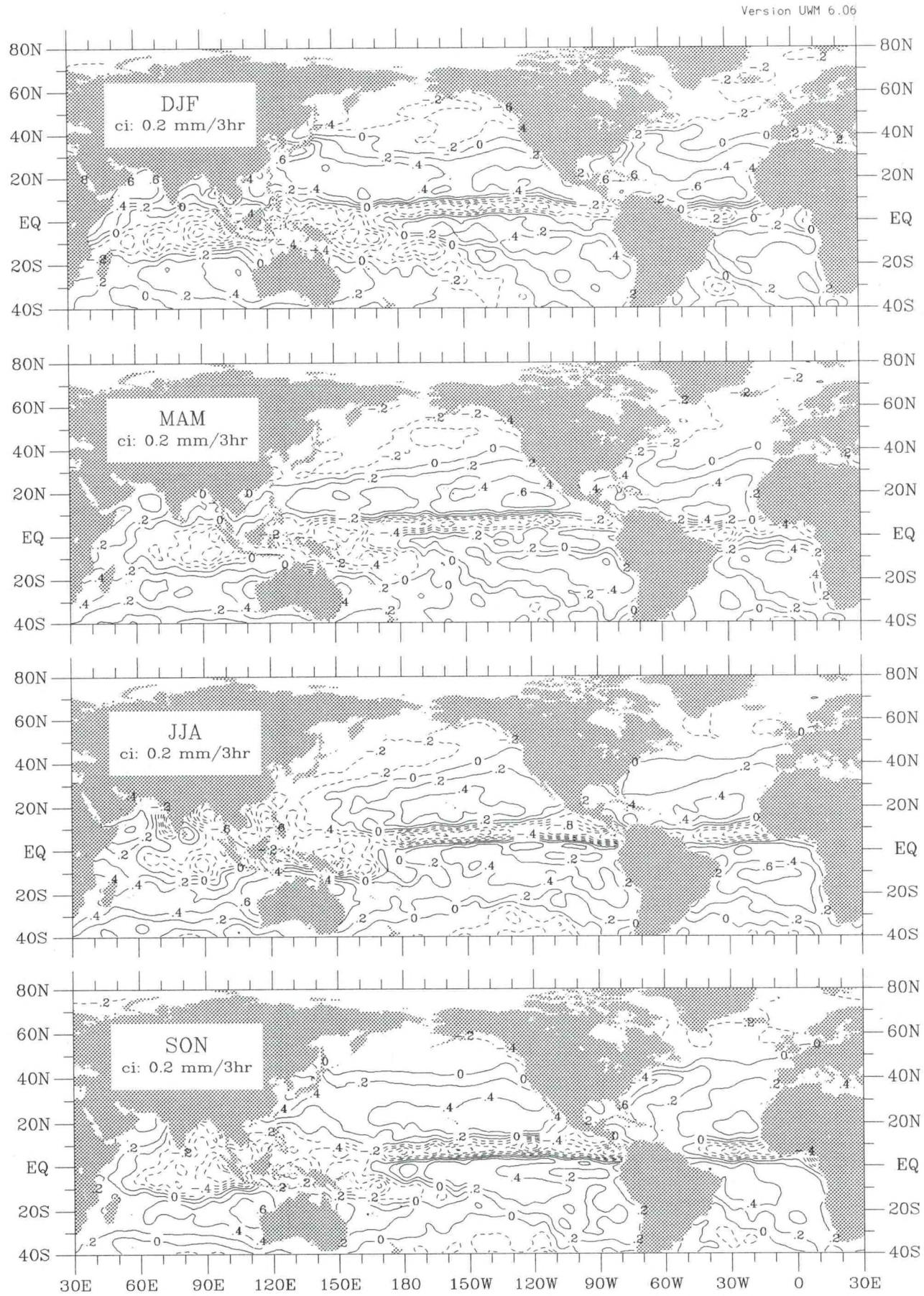

Figure E-P-2. Constrained E minus P seasonal climatology (1945-89).

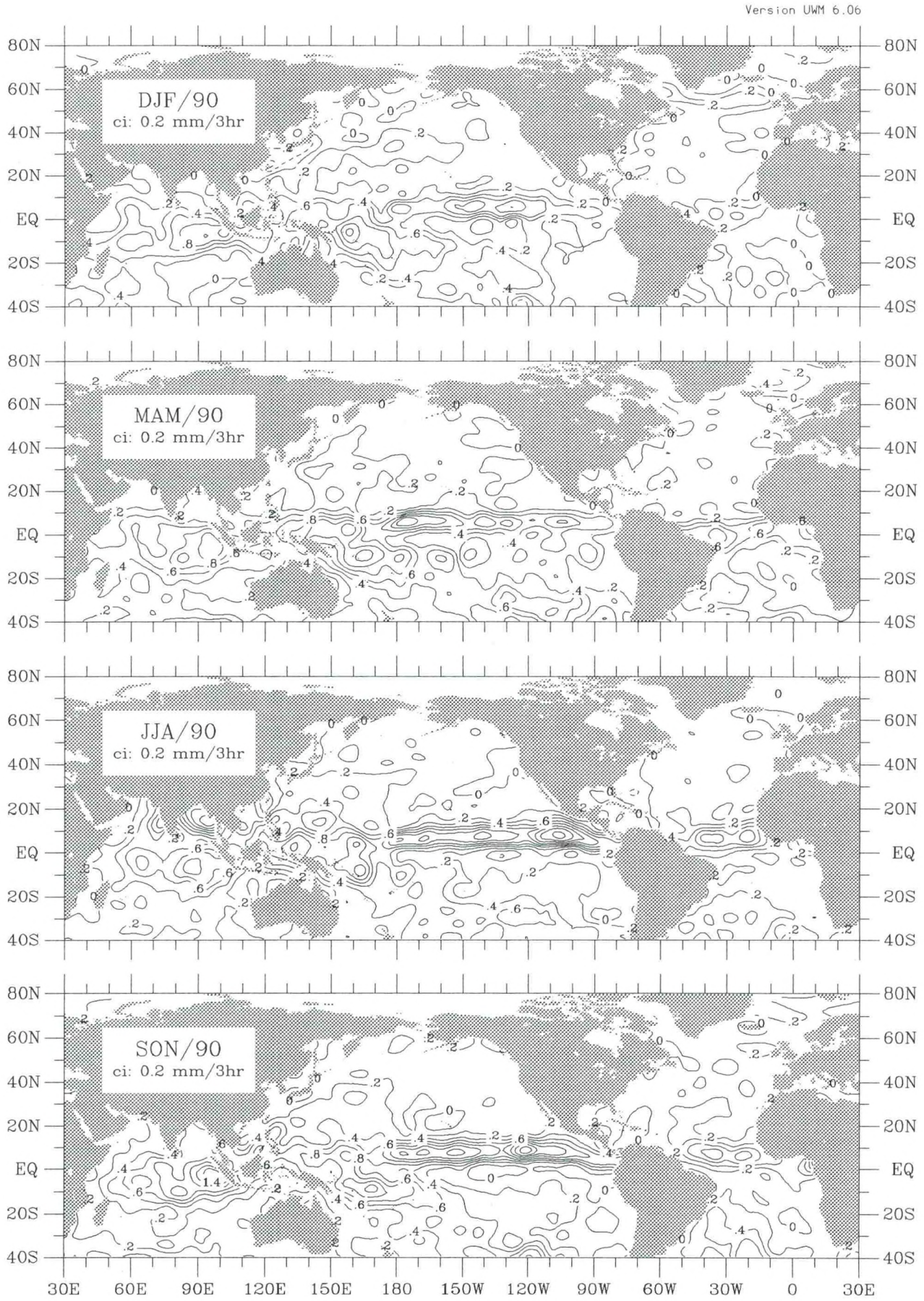

Figure E-P-3. Constrained E minus P seasonal anomaly for 1990.

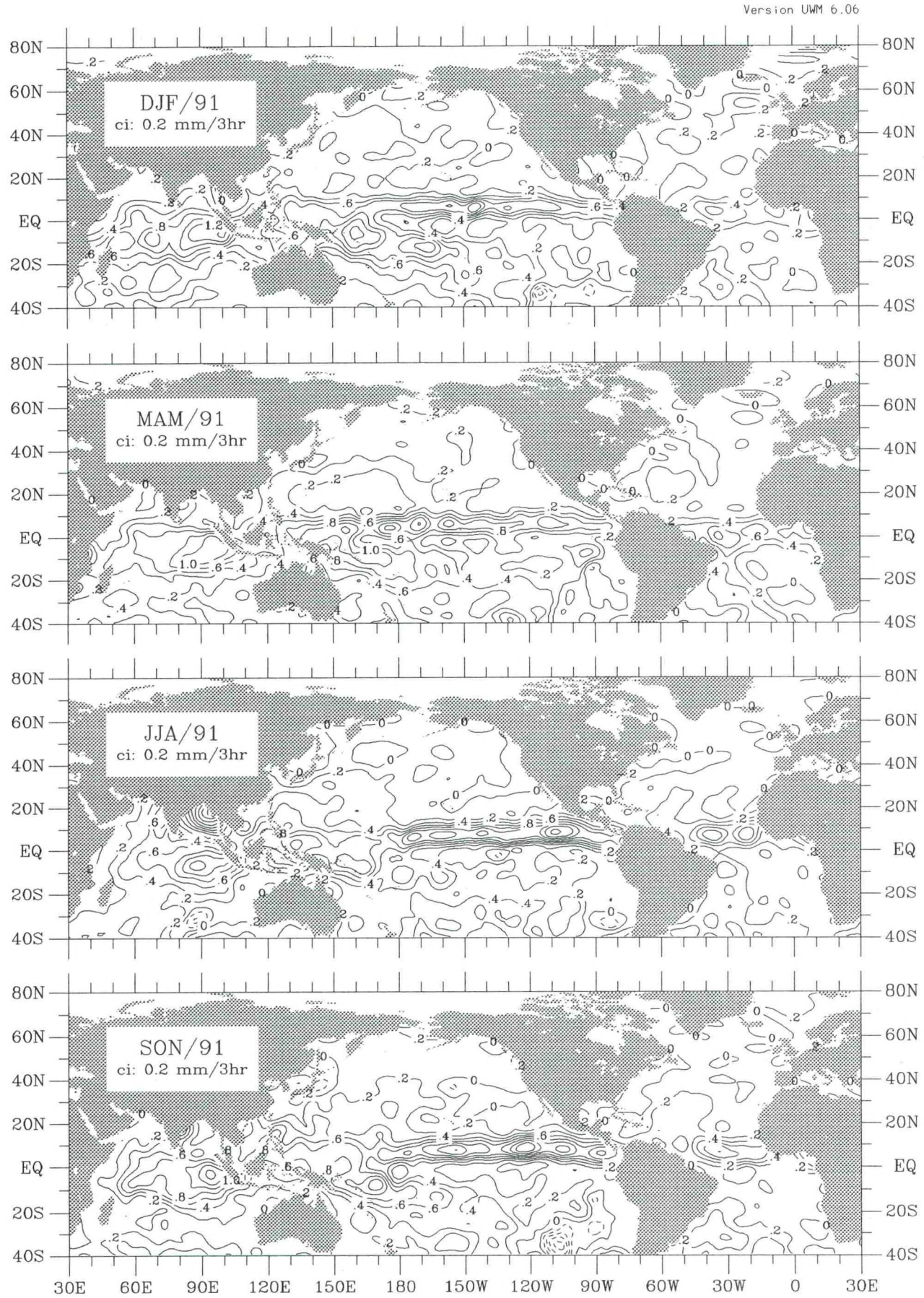

Figure E–P–4. Constrained E minus P seasonal anomaly for 1991.

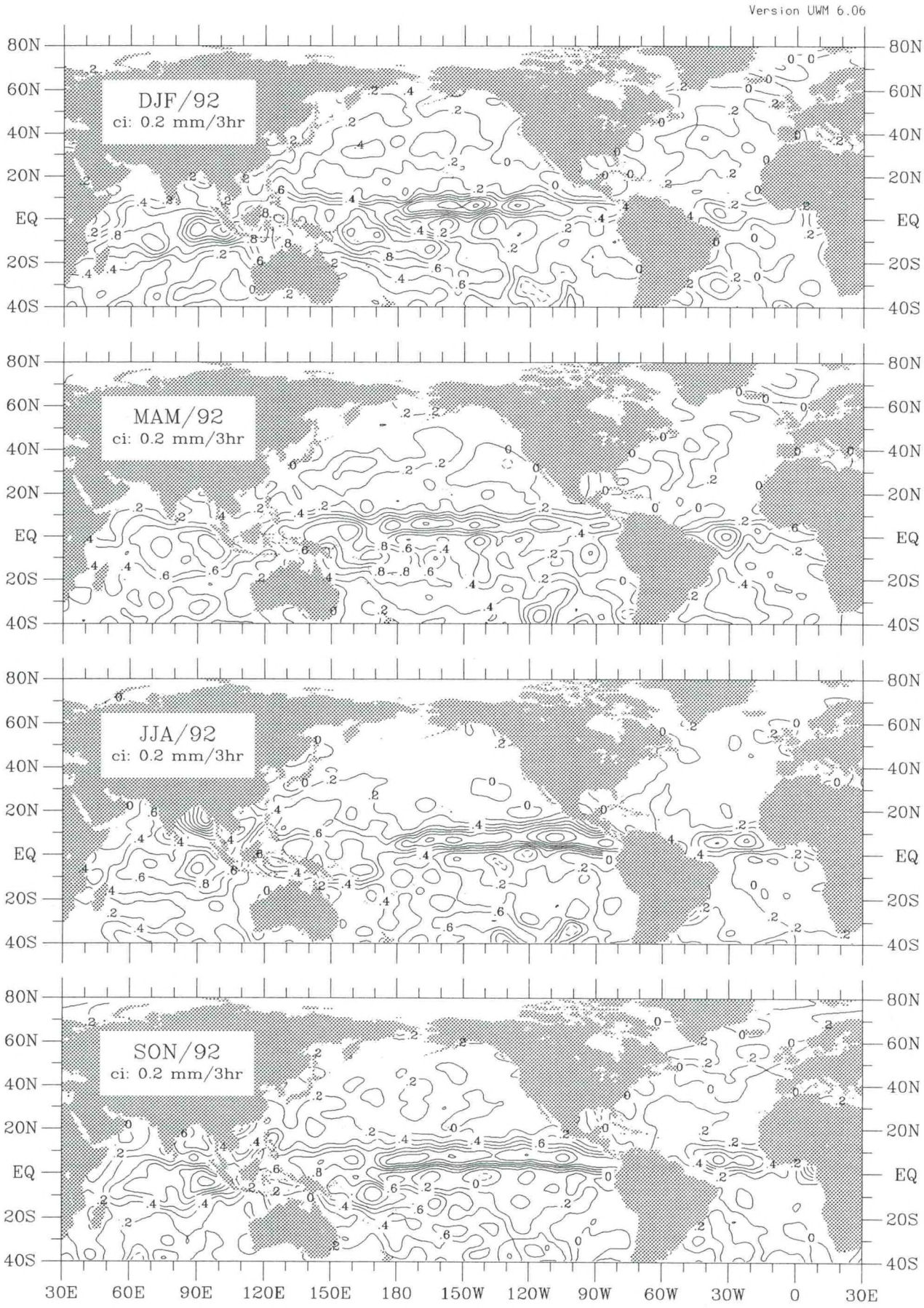

Figure E–P–5. Constrained E minus P seasonal anomaly for 1992.

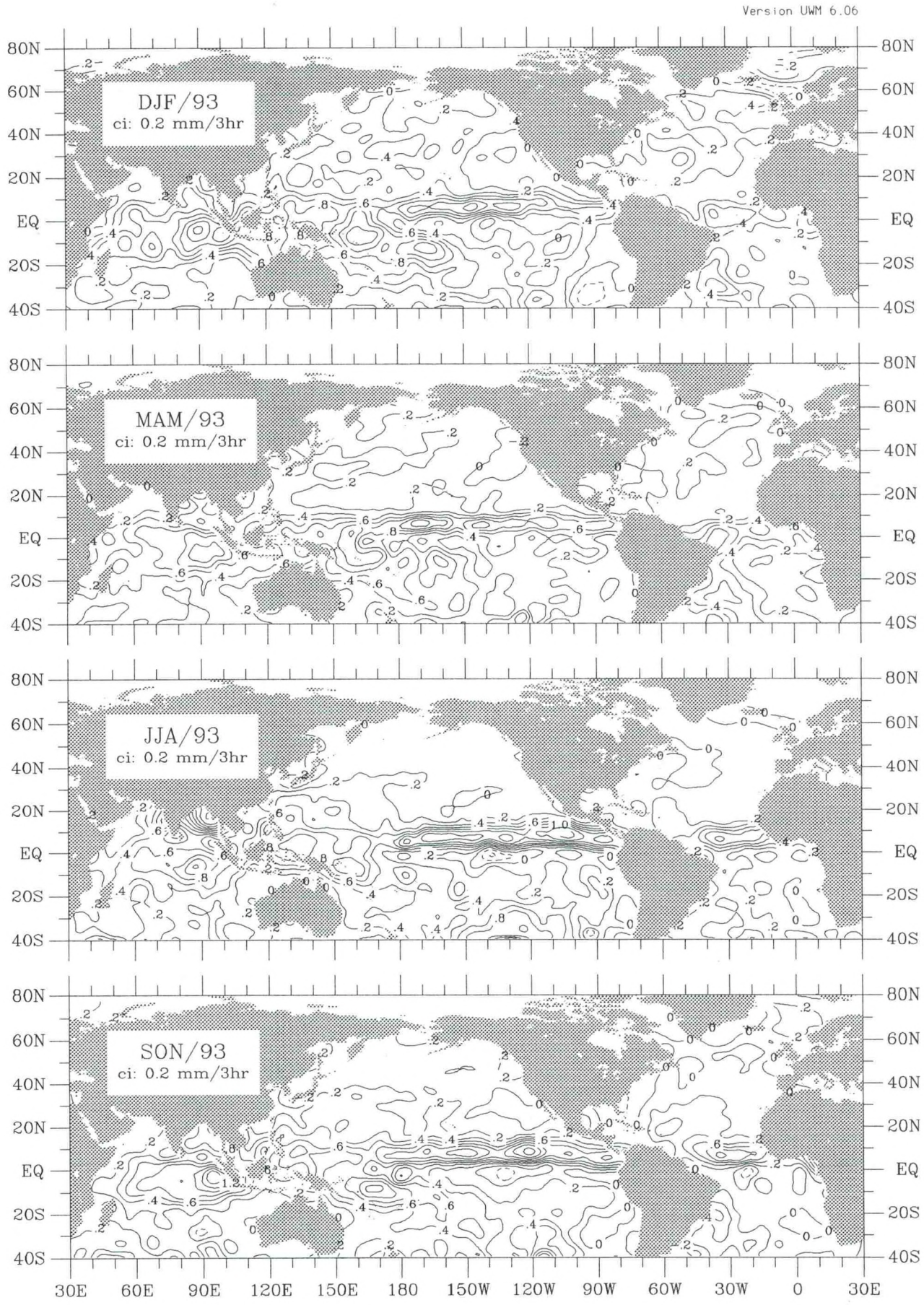

Figure E-P-6. Constrained E minus P seasonal anomaly for 1993.

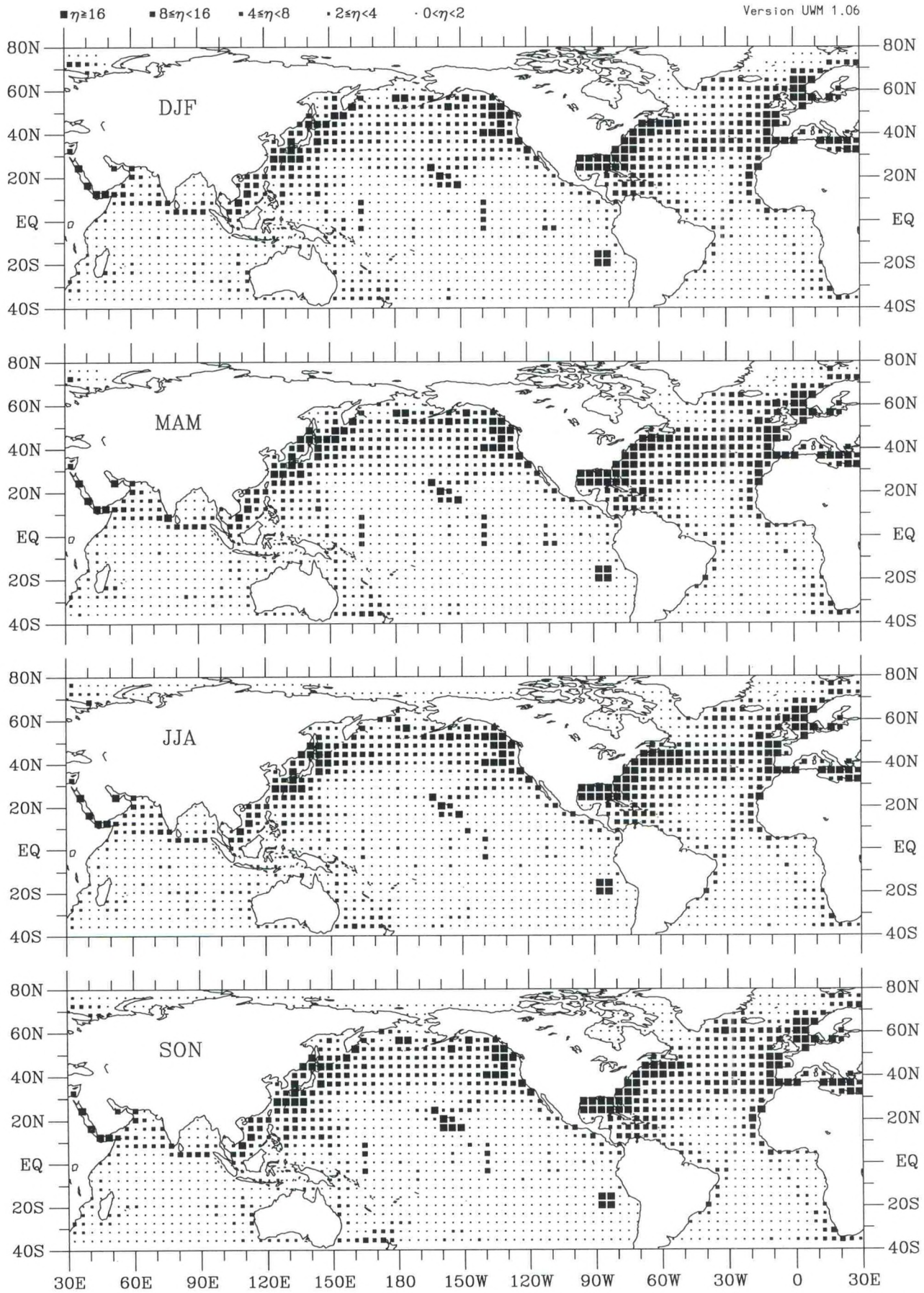

Figure dT−1. Sea minus air temperature seasonal observation density (1990−93).

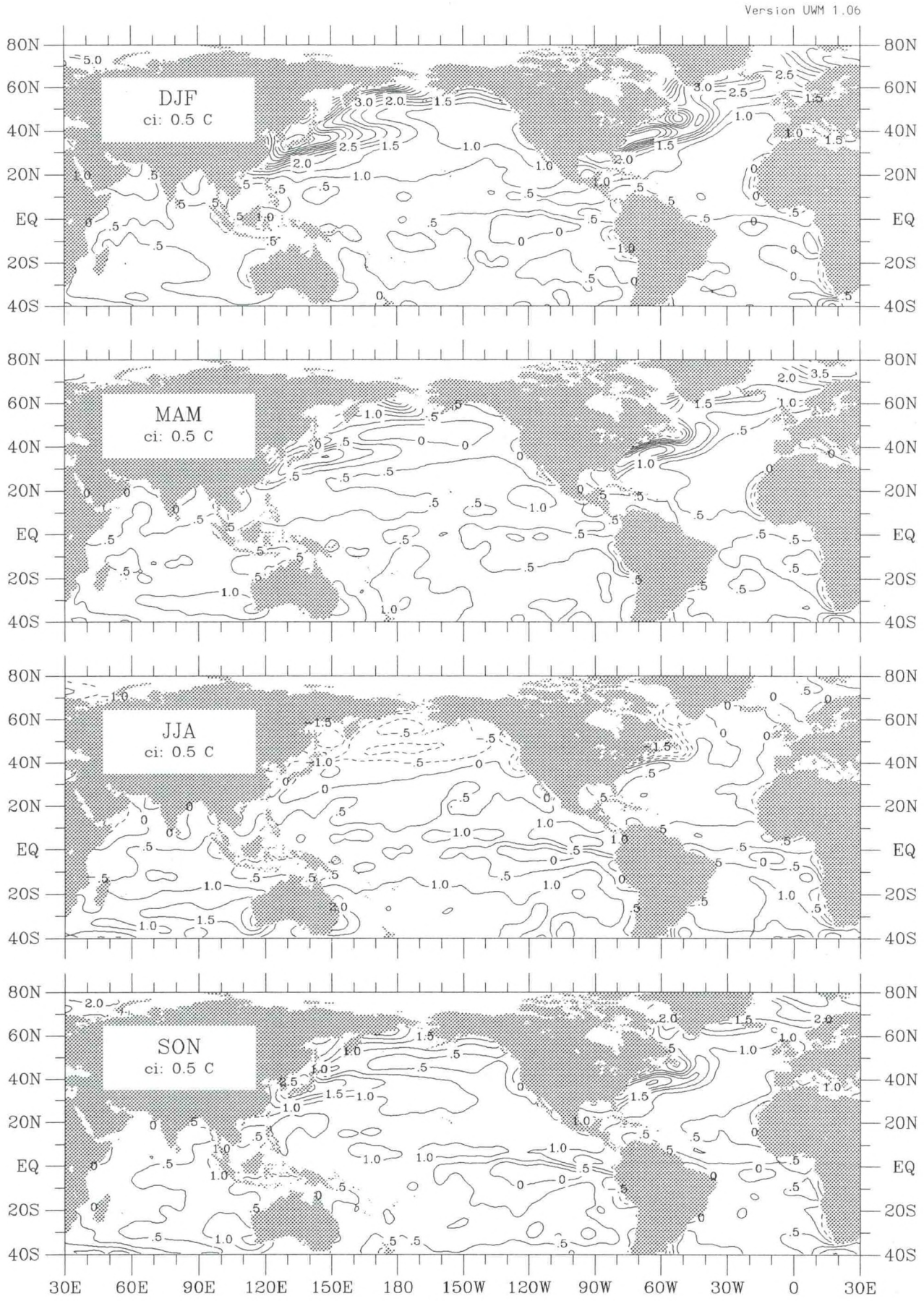

Figure dT-2. Sea minus air temperature seasonal climatology (1945-89).

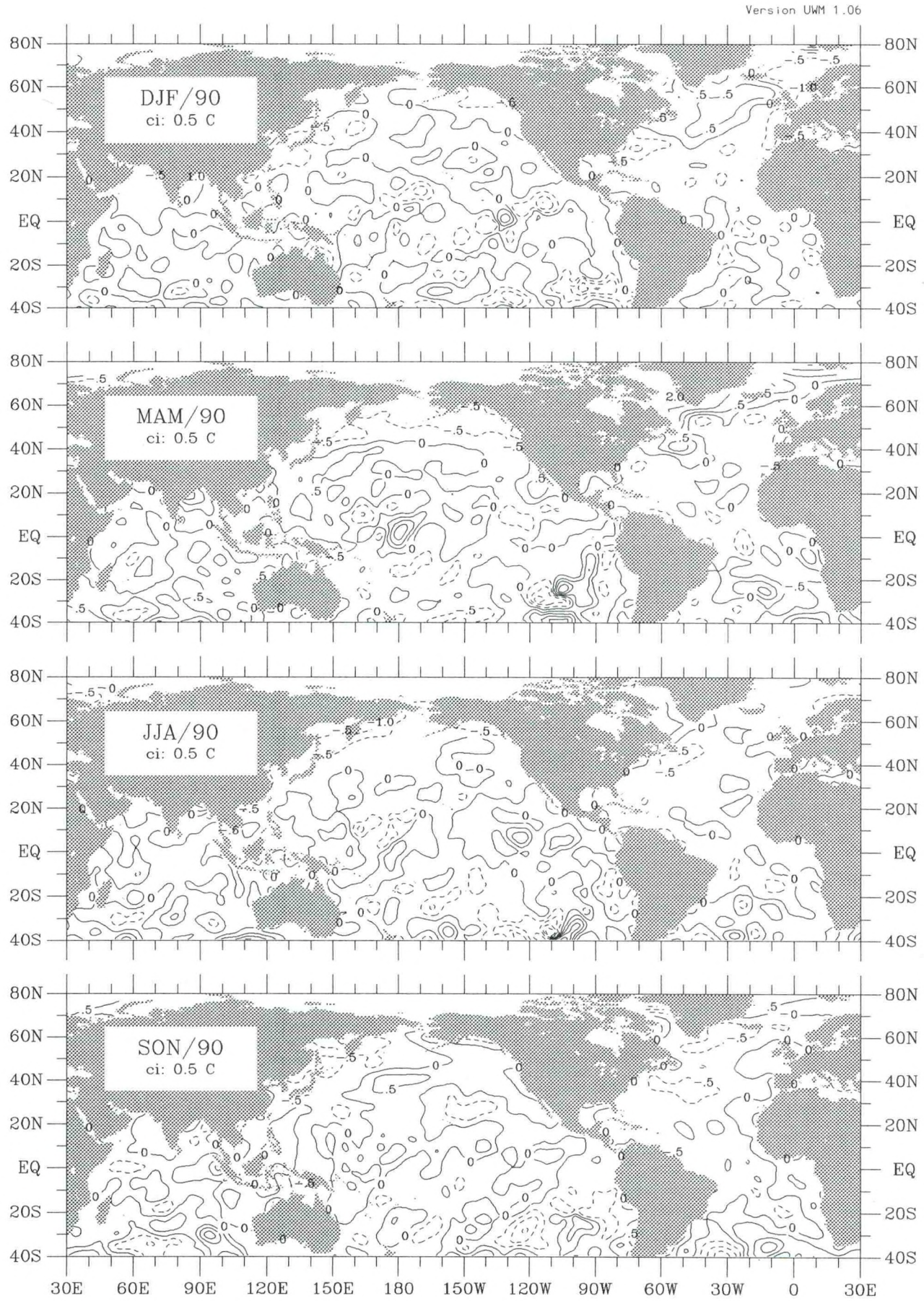

Figure dT-3. Sea minus air temperature seasonal anomaly for 1990.

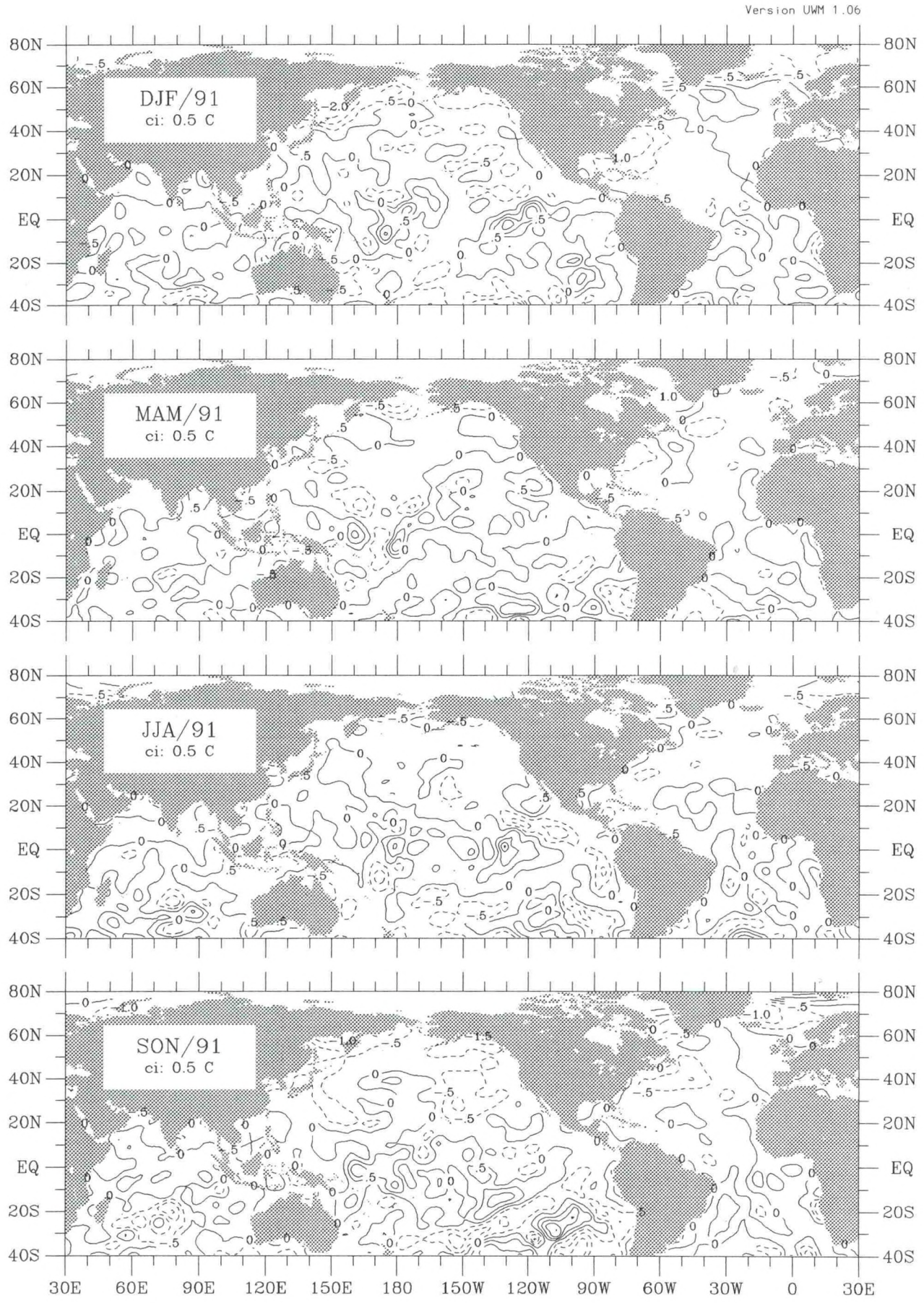

Figure dT-4. Sea minus air temperature seasonal anomaly for 1991.

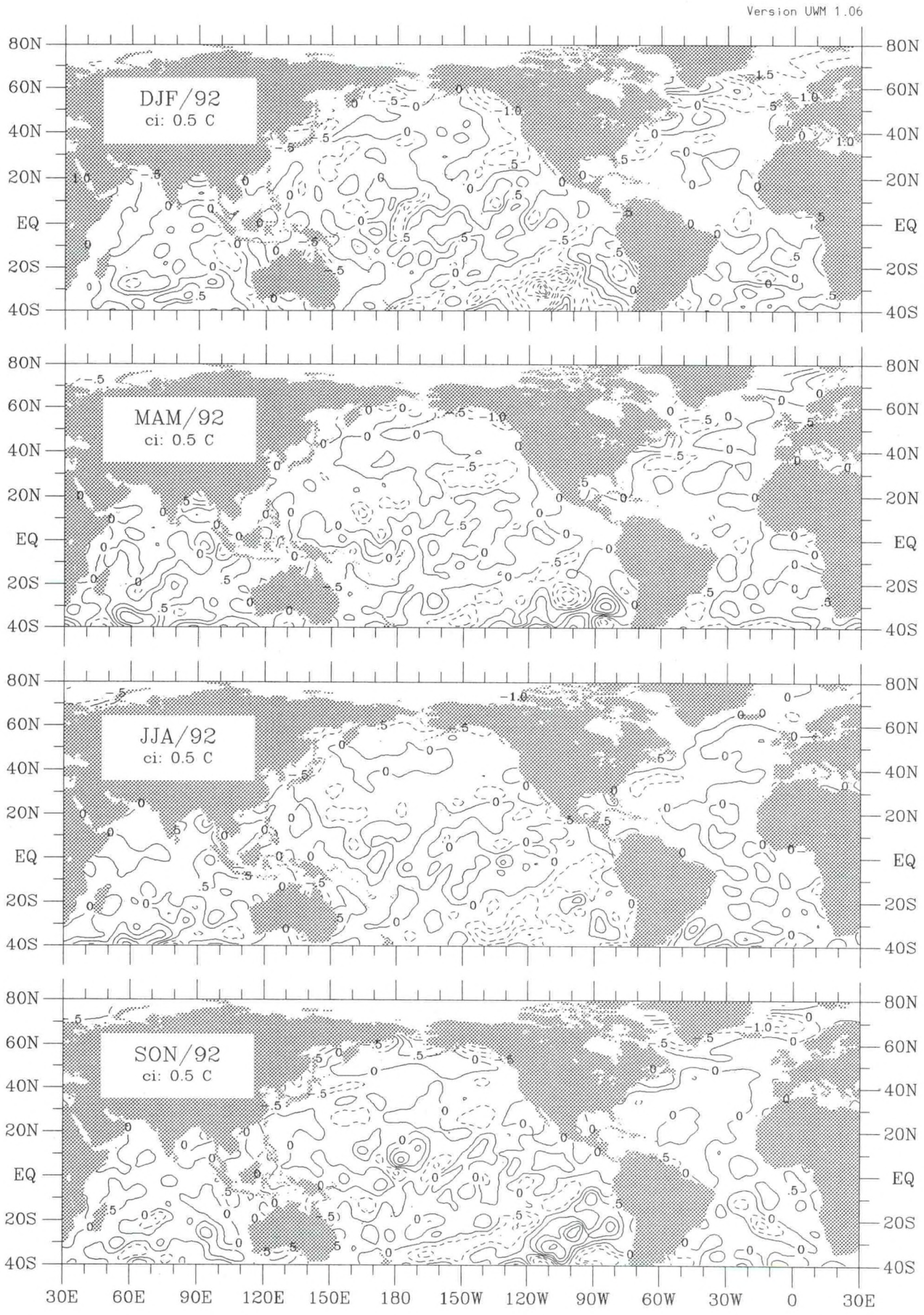

Figure dT-5. Sea minus air temperature seasonal anomaly for 1992.

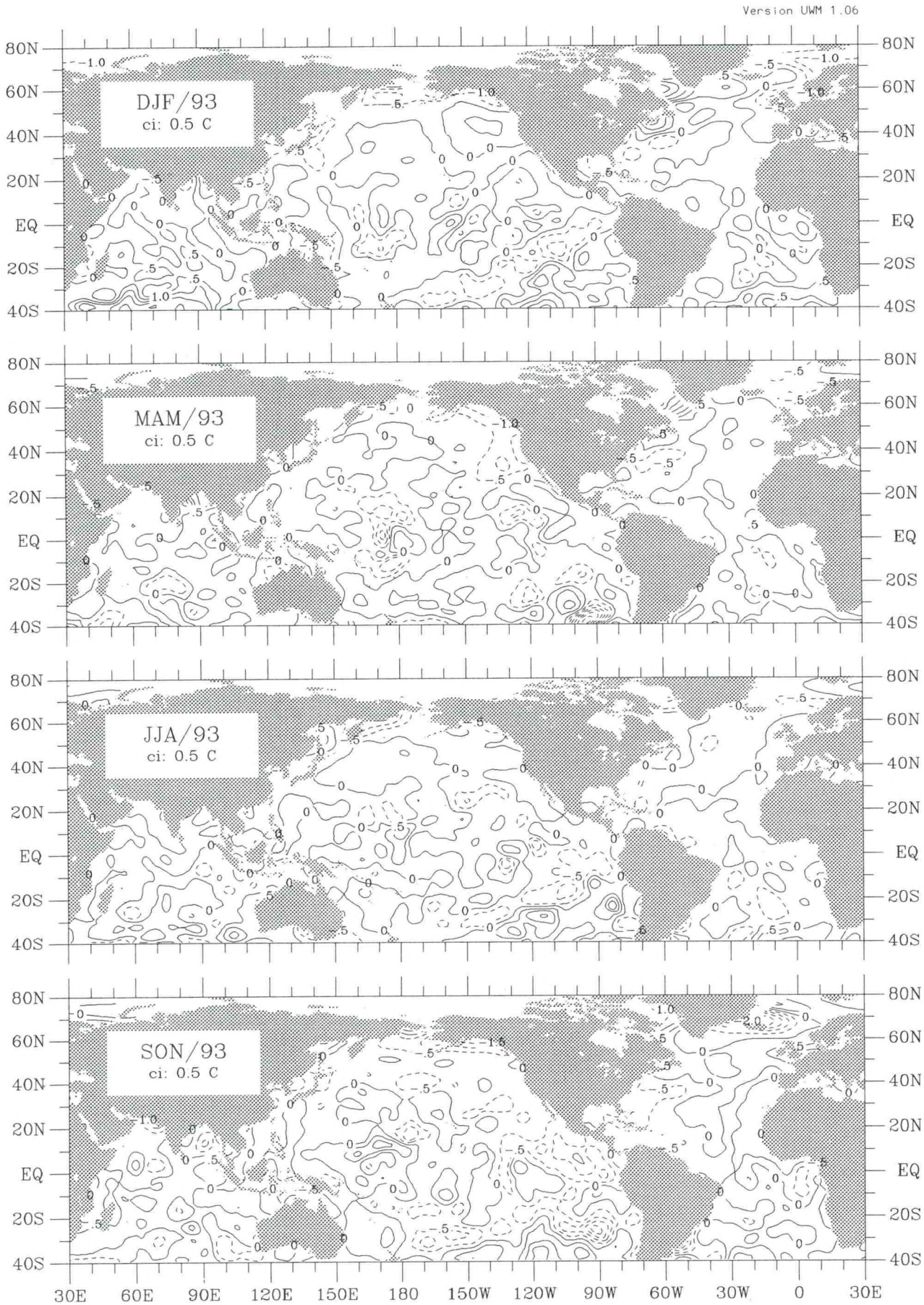

Figure dT-6. Sea minus air temperature seasonal anomaly for 1993.

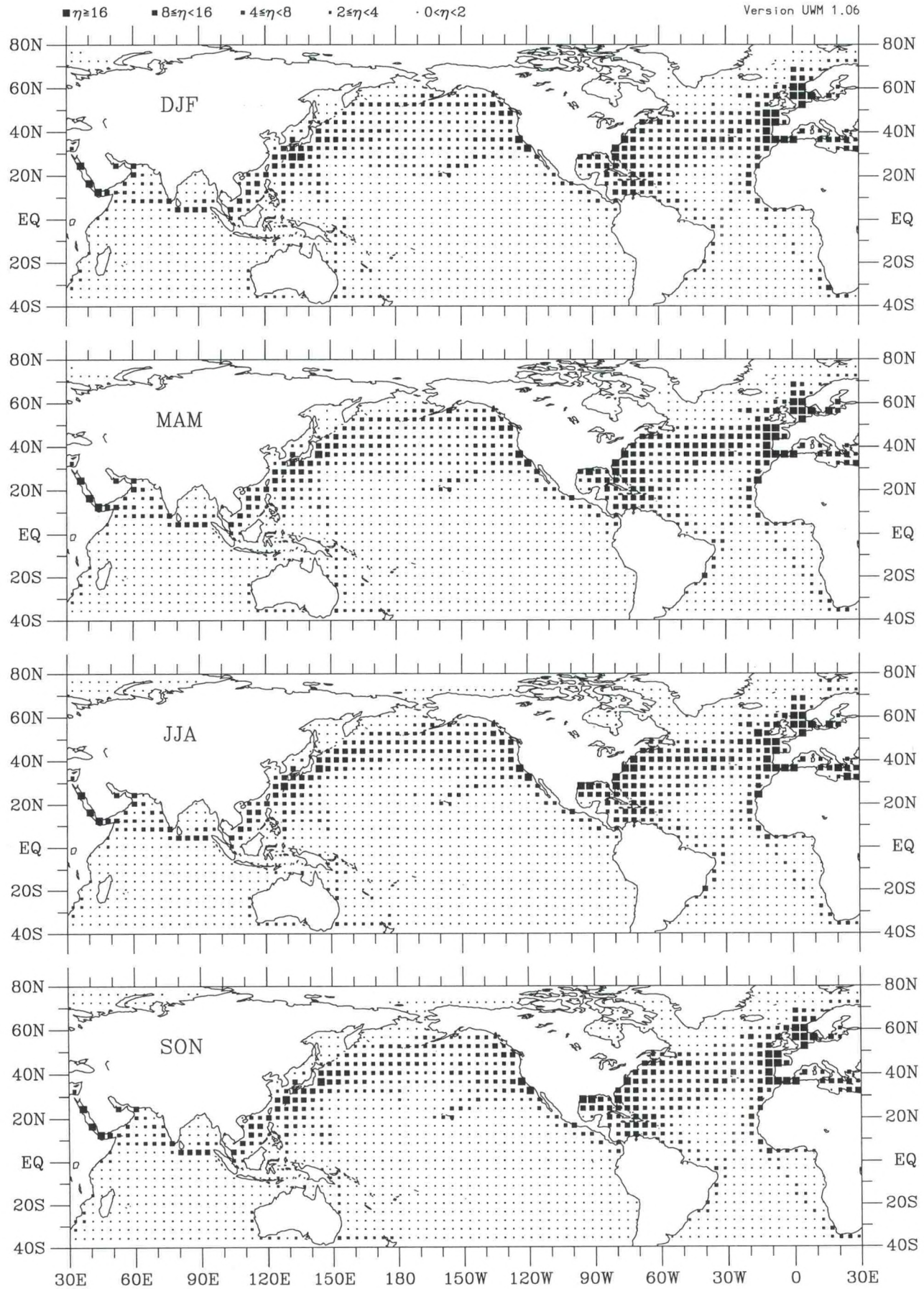

Figure dq-1. qs minus q seasonal observation density (1990-93).

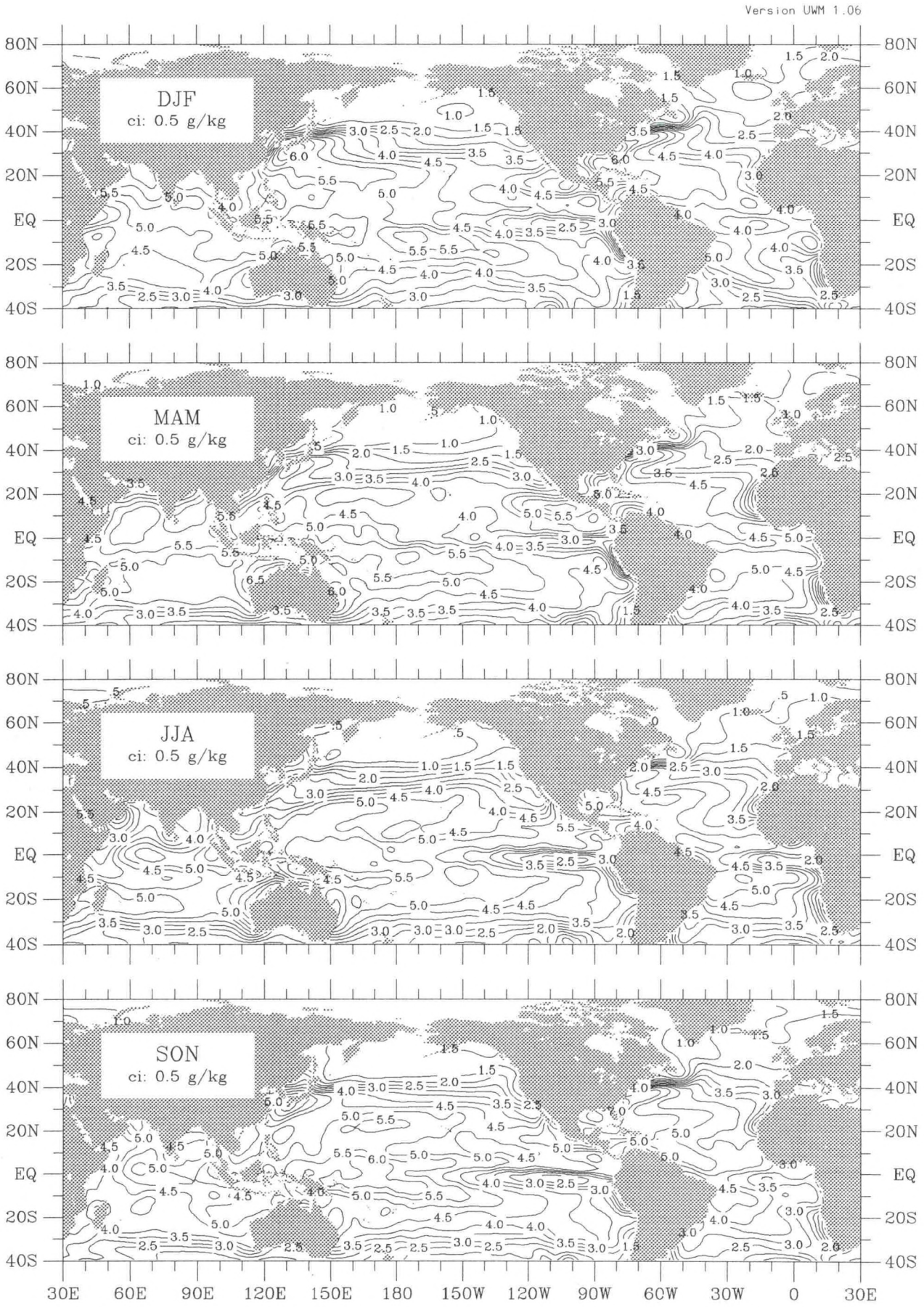

Figure dq-2. qs minus q seasonal climatology (1945-89).

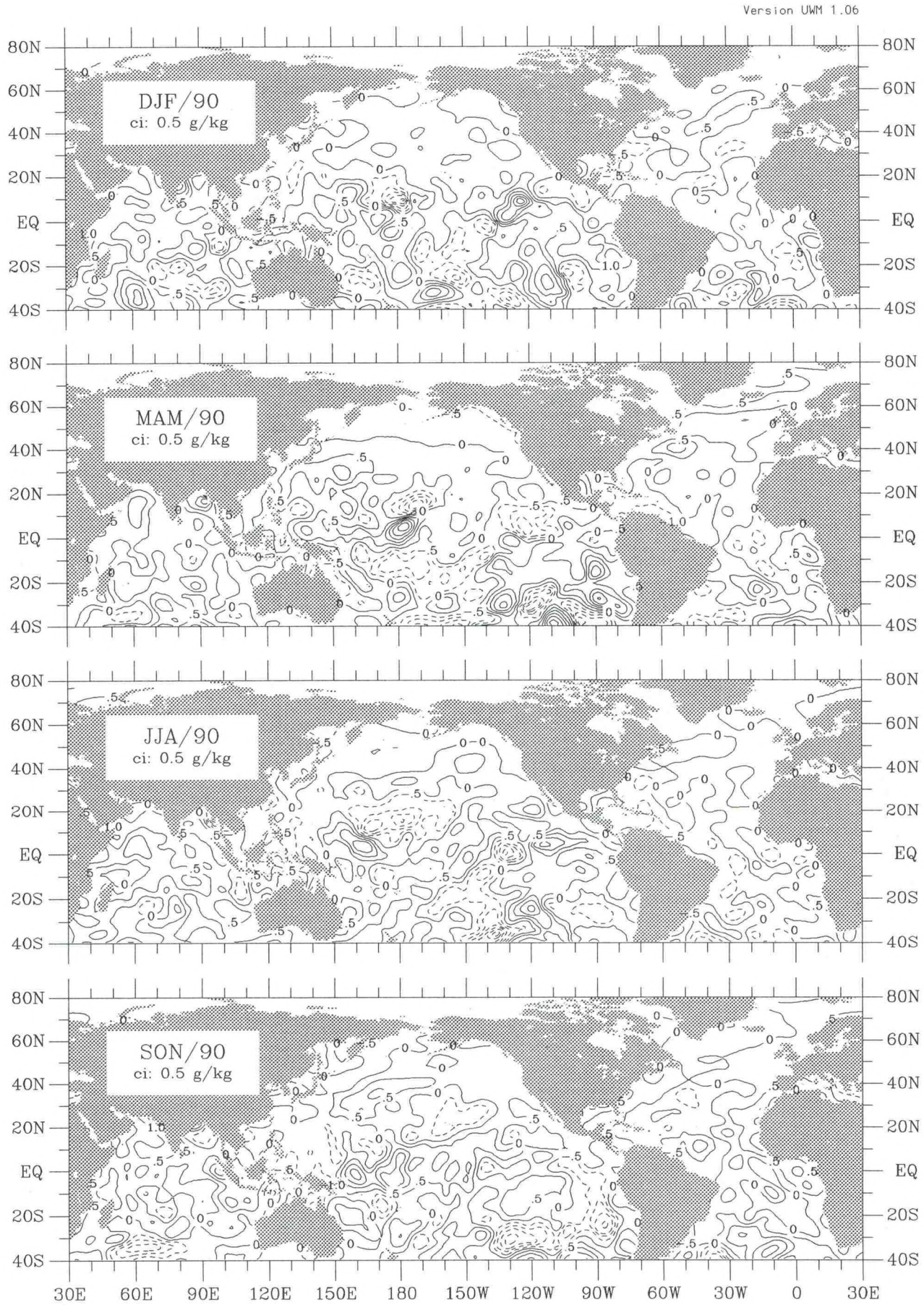

Figure dq-3. qs minus q seasonal anomaly for 1990.

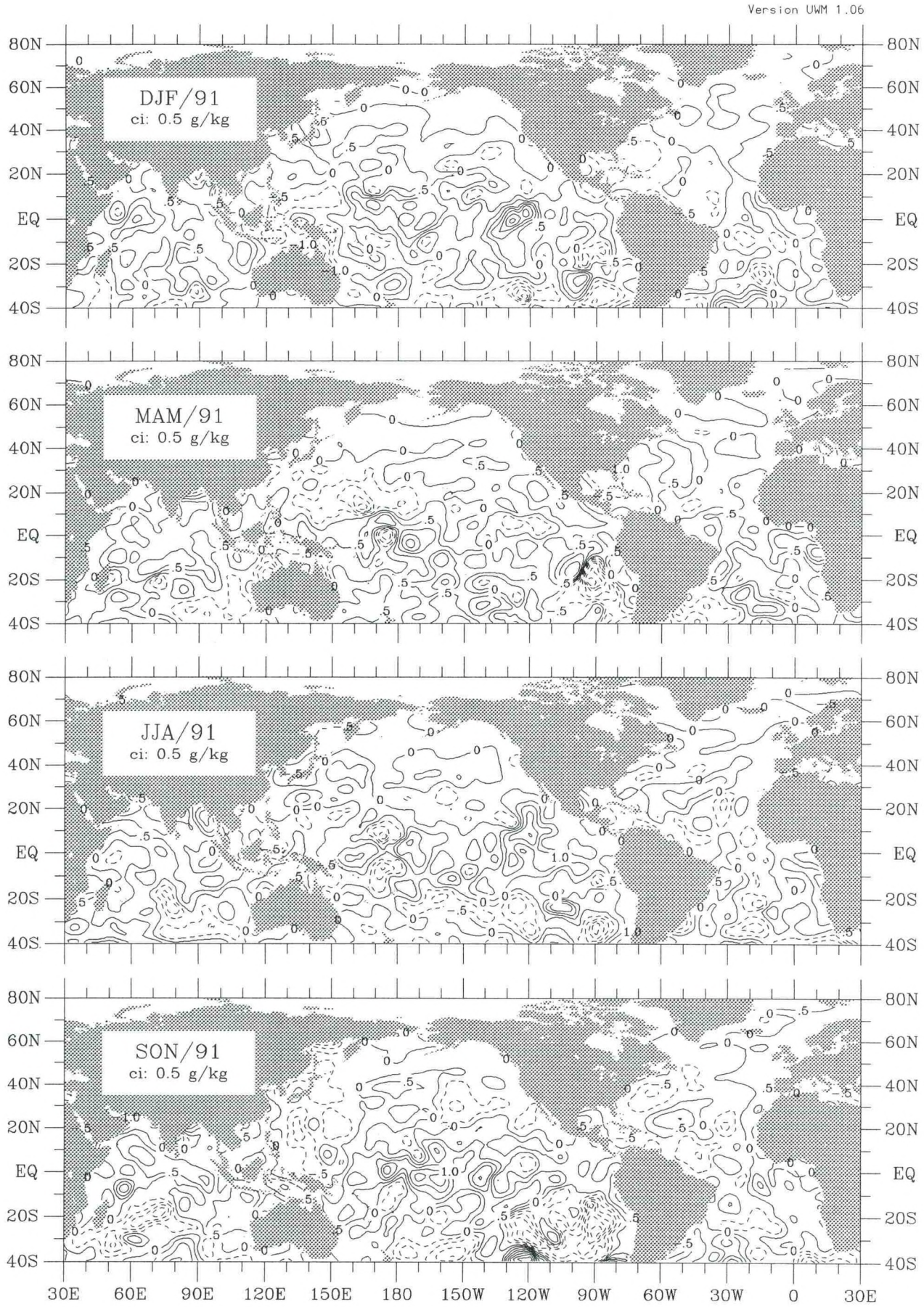

Figure dq-4. qs minus q seasonal anomaly for 1991.

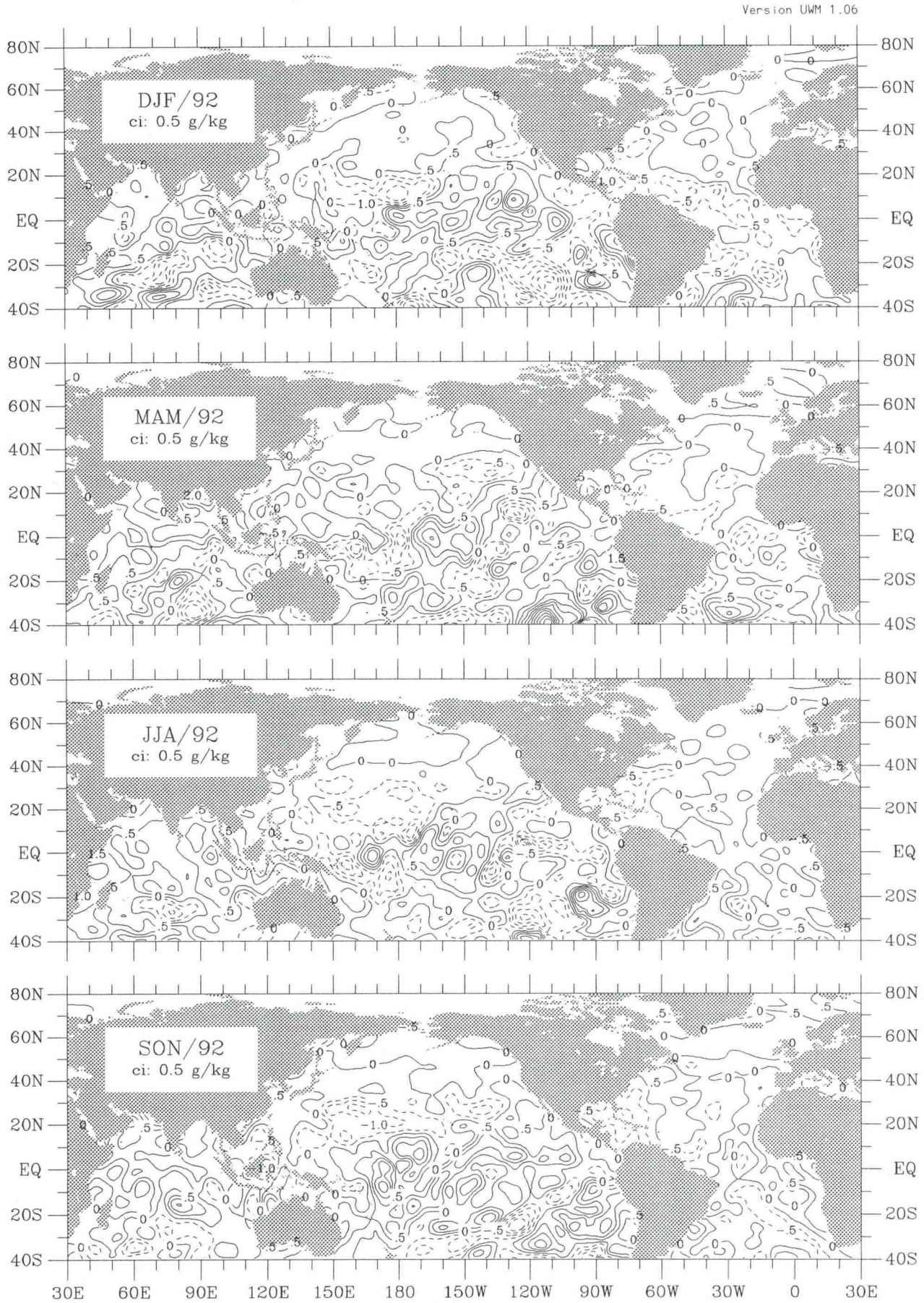

Figure dq-5. qs minus q seasonal anomaly for 1992.

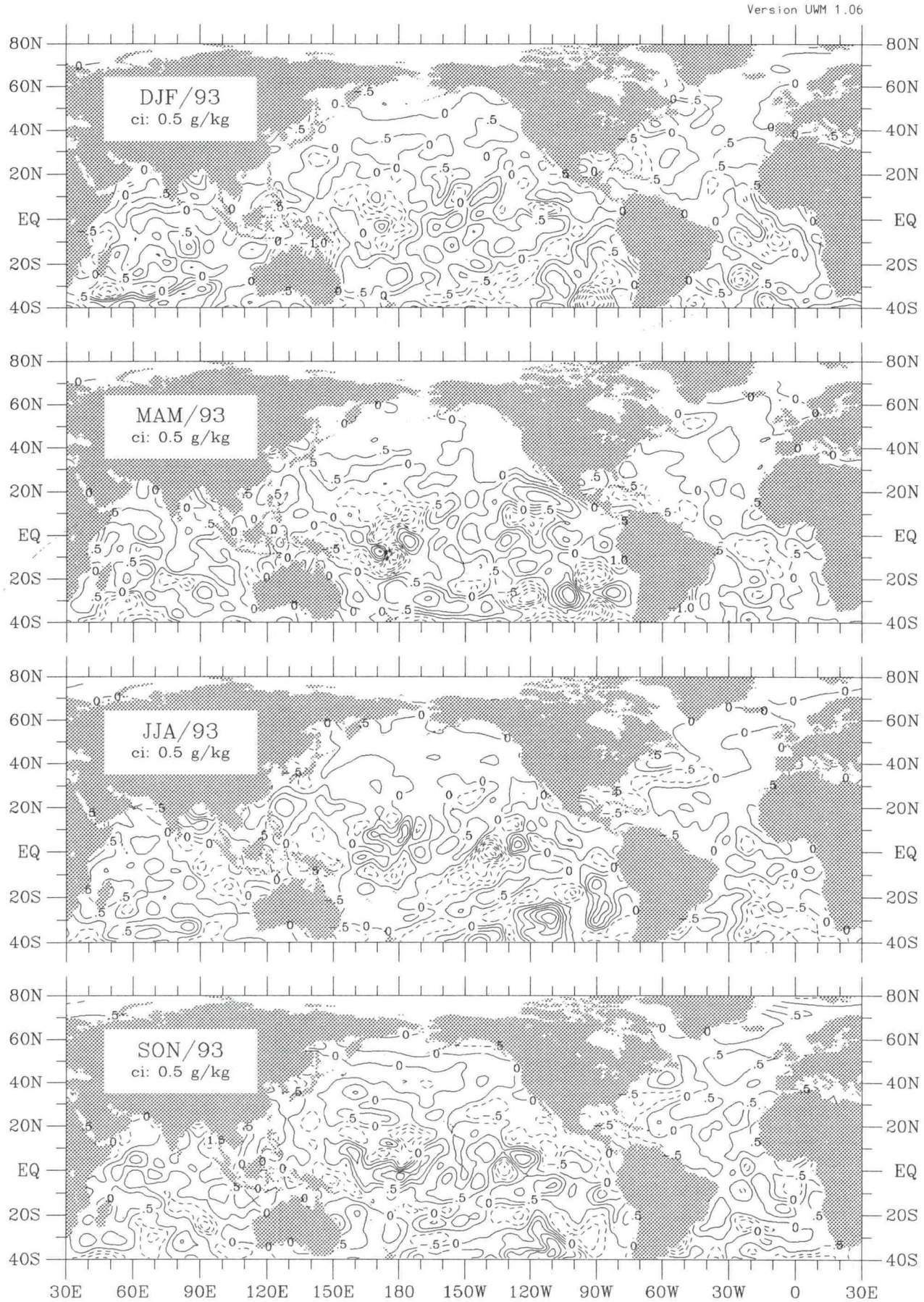

Figure dq-6. qs minus q seasonal anomaly for 1993.

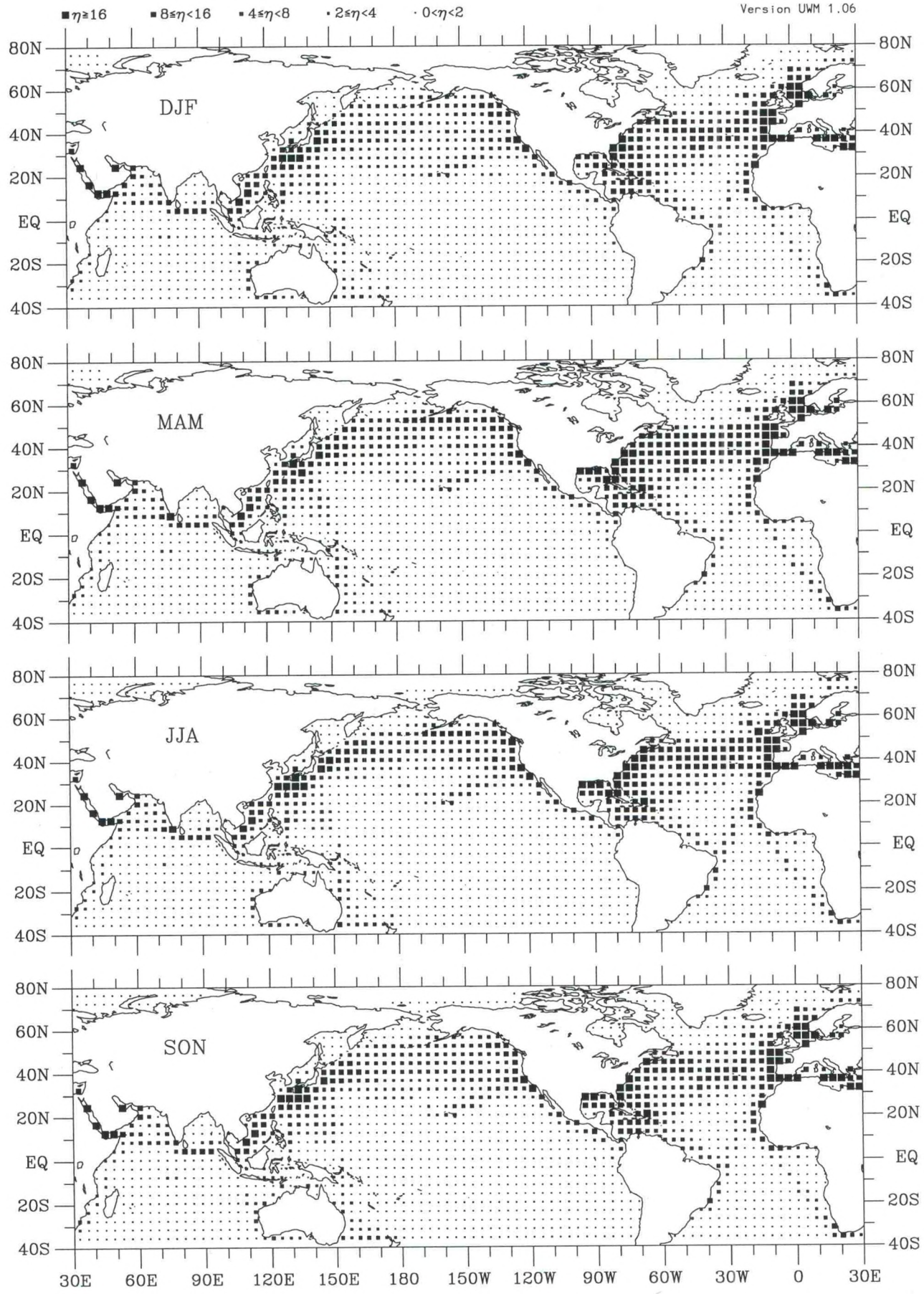

Figure e−1. Vapor pressure seasonal observation density (1990−93).

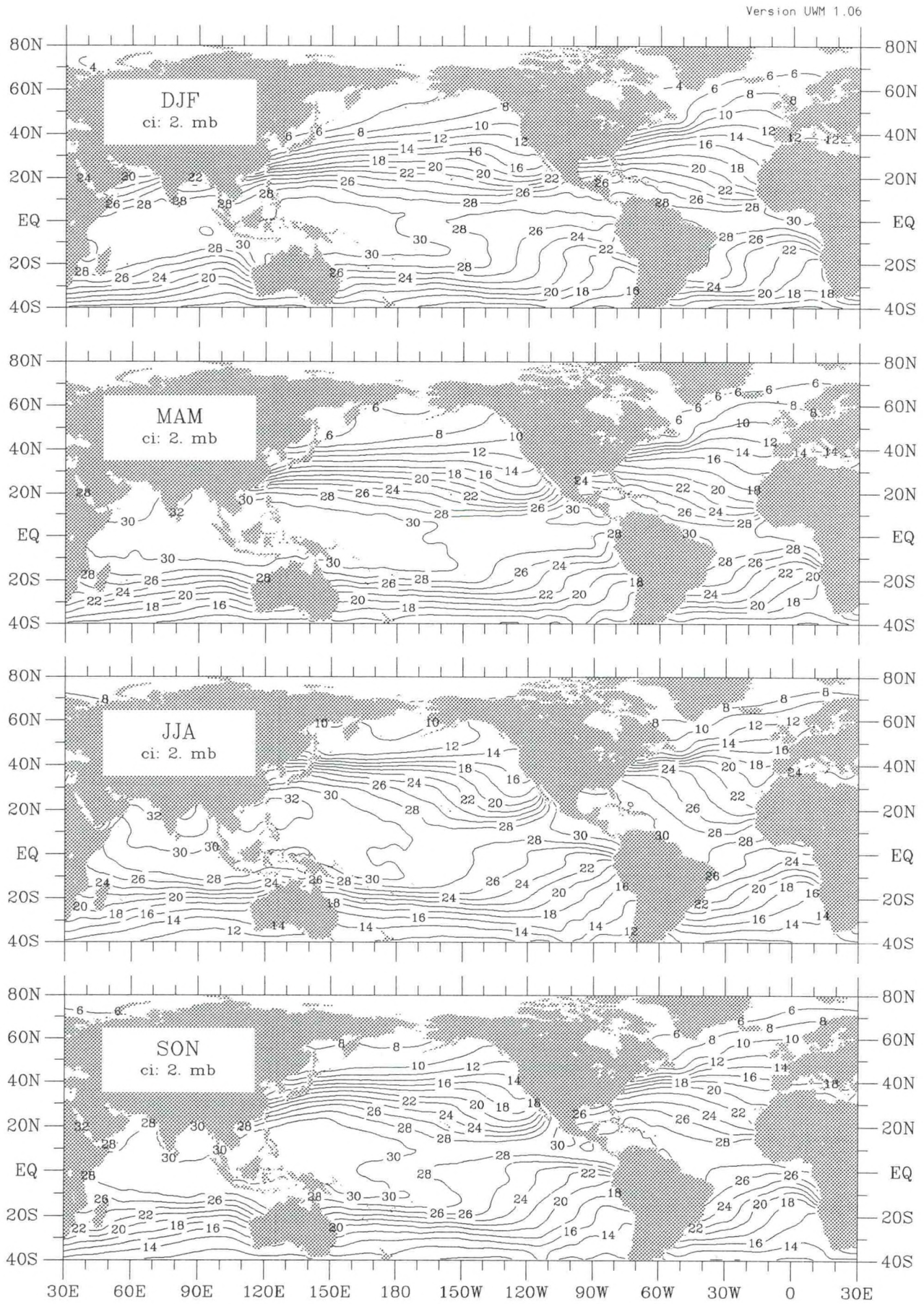

Figure e–2. Vapor pressure seasonal climatology (1945–89).

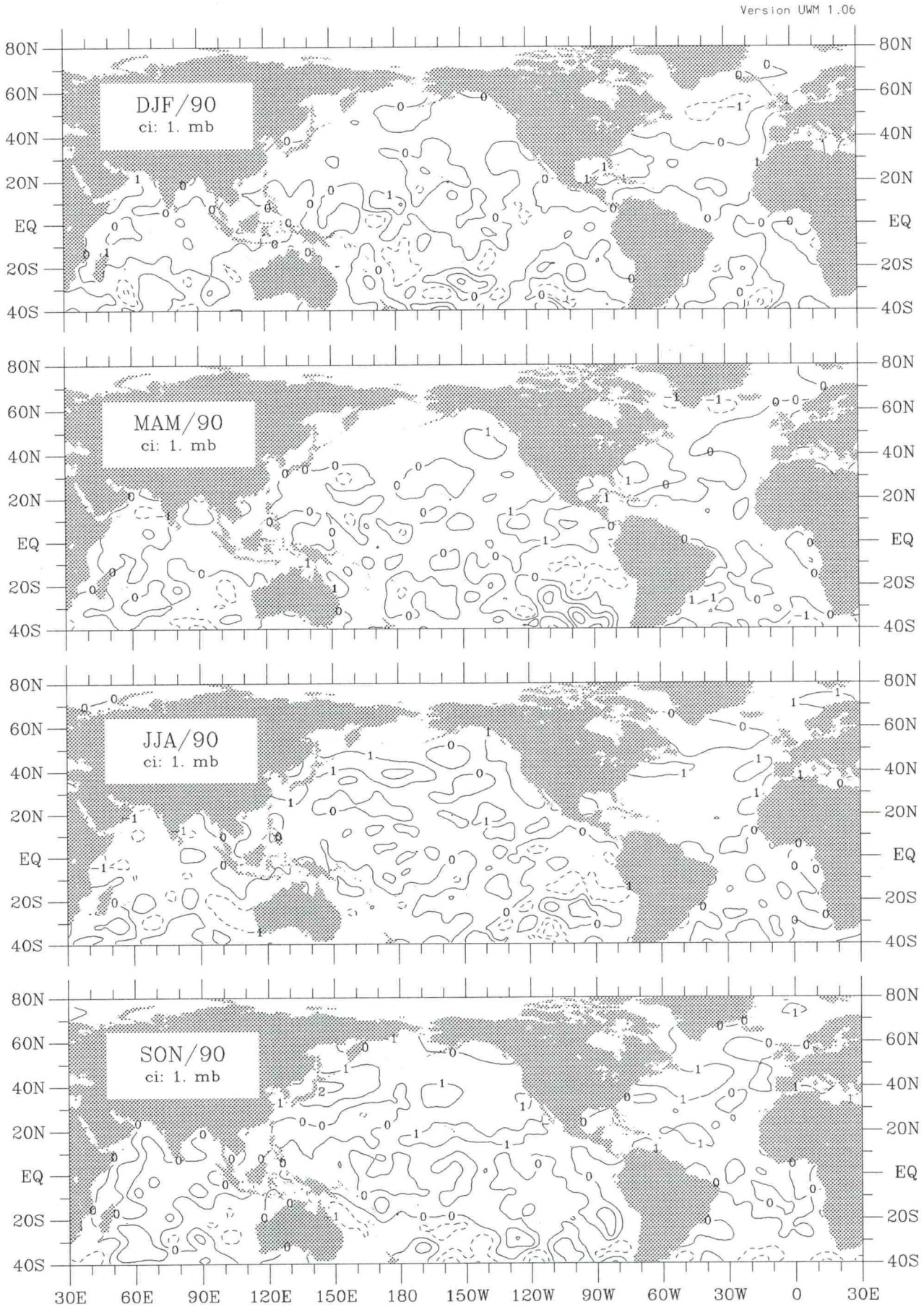

Figure e-3. Vapor pressure seasonal anomaly for 1990.

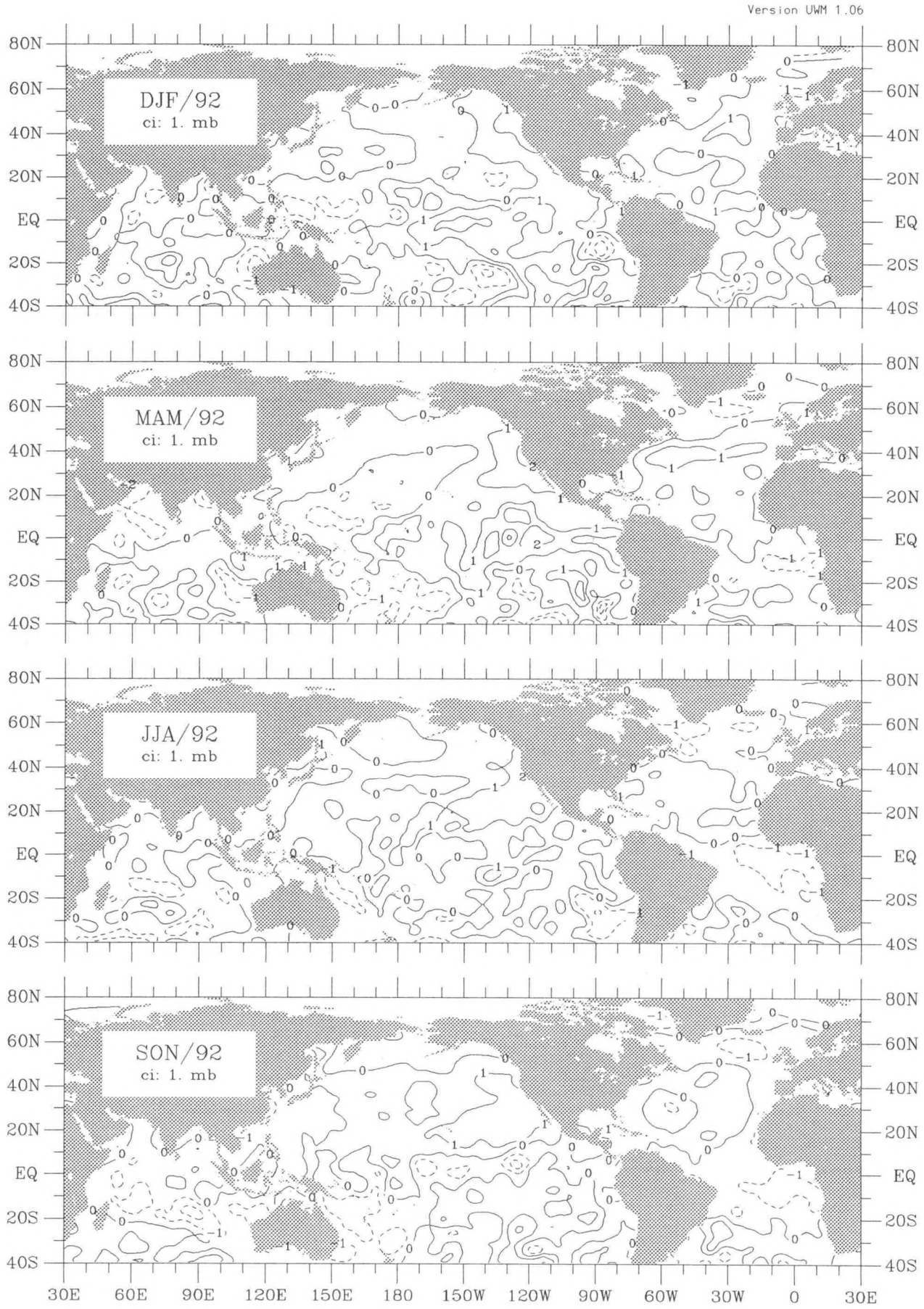

Figure e-5. Vapor pressure seasonal anomaly for 1992.

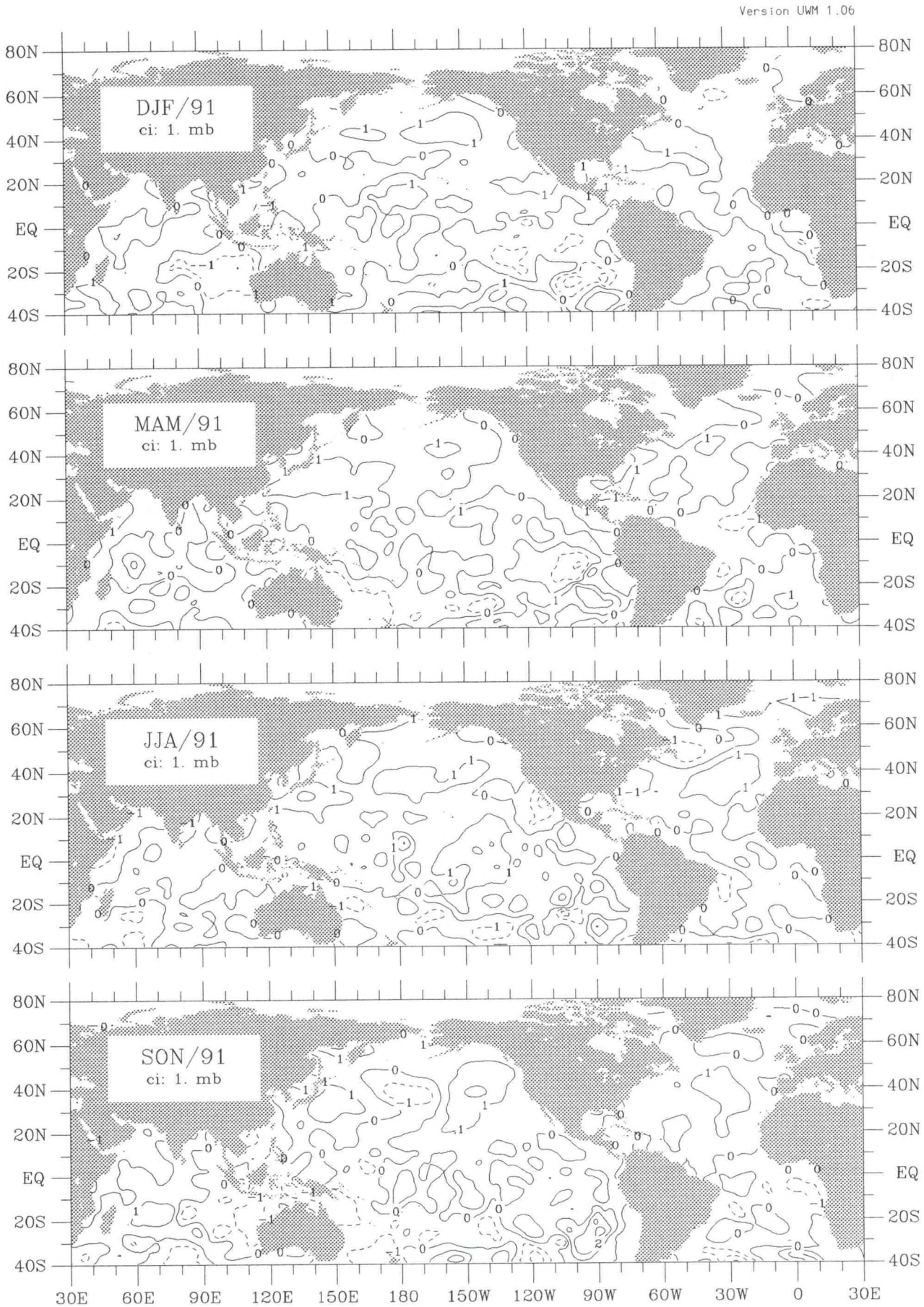

Figure e-4. Vapor pressure seasonal anomaly for 1991.

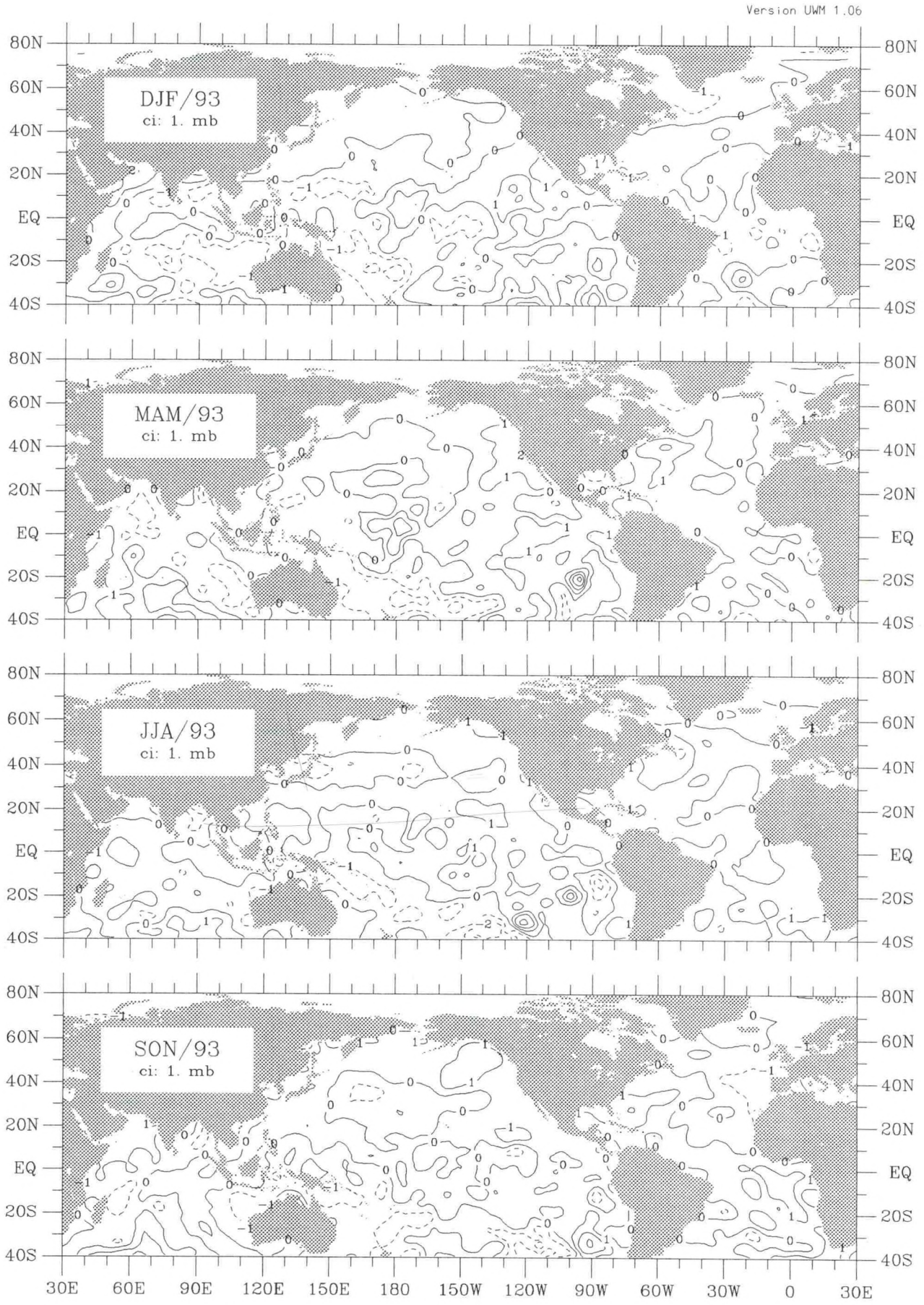

Figure e–6. Vapor pressure seasonal anomaly for 1993.

☆ U.S. GOVERNMENT PRINTING OFFICE: 1997 418-592/40022

NOAA SCIENTIFIC AND TECHNICAL PUBLICATIONS

The National Oceanic and Atmospheric Administration was established as part of the Department of Commerce on October 3, 1970. The mission responsibilities of NOAA are to assess the socioeconomic impact of natural and technological changes in the environment and to monitor and predict the state of the solid Earth, the oceans and their living resources, the atmosphere, and the space environment of the Earth.

The major components of NOAA regularly produce various types of scientific and technical information in the following kinds of publications:

PROFESSIONAL PAPERS - Important definitive research results, major techniques, and special investigations.

CONTRACT AND GRANT REPORTS - Reports prepared by contractors or grantees under NOAA sponsorship.

ATLAS - Presentation of analyzed data generally in the form of maps showing distribution of rainfall, chemical and physical conditions of oceans and atmosphere, distribution of fishes and marine mammals, ionospheric conditions, etc.

TECHNICAL SERVICE PUBLICATIONS - Reports containing data, observations, instructions, etc. A partial listing includes data serials; prediction and outlook periodicals; technical manuals, training papers, planning reports, and information serials; and miscellaneous technical publications.

TECHNICAL REPORTS - Journal quality with extensive details, mathematical developments, or data listings.

TECHNICAL MEMORANDUMS - Reports of preliminary, partial, or negative research or technology results, interim instructions, and the like.

U.S. DEPARTMENT OF COMMERCE
National Oceanic and Atmospheric Administration
National Environmental Satellite, Data, and Information Service
Washington, D.C. 20233